Seismic Vulnerability Assessment for Montreal

-An Application of HAZUS-MH4

By

Keyan Yu

Department of Civil Engineering and Applied Mechanics
McGill University
Montreal, Canada

February 2011

A Thesis submitted to the

Faculty of Graduate Studies and Research

in partial fulfillment of the requirements for the degree of

Master of Engineering

Abstract

Seismic loss estimation for Montreal, Canada is performed for a 2% in 50 years seismic hazard using the HAZUS-MH4 tool developed by US Federal Emergency Management. The software is manipulated to accept a Canadian setting for the Montreal study region, which includes 522 census tracts. The accuracy of loss estimations using HAZUS is dependent on the quality and quantity of data collection and preparation. The data collected for Montreal study region comprise: 1) the building inventory 2) hazard maps regarding soil amplification, liquefaction, and landslides 3) population distribution at three different times of the day 4) census demographic information and 5) synthetic ground motion contour maps using three different ground motion prediction equations. All these data are prepared and assembled into geodatabases that are compatible with the HAZUS software. The study estimated that roughly 5% of the building stock would be damaged with direct economic losses evaluated at 1.4 billion dollars for a scenario corresponding to the 2% in 50 years scenario. The maximum number of casualties associated with this scenario corresponds to a time of occurrence of 2pm and would result in approximately 500 people being injured. Epistemic uncertainty was considered by obtaining damage estimates for three attenuation functions that were developed for Eastern North America. The results indicate that loss estimates are highly sensitive to the choice of the attenuation function and suggests that epistemic uncertainty should be considered both for the definition of the hazard function and in loss estimation methodologies. The next steps in the study should be to increase the size of the survey area to the Greater Montreal which includes more than 3 million inhabitants and to perform more targeted studies for critical areas such as downtown Montreal, and the south-eastern tip of Montreal. The current study was performed mainly for the built environment; the next phase will need to include more information relative to lifelines and their impact on risks.

Résumé

Une analyse de risques sismiques est effectuée pour Montréal, pour un scénario de tremblement de terre correspondant à un aléa de 2% en 50 ans avec le logiciel HAZUS-MH4 développé par le FEMA (Federal Emergency Management Agency). Les fichiers d'entrée des données ont été adaptés afin d'accepter les données pour la région de Montréal. L'analyse est effectuée en discrétisant le territoire selon les secteurs de recensement, soit 522 au total. La précision des estimations sur les conséquences d'un séisme dépend de la qualité et la quantité des données compilées. Les données recueillies pour la présente étude sur la région de Montréal incluent: 1) l'inventaire des bâtiments 2) les cartes de risques pour les effets de site, la liquéfaction et les glissements de terrain et 3) la répartition de la population à trois moments différents de la journée 4) le recensement démographique et 5) les cartes des mouvements du sol pour trois différentes équations de prédiction. Toutes ces données ont préparées et compilées dans es bases de données géo-référencées en format compatible avec le logiciel HAZUS. L'étude indique qu'environ 5% du parc immobilier serait endommagé pour des pertes économiques directes de 1,4 milliards de dollars. Le nombre de victimes maximum est associé avec un scénario d'occurrence à 14 :00 heures avec environ 500 personnes blessées. L'incertitude épistémique a été considérée en considérant trois modèles d'atténuation proposés dans la littérature pour l'est de l'Amérique du Nord. Les résultats indiquent que les risques sont très sensibles à l'incertitude épistémique et il est recommandé de considérer cette incertitude autant dans les études de risque que pour les analyses de l'aléa sismique. Les prochaines étapes d'un projet d'évaluation des risques devrait étendre l'étude à la grande région métropolitaine et cibler des secteurs critiques tels que le centre-ville et le sud-est de l'île de Montréal. La présente étude est limitée aux dommages aux bâtiments. Il serait important de modéliser la vulnérabilité des lignes de vie et de quantifier leur impact sur l'estimation des risques.

Acknowledgement

I would like to convey my gratitude, first and foremost to Professor Luc E. Chouinard for giving me the opportunity to work in this project. His guidance and time to time advice and constructive discussions throughout this project have been invaluable.

I would also like to thank the office of City of Montreal for providing the database, which is an indispensable part of this research. I would like to express my gratitude towards Dr. Philippe Rosset and Mr. Salman Sead for their advices and helps through out the project.

I also wish to thank my parents for their encouragement and support. Last but not the least I would like to thank all my friends and colleges at McGill for being supportive.

Table of Content

List of Figures

List of Tables

Chapter 1. Introduction

1.1 Background and Project Scope

Montreal is the second largest city in Canada, and the largest city in Quebec. Based on Census 2006 data, there are 3.6 million people live in the vicinity of Montreal. It is also one of the oldest cities in North America: the first permanent settlements in Montreal were established in 1642. (Marsan, 1981) Over the years, it has developed into the economical capital of the province, and an international exchange center. However, due to its aging infrastructures and old building inventories, it has become particularly vulnerable to seismic events. One remarkable example is the case of the City Hall in Montreal-East. During the 1988 Saguenay earthquake of Magnitude 6 (300km far away), the masonry cladding of the city hall was severely damaged. The potential damage caused by seismic events if of great interest to different level of governments.

During the past few years, there have been several research projects going on at McGill University for seismic hazard analysis and vulnerability assessment for Montreal Urban Community. Microzonation project (Rosset & Chouinard, 2009) has investigated the potential soil amplification; liquefaction study conducted by (Joseph, 2005) investigated the occurrence probability of such hazard in Montreal. Numerous data has been gathered regarding soil amplification effect in seismic events. Under such background, it is desirable to conduct a preliminary study of the overall seismic vulnerability in Montreal. Such study can be used as a stepping stone for future seismic risk analysis in Montreal and other urban centers. The result of this study will also be useful in seismic risk mitigation and decision making. The aim of this project is to set up a data framework for vulnerability studies in Montreal and to test the performance of loss estimation tool HAZUS software on large scale.

Demonstrated by (Elnashai & Sarno, 2008) in Figure 1-1, earthquakes usually cause severe consequences. Comprehensive regional earthquake impact assessment requires an interdisciplinary framework that encompasses the definition of the hazard event, physical damage, and social and economic consequences. A full impact assessment requires the analysis of all components involved in a seismic event: namely building stock, transportation system, infrastructure system and critical facilities. However, the collection of such data is often costly and time-consuming. Therefore, this project focuses on the physical damage of building stock and its corresponding social-economic damages.

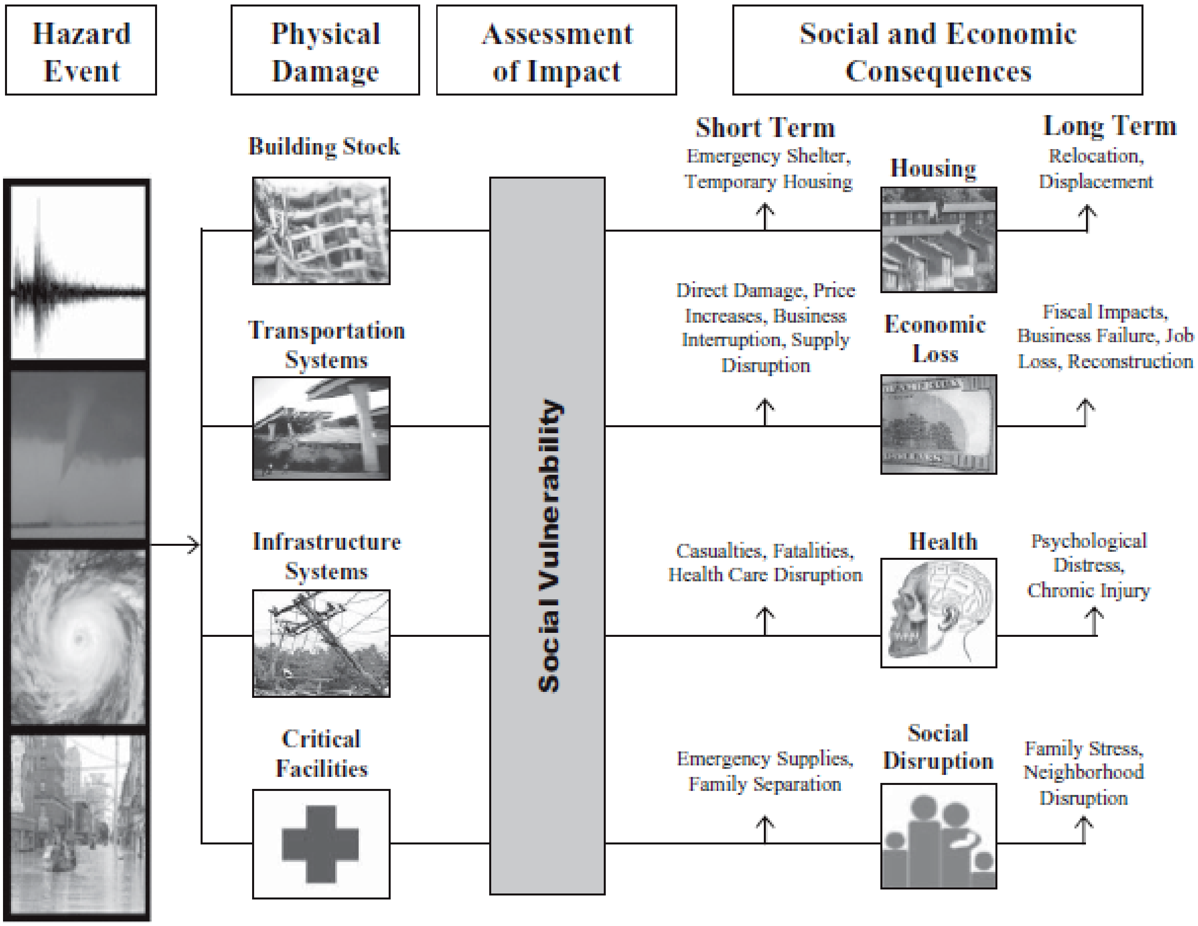

Figure 1-1: Correlation of Natural Hazard Event and Social Economic Consequences (Elnashai & Sarno, 2008)

1.2 HAZUS

HAZUS-MH4 software is chosen to carry out the analysis in this project. HAZUS-MH4 is a GIS based software developed by Federal Emergency Management Agent (FEMA) for the purpose of regional hazard loss estimation. The methodology used in the earthquake model is based on a multi-year project conducted for National Institute of Building Science (NIBS). It is developed by a team of earthquake loss experts composed of earth scientists, engineers, architects, economists, emergency planners, social scientists and software developers. The framework of the methodology is illustrated in Figure 1-2. The major components in seismic loss estimation are included in the framework: Potential Earth Science Hazard, Inventory, Direct Physical Damage, Induced Physical Damage, Direct Economic and Social Loss, and Indirect Economic Loss. Within each component, different modules dealing with different groups of inputs are presented, allowing one to adjust to the degree of sophistication needed in each analysis.

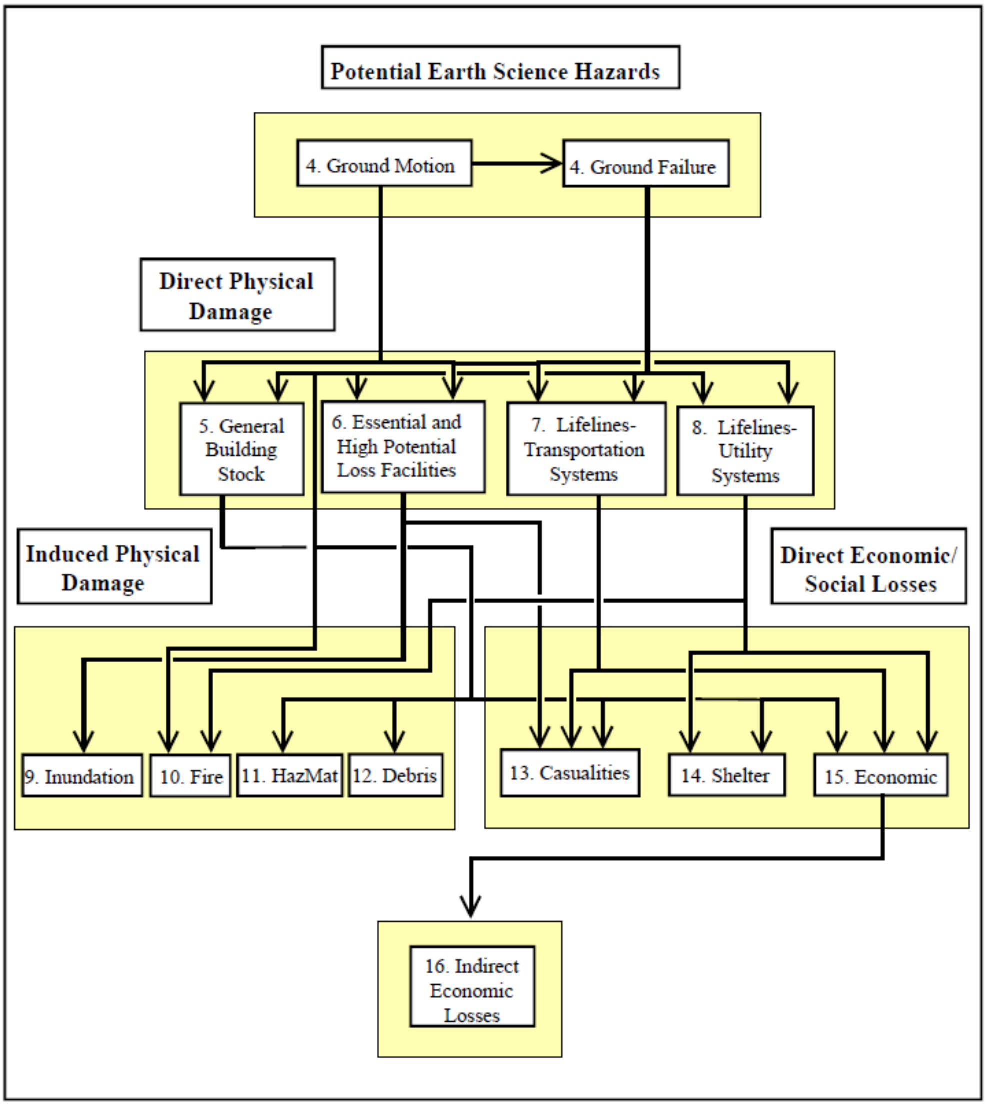

Figure 1-2: Flowchart of Earthquake Loss Estimation Methodology Used in HAZUS(FEMA, 2003)

The methodology is tested against the judgment of experts and past earthquake records. The Earthquake Model has been partially tested using actual inventories of structures plus correct soils maps, it has performed reasonably well. However, this software has some drawbacks: Based on several initial studies, the losses from small magnitude earthquakes (less than M6.0) centered within an extensive urban region appear to be overestimated (FEMA, 2003). There is considerable uncertainty related to the characteristics of ground motion in the Eastern North America. The embedded attenuation relations in the Earthquake Model, which are those commonly recommended for design, tend to be conservative. Hence use of these relations may lead to overestimation of losses in this region, both for scenario events and when using probabilistic ground motion (FEMA, 2003).

Since the Software is developed in a US setting, international application requires user supplied building inventories and other localized data. There are a few known Canadian HAZUS applications: North Vancouver study by Geological Survey of Canada (Journeay & Hastings) and Ottawa study by Ploeger (2008). The Ottawa project investigated the seismic vulnerability of 2 census tract in downtown Ottawa. Building inventory, census information, ground motion parameters and soil condition were collected and prepared according to HAZUS standards. Using these user supplied data, the analysis were performed to determine the most loss during different scenarios. The study concluded that HAZUS can be used as an effective tool in seismic loss estimation in a Canadian setting. It also severed as an important stepping stone in implementing HAZUS in Canada (Ploeger, 2008).

Chapter 2. Literature Review

2.1 Study Region and Seismicity

Regional Seismicity

Although eastern Canada is located on a stable continental region in North American Plate, large and damaging earthquakes have occurred here in the past and will inevitably occur in the future. Montreal is located in the Western Quebec Seismic Zone, which had at least three significant earthquakes in the past (Lamontage et al., 2007). In 1732, an earthquake estimated at 5.8 on the Richter scale shook Montreal, causing significant damage. During the past century, earthquakes of M6.2 occurred near Lake Timiskaming in 1935 and M5.6 near Cornwall, Ontario in 1944(Adams, 1989). Both historical and recent seismic records from Natural Resources Canada also show various seismic activities in the region(Earthquakes Canada, 2010). Most of the earthquakes in this region occur at depth between 5 and 25 km within the Grenville basement (Adams, 1989).

Based on historical and recent seismicity records, the earthquakes in this region occurred in two bands. The first one is along Ottawa River, and the second is along Montreal-Maniwaki axis (Adams, 1989). The first band includes all three major historical earthquakes in this region, and is believed to be associated with rift faults along the Ottawa River (Forsyth, 1981). The second band is more active, but produces smaller earthquake events. The seismicity of the sceond band is believed to be is believed to be related to the passage of a hotspot 130 million years ago (Adams, 1989).

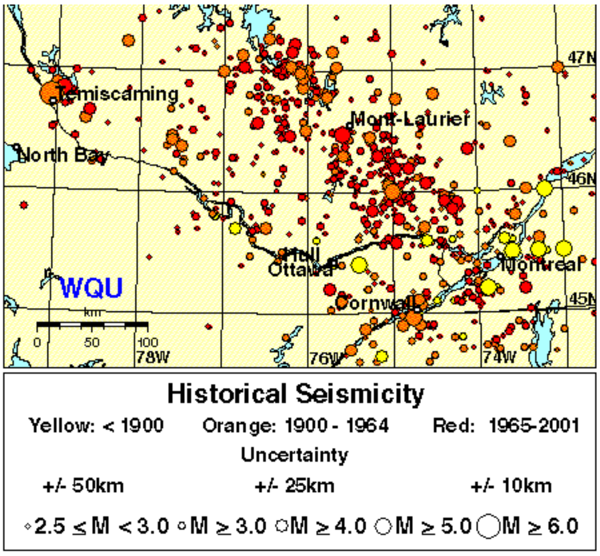

Figure 2-1: Historical Seismicity in Western Quebec Seismic Zone. (GSC, 2010)

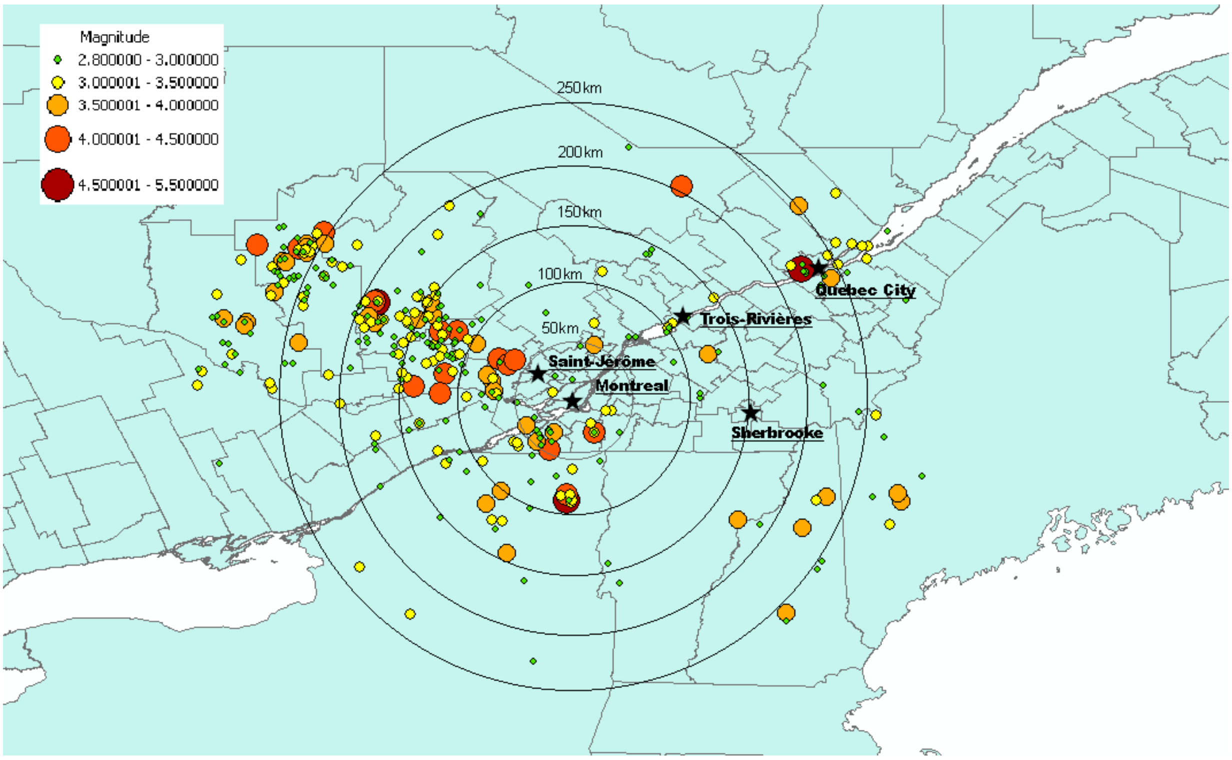

Figure 2-2: Recent Seismic Activities in Western Quebec Seismic Zone. (GIS Data Source: (Earthquakes Canada), 2010)

The seismicity in Montreal is controlled by both bands. The largest historical earthquake felt in Montreal is the 1732 Montreal earthquake of Magnitude 5.8. Considerable damage was observed in the city of Montreal with hundreds of chimneys and walls cracked (Leblanc, 1981). Other than that, four more major historical earthquakes were felt in Montreal. The location and magnitude of these earthquakes are presented in Table 2-1.

Table 2-1: Major Historical Earthquakes Felt in Montreal (Chouinard et al., 2004)

Date	Latitude North	Longitude West	Magnitude ML	Epicentral distance (km)	Estimated MMI	Estimated PGA (g)
1732/09/16	45.5	73.6	5.8	0	VIII	0.241
1816/09/09	45.5	73.6	5.7	0	VIII	0.212
1816/09/16	45.5	73.6	5	0	VI	0.085
1893/11/27	45.5	73.3	5.7	23	VI	0.091
1897/03/23	45.5	73.6	5	0	VI	0.085

Study Region

Montreal is the second largest city in Canada, and the largest city in the province of Quebec. Based on Census survey conducted in 2006, there are 3.6 million people residing in Metropolitan Montreal, and roughly 50% of the population lives on the island of Montreal(Statistic Canada, 2006). It is the cultural and economic center of the region. In Montreal, a significant portion of structures is old and designed according to codes before modern seismic standards. Therefore, Montreal is rated the second most seismic vulnerable city in Canada, and composed of 17.8% of the total seismic risk in Canada (Adams, 1989).

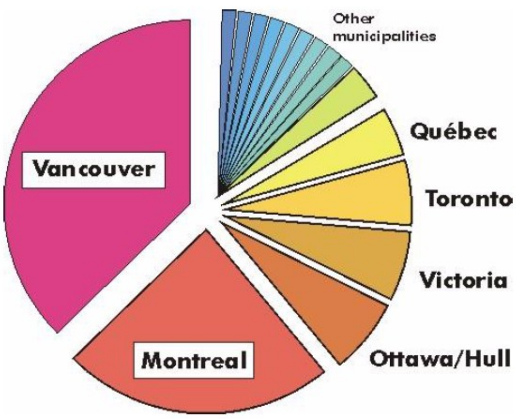

Figure 2-3: Seismic Risk Distribution in Canada (Adams et al., 2002)

The study region of this project is the City of Montreal. The base units of the project are the 522 census tracts within the city limit (Figure 2-4). The input and output data sets are based on these units. These census tracts are located in the 34 boroughs (Arrondissement) designated by the city of Montreal. When presenting the outputs, these neighborhoods are referred to in order to help readers identifying the location of the census tracts. In order to use HAZUS, the name of each census tract is converted into a standard US census tract name. The Canadian census tract name is a number series of 9 digits. The first three representing the Census Metropolitan Area (CMA), and the last 6 digits including 2 digits after the decimal point represent the individual census tract within the CMA. In the US census system, the name of the census tract is composed of 11 digits. The first 5 digits are the county name, and the last 6 are the tract name. In this project, the County name "36061"of New York City is used to replace the CMA name "462" of Montreal. The remaining digits of each census tract are preserved. For example, census tract 4620014.02 in the Canadian census system is recorded as 36061001402 in HAZUS for this project. By doing so, one can easily identify the output of this study by its location in a Census tract map.

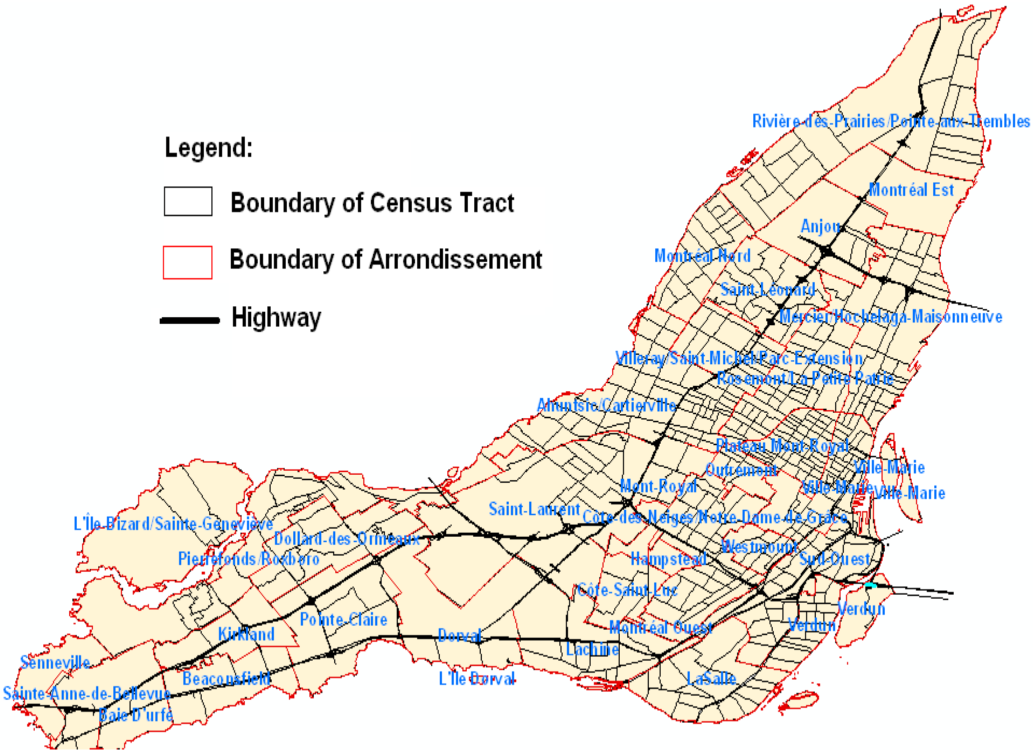

Figure 2-4: Map of Study Region showing the Boundary of 522 Census Tracts. (GIS Data source: StatisticCanada, City of Montreal)

2.2 Geology Setting in Montreal

The basement of Montreal consists of rock dated back to Precambrian age. It is covered by Ordovician sedimentary rocks (ca60000-ca.125000). The predominant rocks in the Montreal area are dolomite and limestone of Beekmantown, Chazy, BlackRiver and Trenton groups. The exception would be the area near of St. Lawrence River and east tip of the island, where the rock is constituted of shale from the Utica, Lorraine, and Richmond group (Boyer, 1985). Mont-Royal is referred as a stock of alkaline igneous rock and is part of eight hills known as the Monteregian hills (Rosset et al., 2003). The location of different rock groups can be seen in Figure 2-5.

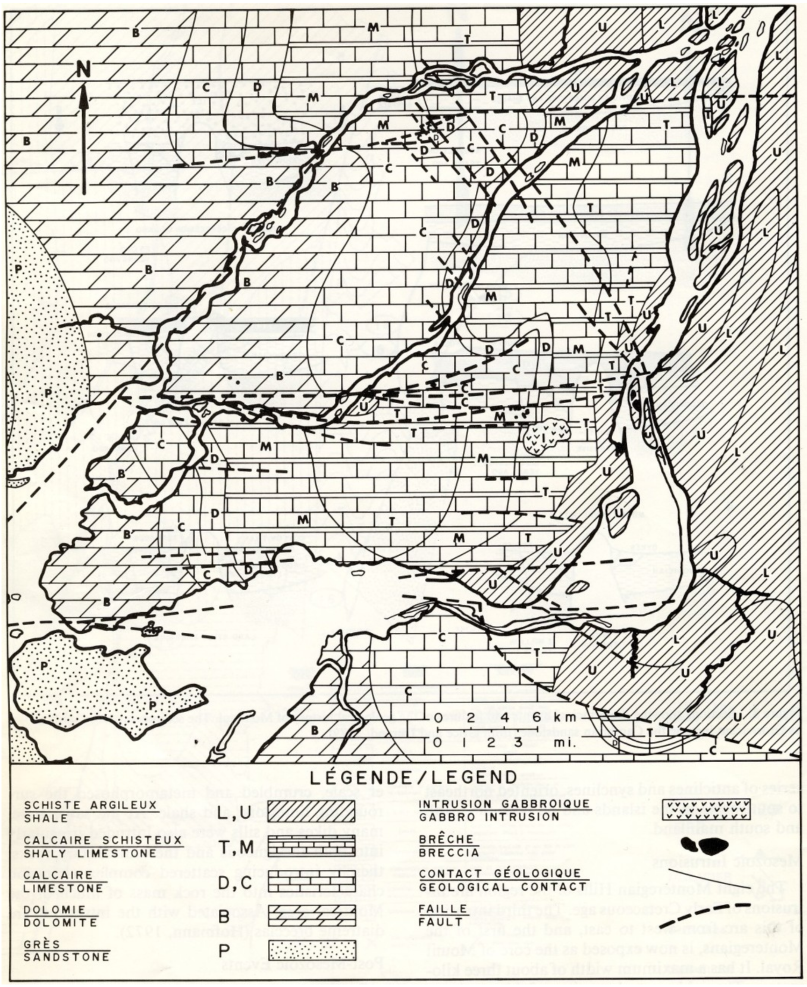

Figure 2-5: Bedrock Geology Map of Montreal(Boyer, 1985)

More recent sediments overlay the bedrock. Two main groups of these deposits are composed of glacial till deposits and post-glacial deposits. The oldest glacial deposit is

Malone Till, followed by Middle Till Complex and the Fort Covington Till. The three tills cover more than 50 percent of the Montreal Island surface(Boyer, 1985). The tills are a mix of boulders, gravel, sand and silt in varying proportions that can be distinguished by their relative values of N-SPT. All post glacial deposits (clay, sand and silt) originate from Champlain Sea and subsequent wanderings of the St-Lawrence riverbed (Rosset, et al., 2003). Figure 2-6 shows the location of these deposits. During an earthquake, the characteristics of seismic waves are altered as they travel from the source to the site of civil engineering work, known as the distance-travel path effect. Moreover, soil characteristics of the site can affect the frequency and duration of ground motion. This is known as the site effect. Therefore, soil characteristics are of high importance in predicting ground shaking and ground failure of a site. One of the most important soil characters is its shear-wave velocity (V_s). By knowing the V_s and depth of each soil layer on site, the natural period of a site can be estimated. Based on the computation of various studies, Rosset and Chouinard (2008) provide a summary of V_s for different deposits found in Montreal (Table 2-2).

Table 2-2: Properties of Selected Deposit in Montreal(Rosset & Chouinard, 2008)

Age in years(a)	Episode of deposit	Nomenclature	Type of Deposit	Density (kg/m3)	S-wave Velocity (m/s)	reference
0 - ca.9500	Late	Bog–pond deposit	Peat, muck, filled ground	2000	150	(a)
	Fluvial	St-Lawrence deposit	Sand, gravel	2054	400	(a,b,d)
ca.9500-ca.12500	Marine	Offshore sediments	Clay-silt, marine shells	1720	150	(a,d)
ca.12500 -ca.60000 to 70000	Glacial	Fort Covington Till	Undifferentiated tills	2080	600	(a,c,e)
		Intermediate Till	Sand, gravel, silt, cobbly	2160	800	(a)
		Malone Till	Boulders, sand, silt	2400	1000	(a)
ca.60000 to 70000 - ca. 125000	Rock	Trenton Limestone	Limestone	2730	2300	(a,c,e)
		Shale of Utica	Shale	2670	2100	(a,c,e)

Note: (a) Prest and Hode-Keyser (1977); (b) Robert (1980); (c) Decroix (1984); (d) National Resource Canada (2003); (e) Benjumea et al. (2001)

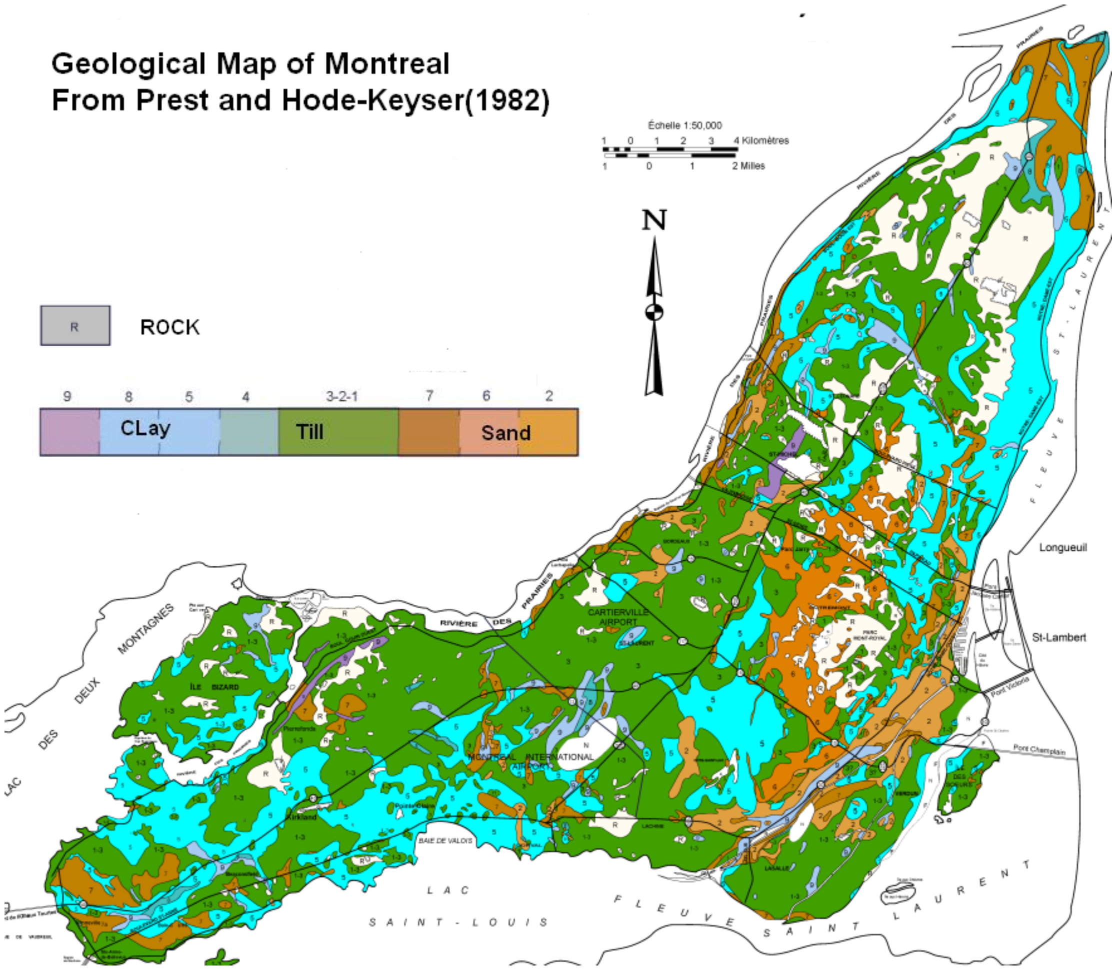

Figure 2-6:Surfacial Geological Map of Montreal(Prest & Hode-Keyser, 1982)

2.3 Potential Earthquake-induced Ground Failure

Analysis of earthquake induced damage indicates that ground effect is a serious contributor to damage of the built environment (Elnashai & Sarno, 2008). The amplitude of ground motion is not only influenced by the distance and magnitude of the earthquake event, but also affected by the local soil and topographic conditions. In general, unconsolidated soils such as soft river deposits and landfills would amplify ground motion in comparison to ground motions measured on consolidated sediments or bedrock. In addition to ground motion, ground failures caused by various mechanisms can result in significant structural damages. The major mechanisms of concern in Montreal region are listed as followings:

Liquefaction

By definition, liquefaction is a state of instability due to the transformation of a saturated granular or cohesionless soil from a solid to a liquefied state as a result of increased pore water pressure and reduced effective stress when subjected to monotonic, cyclic or shock loading (Marcusson, 1978). During an earthquake, the loosely packed soil particles will collapse under the effect of seismic waves. This leads to the increase of pore water pressure, and results in the loss of stiffness and strength of soil (Elnashai & Sarno, 2008). Liquefaction is known to be one of the principal causes of structural damage from earthquake. The damage can result from different sources: flow failure, lateral spreads, ground oscillation and loss of bearing strength (Gates & Ritchie, 2007). Flow failure occurs when large masses of soil flow downslope, and is generally found on sites where the slope is greater than 3^{o}. Lateral spread is another source of property damage from liquefaction. In this phenomenon, the surface soil block slides sideways because of liquefaction of an underlying layer. Lateral spread may not be as dramatic as flow failure and may result in displacements of only a few feet. However, it can cause dramatic damage in underground structures such as pipelines. Ground oscillation is cause by Liquefaction at depth, which may decouple overlying soil layers from underlying ground, causing wavelike rippling and fissures. Finally, the soil could lose bearing capacity due to the effect of liquefaction, causing structures built above to tilt over or sink (Gates & Ritchie, 2007).

Previous research conducted by Joseph (2005) studied the liquefaction potential in Montreal. A factor of safety against liquefaction was generated for earthquake of magnitude 5.5 and 7.5. It is found that a few areas in Montreal do have potential liquefaction hazard. These regions of high liquefaction susceptibility or factor of safety less than and equal to one are the east end, some scattered areas in the central east and west and central portion in Dorval in the west Island (Figure 2-7). Therefore, the potential damage cause by liquefaction susceptibility is investigated in this study.

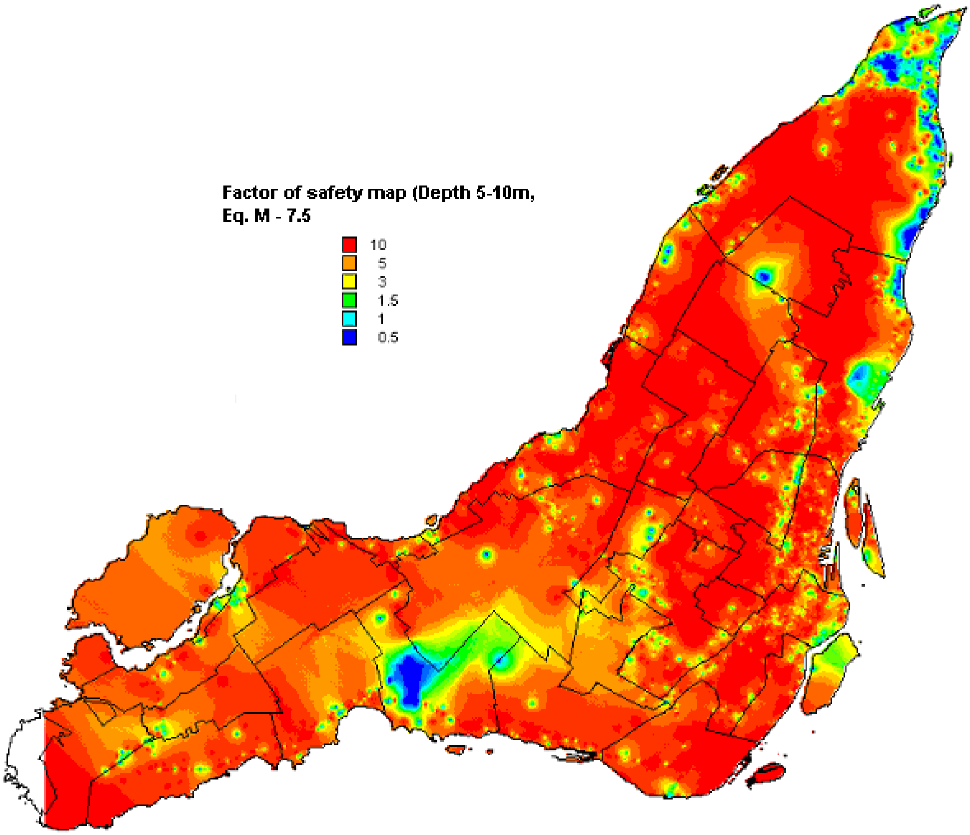

Figure 2-7: Interpolated Map for the Factor of Safety Against Liquefaction for Depth 5 m to 10 m and Earthquake Magnitude 7.5 for the Island of Montreal (Joseph, 2005)

Landslides

Landslides are the rapid downward motion of soil and rock materials occurring in sloping terrains. The triggering mechanism of landslide includes earthquake, excessive participation, and deforestation (Singhroy, Mattar, & Gray, 1998). Landslide occurs when soil losses its shear strength, and can cause more damages than the earthquake triggered it (Elnashai & Sarno, 2008). It is well documented in literature that landslides can results in the destruction of buildings and utility lines. During the 1964 Alaska earthquake, landslides involving about 9.6 million cubic metres of soil, took place in the Anchorage area. The largest one of them occurred in Turnagain residential area, and destroyed about 75 private houses. Water mains and gas, sewer, telephone, and electrical systems were also disrupted throughout the area (U.S.Geological Survey, 2006). Landslides have also occurred in Canada during past earthquakes. Landslides found in different regions of Canada are associated with different soil type, geologic structures, and topographic settings (Singhroy, et al., 1998). In eastern Canada, sensitive postglacial clay soils (quickclays) found in the valley of St.Lawrence is known to induce landslides (Crawford, 1968). One of the most famous quickclay landslides in Canada occurred on the 7 May 1898 at St. Thuribe in St-Lawrence River valley: 3,000,000m^3 of soil material was involved and one person was killed(Smalley, 1976). Due to the existence of quick clay on the island of Montreal, landslide is included as one of the ground failure mechanisms in this project.

Chapter 3. Data Collection

The input required in HAZUS can be grouped into three different categories: Ground Motion and Ground Failure, Structural Inventory, and Demographic Inventory. The first one includes: hazard scenario definition, ground motion parameters calculation, and potential earthquake induced ground failure mapping. Structural inventory covers building structural information and building economic statistics. The last one provides information regarding population distribution and other social-economic data. The information collected for this study is listed in Table 3-1. The source and method used in processing these data are described in this chapter.

Table 3-1: List of Data Collected for the Study

Data Category	Sub Category	Fields
Building Inventory	General Building Stock	*Area* *Building Value* *Structural Type* *Occupancy Class* *Age/Yr of Construction*
	Essential Facilities	*Location*
PESH	Soil Classification Map	
	Liquefaction Susceptibility Map	
	Landslide Susceptibility Map	
Ground Motion Parameters	Ground Motion Maps of Scenario earthquakes	*AB95, AB06, AB08*
Demographics	Household and Income	*Household number and income*
	Population	*Population at 2am, 2pm, and 5pm*

3.1 Ground Motion

Ground motion is the direct effect of a seismic event. Several parameters derived from the recording signals are used to characterize it. The most common way to describe ground motion is by citing the spectral response for a given period, peak ground acceleration (PGA), peak ground velocity (PGV), and Peak Ground Displacement. When accessing the seismic vulnerability of a region, ground motion is the basic and one of the most sensitive inputs. There are several options in choosing ground motion inputs: real records of past events in the region or ones similar to the tectonic context of the region, or synthetic records derived from strong Ground Motion Predictions Equations (GMPEs). In eastern Canada, the first option is not valid because no strong seismic events were recorded in the past. Therefore, the ground motion inputs used in this study are generated by different GMPEs for specific magnitude-distance seismic events chosen. Although the dispersion of energy is a function of distance and source is described by the GMPEs, local site conditions can also significantly affect the amplitude of ground motions. This phenomenon is known as soil amplification. The choice of seismic events, GMPEs, and soil amplification factors are discussed in the following sections.

3.1.1 Hazard Scenario Selection

Seismic hazards are the intrinsic natural occurrence of earthquakes and the resulting ground motion and other effects. There are two approaches in evaluating the seismic hazard of a region: deterministic or probabilistic. Deterministic Seismic Hazard Analysis (DSHA) is performed by choosing the maximum event that can be produce at a seismic source. Probabilistic Seismic Hazard Analysis (PSHA) is a technique established by Cornell (1968) to estimate the mean frequencies of earthquake ground motions occurring at the site in any given time period due to all known and suspected earthquake sources. The mathematical models of these two methods are as followings:

DSHA:

$$E[S_a|x_0, M_i, R_i] = \text{GMPs}$$

Where x0 is the coordinate of the site, M_i and R_i are the magnitude and distance of seismic source.

PSHA:

$$\lambda_{S_a>x} = \sum_{i=1}^{N} (\lambda_{S_a>x})_i = \sum_{i=1}^{N} v_i \left\{ \iiint I[S_a > x|m, r, \varepsilon]\, f_{M,R,\varepsilon}(m, r, \varepsilon) dm\, dr\, d\varepsilon \right\}$$

Where

- V_i is the mean annual rate of occurrence of earthquakes generated by source i with magnitude greater than specified lower bound.
- $I[Sa>x|m,r,\varepsilon]$ is an indicator function for the Sa of a ground motion of magnitude m, distance r, and ε standard deviations away from the median with respect to level x.
- $f_{M,R,\varepsilon}(m,r,\varepsilon)$ is the joint probability density function of magnitude M, Distance R,

and εfor source i.

(Bazzurro & Allin Cornell, 1999)

Each method has its own advantages and disadvantages. In DSHA, the maximum event that can be produced by a specific seismic source and a single GMP are chosen. All variables are treated in a deterministic framework. DSHA is based on hypothesis that future seismicity of a region behaves with a pattern similar to that observed in the past (Oliveira, Roca, & Goula, 2006). This is particularly difficult to perform in Montreal, where little information is known about seismic sources, and large uncertainties are associated with the GMPEs available. In an attempt to account for these uncertainties, several options are investigated by selecting different GMPEs and earthquake scenarios based on deaggregation results.

In PSHA, the combined effects of the various seismic sources to the total seismic hazard are plotted as hazard curves. Since all seismic events of different distances and magnitudes are mixed together, it is difficult to analyze the controlling event of a hazard. Therefore, deaggregation is performed to analyze the relative contribution of each seismic event with different parameters. The most commonly used parameters are Magnitude (M) and Distance (R) of an earthquake scenario(Harmsen, Perkins, & Frankel, 1999). In deaggregation, scenarios with similar M and R are grouped together, and the total contribution of a group is calculated by computing the conditional probability of a ground motion being generated by an earthquake in the magnitude range $M_1<M<M_2$ and distance range $R_1<R<R_2$:

$$Deagg(Sa > z, M_1 < M < M_2, R_1 < R < R_2) = \frac{\sum_{i=1}^{nSource} N_i(M_{\min}) \int_{r=R1}^{R2} \int_{m=M_1}^{M_2} \int_{\varepsilon=\varepsilon_{\min}}^{\varepsilon_{\max}} f_{m_i}(m)\, f_{r_i}(r)\, f_{\varepsilon}(\varepsilon)\, P(Sa > z \mid m, r, \varepsilon)\, dr\, dm\, d\varepsilon}{\nu\ (Sa > z)}$$

(Abrahamson, 2007)

Deaggregation is used to select individual scenarios consistent to the chosen hazard level for this study. Deaggregation is determined by CRISIS-2007 V.1.2 program developed by (Ordaz, Aguilar, & Arboleda, 2007). The input parameters used are discussed as followings:

Hazard Level

The hazard level chosen is 2% in 50 year, which equals to the annual probability level of 0.0004404. This probability level is recommended by Adams and Halchuk (2004) and adopted by the current national building code NBCC2005 (Adams & Halchuk, 2004).

Ground Motion Prediction Equations

Deaggregation is performed three times using different GMPEs developed by Atkinson and Boore over the past 15 years. The three GMPEs used are: (Atkinson & Boore, 1995)(AB95), (Atkinson & Boore, 2006)(AB06), and (Atkinson, 2008)(A08). The attenuation table inputs are prepared by (Belvaux, 2009a) and (Elkady, 2010).

Seismicity Model

In the fourth-generation hazard map used in NBCC2005, four seismicity models are created: Historical model (H-model), Robust model (R-model), Floor model(F-model), and Deterministic Model(C-model). The first two models are complete probabilistic models using areal seismic sources. H-model uses smaller source zones drawn around historical seismicity clusters while R-model uses larger, regional zones reflecting seismotectonic units. F-model is created for the relatively stable central Canadian regions. C-model is the deterministic model created to reproduce the large earthquake occurred near Vancouver Island on the Cascadia subduction zone in 1700 A.D(Adams & Halchuk, 2004). In Montreal region, the dominating model with the predicted largest ground motion value is R-model. Therefore, R-model is chosen as the probabilistic seismic hazard model in this study. The input of R-model is prepared by (Belvaux, 2009b).

R-model used in CRISIS includes 8 areal sources contribute to the seismic hazard in Montreal (Figure 3-1). The sources are horizontal planes with depth of 5km or 10km (Adams & Halchuk, 2003).

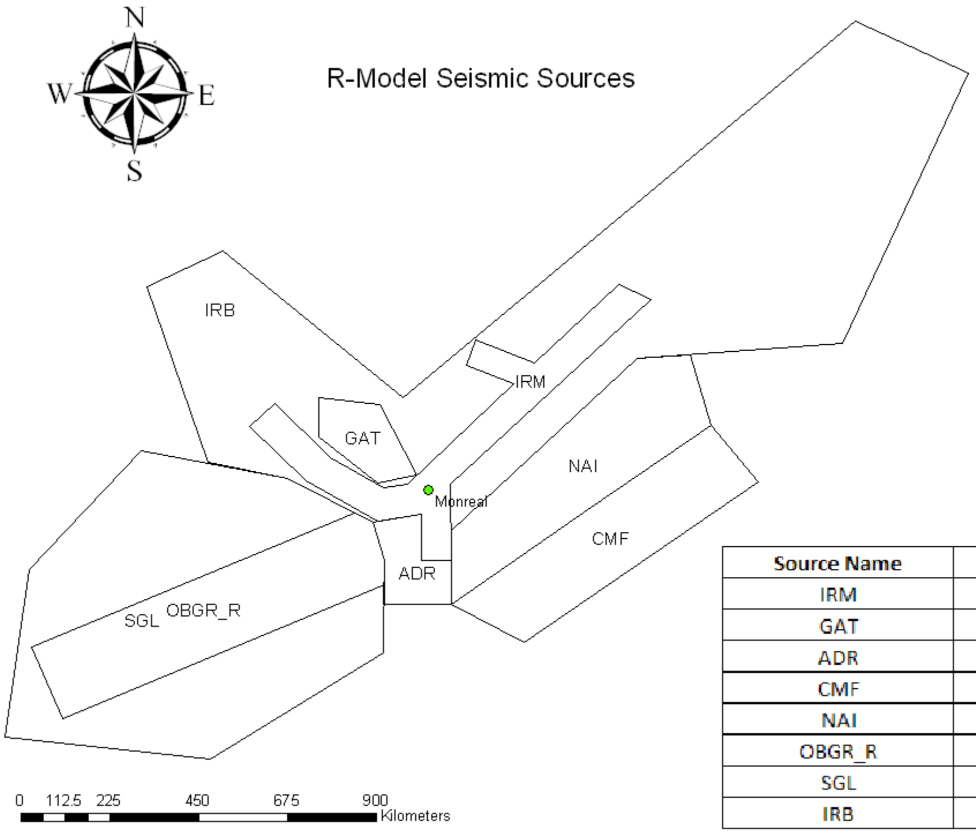

Source Name	Depth_km
IRM	10
GAT	10
ADR	10
CMF	10
NAI	5
OBGR_R	5
SGL	5
IRB	10

Figure 3-1: Location of all R-Model Seismic Sources (GIS Data Source: (Belvaux, 2009b))

Slice and Bin Sizes

The deaggregation slice size used in CRISIS is 2.5km in distance and 0.333M in Magnitude. The size of distance slice is chosen based on the recommendation of (Halchuk, Adams, & Anglin, 2007). The size of magnitude slice is the default value in CRISIS, which is a function of the lower and upper limits of input magnitude. The maximum distance integrated is 400km from a given site since the contribution of seismic source further than this distance is very limited (Halchuk, et al., 2007). CRISIS calculates the contribution of each slice and integrates the results into 20km distance and 0.333 magnitude bins. The bin size of distance and magnitude in CRISIS is defined by the inputs of maximum distance integrated and magnitude limits respectively. Therefore, the bin size used in this study is the default CRISIS value.

The mean and mode events of each deaggregation result are calculated and compared with the GSC results (Figure 3-2). As seen in Table 3-2, the CRISIS results generally agree with GSC results. The difference is mainly caused by the difference in bin size and maximum distance integrated. This is expected since the process of deaggregation is proven to be sensitive to the change in bin sizes (Bazzurro & Cornell, 1999).

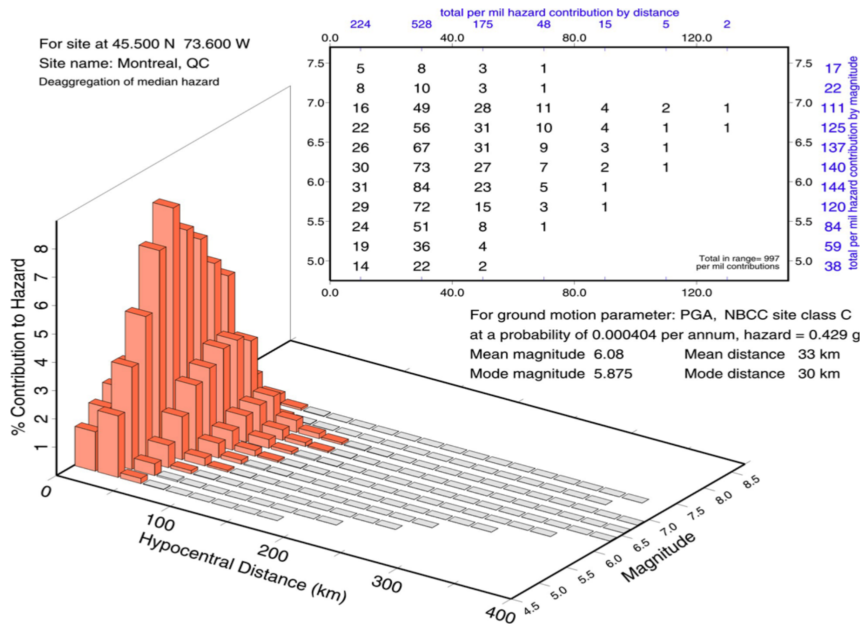

Figure 3-2: Deaggregation of Montreal PGA for a Probability of 2%/50 years Hazard from Study Conducted by Geological Survey of Canada (Halchuk, et al., 2007)

Table 3-2: Comparison of Deaggregation Results from CRISIS Model and GSC Model

Sa(x)	GSC (Mean)		GSC(Mode)		CRISIS AB95 (Mode)		CRISIS AB95 (Mean)	
	D(km)	M	D(km)	M	D_{hypo}	M	D_{hypo}	M
PGA	33	5.73	30	5.47	30	5.65	34	6.03
Sa(0.2)	39	6.28	30	6.11	30	5.99	44	6.34
Sa(0.5)	54	6.65	30	6.45	30	6.33	64	6.68
Sa(1.0)	62	6.85	30	6.81	30	6.33	58	6.75
Sa(2.0)	73	6.85	30	6.81	30	6.33	83	6.85

***GSC Model values are based on the study conducted by (Halchuk, et al., 2007) using GSCFRISK, a customized version of the FRISK88 hazard code (FRISK88 is a proprietary software product of Risk**

Engineering Inc.)

The results of deaggreagtion are usually summarized into central statistics such as means and modes. (Bazzurro & Allin Cornell, 1999) When interpreting the deaggregation results, it is important to understand the difference between the mean and mode event. The means are the weighted average of magnitude and distance, with weight given by deaggregation results. The mean magnitude ($\overline{M}$) can be calculated by multiply the magnitude within the hazard integral.

$$\overline{M} = \frac{\sum_{i=1}^{nSource} N_i(M_{\min}) \int_{r=0}^{\infty} \int_{m=M_{\min}}^{M_{\max}} \int_{\varepsilon=\varepsilon_{\min}}^{\varepsilon_{\max}} m\, f_{m_i}(m)\, f_{r_i}(r)\, f_{\varepsilon}(\varepsilon)\, P(Sa > z \mid m,r,\varepsilon)\, dr\, dm\, d\varepsilon}{\nu\ (Sa > z)}$$

The mean distance ($\bar{R}$) can be calculated using similar method

$$\overline{R} = \frac{\sum_{i=1}^{nSource} N_i(M_{\min}) \int_{r=0}^{\infty} \int_{m=M_{\min}}^{M_{\max}} \int_{\varepsilon=\varepsilon_{\min}}^{\varepsilon_{\max}} r\, f_{m_i}(m)\, f_{r_i}(r)\, f_{\varepsilon}(\varepsilon)\, P(Sa > z \mid m,r,\varepsilon)\, dr\, dm\, d\varepsilon}{\nu\ (Sa > z)}$$

(Abrahamson, 2007)

On the other hand, the mode values are defined as the magnitude-distance bin that has the highest contribution to the total hazard. The bin with mode magnitude (M*) and mode distance (R*) are defined as mode event. (Bazzurro & Cornell, 1999)

While mode event (M*, R*) is an event with a realistic seismic source, the mean event ($\overline{M}, \bar{R}$) is the central statistics of the marginal distributions of M and R that do not capture any dependence between the two variables. (Bazzurro & Cornell, 1999) Therefore, a mode event is more preferable in defining the dominant event of certain hazard. However, it should be noted that the mode event is sensitive to the changes in bin sizes. Most of the time, the mode event is not the single high contribution event to the hazard. Other events in adjacent bins also have similar contribution levels. An example is given in (Figure 3-3). Although a magnitude of 5.7 at 30 km seismic event is identified as the highest contribution event, the event of M6 in the adjacent magnitude bin has the same level of contribution of 15%. Within the same GMP, deaggregation results for different ground motion parameters also have different mode events. However, it is noticed that most contributing events are within the range of M5.3 - M7.0 and distance 30-50km. Based on these observations, not only the mode events, but all the events with high contributions to the total hazard were considered. For each GMP investigated, the significant contributing events from deaggregation results of all four ground motion parameters are listed in Appendix A.

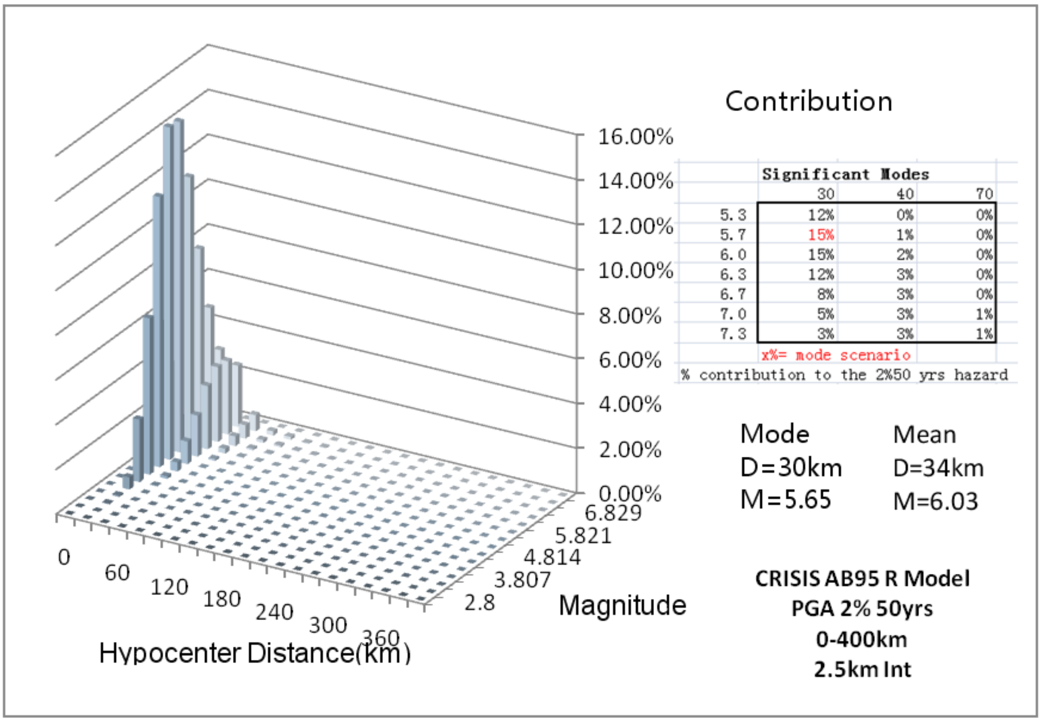

Figure 3-3: CRISIS R-Model Deaggregation Result PGA using AB95 GMPE

Comparing the percentage hazard contribution of each M-R event to all ground motion parameters, the highest percentage contribution of each M-R event is recorded as the contribution index. The M-R event with the highest contribution index is chosen within each magnitude. The M-R events chosen are highlighted in Table 3-3.

Table 3-3: Summary of Maximum Percentage Hazard Contribution for all Significant M-R Couple from Deaggregation results on PGA, Sa(0.2s), Sa(0.5s),Sa(1.0s), and Sa(2.0s).

	M/R (km)	30	50	70
AB95	5.3	12.1%	0.4%	0.0%
	5.7	14.8%*	1.0%	0.0%
	6	14.8%*	2.3%	0.5%
	6.3	12.2%*	4.8%	1.6%
	6.7	9.1%	7.4%	4.0%
	7	6.8%	7.8%	5.1%
	7.3	4.2%	6.0%	4.8%
AB06	M/R (km)	30	50	70
	5.3	9.9%	0.1%	0.0%
	5.7	12.4%	0.6%	0.0%
	6	13.2%*	1.7%	0.3%
	6.3	12.2%*	3.8%	0.9%
	6.7	9.6%	6.2%	2.5%
	7	6.9%	7.2%	3.8%
	7.3	4.3%	5.9%	4.2%
A08	M/R (km)	30	50	70
	5.3	7.2%	1.6%	0.4%
	5.7	8.7%*	2.8%	0.9%
	6	9.6%*	4.1%	1.8%
	6.3	8.9%*	5.3%	2.8%
	6.7	7.6%	6.3%	3.7%
	7	5.5%	6.1%	4.0%
	7.3	3.3%	4.7%	3.4%

Since deaggregation from CRISIS only provides the distance and magnitude of the event, the location of the event is chosen based on the recent and historical seismicity of the region. As mentioned in Chapter 2, there are two axes of seismic events in the region. One is NW towards Mont-Laurier, the other is SW towards Cornwall. Therefore, two scenarios were selected in these two directions for each distance and magnitude couple chosen from deaggregation results. The 38 scenarios chosen are summarized in Table 3-4. The depth of all events is assumed to be at 10km since they all occur within the boundary of IRM seismic source zone.

Table 3-4: Summary of Scenarios Chosen

	GMP	ID	Magnitude	Rhypo_km	Depth_km	Repic_km	X	Y
NW towards Mont-Laurier	AB95	95M53R30NW	5.3	30	10	28.3	-73.87	45.67
		95M57R30NW	5.7	30	10	28.3	-73.87	45.67
		95M60R30NW	6	30	10	28.3	-73.87	45.67
		95M63R30NW	6.3	30	10	28.3	-73.87	45.67
		95M67R30NW	6.7	30	10	28.3	-73.87	45.67
		95M70R50NW	7	50	10	49.0	-74.08	45.79
	AB06	06M53R30NW	5.3	30	10	28.3	-73.87	45.67
		06M57R30NW	5.7	30	10	28.3	-73.87	45.67
		06M60R30NW	6	30	10	28.3	-73.87	45.67
		06M63R30NW	6.3	30	10	28.3	-73.87	45.67
		06M67R30NW	6.7	30	10	28.3	-73.87	45.67
		06M70R30NW	7	30	10	28.3	-73.87	45.67
		06M70R50NW	7	50	10	49.0	-74.08	45.79
	A08	08M53R30NW	5.3	30	10	28.3	-73.87	45.67
		08M57R30NW	5.7	30	10	28.3	-73.87	45.67
		08M60R30NW	6	30	10	28.3	-73.87	45.67
		08M63R30NW	6.3	30	10	28.3	-73.87	45.67
		08M67R30NW	6.7	30	10	28.3	-73.87	45.67
		08M70R50NW	7	50	10	49.0	-74.08	45.79
SW towards Cornwall	AB95	95M53R30SW	5.3	30	10	28.3	-73.91	45.37
		95M57R30SW	5.7	30	10	28.3	-73.91	45.37
		95M60R30SW	6	30	10	28.3	-73.91	45.37
		95M63R30SW	6.3	30	10	28.3	-73.91	45.37
		95M67R30SW	6.7	30	10	28.3	-73.91	45.37
		95M70R50SW	7	50	10	49.0	-74.14	45.28
	AB06	06M53R30SW	5.3	30	10	28.3	-73.91	45.37
		06M57R30SW	5.7	30	10	28.3	-73.91	45.37
		06M60R30SW	6	30	10	28.3	-73.91	45.37
		06M63R30SW	6.3	30	10	28.3	-73.91	45.37
		06M67R30SW	6.7	30	10	28.3	-73.91	45.37
		06M70R30SW	7	30	10	28.3	-73.91	45.37
		06M70R50SW	7	50	10	49.0	-74.14	45.28
	A08	08M53R30SW	5.3	30	10	28.3	-73.91	45.37
		08M57R30SW	5.7	30	10	28.3	-73.91	45.37
		08M60R30SW	6	30	10	28.3	-73.91	45.37
		08M63R30SW	6.3	30	10	28.3	-73.91	45.37
		08M67R30SW	6.7	30	10	28.3	-73.91	45.37
		08M70R50SW	7	50	10	49.0	-74.14	45.28

3.1.2 Ground Motion Prediction Equations

Earthquakes are caused by a rupture of a fault in the earth's crust. During an earthquake, the fault is mechanically broken, and seismic waves are generated. Seismic waves propagate through crust, causing ground motions. While traveling through the crust, seismic waves experience energy dispersion influenced by the magnitude, distance, and site condition of an event. These phenomena are described by Ground Motion Prediction Equations (GMPEs). It estimates both the expected ground motion at a site from a specified magnitude-distance event and the uncertainty associated with the prediction (Elnashai, Di Sarno, & Wiley, 2008). It can be derived in two ways: empirically using strong ground motion records or theoretically using seismology models. There have been many GMPEs developed for different regions of the world. Several GMPEs have been derived for North America since the early 1970s (e.g. Esteva and Villaverde, 1973 ; McGuire, 1978 ; Joyner and Boore, 1981 , 1988 ; Boore *et al.* , 1997 ; Chapman, 1999 , among others) (Elnashai, et al., 2008). Most of them are calibrated to the Western North America (WNA) earthquakes. A few attenuation relationships can be used in the eastern North America (ENA) zones have been developed by (Atkinson, 2008; Atkinson & Boore, 1995, 2006; Campbell, 2003; Somerville, Collins, Abrahamson, & Saikia, 2001; Toro, Abrahamson, & Schneider, 1997). In eastern North America, strong earthquakes are less documented, and therefore, the GMPEs are developed mainly based on stochastic methods using synthetic data.

The GMPEs used in this study are: Atkinson and Boore (1995)-AB95; Atkinson and Boore (2006)-AB06; Atkinson (2008)-A08. AB95 is the function used in the current NBCC2005 building code. AB06 and A08 are the updates of this GMPE, and were chosen to compare the results from AB95. The choice of attenuation relationships has a strong impact on the results, which will be discussed in Chapter 5. Since HAZUS is very sensitive to the ground motion inputs, the uncertainty in attenuation relationships is one of the major contributors to overall uncertainties.

AB95

AB95 was developed based on a stochastic model, where ground motion is modeled as bandlimited Gaussian noise(Atkinson & Boore, 1995). The ground motion prediction equation is of this form:

$$logY = C_1 + C_2(M-6) + C_3(M-6)^2 - logR - C_4 * R$$

(Atkinson & Boore, 1995)

Where Y is the ground motion parameters to be predicted (PGA, PGV, Spectral

Acceleration), M is the moment magnitude, and R is the hypo-center distance (Figure 3-4).

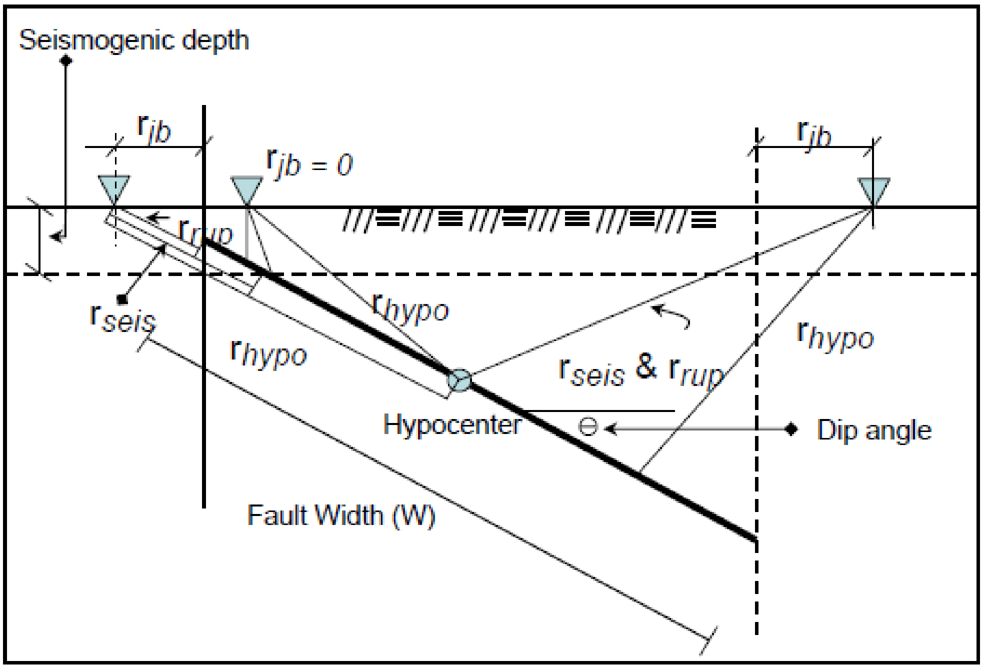

Figure 3-4: Sketch Showing Different Source to Site Distances (Hypocenter distance r_{hypo}, Joyner-Boore distance r_{jb}, and Closest distance to rupture r_{rup}) (FEMA, 2003)

AB95 is the GMPE used for the current NBCC2005 building code. It appears to be consistent to the 1988 Saguenay (M 5.8) and 1985 Nahanni (M 6.8) earthquakes (Atkinson & Boore, 1995). It predicts the strong ground motion on ENA bedrock sites. The site amplification factor for different soil types is not included in this GMPE. Therefore, the soil classification and amplification factors used in this project are based on standards set up by NEHRP (1994).

AB95 is included in HAZUS-MH4 program as one of the attenuation relationships for central and eastern America study regions. When using AB95 for a deterministic event, the only inputs required by HAZUS are the location, depth, and magnitude of the event. HAZUS calculates the ground motion parameters (PGA, PGV, Sa(0.3s), Sa(1.0s)) using the relationship provided by AB95 and applies a soil amplification factor based on the soil class of the site. The classification of soil type and its amplification factors are discussed in section 3.1.3.

AB06

Using new data collected in ENA rock and soil sites during the period from 1995 to 2005, Akinson and Boore (2006) developed new ground motion prediction equations using a stochastic finite fault model. Compared to AB95, AB06 provides lower amplitude for high frequency range (f≥5Hz), but otherwise is similar to AB95. It generally agrees well with the ENA ground motion data, but shows a tendency of overestimating moderate events at high frequency in the distance range from 30 to 100km (Atkinson & Boore, 2006). It is considered to be the most robust attenuation relationships among all three relationships investigated, and therefore is given the highest weight (Atkinson, 2008).

The form of this ground motion prediction equation is as following:

$$LogY = c_1 + c_2M + c_3M^2 + (c_4 + c_5M)f_1 + (c_6 + c_7M)f_2 + (c_8 + c_9M)f_0 + c_{10}R_{cd} + S$$

(Atkinson & Boore, 2006)

Where Y is the ground motion parameters to be predicted, M is the moment Magnitude, R is the closest distance to fault (Figure 3-4), and S is the soil amplification factor taken both linear and non linear effects into account. Two sets of coefficients are given for hard rock site (soil class A) and soft rock/stiff soil boundary (B/C boundary). For sites other than hard rock (soil class A), the S factor is added to the predicted ground motion parameters using B/C boundary coefficients. The soil amplification factor S is developed empirically using ground motion data from regions with more ground motion records (Atkinson & Boore, 2006). It is described by the following equations from Atkinson and Boore (2006):

$$S = \log\left\{exp\left[b_{lin}\ln\left(\frac{V_{30}}{V_{ref}}\right) + b_{ln}\ln\left(\frac{60}{100}\right)\right]\right\} \quad for\ pgaBC \le 60cm/sec^2$$

and

$$S = \log\left\{exp\left[b_{lin}\ln\left(\frac{V_{30}}{V_{ref}}\right) + b_{ln}\ln\left(\frac{pgaBC}{100}\right)\right]\right\} \quad for\ pgaBC > 60cm/sec^2$$

Where

b_{nl} is slope controlling the non-linear factor, defined by the following equations

$$b_{nl} = b_1 \qquad for\ V_{30} \leq V_1$$

$$b_{nl} = \frac{(b_1 - b_2)\ln\left(\frac{V_{30}}{V_2}\right)}{\ln\left(\frac{V_1}{V_2}\right)} + b_2 \qquad for\ V_1 < V_{30} \leq V_2$$

$$b_{nl} = \frac{b_2\ln\left(\frac{V_{30}}{V_{ref}}\right)}{\ln\left(\frac{V_2}{V_{ref}}\right)} \qquad for\ V_2 < V_{30} \leq V_{ref}$$

$$b_{nl} = 0.0 \qquad for\ V_{30} > V_{ref}$$

The coefficients b_1, b_2, b_{lin} used are also from Atkinson and Boore (2006), listed in Table 3-5. V_1=180m/s, V_2=300m/s, and V_{ref}=760m/s

Table 3-5: Coefficient Used in the Calculation of Soil Amplification Factor S

Period(s)	**b_{lin}**	**b_1**	**b_2**
Sa(1.0s)	-0.7	-0.44	0
Sa(0.3125s)	-0.445	-0.513	-0.13
Sa(0.25s)	-0.39	-0.518	-0.16
Sa(0.3s)*	-0.434	-0.514	-0.136
PGA	-0.361	-0.641	-0.144
PGV	-0.6	-0.495	-0.06

*** blin, b1, and b2 used for Sa(0.3 s) is interpolated from coefficients for Sa(0.3125s) and Sa(0.25s)**

Since AB06 is not available in HAZUS-MH4, the ground motion parameters are imported as user-supplied maps. For each earthquake scenario, a set of four contour maps (PGA, PGV, Sa(0.3s), and Sa(1.0s)) is produced using AB06 GMPE. A grid of 350mx500m was created and assigned a soil class based on its spatial location. The value of PGA, PGV, Sa(0.3s) and Sa(1.0s) caused by scenario earthquake at each grid point is calculated using AB06 GMPE. The value is then interpolated using ArcGIS, creating one contour map for each ground motion parameter.

A08

A08 is the latest attenuation relationship developed by Atkinson (2008) using referenced empirical approach. Using ENA ground motion database, this technique calibrates the attenuation relationship developed by Boore and Atkinson (2008) for Western North American (WNA) region to be used in ENA. Different from previous GMPEs developed using stochastic approach, it is an attempt to use empirical approach to develop a GMPE for the ENA region(Atkinson, 2008). It is included as a mean of accounting for epistemic uncertainty in this study.

This GMPE is largely based on the relationship developed by Boore and Atkinson (2008). Using the database developed for the PEER-NGA project, BA08 empirically developed an GMPE that describes ground motion parameter(Y) as a function of magnitude scaling (F_M), distance function (F_D), and site amplification (F_s) as shown in the following equation:

$$lnY = F_M(M) + F_D(R_{JB}, M) + F_s(V_{s30}, R_{JB}, M) + \varepsilon\sigma_T$$

(Boore & Atkinson, 2008)

Where M is the moment magnitude, R_{JB} is the Joyner-Boore distance (Figure 3-4).(Boore & Atkinson, 2008)

A08 adopts this relationship and calibrates the equation with ENA database, adding a correction factor F to the equation. This F factor is expressed as a quadratic function of distance R, shown in equation:

$$logF = c_0 + c_1 R_{jb} + c_2 R_{jb}^2$$

(Atkinson, 2008)

The A08 ground motion prediction is simply the product of the ground motion predicted using BA08 equation and the correction factor F.(Atkinson, 2008)

$$Y_{ENA} = FY_{BA07}$$

Using the same method as in AB06, the ground motion parameters are calculated at each grid site taken into account of the soil class, and interpolated using ArcGIS to produce a contour map as input for HAZUS. Since the soil amplification factors only apply to sites where Vs30 are less than 1300m/s, the ground motion predictions on hard rock site(class A) are calibrated from B/C boundary condition using the results from AB06 (Boore & Atkinson, 2008). These factors are obtained as functions of M and R by taking the ratio AB06(B/C)/AB06(A). (Atkinson, Personal communication, 2010).The full procedure used in the producing ground motion parameter contour map is described in Appendix B.

3.1.3 Site Amplification

Seismic wave energy disperses as it travels from the source. GMPEs are a mean to estimate the decrease of energy (i.e. the amplitude of seismic waves) as a function of the travelling distance and the type of source (i.e. fault mechanism that induced the seismic waves). Locally, site conditions can affect significantly the amplitude of the ground motions. Due to energy conservation laws, the amplitude of the ground motion is negatively related to the shear wave velocity (V_s) of the soil layer. The shear wave velocity of soil depends on soil density and other characteristics, and is smaller in softer layers close to the surface. As seismic wave travels through different soil layers, the amplitude of the ground motion increases as the shear wave velocity decreases towards surface. The amplification is maximized when the frequency of the wave matches the fundamental frequency of soil (f_0). An example of this is the 1985 Mexico City earthquake. Mexico City sits on an old lakebed, which has very soft soil deposits up to 40m in thickness. The geological setting makes it highly vulnerable to site amplification effects. Although the epicenter of this earthquake was 410km away from Mexico City, the event caused the collapse and server damage of roughly 500 building and the death of over 8000 people (Gates & Ritchie, 2007). This example showcased the importance of local soil amplification as an essential factor in assessing seismic risk of a region.

3.1.3.1 Soil Map

In urbanized areas like Montreal, it is important to identify the zones where one could expect soil amplification and quantify the effect with a good resolution. This is what is called microzonation. During the past few years, the microzonation project at McGill has extensively investigated soil conditions in the Montreal vicinity using various non-intrusive approaches like H/V ambient noise analysis, 1-D modeling using borehole data and more recently seismic reflection and refraction methods. The location of all measured sites is presented in Figure 3-5. A microzonation map combining ambient noise analysis and 1-D modeling is proposed by Rosset and Chouinard (2008).

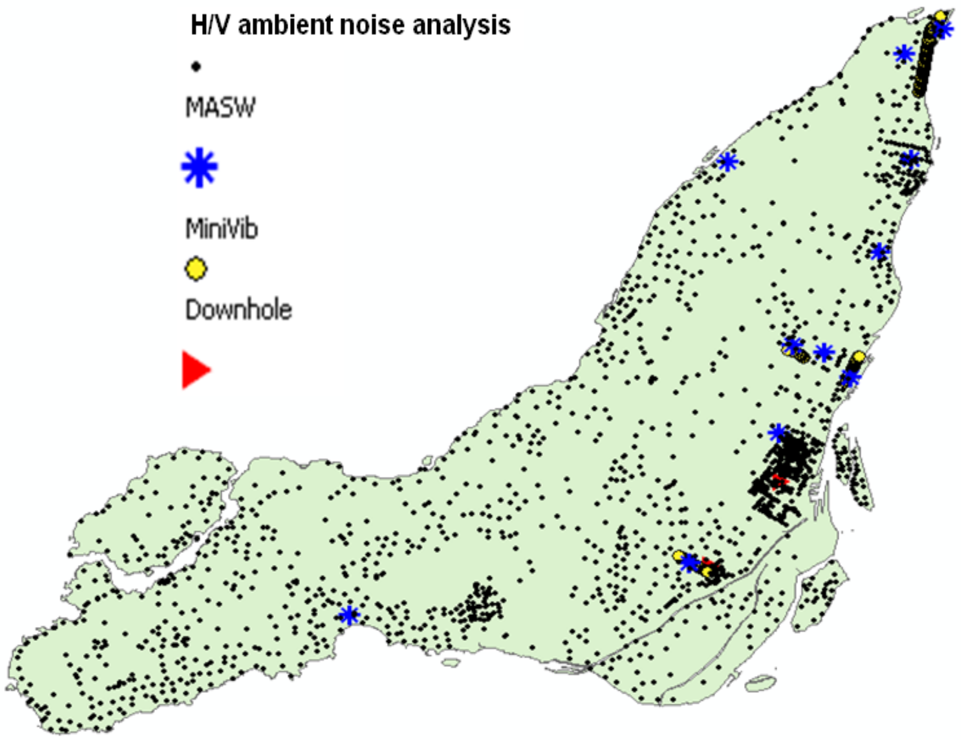

Figure 3-5: Location of All Soil Characteristic Measurement Sites

Among all methods used, ambient noise analysis is a useful and fast method to retrieve the fundamental mode of resonance of the soil. Fundamental resonance frequency of a site is strongly correlated to the type and thickness of the soft soil deposits. A general relationship between the fundamental frequency and the shear wave velocity of the soil layer is given by the following formula:

$$\frac{1}{f_0} = \frac{4H}{V_s}$$

(Elnashai, et al., 2008)

Where H is the thickness of the soft soil layer, and V_s is its shear-wave velocity.

By applying this equation, the shear-wave velocity of a soil layer can be estimated by converting the fundamental frequency (f_0) to V_s. Although the above formula is an approximation for multi-layer soil deposits, it is used to estimate the average shear wave velocity of soft soil layer in the absence of detailed soil layer information. The thickness of the soil layer H is interpolated from the borehole data provided by the city of Montreal. (City of Montreal, Personal communication, 2009) as shown in Figure 3-6. The thickness of soft soil of sites where f_0 is available is extracted from this map.

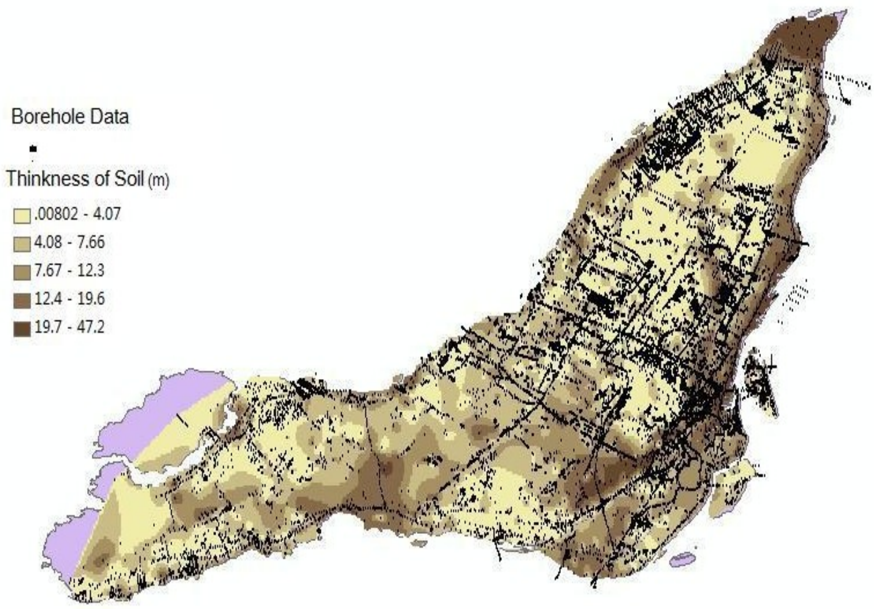

Figure 3-6: Interpolated Thickness of Soft Soil in Montreal (GIS data source: City of Montreal)

With the Vs for soft soil, one can estimate the average Vs for the 30 meters of soil (Vs30). In Montreal, the maximum thickness of soft soil is around 25m, and commonly is lower than 10m. Based on the studied conducted by (Boyer, 1985), two main bedrock categories presented on the island of Montreal are shown in Figure 2-5 in chapter 2. The shear wave velocity of limestone and shale are 2100m/s and 2300m/s respectively as determined by (Prest & Hode-Keyser, 1982). The V_s obtained for soft soil layer and the V_s of the rock of the site are then combined to obtain the V_{s30} using the following formula:

$$V_{s30} = \frac{30}{h_{soft}/V_{s-soft} + (30 - h_{soft})/V_{s-rock}}$$

A lower value for the Vs of bedrock is considered in the eastern part of Montreal where a thick layer (5-25m) of clay underlies a till layer. In this zone the fundamental frequency seems to be influenced by the contrast of Vs between these two layers instead of the bedrock. For this reason, the shear wave velocity of rock is modified to be 1000m/s to represents the actual layers measured in these regions (Figure 3-7).

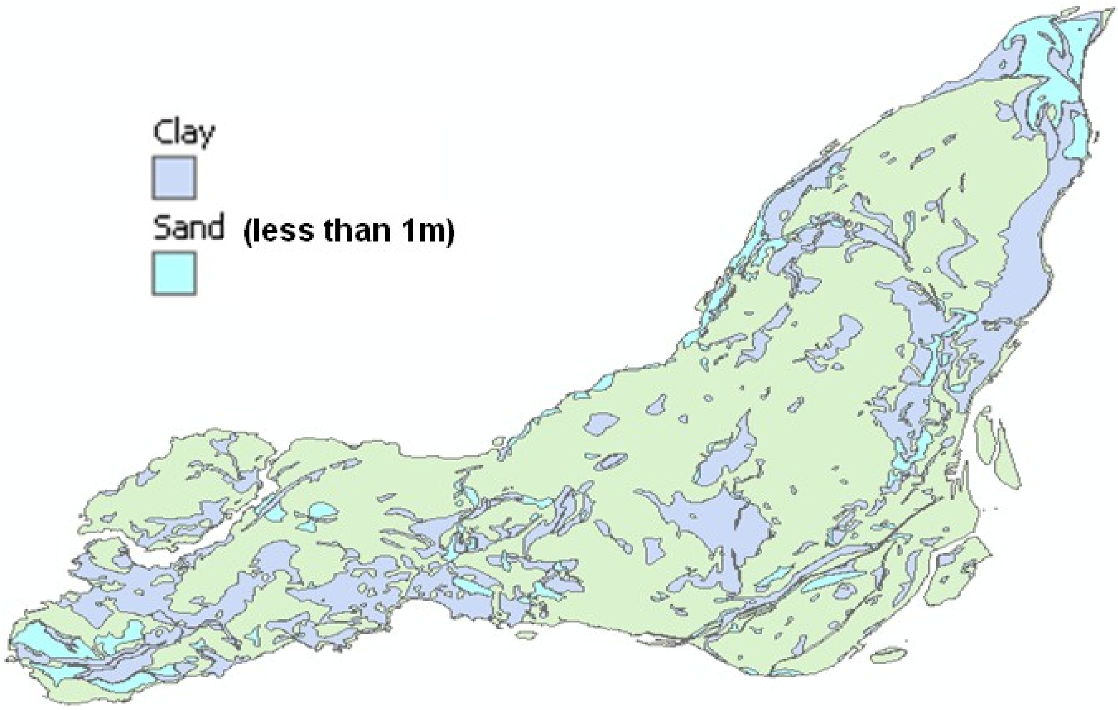

Figure 3-7: Clay Layer Location on the Island of Montreal

In addition to the estimated Vs30 from ambient noise analysis results, several V_s30 measurements are also available, including 11 lines of 1-D Multichannel Analysis of Surface Wave (MASW) measurement, 4 high-resolution seismic imaging investigations (MiniVib) profiles, and 2 downhole measurements.

During the summer of 2009, a total of 20 sites on the island of Montreal were investigated using 1-D MASW method. MASW is a geophysical method, which generates a shear-wave velocity (Vs) profile by analyzing Raleigh-type surface waves on a multichannel record. The source to receiver distance, receiver spacing, and source type has been adjusted so that the required depth information can be obtained. Among all the 20 sites, 11 of them have been processed to get shear-wave velocity profile along the depth (Park, 2010). The V_{s30} of each site was derived from the profile using the following formula.

$$V_{s30} = \frac{30}{h_1/V_1 + h_2/V_2 + h_3/V_3 + \cdots + h_{i-1}/V_{i-1} + (30 - \sum_1^{i-1} h_i)/V_i}$$

Where

h_i=thickness of soil layer i

V_i=shear wave velocity of soil layer i

A summary of V_{s30} results can be seen in Table 3-6:

Table 3-6: Summary of Vs30 (m/s) Results from MASW measurements

Site	X_Longitude	Y_Latitude	Vs30(Low)	Vs30(High)	Vs30(Avg)	Vs30(Std.Dev.)	Vs30(Passive)
MM05	-73.60	45.64	384.04	489.39	**445.35**	32.08	485.97
MM07	-73.79	45.45	237.68	335.85	**291.78**	36.49	285.04
MM12	-73.57	45.53	153.35	193.76	**180.09**	14.12	
MM13	-73.50	45.64	294.07	324.23	**303.27**	10.80	342.96
MM14	-73.51	45.60	240.23	293.50	**274.10**	16.86	286.76
MM15	-73.53	45.55	388.13	471.55	**444.22**	31.35	399.55
MM16	-73.54	45.56	435.37	515.94	**489.05**	25.14	
MM18	-73.56	45.56	435.32	532.10	**480.07**	30.38	
MM19	-73.50	45.68	204.51	225.85	**211.53**	8.35	207.36
MM20	-73.48	45.69	188.45	226.73	**205.08**	14.89	206.42
MP11	-73.62	45.47					517.98

The results of 4 Mini-vib surveys and 2 downhole surveys were are also available. Mini-vib is a 2-D geophysical survey, where a device gently shakes the ground both vertically and horizontally, sending and receiving P-wave and S-wave reflected from various geologic structures beneath. The survey investigated 4 profiles in 3 areas, where the soil thickness is the highest on the island of Montreal. In each profile, the V_{s30} of each survey point is interpolated or extrapolated from the profile. Two downhole surveys with detailed soil layer information and Vs30 results are available for Decaire and Jeanne-Mance sites. The results can be seen in Appendix C.

All the calculated Vs30 data is georefereced and plotted using ArcGIS. A V_{s30} map is interpolated using natural neighborhood method (Figure 3-8).

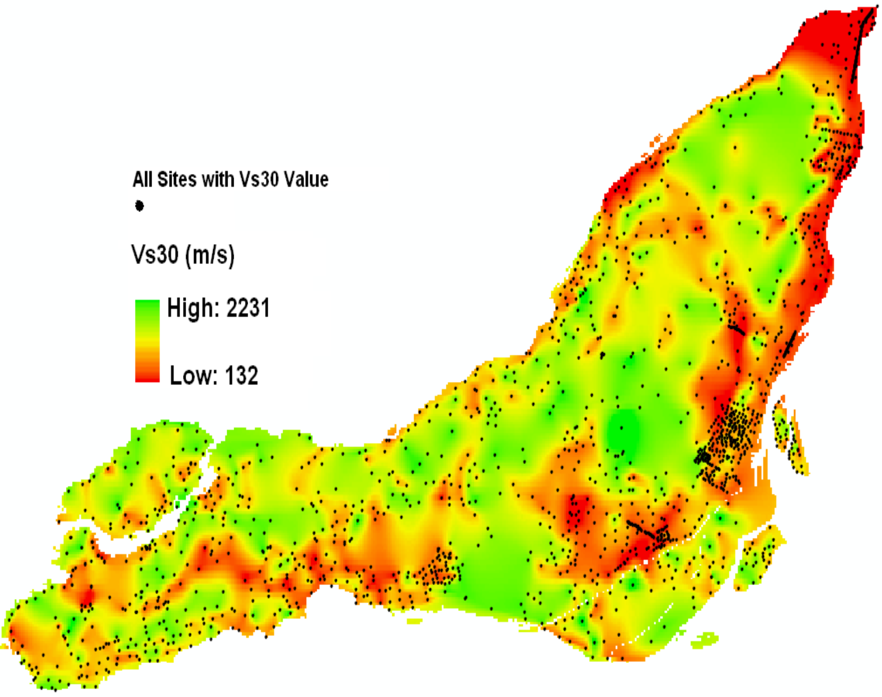

Figure 3-8: Interpolated V_{s30} (m/s) Map of Montreal

Since all soil characteristic surveys were planned to cover the region where soil thickness is significant, very few data points were available for rock sites, where Vs30 is in the range of 2100 to 2300m/s (Figure 3-9). The interpolated V_{s30} map is then combined with known rock sites from surfacial geological map to produce a more accurate soil map using NEHRP classification system (Figure 3-10). This soil classification map is used as an input in HAZUS as well as in ground motion prediction equations, namely AB06 and A08 attenuation relationships, to calculate soil amplification factors.

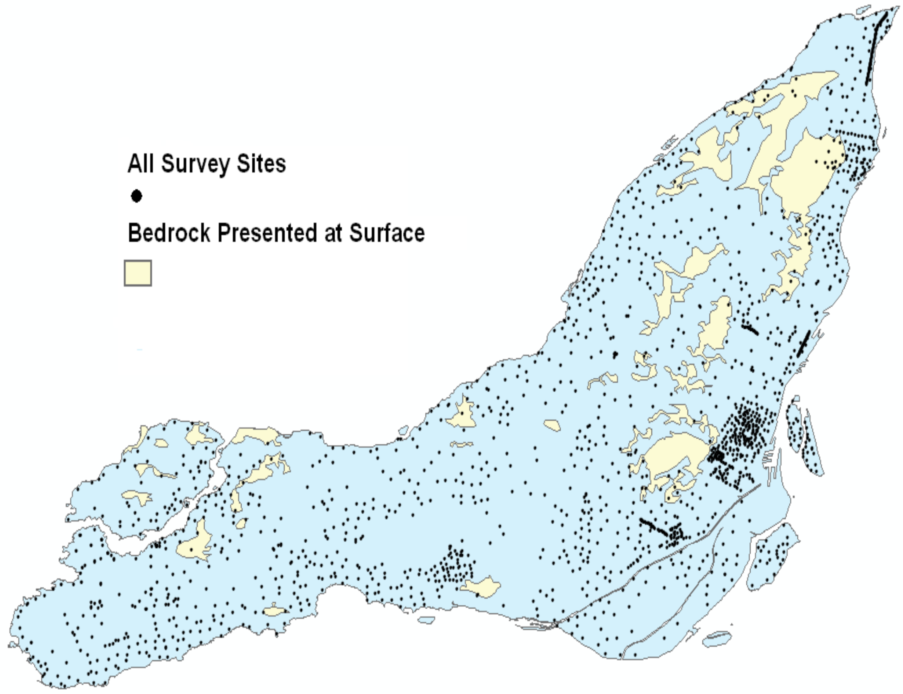

Figure 3-9: Surface Bedrock Location Vs. all Survey Sites

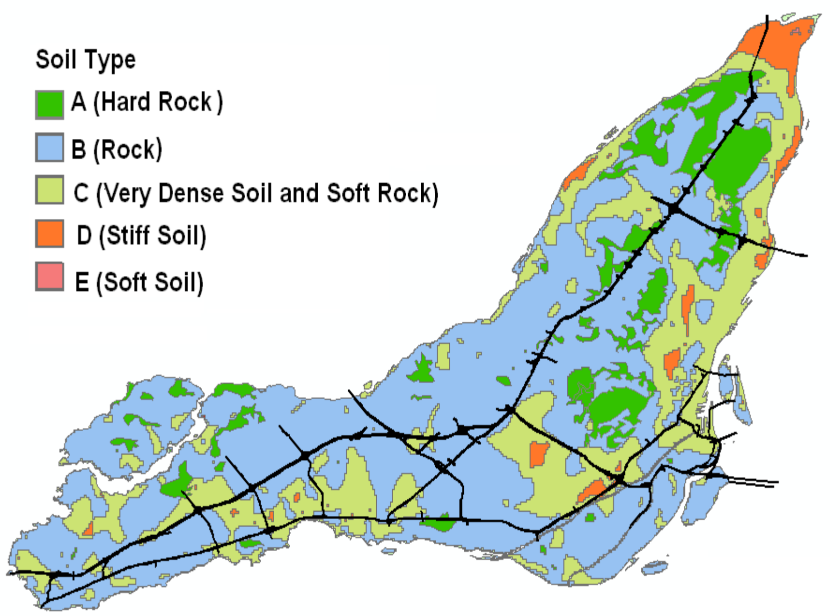

Figure 3-10: Soil Classification Map for Montreal Based on NEHRP Soil Classification

(Soil Type depends on its Vs30, Type A: Vs30 > 1500m/s, Type B: 760m/s <Vs30≤ 1500m/s, Type C: 360m/s <Vs30≤760m/s, Type D: 180m/s <Vs30≤360m/s, Type E: Vs30≤180m/s)

3.1.3.2 Soil Amplification Factor

Using the soil map developed for Montreal, soil amplification factors can be calculated. The current Canadian Building Code (NBCC2005) seismic provision adopts the NEHRP (1994) provisions for soil classification and amplification factors, where average shear-wave velocity in the first 30 m of subsoil (V_{s30}) is a key parameter for site amplification effects. As shown in Table 3-7(FEMA, 1997), a soil class is assigned to a site depending on its V_{s30} value. A corresponding site amplification factor is then applied to the predicted ground motions from different attenuation functions. Among all three attenuation relationships used, only AB95 is available in HAZUS, where the amplification factor are the same as the NEHRP soil amplification factors (Table 3-8). The ground motion parameters are amplified based on both the soil class and the scale of peak ground acceleration (PGA) of the site. Spectral acceleration at a period of 0.3s (Sa(0.3s))and PGA are amplified by the short period factor F_A. Spectral acceleration at a period of 1.0s (Sa(1.0s)) and peak ground velocity (PGV) are amplified by the long period factor F_V (FEMA, 2003). One should be aware that the HAUZS and NEHRP amplification factors are developed using Soil class B (760m/s$<V_{s30}<$1500m/s) as reference site. In the NBCC 2005 seismic provision, although the definition of soil class remain the same, the reference site is a soil class C (360m/s$<V_{s30}<$760m/s) site. This difference of references imposed the need to adjust the amplification factors applied to the ground motions.

For the ground motion parameters developed using AB06 and A08 attenuation relationships, the amplification factors used are the ones recommended in the attenuation function described in the previous section. A sample input ground motion map of Scenario AB06_M6.3D30NW is presented in Figure 3-11.

Table 3-7: NEHRP Soil Classification (FEMA, 2003)

Site Class	Site Class Description	Shear Wave Velocity (m/sec)	
		Minimum	Maximum
A	**HARD ROCK** Eastern United States sites only	1500	
B	**ROCK**	760	1500
C	**VERY DENSE SOIL AND SOFT ROCK** Untrained shear strength $u_s \geq 2000$ psf ($u_s \geq 100$ kPa) or $N \geq 50$ blows/ft	360	760
D	**STIFF SOILS** Stiff soil with undrained shear strength 1000 psf $\leq u_s \leq 2000$ psf (50 kPa $\leq u_s \leq 100$ kPa) or $15 \leq N \leq 50$ blows/ft	180	360
E	**SOFT SOILS** Profile with more than 10 ft (3 m) of soft clay defined as soil with plasticity index PI > 20, moisture content *w* > 40% and undrained shear strength $u_s < 1000$ psf (50 kPa) ($N < 15$ blows/ft)		180
F	**SOILS REQUIRING SITE SPECIFIC EVALUATIONS** **1. Soils vulnerable to potential failure or collapse under seismic loading:** e.g. liquefiable soils, quick and highly sensitive clays, collapsible weakly cemented soils. **2. Peats and/or highly organic clays** (10 ft (3 m) or thicker layer) **3. Very high plasticity clays:** (25 ft (8 m) or thicker layer with plasticity index >75) **4. Very thick soft/medium stiff clays:** (120 ft (36 m) or thicker layer)		

Table 3-8: NEHRP Soil Amplification Factor used in HAZUS (FEMA, 2003)

Site Class B Spectral Acceleration	Site Class				
	A	B	C	D	E
Short-Period, S_{AS} (g)	**Short-Period Amplification Factor, F_A**				
≤ 0.25	0.8	1.0	1.2	1.6	2.5
0.50	0.8	1.0	1.2	1.4	1.7
0.75	0.8	1.0	1.1	1.2	1.2
1.0	0.8	1.0	1.0	1.1	0.9
≥ 1.25	0.8	1.0	1.0	1.0	0.8*
1-Second Period, S_{A1} (g)	**1.0-Second Period Amplification Factor, F_V**				
≤ 0.1	0.8	1.0	1.7	2.4	3.5
0.2	0.8	1.0	1.6	2.0	3.2
0.3	0.8	1.0	1.5	1.8	2.8
0.4	0.8	1.0	1.4	1.6	2.4
≥ 0.5	0.8	1.0	1.3	1.5	2.0*

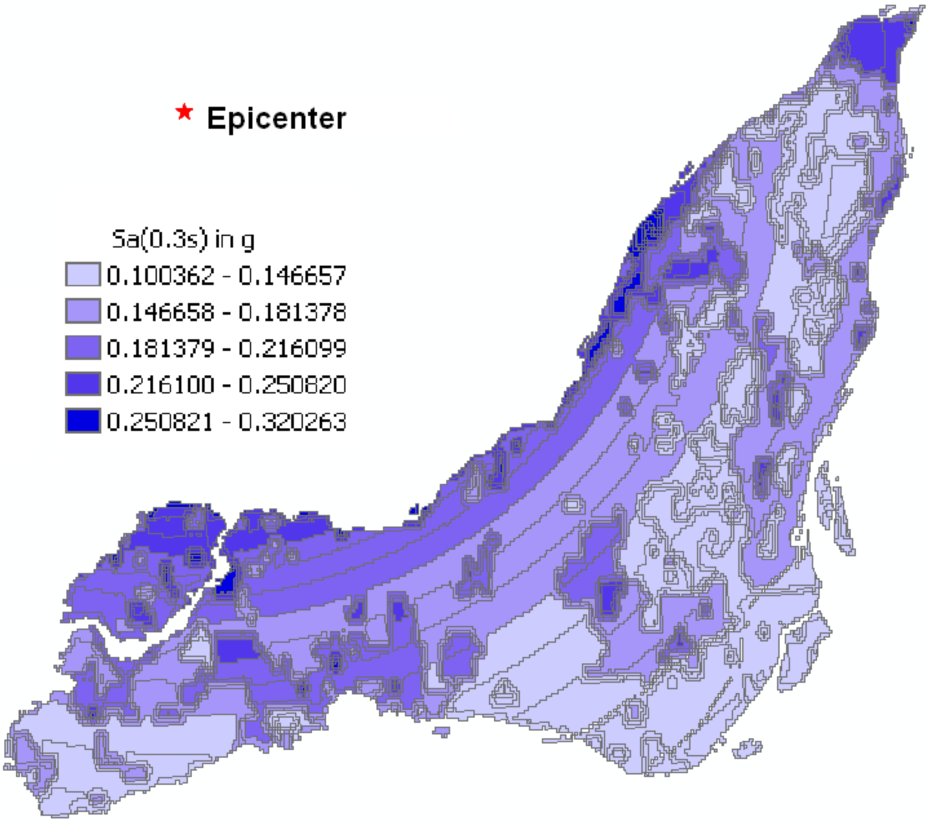

Figure 3-11: Sample User Defined Ground Motion Map: Spectral Acceleration at 0.3s Contour Map for AB06_M6.3D30NW Scenario

3.2 Potential Earth Science Hazards (PESH)

3.2.1 Liquefaction

Previous study done by Joseph (2005) has shown that Montreal is subjected to moderate liquefaction risk under an earthquake event of magnitude 5 to 7 (Joseph, 2005). Therefore, the liquefaction probability and its induced ground failure is investigated based on the method recommended by HAZUS-MH4 technical manual (FEMA, 2003). The method developed by Youd and Perkins (1978) provides a simplified and conservative method in evaluating liquefaction probability. The method evaluates the liquefaction probability based on liquefaction susceptibility map and ground shaking parameters. The first step in this method is to develop a susceptibility map based on geologic information of the study region. A susceptibility index ranging from 0 to 5 was assigned according to the classification system presented in Table 3-9 (Youd & Perkins, 1978).

Table 3-9: Liquefaction Susceptibility Classification based on Surfacial Geological Deposits (Youd & Perkins, 1978)

Type of Deposit	General Distribution of Cohesionless Sediments in Deposits	Likelihood that Cohesionless Sediments when Saturated would be Susceptible to Liquefaction (by Age of Deposit)			
		< 500 yr Modern	Holocene < 11 ka	Pleistocene 11 ka - 2 Ma	Pre-Pleistocene > 2 Ma
(a) Continental Deposits					
River channel	Locally variable	Very High	High	Low	Very Low
Flood plain	Locally variable	High	Moderate	Low	Very Low
Alluvial fan and plain	Widespread	Moderate	Low	Low	Very Low
Marine terraces and plains	Widespread	---	Low	Very Low	Very Low
Delta and fan-delta	Widespread	High	Moderate	Low	Very Low
Lacustrine and playa	Variable	High	Moderate	Low	Very Low
Colluvium	Variable	High	Moderate	Low	Very Low
Talus	Widespread	Low	Low	Very Low	Very Low
Dunes	Widespread	High	Moderate	Low	Very Low
Loess	Variable	High	High	High	Unknown
Glacial till	Variable	Low	Low	Very Low	Very Low
Tuff	Rare	Low	Low	Very Low	Very Low
Tephra	Widespread	High	High	?	?
Residual soils	Rare	Low	Low	Very Low	Very Low
Sebka	Locally variable	High	Moderate	Low	Very Low
(b) Coastal Zone					
Delta	Widespread	Very High	High	Low	Very Low
Esturine	Locally variable	High	Moderate	Low	Very Low
Beach					
High Wave Energy	Widespread	Moderate	Low	Very Low	Very Low
Low Wave Energy	Widespread	High	Moderate	Low	Very Low
Lagoonal	Locally variable	High	Moderate	Low	Very Low
Fore shore	Locally variable	High	Moderate	Low	Very Low
(c) Artificial					
Uncompacted Fill	Variable	Very High	---	---	---
Compacted Fill	Variable	Low	---	---	---

As mentioned in the geologic setting of Montreal (Section 2.2), most of the Montreal region is covered by glacial till aged over 10000 years, which has liquefaction susceptibility index of 1 or "very low" in Table 3-9. The two groups of clay and sand fall into flood plain and marine plain categories which ages are less than 10000 years and 12000 years respectively. Therefore, they are assigned the indexes of 3 and 2 respectively, representing moderate and low liquefaction susceptibilities. There are a few old river channel, lakebed, and uncompacted fills presented in Montreal. The liquefaction susceptibility levels assigned to these areas are 5 or "very high". The area with surface bedrock is given a susceptibility of 0 since liquefaction is not possible with rock sites.

The input liquefaction susceptibility map for HAZUS is shown in Figure 3-12.

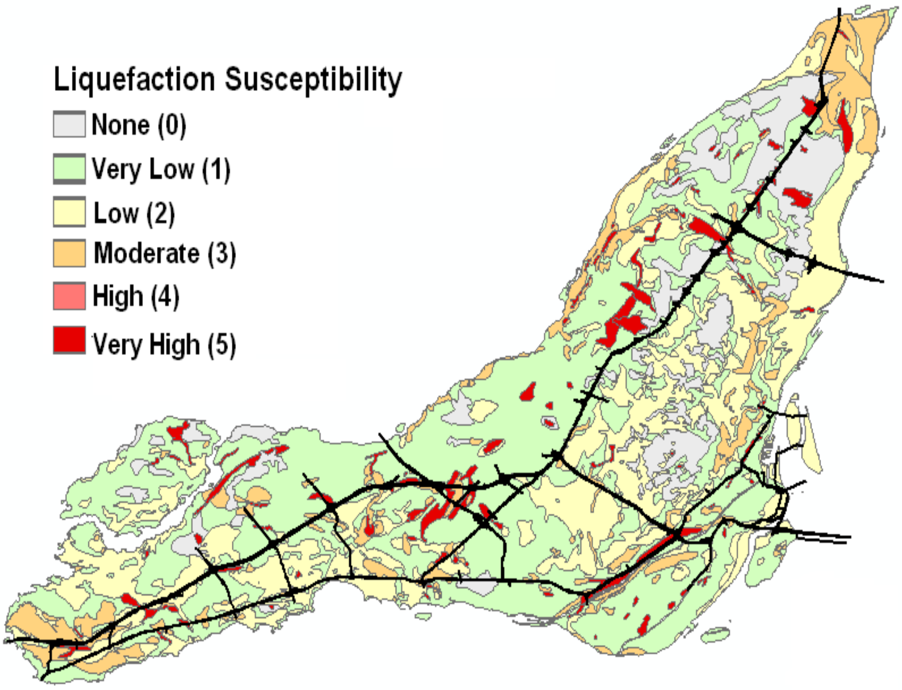

Figure 3-12: Liquefaction Susceptibility Map for Montreal

The liquefaction probability is determined by susceptibility, ground water depth, and ground shaking amplitude. The probability is calculated using the following equation (FEMA, 2003):

$$P[liquefaction_{sc}] = \frac{P[liquefaction_{sc}|PGA = a]}{K_M . K_W} . P_{ml}$$

Where

$$K_M = 0.0027M^3 - 0.0267M^2 - 0.2055M + 2.9188$$

$$M = moment\ magnitude$$

$$K_W = 0.022d_w + 0.93$$

d_w = ground water depth

Where P [liquefaction$_{sc}$|PGA=a] is the conditional probability of liquefaction obtained from the model proposed by Liao et al. (1988)(Figure 3-13); K_M and K_W are the correction factors for Magnitude and ground water depth respectively (Seed & Idriss, 1982). Due to the conservative nature of the method, a correction factor P_{ml} is added to bring the liquefaction probability estimate closer to reality. It is the percentage of map unit subject to liquefaction, determined from various regional liquefaction studies (Power, et al, 1982). The value of P_{ml} is listed in Table 3-10.

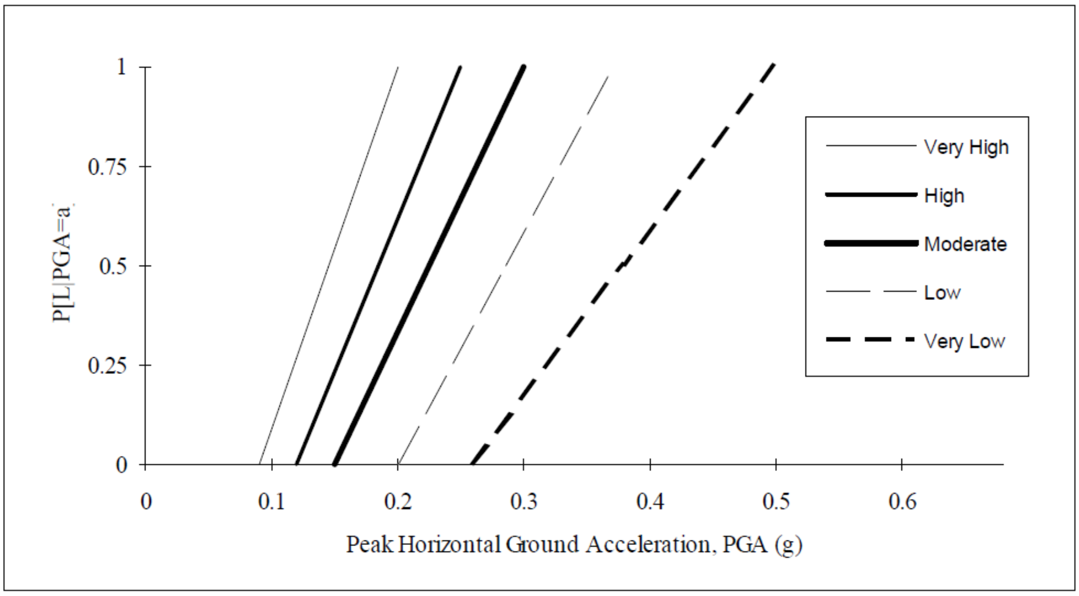

Figure 3-13: Conditional Liquefaction Probability Relationships for Liquefaction Susceptibility (Liao, Veneziano, & Whitman, 1988)

Table 3-10: Proportion of Map Unit Subject to Liquefaction (Power, et al., 1982)

Mapped Relative Susceptibility	Proportion of Map Unit
Very High	0.25
High	0.20
Moderate	0.10
Low	0.05
Very Low	0.02
None	0.00

Based on the same concept, the expected permanent ground displacement (PGD) was estimated based on the amplitude of ground shaking and liquefaction susceptibility. Presented by Youd and Perkin (1987), the expected PGD is a function of PGA and threshold PGA triggering liquefaction for different susceptibility group (PGA(t)). A modification factor K_{Δ} (Seed & Idriss, 1982)for magnitude less than M7.5 is added for smaller events. The calculated PGD is an important parameter in determining the damaged caused by ground failure, which will be discussed in Chapter 5.

$$K_{\Delta} = 0.0086M^3 - 0.0914M^2 + 0.4698M - 0.9835$$

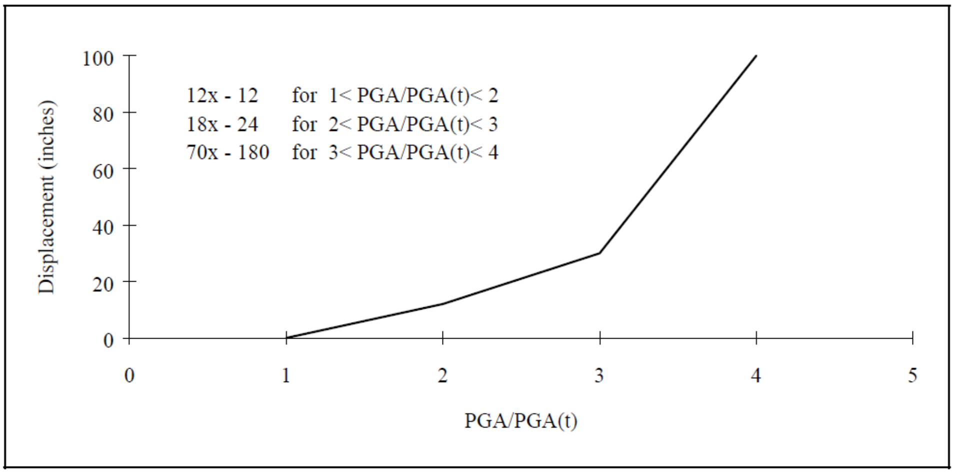

Figure 3-14: Permanent Ground Displacement Relationship with PGA and PGA(t)(Sadigh, Egan, & Youngs, 1986.; Youd & Perkins, 1978)

3.2.2 Landslide

Landslide susceptibility is investigated using the method recommended by HAZUS-MH4 Technical Manual(FEMA, 2003). Similar to liquefaction, the effect of landslide was evaluated using a landslide susceptibility map along with ground shaking parameters and ground water table. The landslide susceptibility map was developed using surfacial geological map, topographic map and ground water table. A susceptibility index of 0 to 10 (Table 3-11) is assigned to the map area according to the classification system developed by Wilson and Keefer (1985). In which the critical acceleration to cause landslide is a function of the slope angle, soil type and ground water table.

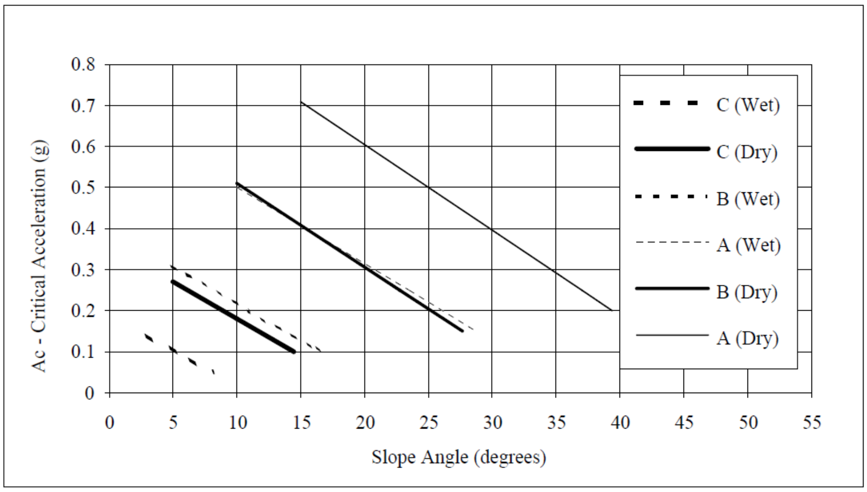

Figure 3-15: Critical Acceleration for Landslide as a Function of Slope Angle and Soil Group(Wilson & Keefer, 1985)

Table 3-11: Landslide Susceptibility Classification (FEMA, 2003)

Geologic Group		Slope Angle, degrees					
		0-10	10-15	15-20	20-30	30-40	>40
(a) DRY (groundwater below level of sliding)							
A	Strongly Cemented Rocks (crystalline rocks and well-cemented sandstone, c' =300 psf, ϕ' = 35°)	None	None	I	II	IV	VI
B	Weakly Cemented Rocks and Soils (sandy soils and poorly cemented sandstone, c' =0, ϕ' = 35°)	None	III	IV	V	VI	VII
C	Argillaceous Rocks (shales, clayey soil, existing landslides, poorly compacted fills, c' =0 ϕ' = 20°)	V	VI	VII	IX	IX	IX
(b) WET (groundwater level at ground surface)							
A	Strongly Cemented Rocks (crystalline rocks and well-cemented sandstone, c' =300 psf, ϕ' = 35°)	None	III	VI	VII	VIII	VIII
B	Weakly Cemented Rocks and Soils (sandy soils and poorly cemented sandstone, c' =0, ϕ' = 35°)	V	VIII	IX	IX	IX	X
C	Argillaceous Rocks (shales, clayey soil, existing landslides, poorly compacted fills, c' =0 ϕ' = 20°)	VII	IX	X	X	X	X

A slope angle map is interpolated using the digital topographic model of Montreal (Quebec Ressources Naturelleset Faune, 1999). The ground water depth map is provided by the City of Montreal (City of Montreal, Personal Communication, 2009) (Figure 3-16). Geologic group is based on the surfacial geological map (Prest & Hode-Keyser, 1982). The input for HAZUS is the landslide susceptibility map shown in Figure 3-18. Most of the Montreal is not subject to high landslide susceptibility thanks to low slope angle and glacial till deposits. However, a small region with steep slope angle and clay deposit in south west Montreal is assigned a high susceptibility, indicating possible landslide hazards. It should be noted that high landslide susceptibility does not equal to landslide hazard. Since the method used by Wilson and Keefer (1985) is conservative, a factor is used in HAZUS to bring the result closer to reality. Based on the work of Wieczorek et al. (1985), the factor is given as the percentage of map area subject to landslide in certain susceptibility class (Table 3-12). Within the same susceptibility category, the probability of landsliding is the same. It is either 1 or 0 depending on whether the induced ground acceleration (a_{is}) is greater or smaller than the critical acceleration (a_c) presented in Table 3-13.

Table 3-12: Percentage of Map Area subject to Landslide in Certain Susceptibility Class (FEMA, 2003; Wieczorek, Wilson, & Harp, 1985)

Susceptibility Category	None	I	II	III	IV	V	VI	VII	VIII	IX	X
Map Area	0.00	0.01	0.02	0.03	0.05	0.08	0.10	0.15	0.20	0.25	0.30

Table 3-13: Critical Acceleration (a_c) for Susceptibility Categories(FEMA, 2003)

Susceptibility Category	None	I	II	III	IV	V	VI	VII	VIII	IX	X
Critical Accelerations (g)	None	0.60	0.50	0.40	0.35	0.30	0.25	0.20	0.15	0.10	0.05

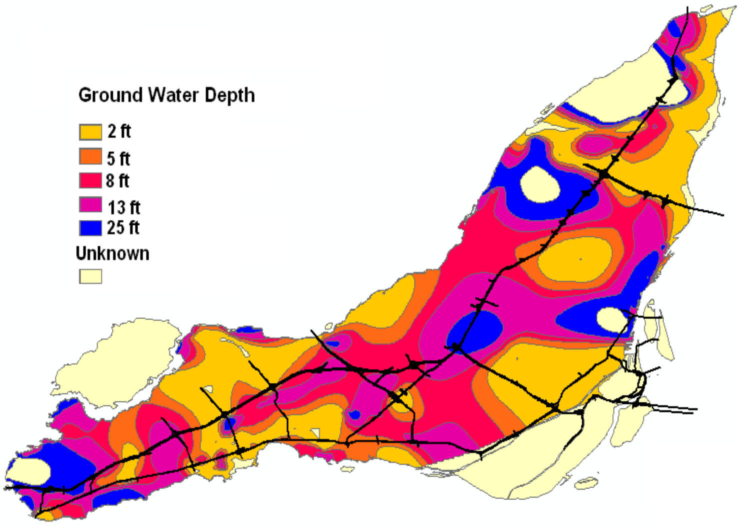

Figure 3-16: Typical Ground Water Depth on the Island of Montreal (GIS Data Source: City of Montreal)

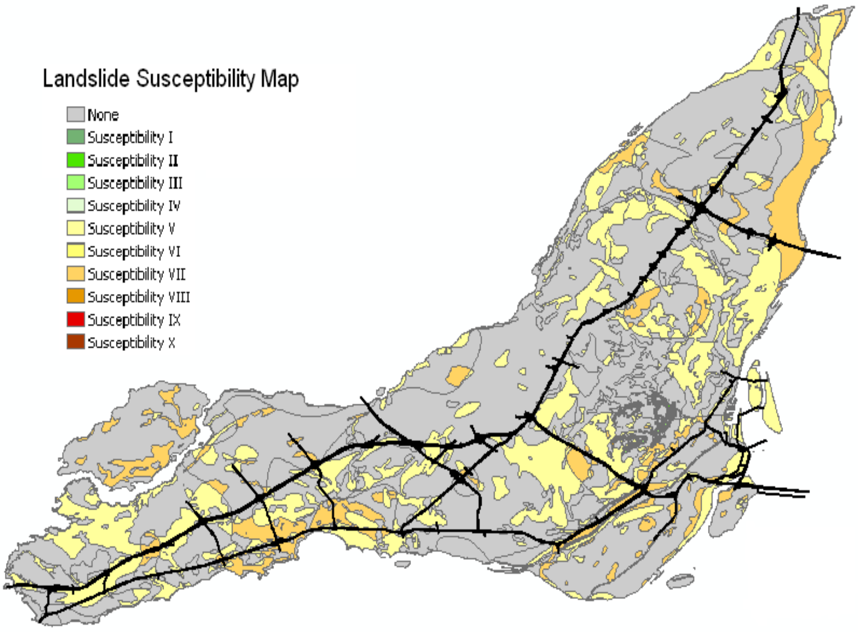

Figure 3-17: Landslide Susceptibility Map for Montreal

The Permanent Ground Displacement (PGD*) induced by landslide is calculated as a function of ground shaking amplitude, critical acceleration and number of circles. Shown in the following equation, the expected PGD* is the product of expected displacement factor (Figure X), induced acceleration (a_{is}) and number of cycle (n). Same as the PGD calculated from liquefaction, it is an important parameter in determining the damage caused by ground failure.

$$E[PGD *] = E\left[{}^{d}/_{a_{is}}\right] . a_{is} . n$$

where

$$n = 0.3419M^3 - 5.5214M^2 + 33.6154M - 70.7692 \text{(Seed \& Idriss, 1982)}$$

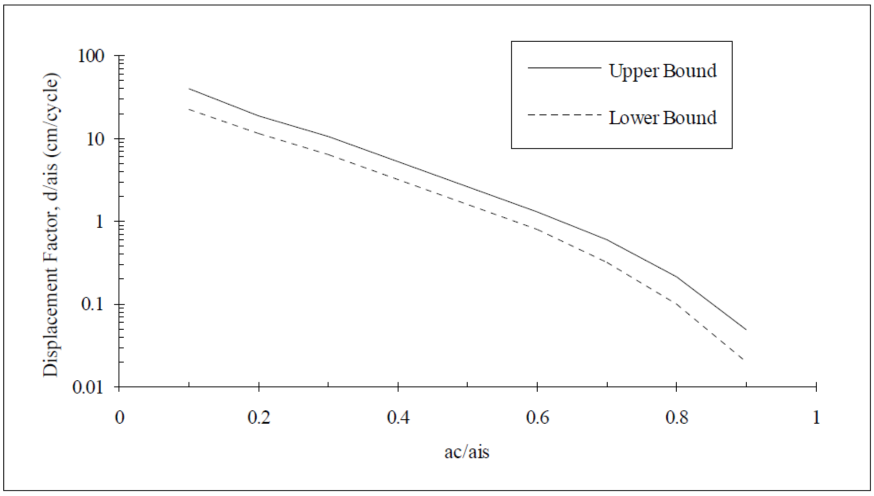

Figure 3-18: Relationship between Displacement Factor and Ratio of Critical Acceleration and Induced Acceleration (Makdisi & Seed, 1978)

3.3 Building Inventory

In HAZUS, the information regarding structures is divided into several categories: general building stock (GBS), essential facilities (EF), high potential loss facilities, utility systems and lifelines. For the scope of this project, only the general building stock and the essential facilities are investigated.

3.3.1 General Building Stock (GBS)

General Building Stock (GBS) includes information on the residential (RES), commercial (COM), educational (EDU), government (GOV), religion (REG) and agriculture buildings (ARG). The information of all the buildings within each census tract is concentrated at the centroid of the census tract. The general building stock is made up of four key databases described in Table 3-14.

Table 3-14: Key Databases Required in Developing General Building Stock in HAZUS

(FEMA, 2003)

Database	Description
Square footage by occupancy	These data are the estimated floor area by specific occupancy (e.g., COM1).
Full Replacement Value by occupancy	These data provide the user with estimated replacement values by specific occupancy (e.g., RES1).
Building Count by occupancy	These data provide the user with an estimated building count by specific occupancy (e.g., IND1).
General Occupancy Mapping	These data provide a general mapping for the GBS inventory data from the specific occupancy to general building type

Furthermore, the fields needed to construct the above database are listed in Table 3-15 for individual building in each census tract.

Table 3-15: Data Fields Required in Developing General Building Stock in HAZUS

Field	Usage		
Building Value	Full Replacement Value by occupancy		
Occupancy Class	Square footage by occupancy	Full Replacement Value by occupancy	Building Count by occupancy
Year of Construction	General Occupancy Mapping		
Location	Square footage by occupancy	Full Replacement Value by occupancy	Building Count by occupancy
Structural Type	General Occupancy Mapping		
Design Level	General Occupancy Mapping		
Building Area	Square footage by occupancy		

Part of the above information is available from Role_2009 database provided by the city of Montreal (City of Montreal, 2010). The property tax evaluation database Role_2009 is an excellent source for information regarding location, value, construction year, area and occupancy class of the building. However, it is a property based database that does not use building as its basic unit. Hence, it is consolidated to reflect the condition of individual building instead of individual property. The floor area, building value, and dwelling number from properties that share the same X, Y coordinates is summed up. During this step, the non-building properties such as vacant land and parks are also taken out of the database. Shown in Table 3-16, there are some differences in the occupancy classification system used by Role_2009 and HAZUS. Therefore, the role_2009 database is modified to meet the HAZUS occupancy classification standard. The multi-family residential buildings are regrouped by the number of dwellings in each building. The commercial and industrial buildings are categorized based on their fields of business.

Table 3-16: Comparison of Occupancy Classification System between City of Montreal Tax Evaluation Database (Role_2009) and HAZUS-MH4 General Building Stock

Hazus Code	Description	Role_2009 Code	Description
	Residential		**Residential**
RES1	Single Family Dwelling	2A	Unifamilial-1 logement hors-sol
RES2	Mobile Home	2H	Maison mobile
RES3	Multi Family Dwelling		
	RES3A Duplex	2B	Duplex-2 logements hors-sol
	RES3B 3-4 Units	2C	Triplex-3 logements hors-sol
	RES3C 5-9 Units	4A	Immeuble semi-commercial-maximum 11 logements
	RES3D 10-19 Units	2D	Multiplex-4 à 11 logements hors-sol
	RES3E 20-49 Units	3A	Multiplex, 12 log. et plus, 3 étages et moins sans commerce
	RES3F 50+ Units	3B	Multiplex, 12 log. et plus, 3 étages et moins avec commerce
		3D	Multiplex, 12 log. et plus, 4 étages et plus sans commerce (H-Rise)
		3E	Multiplex, 12 log. et plus, 4 étages et plus avec commerce (H-Rise)
RES4	Temporary Lodging	2F	Maison de chambre ou de touriste (autres qu'hôtel/motels)
		4T	Appartement hôtel, résidence de touriste
		2G	Chalet
		4H	Hôtels et motel
RES5	Institutional Dormitory	3G	OMH, SHQ, COOP, SHDM
RES6	Nursing Home	3H	Résidence personnes agées
		3I	CHSLD
	Commercial		**Commercial**
COM1	Retail Trade	4B	Immeubles commercial à usage divers
COM2	Wholesale Trade	4D	Centre commercial-6 commerces ou plus avec stationnement hors rue
COM3	Personal and Repair Services	4G	Poste d'essence
COM4	Professional/Technical Services	4E	Édifice à bureaux avec ou sans commerces
COM5	Banks		
COM5	Hospital	6D	Hôpitaux et autres immeubles du réseau de la santé
COM7	Medical Office/Clinic		
COM8	Entertainment		
COM9	Theaters	4I	Théatres ou stades
COM10	Parkings	2J	Stationnement intérieur
		2K	Stationnement extérieur
		4F	Garage public, de stationnement, de réparation ou d'entretien automobile

Hazus Code	Description	Role_2009 Code	Description
	Industrial		**Industrial**
IND1	Heavy	5B	Usines
IND2	Light	5C	Manufactures légères
		4C	Entrepôt et station de transport de marchandises
IND3	Food/Drugs/Chemicals		
IND4	Metals/Minerals Processing		
IND5	High Technology		
IND6	Construction		
	Agriculture		
AGR1	Agriculture		
	Religion/Non-Profit		**Religion**
REL1	Church/Non-Profit	6E	Églises, lieux de culte, presbytères et autres immeubles religieux
	Government		**Government**
GOV1	General Services	6F	Autres Immeubles publics ou gouvernementaux
		5D	Utilités publiques
GOV2	Emergency Response		
	Education		**Education**
EDU1	Grade School	6C	Écoles, collèges, universités et autres du réseau de l'éducation
EDU2	College/University		
			***Diverse Usage**
		2E	Bâtiment secondaire
		2I	Immeuble en conversion
		2L	Espace de rangement
		3F	Ensemble immobilier
		4J	Lofts
		4M	Autres commerces divers
		5A	Chemins de fer

After these modifications, the building count by occupancy, square footage by occupancy, and building value by occupancy is aggregated for the study region at census tract level. Based on the building value, the building content value is also estimated for each occupancy type at census tract level. As recommended by HAZUS technical manual, the content value is a percentage of the building value as shown in Table 3-17. These four tables are used as inputs for general building stock, replacing the default GBS inventory of New York State in HAZUS.

Table 3-17 : Building Content Value as the Percentage of Building Value by Occupancy(FEMA, 2003)

Hazus Code	Description	Content Value as % of Building Value
	Residential	
RES1	Single Family Dwelling	50
RES2	Mobile Home	50
RES3	Multi Family Dwelling	50
RES4	Temporary Lodging	50
RES5	Institutional Dormitory	50
RES6	Nursing Home	50
	Commercial	
COM1	Retail Trade	100
COM2	Wholesale Trade	100
COM3	Personal and Repair Services	100
COM4	Professional/Technical Services	100
COM5	Banks	100
COM6	Hospital	150
COM7	Medical Office/Clinic	150
COM8	Entertainment	100
COM9	Theaters	100
COM10	Parkings	50
	Industrial	
IND1	Heavy	150
IND2	Light	150
IND3	Food/Drugs/Chemicals	150
IND4	Metals/Minerals Processing	150
IND5	High Technology	150
IND6	Construction	100
	Agriculture	
AGR1	Agriculture	100
	Religion/Non-Profit	
REL1	Church/Non-Profit	100
	Government	
GOV1	General Services	100
GOV2	Emergency Response	150
	Education	
EDU1	Grade School	100
EDU2	College/University	150

There is some information missing from Role_2009. It does not include structural type or design level of the building, which are the required inputs for the general occupancy mapping database. The default occupancy mapping scheme from HAZUS provides information on structural type distribution within each occupancy type. These structural model types are based on FEMA-178(FEMA, 1992) classification, and the detailed description of each type is available in Chapter 5.2 of HAZUS-MH4 Technical Manual (FEMA, 2003). The estimated building structural type distribution of Montreal is shown in Figure 3-19. It is mentioned in the HAZUS-MH4 technical manual that the default occupancy mapping scheme is provided as a guide, and regional mapping scheme can be derived to improve its accuracy.

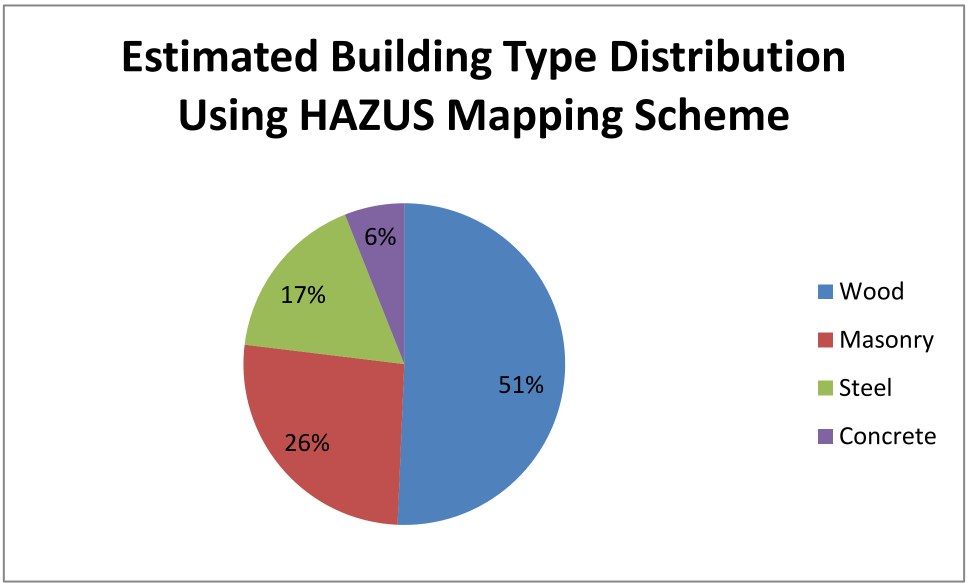

Figure 3-19: Estimated Building Type Distribution in Montreal Using Default HAZUS Mapping Scheme

Ideally, a side walk survey will be able to collect these data. However, it is too costly to conduct this type of survey on a large scale. Based on a similar study conducted by Ploeger (2008) for downtown Ottawa, it's shown that the default occupancy mapping scheme could be used to provide a good initial estimate (Ploeger, 2008). As presented in Table 3-18, when using the default general mapping scheme provided by HAZUS, the physical damage of general building stock is similar to the results from the actual building mapping scheme. The median difference is 10% of the total damage.

Table 3-18 : Comparison of Building Damage by Using Actual Building Occupancy Scheme and Default HAZUS NY1 Inventory Scheme (Ploeger, 2008)

Scenario		**Building Damage (Number of Building)**		**Comparison**	
M	D(km)	Actual Scheme	Default NY1	Difference	% Difference
5.0	1.0	2	1	1	50%
5.0	5.0	1	1	0	0%
5.5	1.0	30	29	1	3%
5.5	7.0	20	18	2	10%
6.0	1.0	168	145	23	14%
6.0	10.0	112	96	16	14%
6.0	27.5	14	11	3	21%
6.0	53.0	2	1	1	50%
6.5	15.0	265	238	27	10%
6.5	31.0	60	58	2	3%
6.5	56.5	14	12	2	14%
7.0	23.0	395	375	20	5%
7.0	38.5	149	134	15	10%
7.0	64.0	41	38	3	7%
				Median	**10%**

With this in mind, a sampling survey of the general building stock in Montreal is conducted to investigate the typical building types in Montreal. This is done to check if the choice of using the default occupancy mapping scheme of New York State (NY1) is justified.

Building Survey

At the time of the survey, only the older version of the property tax database (Role_2005) was available from the city of Montreal. Therefore, the sampling buildings were selected from this database. The distribution of the general building stock in Montreal is not likely to have changed over the last few years. The Role_2005 database is representative of the current general building stock condition in Montreal. Shown in Figure 3-20, 95% of the buildings in Montreal are residential, and the remaining 5% is divided into commercial and industrial buildings. Due to time constraints, only residential buildings were investigated in this study. A break-down of residential buildings is given in Figure 3-21, single dwelling accounts for 50% of the all residential buildings, followed by duplex (26%), triplex (11%), and small apartment building with less than 12 dwellings (10%). The remaining is made of mid-rise and high-rise apartment buildings with more than 12 dwellings

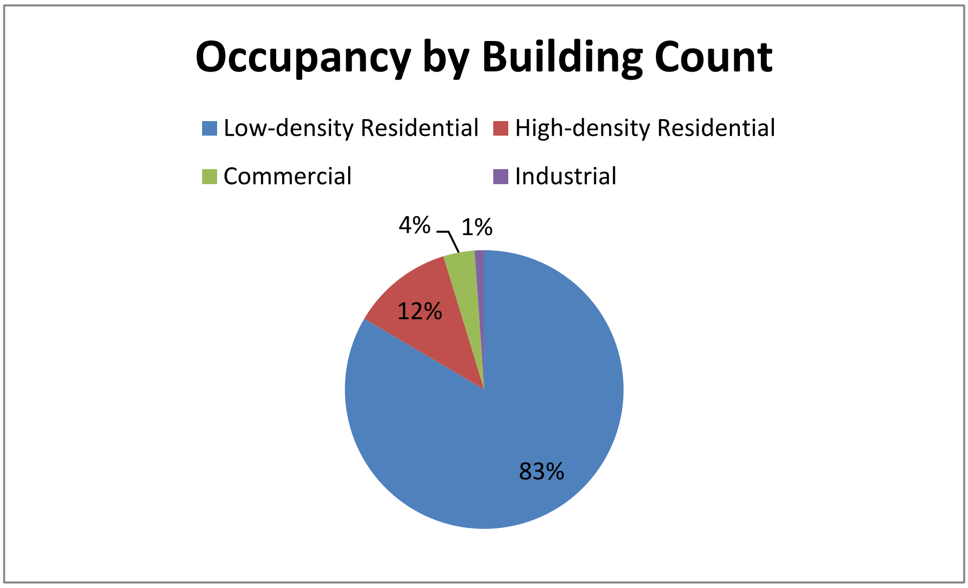

Figure 3-20: Percentage Building Distribution by Occupancy in Montreal

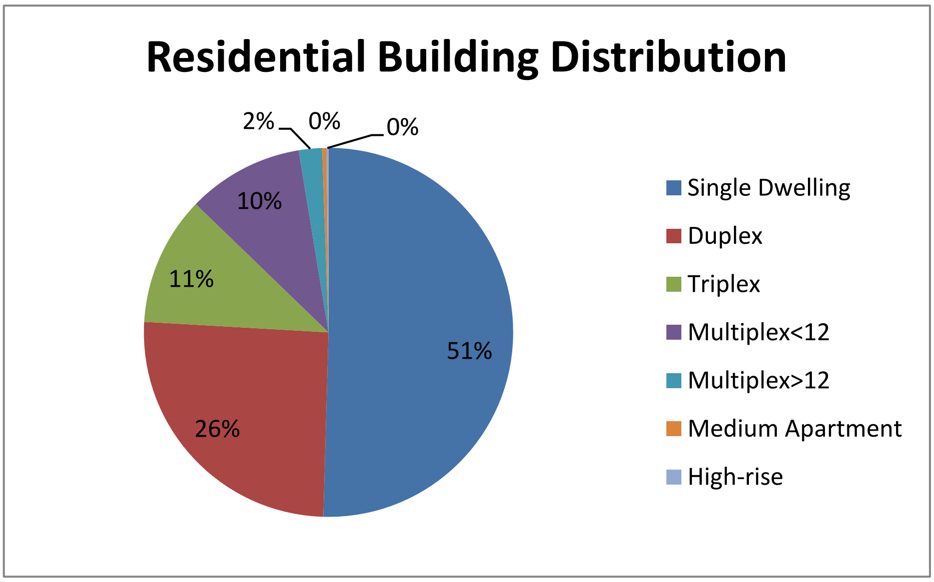

Figure 3-21: Percentage Residential Building Distribution in Montreal

The structural type data comes from two sources: a downtown building survey and a 2009 building survey. The first survey was conducted during the summer of 2008 as part of the research project of Ph.D student Salman Sead from McGill University. The side-walk survey covered 210 buildings in downtown Montreal area bounded by Rue Sherbrooke O., Rue Guy, Rue Notre-Dame O. and Rue Berri (Sead, Personal communication, 2010). Since the buildings surveyed were mostly high-rise buildings, the result of the 2008 survey was used as the source for the structural distribution of high-rise buildings. The 2009 building survey held an emphasis on low to mid-rise residential buildings, and was carried out to complement the results from the 2008 side walk survey.

Given the large number of buildings in Montreal and the time constraint of this project, it is unrealistic to perform a complete side-walk survey on the whole island of Montreal for low and mid-rise buildings. A sampling plan was carried out in an attempt to reduce the number of samples without compromising the quality of the distribution. The type of a building is a function of its construction year, number of storey and occupancy type (Auger & Roquet, 1998; Smith & Coull, 1991). It is observed that within a given time period, only a few construction techniques are popular. The types of construction technique used are usually determined by the size and the usage of the building (Auger & Roquet, 1998). Therefore, by separate buildings into different categories according to their construction year, occupancy type and size, the structural type of buildings will likely to be more consistent within each category. By doing so, fewer samples need to be taken to investigate the building types presented in Montreal.

From the Role_2005, the construction year and occupancy type of each building is available. The occupancy type is divided into five groups: medium-density residential buildings (2x), high-density residential buildings (3x), commercial buildings (4x), industrial buildings (5x), and public and government buildings (6x). Each group is further divided into several categories to differentiate the size and specific occupancy within the group. Five general construction periods were identified based on the literatures on the construction history of Montreal (Auger & Roquet, 1998; Marsan, 1981).

Shown in Table 3-19, the sample size is the smaller of 20 and 5% of the total building population in each building group defined by the size and construction period of the building. The exceptions are the single family dwelling from pre-1840 and 1841-1900 periods, where additional second sets of sample are surveyed to verify the adequacy of sample size. Therefore, a total of 40 buildings are surveyed in these two building groups. The survey was done with the help of Google map, which publishes high resolution photos of buildings. This technique works well for residential buildings in urban areas.

Table 3-19: Number of Residential Building Surveyed in Each Building Occupancy and Age Group

# of Storeys	Low-rise Buildings (<3)					Med-rise (4~5)	High-rise (>=6)
Type	Single Family Dwelling	Duplex	Triplex	Multiplex <12 Dwelling	Multiplex >12 Dwelling	Medium Apt. Building	High-rise Building*
Role Code	2A, 2G	2B	2C, 2F	2D	3A,3B	3D, 3E, 4H(<6)	3D, 3E, 4H(>=6)
# of building	155156	78315	34834	31295	6271	1181	509
	Number of Building Constructed in Each period (Number of Building Surveyed)						
-1840	96(40)	15(15)	9(9)	1	10	-	-
1841-1900	3339(40)	4203(20)	2331(20)	1411(20)	91(5)	68(3)	2
1901-1940	15268(20)	15316(20)	10260(20)	8417(20)	503(20)	248(13)	21
1941-1980	86484(20)	52089(20)	14720(20)	11207(20)	3027(20)	805(20)	420
1981-Now	41385(20)	2034(20)	2283(20)	1412(20)	242(13)	53(3)	58

*** For high-rise buildings, the structural type distribution data was derived from the summer 2008 downtown survey.**

The survey identified 13 model types for low density residential buildings, which has less than 12 dwellings. A list of these model building types is available in Appendix D. Based on the work of (Auger & Roquet, 1998) and expert opinion (Bermington, Personal Communication, 2010), the structural type of each model type surveyed is determined based on the lateral force resisting system of the building (Table 3-20).

Table 3-20: Model Building Types of Low- Rise Residential Buildings Observed in Montreal

Time	Model Type	Material	Structure
-1880	17	Stone/Wood	Masonry Bearing Wall /Wood Frame
	2	Wood/Brick	Wood Frame/Masonry Bearing Wall
	3	Wood/Brick	Wood Frame/Masonry Bearing Wall
	4	Wood/Brick	Wood Frame/Masonry Bearing Wall
	5	Wood/Brick	Wood Frame/Masonry Bearing Wall
	7	Wood/Brick	Wood Frame/Masonry Bearing Wall
1880-1930's	18	Wood/Brick	Wood Frame/Masonry Bearing Wall
	6	wood	wood frame
	8	wood	wood frame
	16	wood	wood frame
	19	wood	wood frame
1940's-NOW	20	wood	wood frame

*Personal communication with building inspector Mr. Normand Remington

Among all the model types, wood frame is the most common structural system. However, it was noticed that many of the buildings constructed before World War I share masonry walls with adjacent buildings. This wall known as the "firewall" usually acts as bearing wall for the building. Although mainly made of wood frames, these buildings would behave like unreinforced masonry structures rather than wood frame buildings.

As summarized in Table 3-21, according to the 134 single family buildings surveyed, it can be observed that wood frame construction was getting popular in the early 20th century, when the structural type distribution shows a significant change. For low density multifamily housing, the structural type distribution is similar to the single family dwelling distribution. Compared to low-density low-rise housing, high density housing shows a more complicated structural distribution. Concrete moment frame, shear wall structures and steel moment frames were observed during the survey.

Using the above information, the structural type of individual buildings surveyed was determined by matching the architectural feature of each building to each model type. The result of the estimated occupancy and structural type distribution is shown in Table 3-22. It was estimated that about 94% of the single-family residential buildings are wood frame buildings, and 6% are unrienforced masonry buildings. For multifamily residential buildings, 22% were found to be unreinforced masonry buildings while 78% were found to be wood frame buildings. Compared with the default New York occupancy mapping from HAZUS, the estimated structural occupancy distribution in Montreal generally agrees with the default mapping scheme. Shown in Table 3-23, the Montreal building stock has more wood frame structures and less masonry structures compare to the default mapping scheme for both single family and multifamily buildings. Since wood frame buildings generally have higher lateral force resistance than masonry buildings, the choice of using default mapping scheme is a more conservative approach. Due to the sample size limit of the building survey, the results hold a high level of uncertainty. Therefore, the default New York State (NY1) occupancy mapping is used in this study. However, the difference between default HAZUS mapping scheme and survey results indicates that it is necessary to develop a regional mapping scheme for Montreal in future projects.

Table 3-21: Summary of Building Survey Result Showing Structural Type Distribution by Occupancy Type

	Number of Building Surveyed																
	Single Family Dwelling		Duplex-Multiplex (<12Dwellings)		Low-rise Apartment				Med-rise Apartment					High-rise Apartment*			
Role Code	2A,2G		2B,2C,2D,2F		3A,3B				3D,3H,3F(<6)					3D,3H,3F(>=6)			
Periods	WF	MB	WF	MB	CMF	CSW	WF	MB	CMF	CSW	WF	SMF	MB	CMF	CSW	SMF	MB
-1840	10	24	12	11	0	0	0	0	0	0	0	0	0	0	0	0	0
1841-1900	11	28	11	48	0	0	1	2	0	0	0	0	4	0	0	0	1
1901-1940	13	8	23	37	0	4	3	12	0	2	0	4	7	5	0	0	0
1941-1980	20	0	60	0	0	1	19	0	2	4	3	9	0	13	3	3	0
1981-now	20	0	53	1	1	3	6	0	3	0	0	0	0	12	2	1	0

***From Summer2008 Building Survey, CMF=Concrete Moment Frame, CSW=Concrete Shear Wall, WF=Light Wood Frame, MB=Masonry Building, SMF=Steel Moment Frame**

Table 3-22: Estimated Structural Distribution of Residential Buildings in Montreal

	Single Family		Duplex-Multiplex		Low-rise Apartment				Med-rise Apartment					High-rise Apartment			
Role2005 Code	**2A,2G**		**2B,2C,2D,2F**		**3A,3B**				**3D,3H,3F(<6)**					**3D,3H,3F(>=6)**			
Periods	**WF**	**MB**	**WF**	**MB**	**CM**	**CSW**	**WF**	**MB**	**CM**	**CSW**	**WF**	**SMF**	**MB**	**CM**	**CSW**	**SMF**	**MB**
-1840	30	72	15	13	0	0	0	0						0	0	0	0
1841-1900	997	2538	1711	7467	0	0	49	98	0	0	0	0	68	0	0	0	2
1901-1940	10005	6157	15369	24723	0	171	129	514	0	38	0	76	134	21	0	0	0
1941-1980	91549	0	88328	0	0	245	4656	0	89	179	134	403	0	287	66	66	0
1981-now	43809	0	6691	126	39	118	235	0	53	0	0	0	0	46	8	4	0
Total	**146390**	**8766**	**112114**	**32330**	**39**	**534**	**5069**	**613**	**142**	**217**	**134**	**479**	**202**	**355**	**74**	**70**	**2**
%	94%	6%	78%	22%	1%	9%	81%	10%	12%	18%	11%	41%	17%	71%	15%	14%	0%

CMF=Concrete Moment Frame, CSW=Concrete Shear Wall, WF=Light Wood Frame, MB=Masonry Building, SMF=Steel Moment Frame

Table 3-23: Comparison of Estimated Montreal Occupancy Mapping and New York State Default Mapping Scheme from HAZUS

			Montreal Survey Results				Default New York (NY1)			
Role Code	**HAZUS Code**		**Wood**	**Masonry**	**Concrete**	**Steel**	**Wood**	**Masonry**	**Concrete**	**Steel**
2A,2G	**Single Family(RES1)**		94%	6%	0%	0%	85%	14%	1%	0%
2B,2C,2D,2F,3A,3B	**Multi-family(RES3)**	low-rise	78%	22%	0%	0%	66%	31%	4%	3%
3D,3H,3F		med-rise	11%	17%	31%	41%	0%	70%	23%	7%
		high-rise	0%	0%	86%	14%	0%	5%	58%	37%

3.3.2 Essential Facilities

The essential facilities in HAZUS-MH4 are made up of the following groups: emergency response facility, medical care facility and school. Each group is further divided into several sub-categories shown in Table 3-24.

Table 3-24: HAZUS Classification of Essential Facilities(FEMA, 2003)

No.	Label	Occupancy Class	Description
		Medical Care Facilities	
1	EFHS	Small Hospital	Hospital with less than 50 Beds
2	EFHM	Medium Hospital	Hospital with beds between 50 & 150
3	EFHL	Large Hospital	Hospital with greater than 150 Beds
4	EFMC	Medical Clinics	Clinics, Labs, Blood Banks
		Emergency Response	
5	EFFS	Fire Station	
6	EFPS	Police Station	
7	EFEO	Emergency Operation Centers	
		Schools	
8	EFS1	Schools	Primary/ Secondary Schools (K-12)
9	EFS2	Colleges/Universities	Community and State Colleges, State and Private Universities

Use a database provided by the city of Montreal, the location of essential facilities is inputted into HAZUS. Other information regarding building area, value, structural type and functionality are obtained from the 2009 Role and government websites for part of the essential facilities. For a preliminary analysis, the inputs required are the location and the structural type of the building. The default building structural type is used when the structural information is missing. The location of the essential facilities is shown in Figure 3-23. Since the information obtained is not complete, only a preliminary analysis on the building damage level is performed using HAZUS. For a complete analysis of essential facilities, the information in Table 3-25 should be collected. Since such analysis is performed on an individual building base, it is important to collect all the necessary information regarding building status and functionality.

Table 3-25: Fields of Information Collected, Partially Collected and Missing for Essential Facilities

	Medical Care Facility	Emergency Operation Center	Police Station	Fire Station	School
Information Collected	EfClass Tract Name Address City Zipcode Latitude Longitude Phone Number	EfClass Tract Name Address City Zipcode Latitude Longitude Contact Person Phone Number	EfClass Tract Name Address City Zipcode Latitude Longitude Phone Number Num of Stories	EfClass Tract Name Address City Zipcode Latitude Longitude Year Built Num of Stories	EfClass Tract Name Address City Zipcode Latitude Longitude
Information Partially Collected	Year Built Num of Stories Num of Beds	Year Built Num of Stories Area Building Type	Year Built Replacement Cost Area Building Type	Replacement Cost Area Building Type	
Information Missing	Contact Person Primary Function Replacement Cost Backup Power (Yes/No) Design Level Building Type Foundation Type Landslide Susceptibility Liquefaction Susceptibility WaterDepth	Replacement Cost Backup Power (Yes/No) Shelter Capacity Kitchen (Yes/No) Design Level Foundation Type Landslide Susceptibility Liquefaction Susceptibility WaterDepth	Contact Person Backup Power (Yes/No) Shelter Capacity Kitchen (Yes/No) Design Level Foundation Type Landslide Susceptibility Liquefaction Susceptibility WaterDepth	Contact Person Phone Number Backup Power (Yes/No) Shelter Capacity Kitchen (Yes/No) Num of Fire Trucks Design Level Foundation Type Landslide Susceptibility Liquefaction Susceptibility WaterDepth	Contact Person Phone Number Year Built Num of Stories Replacement Cost Num of Students Backup Power (Yes/No) Shelter Capacity Area School District Kitchen (Yes/No) Design Level Building Type Foundation Type Landslide Susceptibility Liquefaction Susceptibility WaterDepth

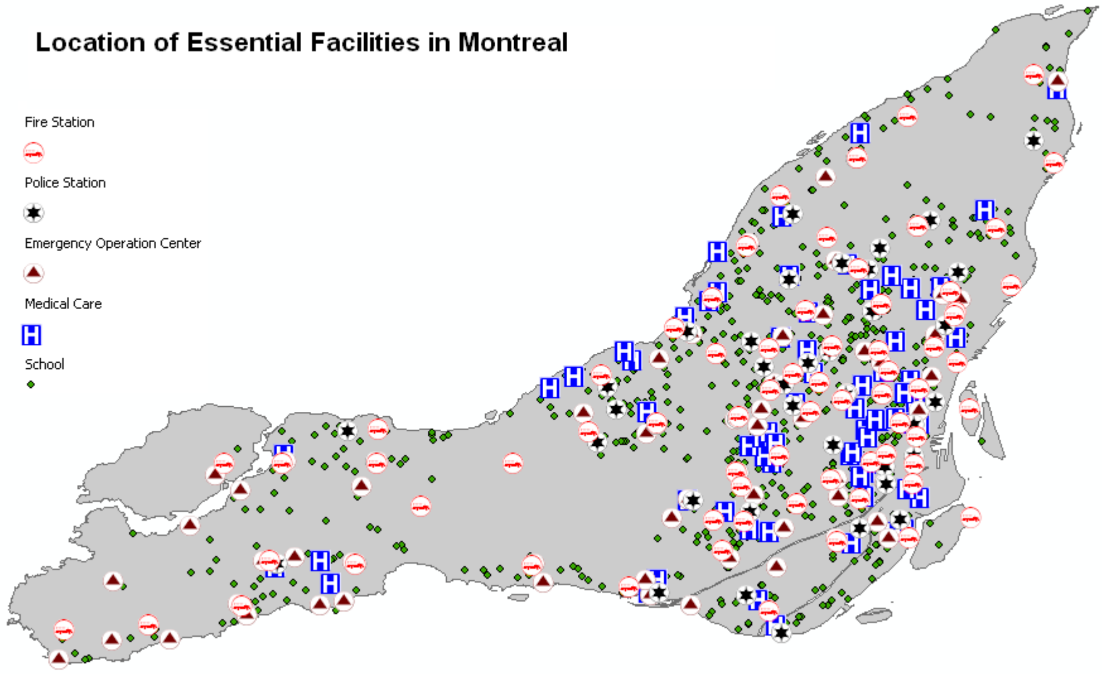

Figure 3-22: Location of Essential Facilities in Montreal

3.4 Demographics

Demographic data is essential in estimating direct economic losses and direct social losses from earthquakes. The required inputs and sources are presented in Table 3-26. These data come from two major sources: Canadian Census 2006 (StatisticsCanada, 2006), and Origin-Destination Survey 2003 (O-D2003) conducted by Centre d'information métropolitain sur le transport urbain(CIMTU, 2003). Census2006 database provides most of the information except for daytime population distribution and median building age within Census Tract, which comes from OD-survey2003 and Role2009 respectively.

Table 3-26: Demographic Data Input, Source and Usage (Adapted from Table 3.26 from HAZUS-MH4 Technical Manual)

Fields	Source	Usage		
		Shelter	Casualty	Occupancy
Population	Census2006	*		
PrivateHouseholds	Census2006	*		
GroupQuarters	Census2006	*		
MaleLess15	Census2006	*		
Male15to64	Census2006	*		
MaleOver64	Census2006	*		
FemaleLess15	Census2006	*		
Female15to64	Census2006	*		
FemaleOver64	Census2006	*		
MalePopulation	Census2006	*		
FemalePopulation	Census2006	*		
White	Census2006	*		
Black	Census2006	*		
NativeAmerican	Census2006	*		
Asian	Census2006	*		
Hispanic	Census2006	*		
PacifiIslander	Census2006	*		
OtherRaceOnly	Census2006	*		
IncLess10	Census2006	*		
Inc10to20	Census2006	*		
Inc20to30	Census2006	*		
Inc30to40	Census2006	*		
Inc40to50	Census2006	*		
Inc50to60	Census2006	*		
Inc60to80	Census2006	*		
Inc80to100	Census2006	*		
IncOver100	Census2006	*		
RessidDay	OD2003		*	
ResidNight	Census2006		*	
Hotel	OD2003		*	
Vistor	OD2003		*	
WorkingCom	OD2003		*	
WorkingInd	OD2003		*	
Commuting5PM	OD2003		*	
OwnerSingleUnits	Census2006	*		
OwnerMultUnits	Census2006	*		
OwnerMultStructs	Census2006	*		
OnwerMHs	Census2006	*		
RenterSingleUnits	Census2006	*		
RenterMultUnits	Census2006	*		
RenterMultStructs	Census2006	*		
RenterMHs	Census2006	*		
TotalVac	Census2006			*
VacantSingleUnits	Census2006			*
VacantMultUnits	Census2006			*
VacantMultStructs	Census2006			*
VacantMHs	Census2006			*
BuiltBefore40	Census2006			*
Built40to49	Census2006			*
Built50to59	Census2006			*
Built60to69	Census2006			*
Built70to79	Census2006			*
Built80-89	Census2006			*
Built90-98	Census2006			*
BuiltAfter98	Census2006			*
MedianYear	Role2009			*
AvgRent	Census2006	*		
AvgValue	Census2006	*		
SchoolEnrollmentKto12	OD2003		*	
SchoolEnrollmentCollege	OD2003		*	

3.4.1 Population Distribution

In order to get the casualty estimates, the population distribution at three different times of the day is required as an input in HAZUS. The night-time population distribution at 2 AM is obtained from the Census2006 survey (Statistics Canada, 2006). The day-time population distribution is estimated from the O-D 2003 survey (CIMTU, 2003). The O-D 2003 survey covers 5% of the total population within the metropolitan Montreal area. The survey records the trip origin, destination, purpose and method of transportation for each trip made during a typical day for all the participants. Using these information, a summary table is made to show all the trips a person made during the day. This table allows one to identify the location of a person at a certain time of the day by determining the trip made closest to that time. Since the purpose of each trip is coded in O-D survey, the working population, residential population, school population, visitor population and commuting population can be calculated separately. The population distributions at 2 PM and 5 PM are calculated using O-D survey. The working population, residential population, school population, and visitor population at 2 PM are used as inputs for the corresponding daytime population fields in HAZUS. The commuting population at 5 PM is used as the input for commuting5pm.

Comparing the daytime (Figure 3-23) and nighttime (Figure 3-24) population distribution, it is observed that the total daytime population at 2pm is greater than the total nighttime population at 2am for the island of Montreal. This is expected since the majority of the daytime population is the population at work, which includes population residing outside of the island. This trend is more obvious in downtown Montreal, where the majority of the buildings are offices and commercial centers. Shown in Figure 3-25, the population in downtown core during the day is more than 10 times the population during the night. This trend is also observed in the industrial areas of the island: Saint-Laurent and Montreal-Est both show a higher population during the day than at night.

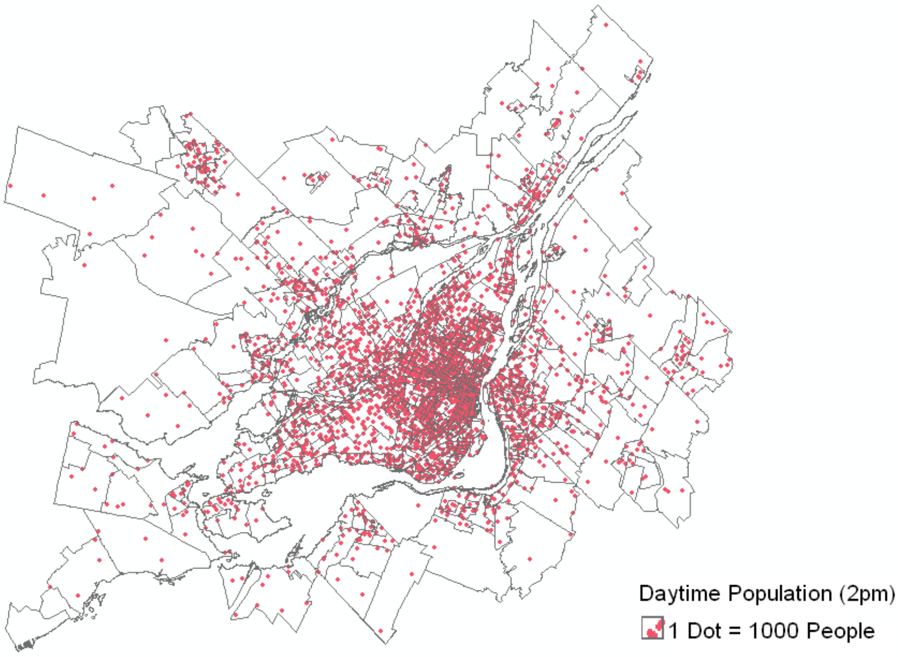

Figure 3-23: Daytime Population of Montreal (OD-2003 survey data)

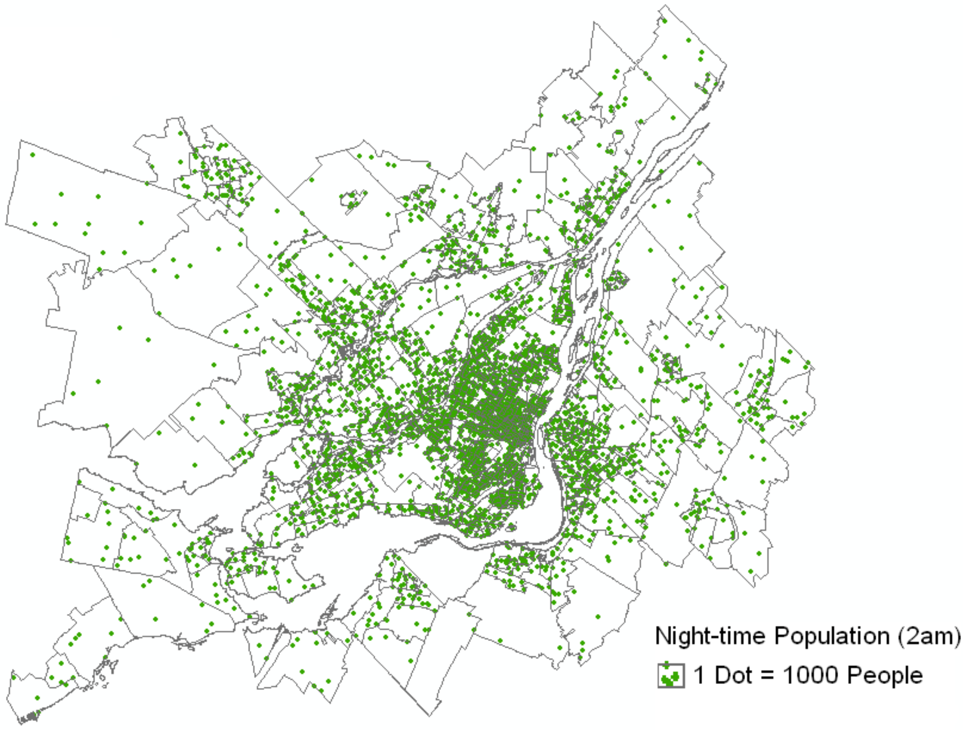

Figure 3-24: Night-time Population of Montreal (Census 2006 data)

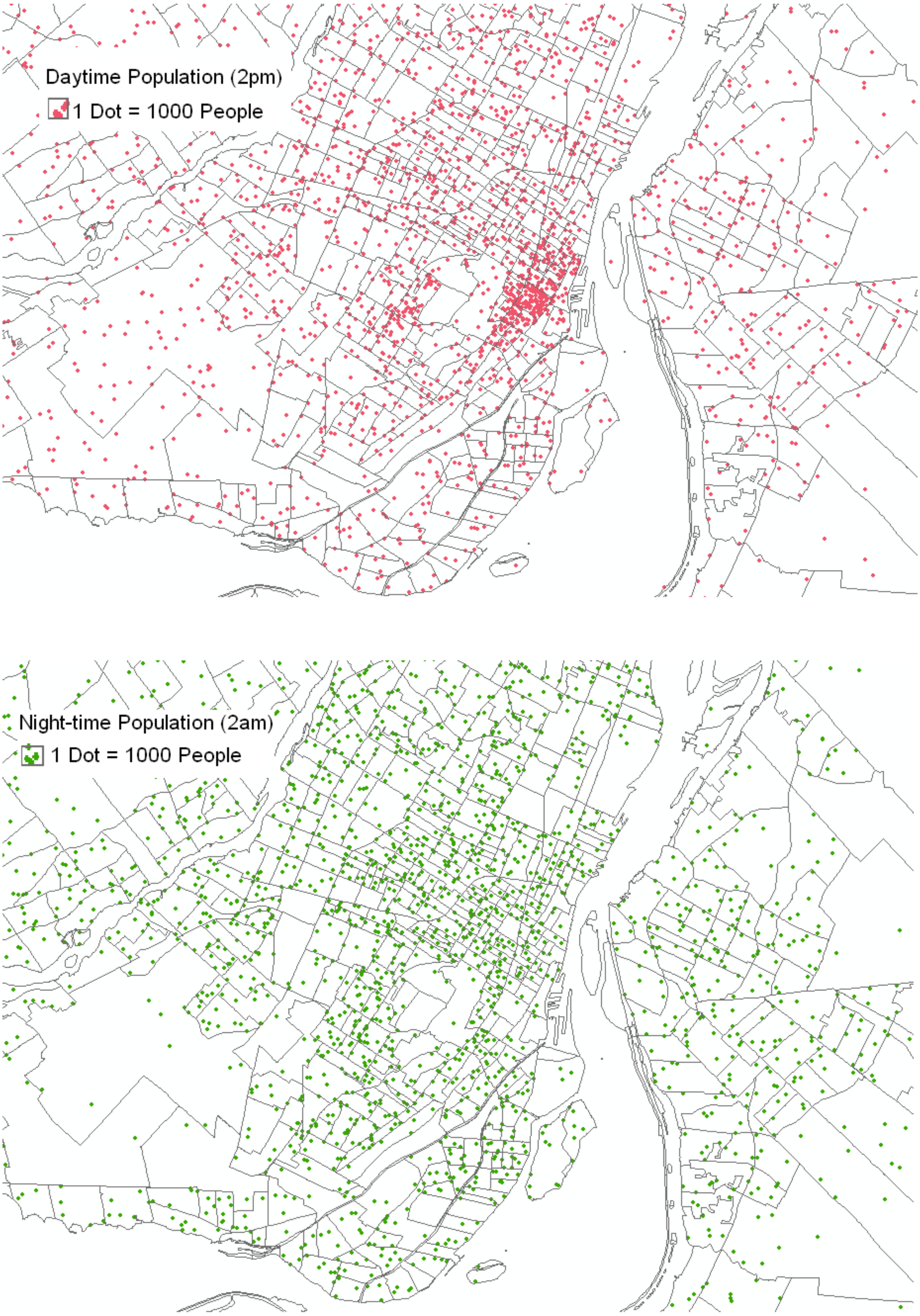

Figure 3-25: Daytime and Night-time Population in Downtown Montreal

3.4.2 Other Demographics Data

Other than population distribution, the income and age distribution are also important parameters in estimating economic and social losses during an earthquake. These data are supplied by the Census 2006 survey and converted into the HAZUS format. Most of the data can be used directly as HAZUS inputs with very minor changes. For example, the family income brackets used in Census 2006 is 10000, which is different from the HAZUS income classification. The census data is therefore regrouped to meet the HAZUS standard. Such minor grouping differences also exist in ethnic origin of the population and age group. Therefore, the information in Census 2006 is converted into the standard HAZUS standard demographic inventory. The raw data taken from Census 2006 and the HAUZS demographic fields in which they are used are presented in Table 3-27. Due to the fact that some of the raw data have been regrouped, some uncertainties are introduced into the demographics data.

Table 3-27: Source Data Fields in Census 2006 for HAZUS Demographics Inventory

HAZUS Fields	2006 Census Data Fields
IncLess10	Under $10,000, household income in 2005 of private households
Inc10to20	$10,000 to $19,999, household income in 2005 of private households
Inc20to30	$20,000 to $29,999, household income in 2005 of private households
Inc30to40	$30,000 to $39,999, household income in 2005 of private households
Inc40to50	$40,000 to $49,999, household income in 2005 of private households
Inc50to60	$50,000 to $59,999, household income in 2005 of private households
Inc60to80	$60,000 to $69,999, household income in 2005 of private households
Inc80to100	$70,000 to $79,999, household income in 2005 of private households
IncOver100	$80,000 to $89,999, household income in 2005 of private households
	$90,000 to $99,999, household income in 2005 of private households
	$100,000 and over, household income in 2005 of private households
ResidNight	Population, 2006 - 100% data
OwnerSingleUnits	Single-detached house, occupied private dwellings by structural type of dwelling
OwnerMultUnits	Other single-attached house, occupied private dwellings by structural type of dwelling
OwnerMultStructs	Semi-detached house, occupied private dwellings by structural type of dwelling
OnwerMHs	Row house, occupied private dwellings by structural type of dwelling
RenterSingleUnits	Apartment, duplex, occupied private dwellings by structural type of dwelling
RenterMultUnits	Apartment, building that has five or more storeys, occupied private dwellings by structural type of dwelling
RenterMultStructs	Apartment, building that has fewer than five storeys, occupied private dwellings by structural type of dwelling
RenterMHs	
TotalVac	
VacantSingleUnits	
VacantMultUnits	
VacantMultStructs	
VacantMHs	
BuiltBefore40	Period of construction, before 1946, occupied private dwellings
Built40to49	Period of construction, 1946 to 1960, occupied private dwellings
Built50to59	Period of construction, 1961 to 1970, occupied private dwellings
Built60to69	Period of construction, 1971 to 1980, occupied private dwellings
Built70to79	Period of construction, 1981 to 1985, occupied private dwellings
Built80-89	Period of construction, 1986 to 1990, occupied private dwellings
Built90-98	Period of construction, 1991 to 1995, occupied private dwellings
BuiltAfter98	Period of construction, 1996 to 2000, occupied private dwellings
	Period of construction, 2001 to 2006, occupied private dwellings
AvgRent	Average gross rent $, number of non-farm, non-reserve private dwellings occupied by usual residents
AvgValue	Average value of dwelling $, number of non-farm, non-reserve private dwellings occupied by usual residents

HAZUS Fields	2006 Census Data Fields
Population	Population, 2006 - 100% data
PrivateHouseholds	Total private dwellings, 2006
GroupQuarters	Population, 2006 - 100% data - Total number of persons in private households - 20% sample data
MaleLess15 **Male15to64** **MaleOver64**	Male, 0 to 4 years Male, 5 to 9 years Male, 10 to 14 years Male, 15 to 19 years Male, 20 to 24 years Male, 25 to 29 years Male, 30 to 34 years Male, 35 to 39 years Male, 40 to 44 years Male, 45 to 49 years Male, 50 to 54 years Male, 55 to 59 years Male, 60 to 64 years Male, 65 to 69 years Male, 70 to 74 years Male, 75 to 79 years Male, 80 to 84 years Male, 85 years and over
FemaleLess15 **Female15to64** **FemaleOver64**	Female, 0 to 4 years Female, 5 to 9 years Female, 10 to 14 years Female, 15 to 19 years Female, 20 to 24 years Female, 25 to 29 years Female, 30 to 34 years Female, 35 to 39 years Female, 40 to 44 years Female, 45 to 49 years Female, 50 to 54 years Female, 55 to 59 years Female, 60 to 64 years Female, 65 to 69 years Female, 70 to 74 years Female, 75 to 79 years Female, 80 to 84 years Female, 85 years and over
MalePopulation	Male, total population
FemalePopulation	Female, total population
White **Black** **NativeAmerican** **Asian** **Hispanic** **PacifiIslander** **OtherRaceOnly**	British Isles origins, population by ethnic origin French origins, population by ethnic origin Aboriginal origins, population by ethnic origin Other North American origins, population by ethnic origin Caribbean origins, population by ethnic origin Latin, Central and South American origins, population by ethnic origin European origins, population by ethnic origin African origins, population by ethnic origin Arab origins, population by ethnic origin West Asian origins, population by ethnic origin South Asian origins, population by ethnic origin East and Southeast Asian origins, population by ethnic origin Oceania origins, population by ethnic origin

Chapter 4. HAZUS Loss Estimation Methodology

4.1 HAZUS Loss Estimation Framework

The HAZUS earthquake loss estimation method consists of several components with some acting as inputs of others. The basic inputs of these components are Potential Earthquake Science Hazards (PESH) and building inventories, from which, a complete analysis can be run to provide estimation in the following fields: direct physical damage, Induced physical damage, direct economic/social damage, and indirect economic damage. The complete list of outputs of the HAZUS earthquake loss estimation is shown in Figure 1-2 in Chapter 1.

Due to limited accessibility to some of the data, the Montreal study only used part of the analysis models in HAZUS, including ground motion and ground failure predictions, direct physical damage of general building stock and essential facility, casualty estimation, shelter needs projections and direct economic losses.

Since this study does not cover transportation systems or lifeline-utility systems, the estimated damage and losses is only a fraction of the actual damage done. When interpreting the results, one should always keep this in mind. In this section, the methodology used by HAZUS for estimating physical and social damage is explained.

4.2 Direct physical damage

Physical damage of structures in HAZUS is described by the probability of four different damage states: slight damage, moderate damage, extensive damage and complete damage. The detailed description of these four states for each model building types can be found in HAZUS-MH4 technical manual Chapter 5.2. This probability is calculated using two sets of data: fragility curves describe the probability of reaching different states for a given building response, and capacity curves that predict such responses in a given earthquake.

The fragility curves relate the probability of being in, or exceeding, a building damage state for a given building response parameters (FEMA, 2003). An example of fragility curve used in HAZUS is given in Figure 4-1, where Ds is the damage, and ds is a particular damage state.

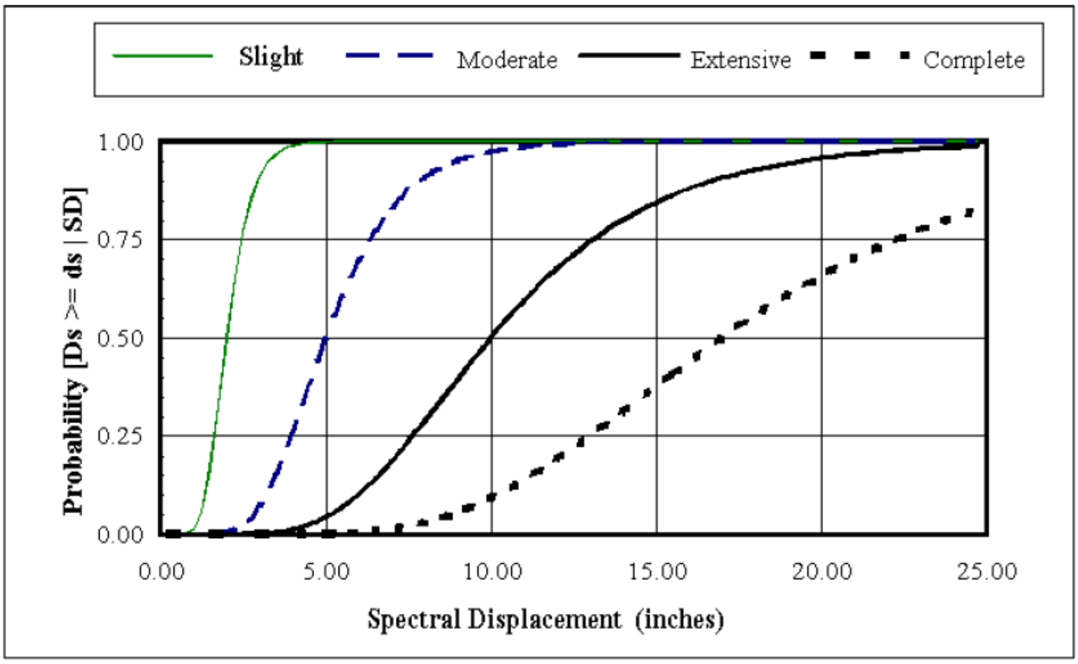

Figure 4-1: Example of Fragility Curves for Slight, Moderate, Extensive and Complete Damage (FEMA, 2003)

The fragility curve for a given damage state is defined by a median value of a PESH parameter (S_d) that corresponds to the threshold of that damage state and by the variability (β_{ds}) associated with that damage state. These two parameters are developed for each of the damaged state and for all three types of building components: structural, nonstructural-drift sensitive, and nonstructural-acceleration sensitive. The conditional probability of being in or exceeding certain damage state is therefore:

$$P[ds|S_d] = \Phi[\frac{1}{\beta_{ds}} \ln\left(\frac{S_d}{\bar{S}_{d,ds}}\right)]$$

where $S_{d,ds}$ is the median value of the PESH parameter of damage state ds, β_{ds} is the standard deviation of the natural logarithm of the PESH parameter for damage state d_s, and S_d is the building response in terms of the PESH parameter chosen (FEMA, 2003).

When determining direct physical damage, HAZUS considers both ground shaking and ground failure induced by an earthquake. For ground failure, the PESH parameter used in fragility curves is permanent ground displacement (PGD). For ground shaking, the PESH parameters used to drive building fragility curves are peak spectral displacement for structural and drift-sensitive nonstructural components and peak spectral acceleration for acceleration sensitive nonstructural components (FEMA, 2003).

4.2.1 Damage due to Ground Shaking

Under high loads, buildings have the capacity of undergoing inelastic deformations before collapsing. In the inelastic range, damage is usually controlled by displacements rather than lateral loads. Therefore, HAUZS methodology uses the total displacement rather than the lateral force to determine the damage probability during an earthquake. The displacement is determined by the intersection of the capacity curve of a building and the demand spectrum derived from the ground motion.

Derived from the static-equivalent base shear and the corresponding building displacement, a capacity curve is a force-displacement plot that reflects the true deflection of a building, which allows one to exam the displacement of a model building type as a function of the applied seismic load. (Mahaney, Paret, Kehoe, & Freeman., 1993) It is defined by three points: design, yield and ultimate. The curve is linear below the yield point. Between yield and ultimate points, the curve transitions in slope. After the ultimate point, the curve remains plastic. The capacity curve of each model building type in HAZUS is estimated by the engineering properties that defines these three points.

The ground motion is characterized as a standardized spectrum, which consists of three regions: the region of constant spectral acceleration, the region of constant spectral velocity, and the region of constant spectral displacement. The boundaries of these regions are defined by the spectral acceleration at 0.3s and 1.0s. The demand spectrum of building is based on the input ground motion spectrum reduced for effective damping. This effective damping parameter is the sum of elastic damping and hysteretic damping, which is a function of the yield and ultimate capacity points of a building's capacity curve.(Molina-Palacios & Lindholm, 2004) An example of the building capacity and demand curve is shown in Figure 4-2. In the figure, the demand spectrum is significantly reduced from the PESH input spectrum and intersects with the capacity curve. The spectral displacement (S_d) of the intersection is used as the input in fragility curve.

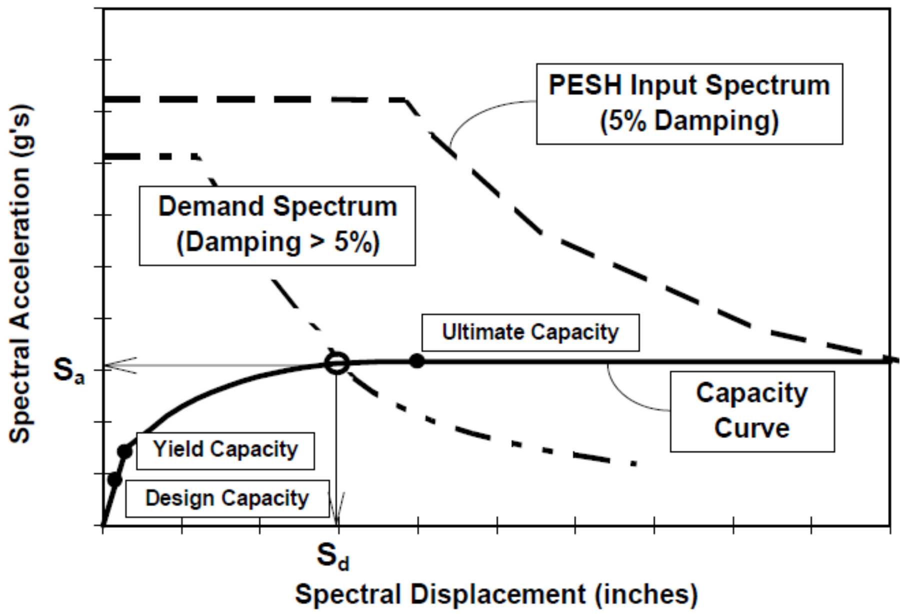

Figure 4-2: Example Building Capacity Curve and Demand Spectrum (FEMA, 2003)

4.2.2 Damage due to Ground Failure

In HAZUS, ground failure is characterized by the Permanent Ground Displacement (PGD). The four damage state used in ground shaking are simplified into one combined damage state: Extensive/Complete Damage. Similar to the method evaluating damage caused by ground shaking, a fragility curve is constructed using the parameters listed in Table 4-1. This fragility curve is used for all model building types to estimate the damage caused by ground failure. The expected PGD at 10% and 50% damage level is shown in Table 4-1:

Table 4-1: Building Damage Relationship to PGD (FEMA,2003)

P[E or C|PGD]	Settlement PGD (inches)	Lateral Spread PGD (inches)
0.1	2	12
0.5 (median)	10	60

Among all the buildings damaged, it is assumed that 20% of the buildings in the Extensive/Complete Damage state are completely damaged, while the remaining 80% are extensively damaged (FEMA, 2003).

HAZUS assumes that damage due to ground failure and damage due to ground shaking are independent of each other. Therefore, the combined damage probability of being in or exceeding certain damage state is the union of the cumulative damage probabilities induced by ground shaking and ground failure (FEMA, 2003).

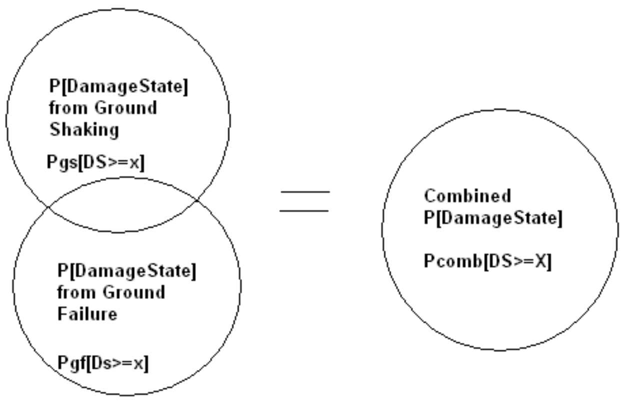

Figure 4-3: Method used in HAZUS to Calculate the Combined Probability of Being in or Exceeding Certain Damage State for Evaluating Direct Physical Damage for Buildings

The discrete probability of being in each damage state is then calculated from the combined cumulative probabilities.

$$P_{COMB}[DS = Complete] = P_{COMB}[DS \geq Complete]$$

$$P_{COMB}[DS = Extensive] = P_{COMB}[DS \geq Extensive] - P_{COMB}[DS \geq Complete]$$

$$P_{COMB}[DS = Moderate] = P_{COMB}[DS \geq Moderate] - P_{COMB}[DS \geq Extensive]$$

$$P_{COMB}[DS = Slight] = P_{COMB}[DS \geq Slight] - P_{COMB}[DS \geq Moderate]$$

$$P_{COMB}[DS = None] = 1 - P_{COMB}[DS \geq Slight]$$

(FEMA, 2003)

This damage probability is then translated into number of damaged buildings at the level of census tract. Number of damaged buildings in each damage state is calculated for each model building type based on the structural type distribution within each census tract. The results are also calculated in terms of square footage, and are used in calculating induced damage such as debris.

4.3 Direct Economic Damages

Direct economic losses related to buildings consist of three parts: building repair and replacement costs, building content losses, and building inventory losses. (FEMA, 2003) The building economic data are either supplied by building economic data from the general building stock or by default values in HAZUS.

The building repair and replacement costs are calculated individually for each building type and summed in the end for each occupancy class within each census tract. It is calculated as the product of direct physical damage probability, ratio of damage in each damage state, cost of repair and replacement per unit area and area of each building type within each occupancy class. The direct physical damage probability is taken from the results of direct physical damage; the ratio of damage is given in HAZUS as a default value for each damage state; and the cost of repair and replacement as well as building area is taken from the building economic data in the general building stock tables. The repair and replacement costs cover both the structural damage and non-structural damage.

The cost of damaged content gives an estimate of the losses in furniture and equipments that are not fixed to the structure. Similar to building repair and replacement costs, it is calculated for each occupancy class as a product of probability of damage for each building type within each occupancy class, ratio of damage in each damage state, cost of content of each occupancy class. The probability of damage used is the non-structural acceleration sensitive damage, which is a good indicator of content damage (FEMA, 2003).

Business inventory loss covers only commercial and industrial buildings. It is estimated based on the default annual gross sales of a business in certain occupancy. Similar to content loss, the inventory loss is calculated as the products of the non-structural acceleration sensitive damage probability, total inventory value, percentage loss of inventory of given damage state. (FEMA, 2003)

4.4 Casualty

The casualty estimated by HAZUS is broken down into four levels indicated in Table 4-2. Based on previous studies (Coburn & Spence, 1992; Durkin & Thiel, 1991), the injury classification scale describes the casualty at four levels. No death is expected to happen with level one to level two injuries. Level three and level four injuries are life-threatening injuries and death respectively.

In HAZUS, the total population is divided into six groups: residential population, commercial population, educational population, industrial population, commuting population and hotel population. The population distribution is estimated using demographics data supplied. Except for commuting population, the indoor and outdoor population at three time of the day is calculated for each population group and assigned into the corresponding building occupancy class. The commuting population in car and using other methods are estimated to calculate the roadway casualties caused by the collapse of highway.

Table 4-2: Casualty Level Description by HAZUS (FEMA, 2003)

Injury Severity Level	Injury Description
Level 1	Injuries requiring basic medical aid that could be administered by paraprofessionals. These types of injuries would require bandages or observation. Some examples are: a sprain, a severe cut requiring stitches, a minor burn (first degree or second degree on a small part of the body), or a bump on the head without loss of consciousness. Injuries of lesser severity that could be self treated are not estimated by HAZUS.
Level 2	Injuries requiring a greater degree of medical care and use of medical technology such as x-rays or surgery, but not expected to progress to a life threatening status. Some examples are third degree burns or second degree burns over large parts of the body, a bump on the head that causes loss of consciousness, fractured bone, dehydration or exposure
Level 3	Injuries that pose an immediate life threatening condition if not treated adequately and expeditiously. Some examples are: uncontrolled bleeding, punctured organ, other internal injuries, spinal column injuries, or crush syndrome.
Level 4	Instantaneously killed or mortally injured

Figure 4-4 shows the indoor casualty estimates the event tree used in HAZUS. A similar event tree is used for outdoor casualty estimates. For all four casualty level, a casualty rate is supplied by HAZUS for each model building type at four structural damage states. The number of people in each building type is estimated based on the same occupancy-structural type distribution table used in direct physical damage loss estimation. Therefore, by knowing the probability of damage at all given damage states for each building type, the number of indoor and outdoor casualty of a particular occupancy class can be calculated. The results are aggregated for the study region at four casualty levels.

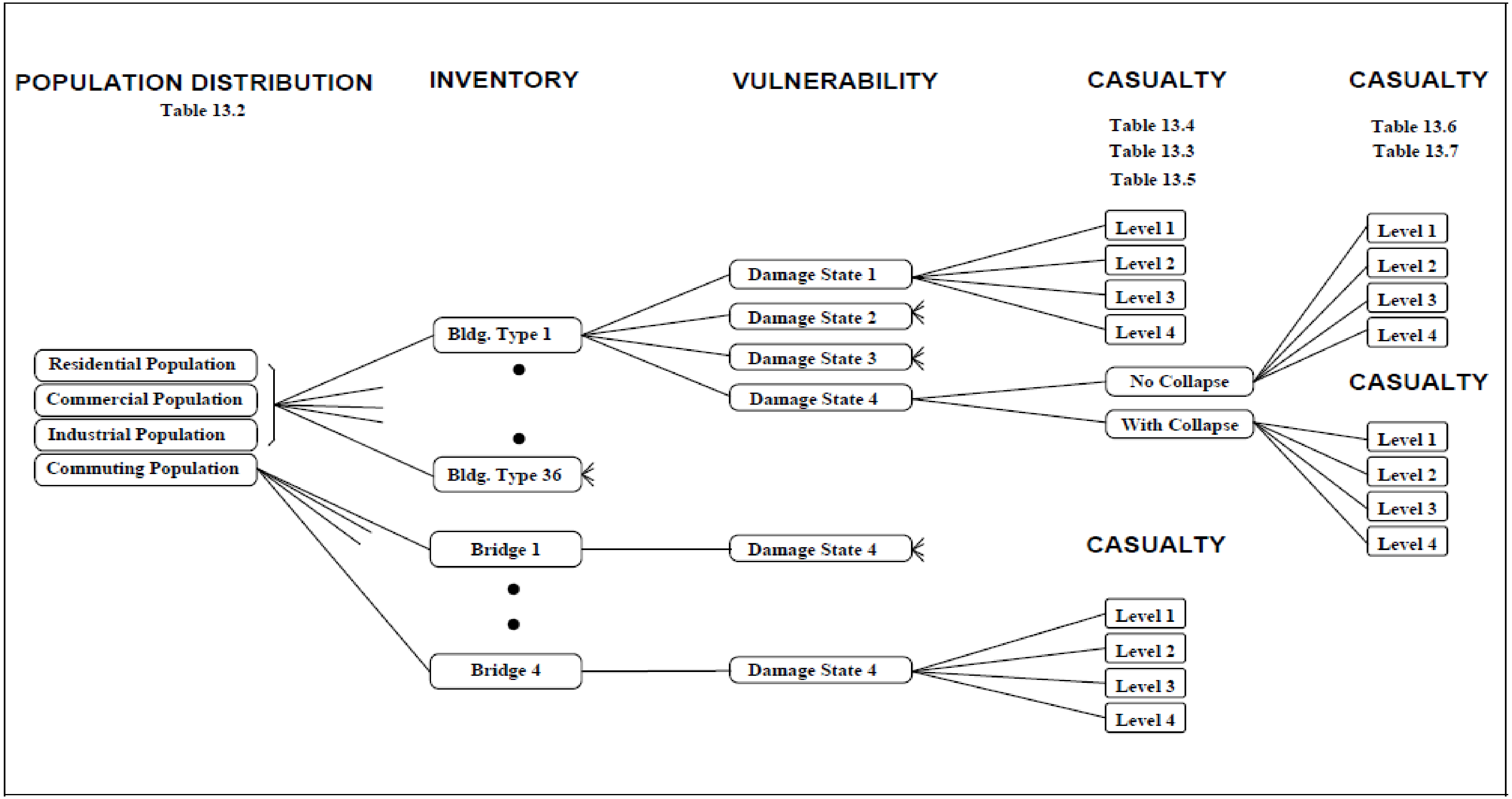

Figure 4-4: Indoor Casualty Methodology Event Tree (FEMA, 2003)

4.5 Displaced Household and Short-term Shelter Needs

The number of uninhabitable dwellings can also be estimated in HAZUS. It is based on the assumption that the total number to displaced household is the sum of complete damaged dwellings and 90% of the extensive damaged multifamily dwellings (Perkins, 1992). The number of household is then calculated based on the ratio of total household and total dwelling units.

The number of people seeking short term shelters is affected by several factors: age, ownership, income and ethnic of the population. The population is divided into subgroups according to these factors. The percentage of population seeking shelters within each subgroup is given in HAZUS based on the research of George Washington University under contract with the Red Cross (Harrald, et al., 1991). The sum of the results from each subgroup is calculated as the total population seeking short-term shelter needs.

Chapter 5. Results and Discussions

Based on deaggregation results, a total of 38 scenarios were run in HAZUS. The scenarios investigated the most likely contributing events to a 2% in 50 years seismic hazard. Three GMPEs are used in these scenarios to investigate the sensitivity of the results. The outputs of each scenario consist of direct physical damage to general building stock and essential facilities, direct economic losses, and direct social losses such as number of casualties and shelter needs. The results are presented and discussed in this chapter.

5.1 Direct Physical Damage

Direct physical damage to the general building stock for a particular scenario is presented as the number of buildings damaged by occupancy and by building type. The number of damaged building is calculated for each damage state at census tract level. A thematic map can be drawn to visualize the level of damage at different locations in Montreal. The results of all 38 scenarios are aggregated at different damage states for the whole study region, and compared in the following section.

5.1.1 Building Damage by Scenario

As shown in Table 5-1 to Table 5-6, the building damage results from scenarios of different magnitudes and locations are summarized for each GMPE. Within each GMPE, the weighted average of scenarios in both North-West and South-West are calculated using the same weights based on their contribution factor from deaggregation results. Table 5-1, 5-3 and 5-5 indicates the number of building damaged at four different damage levels. Table 5-2, 5-4 and 5-6 indicates the same results in terms of percentage of the total building stock. Graphic representations of the results are shown in Figure 5-1 to 5-6.

Table 5-1: Number of Building Damaged at Each Damage Level for Scenarios using AB95 Ground Motion Prediction Equation

Scenarios	Slight	Moderate	Extensive	Complete	Contribution Factor	Weight
AB95_30NW5.3	3563	931	128	13	12.06	17.0%
AB95_30NW5.7	8941	2483	431	52	14.84	21.0%
AB95_30NW6	24131	7744	1527	213	14.75	20.8%
AB95_30NW6.3	42428	16105	3668	605	12.21	17.2%
AB95_30NW6.7	63665	29712	7989	1582	9.12	12.9%
AB95_50NW7	57308	24672	5785	1053	7.81	11.0%
Weighted Avg	**29352**	**11620**	**2730**	**482**		
AB95_30SW5.3	4607	1179	188	22	12.06	17.0%
AB95_30SW5.7	10798	3071	608	89	14.84	21.0%
AB95_30SW6	26476	9142	2130	364	14.75	20.8%
AB95_30SW6.3	43699	18143	4754	926	12.21	17.2%
AB95_30SW6.7	62374	31971	9565	2206	9.12	12.9%
AB95_50SW7	56351	24519	5735	1065	7.81	11.0%
Weighted Avg	**30355**	**12703**	**3288**	**660**		
Total Weighted Avg	**29854**	**12162**	**3009**	**571**		

Table 5-2: Percentage Damage of Total Building Number at Each Damage Level for Scenarios using AB95 Ground Motion Prediction Equation

Scenarios	Slight	Moderate	Extensive	Complete	Contribution Factor	Weight
AB95_30NW5.3	1.13%	0.30%	0.04%	0.00%	12.06	17%
AB95_30NW5.7	2.84%	0.79%	0.14%	0.02%	14.84	21%
AB95_30NW6	7.66%	2.46%	0.48%	0.07%	14.75	21%
AB95_30NW6.3	13.46%	5.11%	1.16%	0.19%	12.21	17%
AB95_30NW6.7	20.20%	9.43%	2.53%	0.50%	9.12	13%
AB95_50NW7	18.18%	7.83%	1.84%	0.33%	7.81	11%
Weighted Avg	9.31%	3.69%	0.87%	0.15%		
AB95_30SW5.3	1.46%	0.37%	0.06%	0.01%	12.06	17%
AB95_30SW5.7	3.43%	0.97%	0.19%	0.03%	14.84	21%
AB95_30SW6	8.40%	2.90%	0.68%	0.12%	14.75	21%
AB95_30SW6.3	13.87%	5.76%	1.51%	0.29%	12.21	17%
AB95_30SW6.7	19.79%	10.14%	3.04%	0.70%	9.12	13%
AB95_50SW7	17.88%	7.78%	1.82%	0.34%	7.81	11%
Weighted Avg	9.63%	4.03%	1.04%	0.21%		
Total Weighted Avg	**9.47%**	**3.86%**	**0.95%**	**0.18%**		

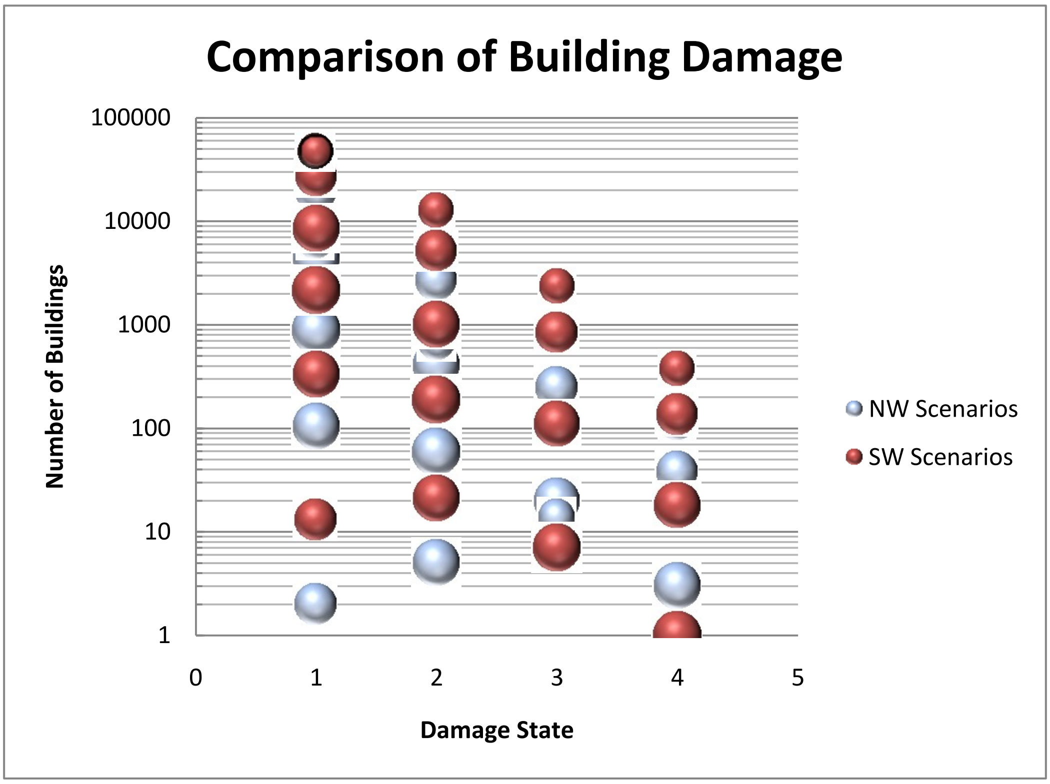

Figure 5-1: Number of Building Damaged at Each Damage Level for Scenarios using AB95 Ground Motion Prediction Equation

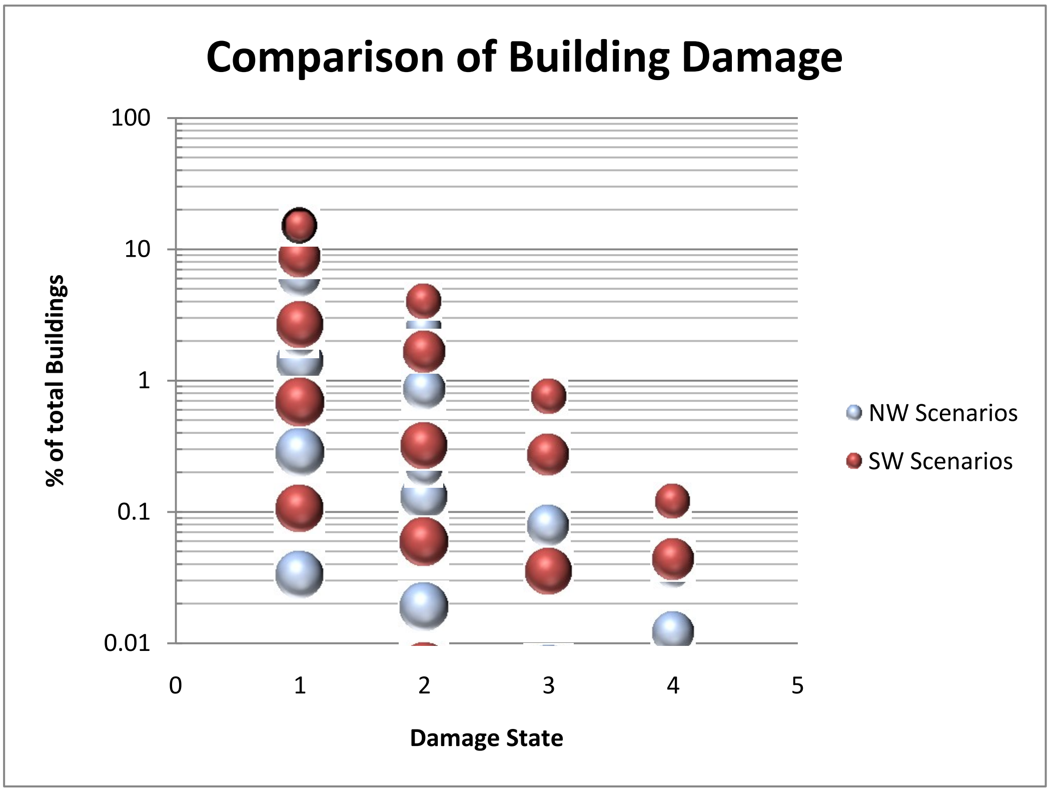

Figure 5-2: Percentage Damage of Total Building Number at Each Damage Level for Scenarios using Ground Motion Prediction Equation

Table 5-3: Number of Building Damaged at Each Damage Level for Scenarios using AB06 Ground Motion Prediction Equation

Scenarios	Slight	Moderate	Extensive	Complete	Contribution Factor	Weight
AB06_30NW5.3	2	0	0	0	9.9	13.9%
AB06_30NW5.7	104	5	0	0	12.4	17.4%
AB06_30NW6	893	59	0	0	13.2	18.5%
AB06_30NW6.3	4405	410	20	3	12.2	17.1%
AB06_30NW6.7	19675	2711	247	38	9.6	13.4%
AB06_30NW7	42368	7861	852	113	6.9	9.7%
AB06_50NW7	6514	678	14	0	7.2	10.1%
Weighted Avg	**8333**	**1274**	**120**	**17**		
AB06_30SW5.3	13	0	0	0	9.9	13.9%
AB06_30SW5.7	331	21	0	0	12.4	17.4%
AB06_30SW6	2145	187	7	1	13.2	18.5%
AB06_30SW6.3	8425	997	110	18	12.2	17.1%
AB06_30SW6.7	27480	5157	849	136	9.6	13.4%
AB06_30SW7	47516	12592	2369	376	6.9	9.7%
AB06_50SW7	7416	789	22	0	7.2	10.1%
Weighted Avg	**10930**	**2198**	**365**	**58**		
Total Weighted Avg	**9631**	**1736**	**243**	**37**		

Table 5-4: Percentage Damage of Total Building Number at Each Damage Level for Scenarios using AB06 Ground Motion Prediction Equation

Scenarios	Slight	Moderate	Extensive	Complete	Contribution Factor	Weight
AB06_30NW5.3	0.00%	0.00%	0.00%	0.00%	9.9	13.9%
AB06_30NW5.7	0.03%	0.00%	0.00%	0.00%	12.4	17.4%
AB06_30NW6	0.28%	0.02%	0.00%	0.00%	13.2	18.5%
AB06_30NW6.3	1.40%	0.13%	0.01%	0.00%	12.2	17.1%
AB06_30NW6.7	6.24%	0.86%	0.08%	0.01%	9.6	13.4%
AB06_30NW7	13.44%	2.49%	0.27%	0.04%	6.9	9.7%
AB06_50NW7	2.07%	0.22%	0.00%	0.00%	7.2	10.1%
Weighted Avg	2.64%	0.40%	0.04%	0.01%		
AB06_30SW5.3	0.00%	0.00%	0.00%	0.00%	9.9	13.9%
AB06_30SW5.7	0.11%	0.01%	0.00%	0.00%	12.4	17.4%
AB06_30SW6	0.68%	0.06%	0.00%	0.00%	13.2	18.5%
AB06_30SW6.3	2.67%	0.32%	0.03%	0.01%	12.2	17.1%
AB06_30SW6.7	8.72%	1.64%	0.27%	0.04%	9.6	13.4%
AB06_30SW7	15.08%	4.00%	0.75%	0.12%	6.9	9.7%
AB06_50SW7	2.35%	0.25%	0.01%	0.00%	7.2	10.1%
Weighted Avg	3.47%	0.70%	0.12%	0.02%		
Total Weighted Avg	**3.06%**	**0.55%**	**0.08%**	**0.01%**		

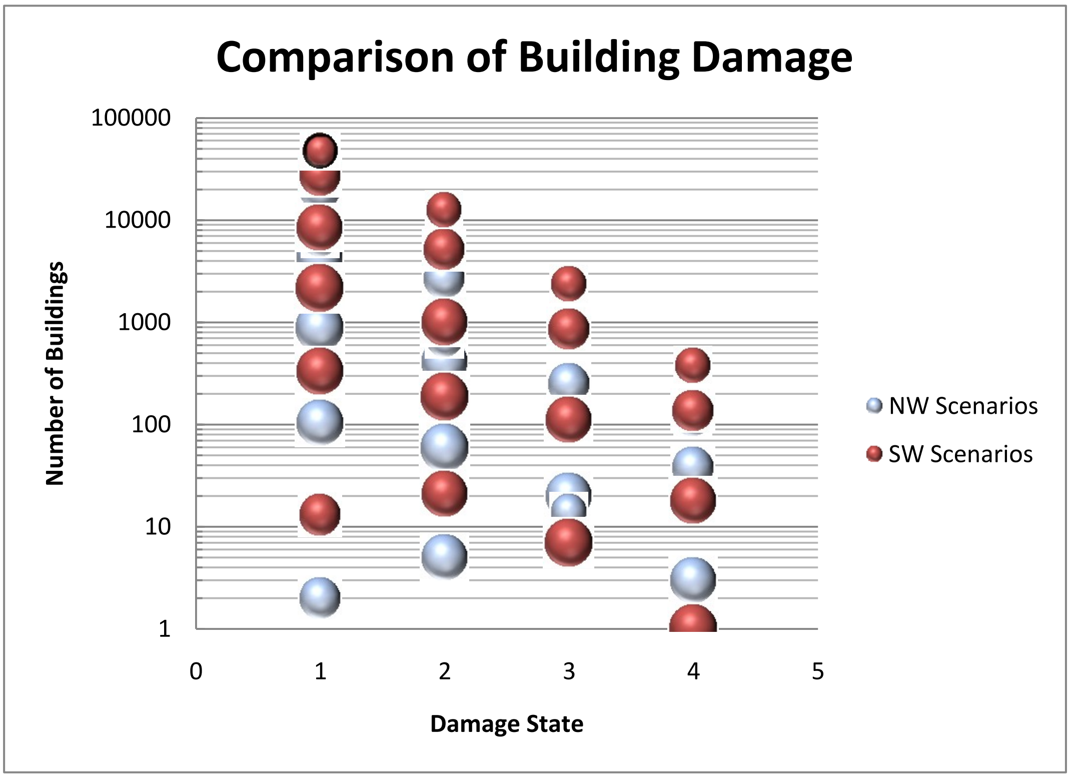

Figure 5-3: Number of Building Damaged at Each Damage Level for Scenarios using AB06 Ground Motion Prediction Equation

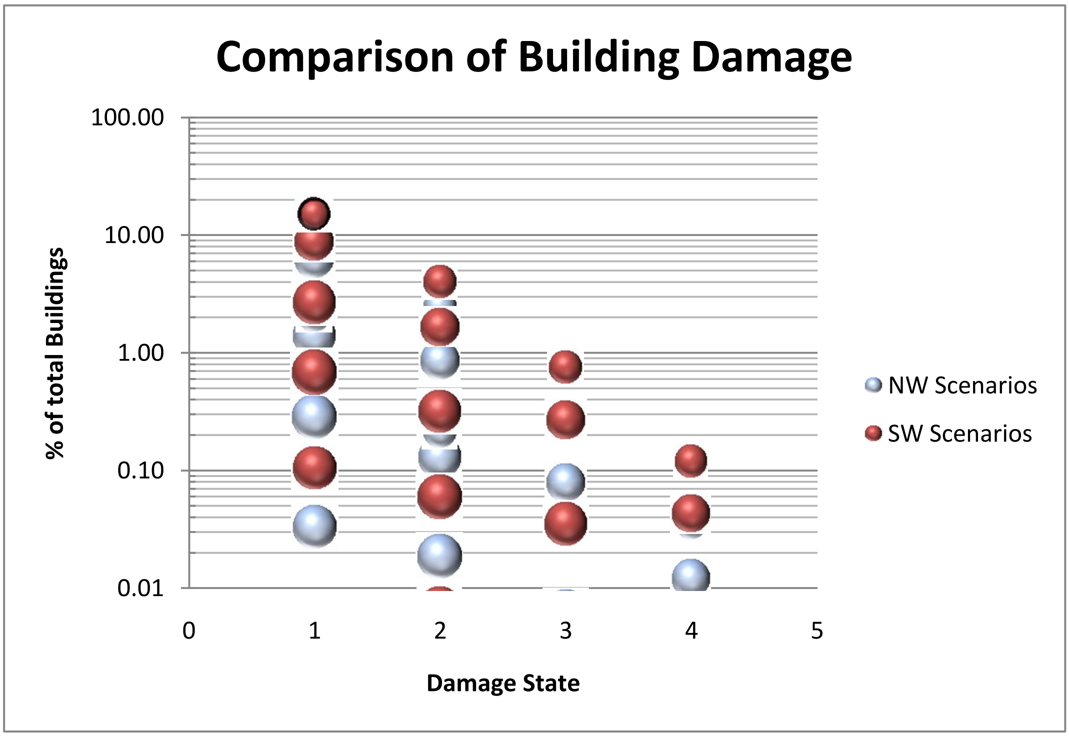

Figure 5-4: Percentage Damage of Total Building Number at Each Damage Level for Scenarios using AB06 Ground Motion Prediction Equation

Table 5-5: Number of Building Damaged at Each Damage Level for Scenarios using A08 Ground Motion Prediction Equation

Scenarios	Slight	Moderate	Extensive	Complete	Contribution Factor	Weight
A08_30NW5.3	0	0	0	0	7.2	15.0%
A08_30NW5.7	14	1	4	0	8.7	18.1%
A08_30NW6	98	13	37	9	9.6	20.0%
A08_30NW6.3	483	67	155	37	8.9	18.5%
A08_30NW6.7	2591	318	437	105	7.6	15.8%
A08_50NW7	1108	127	206	49	6.1	12.7%
Weighted Avg	**661**	**82**	**132**	**31**		
A08_30SW5.3	2	0	0	0	7.2	15.0%
A08_30SW5.7	39	4	9	1	8.7	18.1%
A08_30SW6	224	22	38	8	9.6	20.0%
A08_30SW6.3	915	105	154	37	8.9	18.5%
A08_30SW6.7	4118	528	586	140	7.6	15.8%
A08_50SW7	1115	123	196	47	6.1	12.7%
Weighted Avg	**1013**	**124**	**155**	**37**		
Total Weighted Avg	**837**	**103**	**144**	**34**		

Table 5-6: Percentage Damage of Total Building Number at Each Damage Level for Scenarios using A08 Ground Motion Prediction Equation

Scenarios	Slight	Moderate	Extensive	Complete	Contribution Factor	Weight
A08_30NW5.3	0.00%	0.00%	0.00%	0.00%	7.2	15.0%
A08_30NW5.7	0.00%	0.00%	0.00%	0.00%	8.7	18.1%
A08_30NW6	0.03%	0.00%	0.01%	0.00%	9.6	20.0%
A08_30NW6.3	0.15%	0.02%	0.05%	0.01%	8.9	18.5%
A08_30NW6.7	0.82%	0.10%	0.14%	0.03%	7.6	15.8%
A08_50NW7	0.35%	0.04%	0.07%	0.02%	6.1	12.7%
Weighted Avg	0.21%	0.03%	0.04%	0.01%		
A08_30SW5.3	0.00%	0.00%	0.00%	0.00%	7.2	15.0%
A08_30SW5.7	0.01%	0.00%	0.00%	0.00%	8.7	18.1%
A08_30SW6	0.07%	0.01%	0.01%	0.00%	9.6	20.0%
A08_30SW6.3	0.29%	0.03%	0.05%	0.01%	8.9	18.5%
A08_30SW6.7	1.31%	0.17%	0.19%	0.04%	7.6	15.8%
A08_50SW7	0.35%	0.04%	0.06%	0.01%	6.1	12.7%
Weighted Avg	0.32%	0.04%	0.05%	0.01%		
Total Weighted Avg	**0.27%**	**0.03%**	**0.05%**	**0.01%**		

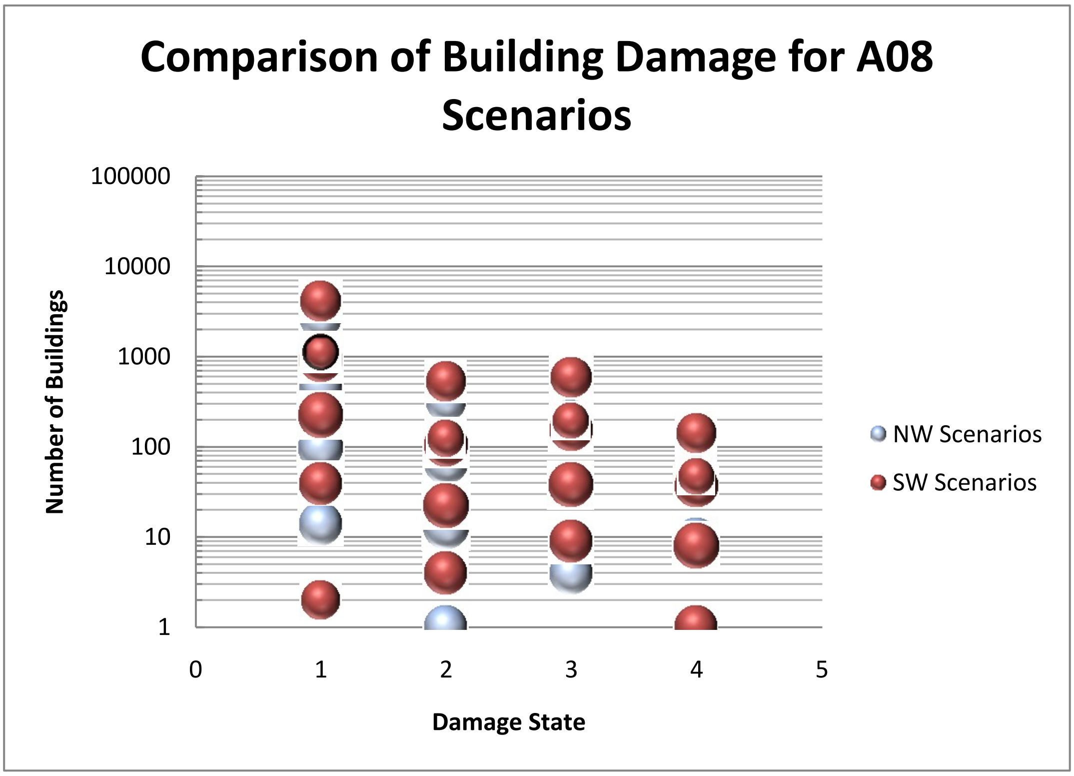

Figure 5-5: Number of Building Damaged at Each Damage Level for Scenarios using A08 Ground Motion Prediction Equation

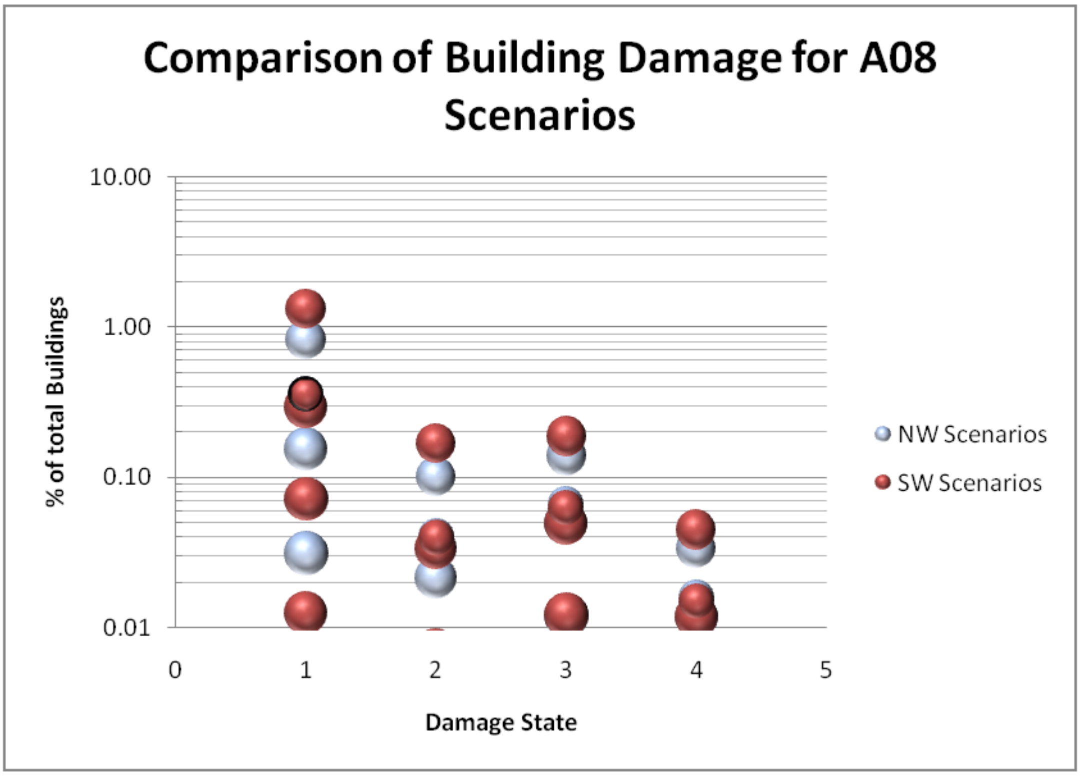

Figure 5-6: Percentage Damage of Total Building Number at Each Damage Level for Scenarios using A08 Ground Motion Prediction Equation

It is observed that the difference between minimum damage and maximum damage is very large for all four damage levels within each GMPE group. For example, the number of building with slight damage ranges from 2 to 42368 within all scenarios using AB06 GMPE. In general, damage increases as magnitude increases. By plotting the number of building damaged versus magnitude for a scenario, it is observed that the damage level is very sensitive towards the change in magnitude within certain magnitude range (Figure 5-7). For scenarios using AB95 GMPE, the slope of the damage-magnitude curve increases around magnitude 5.7, indicating an increasing rate of damage for higher magnitude events. The damage is more sensitive to the increase in magnitude at higher magnitude than at lower magnitude. For example, an increase of 0.2 in magnitude from 6.0 to 6.2 doubles the number of buildings suffering slight damage while such increase from 5.3 to 5.5 only causes 50% more in building damages. As for AB06 and A08 GMPEs, this trend is also observed, but at a higher magnitude level around 6.3.

Scenarios with the same magnitude and distance can result in different damages if the events happen at different locations around the island. For the same magnitude and distance, two scenarios were produced at north-west and south-west of Montreal. The south-west scenario generally results in slightly higher damage than the north-west scenario. Possible explanation is that building density is higher in the southern side of the island. By locating the earthquake scenario closer to this region, more damages are expected.

Generally, during an earthquake, the number of buildings suffering slight damage is always the highest, followed by buildings with moderate, extensive and complete damage. This is true for AB95 and AB06 scenarios. The number of damaged buildings decreases as damage severity level increases. The trend is presented as following:

$$Slight\ Damage > Moderate\ Damage > Extensive\ Damage > Complete\ Damage$$

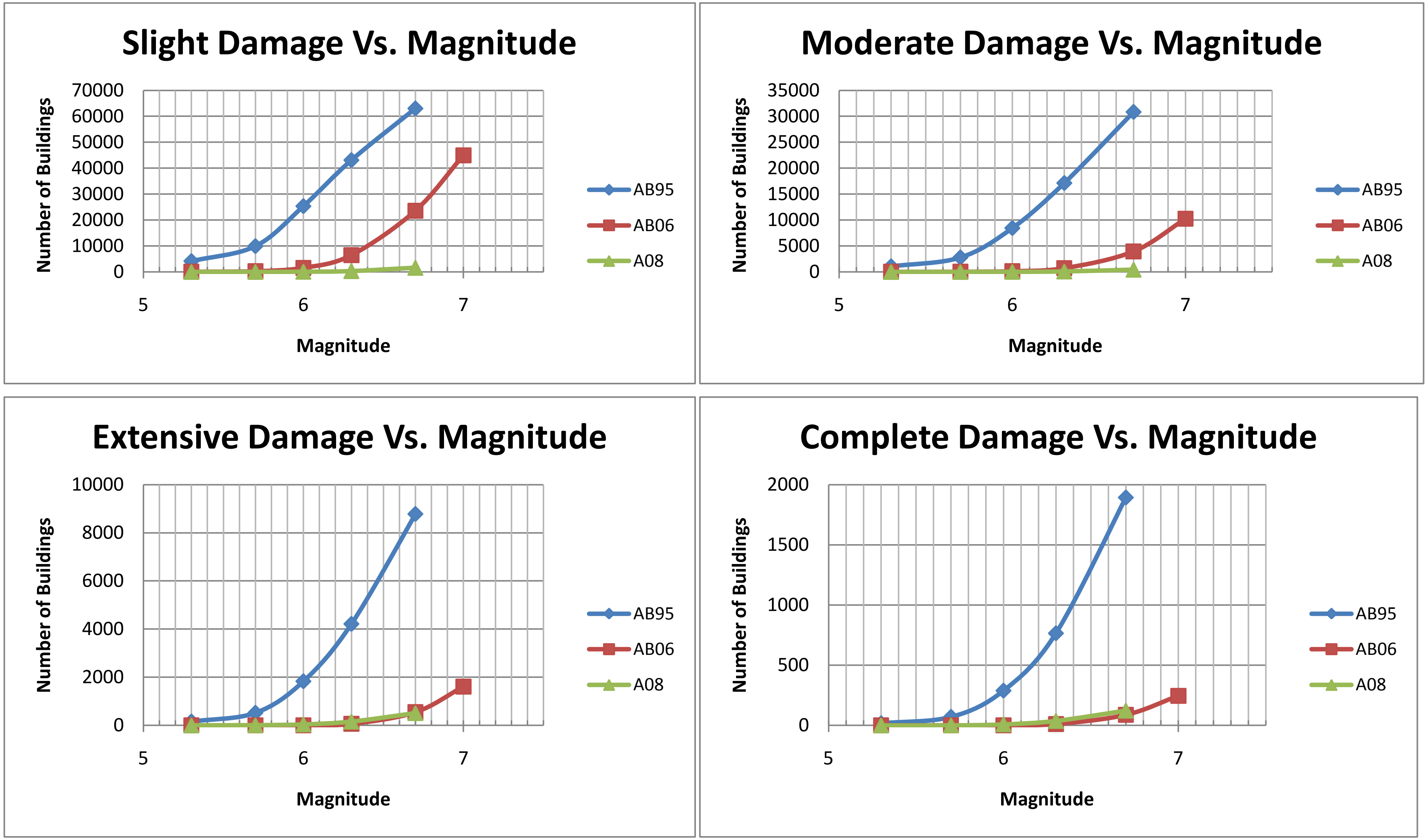

Figure 5-7: HAZUS Estimated Number of Damaged Building as a Function of Earthquake Magnitude at Slight, Moderate, Extensive and Complete Damage Level

However, for scenarios using A08 GMPE, the result shows a reverse trend for moderate and extensive damages. In A08, the number of extensively damaged buildings is higher than the number of moderately damaged buildings. This is due to the unique shape of the response spectrum of A08 and the method HAZUS used to process such information. As explained in Chapter 4, when evaluating the physical damage of buildings, HAZUS considers damages caused by both ground shaking and ground failure. While ground shaking is characterized by standardized response spectrum, ground failure is represented by permanent ground displacement (PGD). By HAZUS default methods, PGD is caused by liquefaction and landslide, and calculated as a function of peak ground acceleration (PGA). The higher PGA is, the larger PGD will be. Shown in the Figure 5-8, the PGA predicted by A08 is 0.63g at soil class C site for a 2% in 50 year hazard. This value is much higher than the PGA predicted by AB95 and AB06, which are 0.44g and 0.31g respectively. The high PGA value of A08 results in a high PGD, contributing to the damage caused by ground failure. In HAZUS, such damage only includes extensive and complete damage. Slight and moderate damage are assumed not likely to occur due to ground failure (FEMA, 2003). By adding up the damages from ground failure and ground shaking, extensive and complete damages are higher due to the large contribution of ground failure.

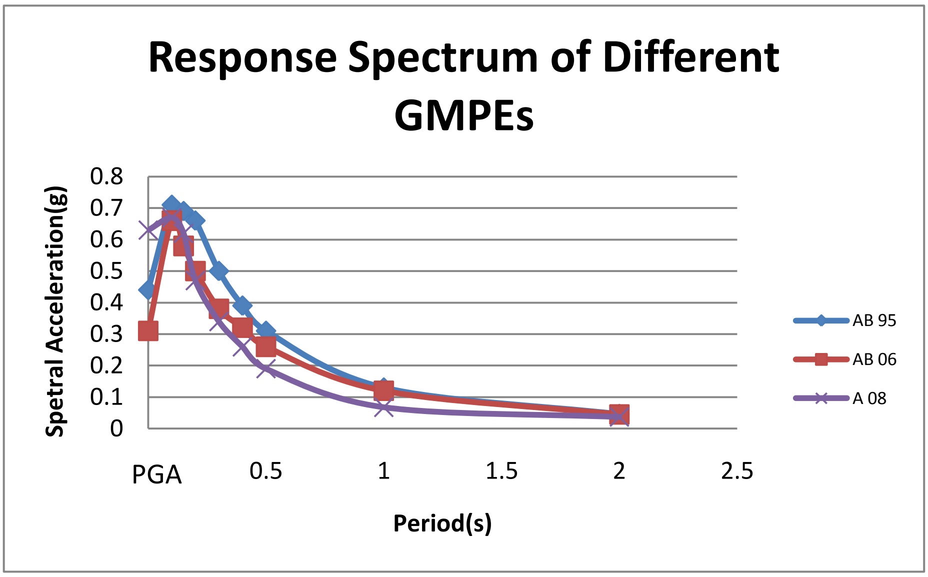

Figure 5-8: Comparison of Response Spectrum of AB95, AB06 and A08 at Soil Class C site

For two scenarios at the same location and magnitude, using different GMPEs can result in very different outcomes. In general, AB95 produces the highest damage, followed by AB06 and A08. The only exceptions are the low and moderate magnitude scenarios, where A08 scenarios have higher extensive and complete damage than AB06 scenarios for the reason explained above. An example is given in Figure 5-9. By using AB95, the number of moderate damaged buildings is 10 times bigger than the result of AB06 scenario, which itself is 10 times bigger than the result of A08. This trend is observed in all scenarios of different magnitudes and locations.

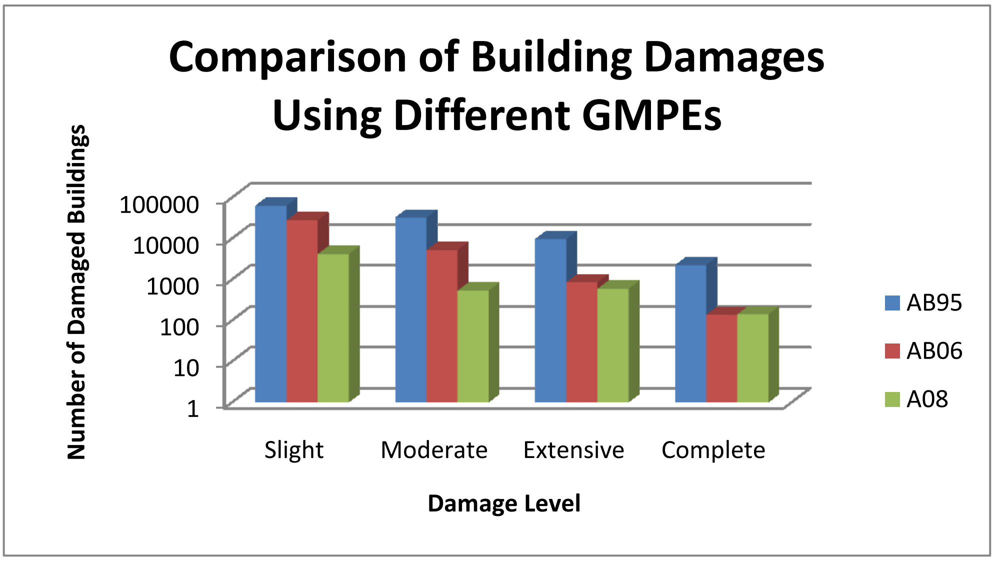

Figure 5-9: Comparison of Number of Damaged Building at Four Damage Level Using Different GMPEs for Scenario Earthquake of Magnitude 6.7 and Distance 30 km South-West of Montreal

This is expected since AB95 gives the highest ground motion predictions and AB08 gives the lowest for the same scenario in general. The standardized response spectrums of AB95, AB06, and A08 on soil class C are shown in Figure 5-10. As explained in Chapter4, the ground motions predicted by different GMPEs are generalized into a standard response spectrum in HAZUS. The spectrum curve was determined by spectral acceleration at 0.3s (S_a(0.3s)) and 1.0s(S_a(1.0s)). Having the highest values at these two periods, AB95 therefore gives the highest ground motion predictions. Compared to AB06, although A08 predicts similar ground motion at 0.3s, it has a significantly low ground motion prediction at 1.0s period. This shifts the standard response spectrum curve of A08 to the left, resulting in a lower spectrum displacement in building response. Compared to AB95 and AB06, the standard response spectrum of A08 is significantly lower than the original response spectrum. This indicates that the standard response spectrum of HAZUS underestimates the ground motion predicted by A08. This explains the low physical damage estimated in all A08 scenarios. However, the large variation in damage results indicates that HAZUS is very dependent on the choice of GMPEs. Any uncertainty in a GMPE will significantly influence the damage estimated by HAZUS.

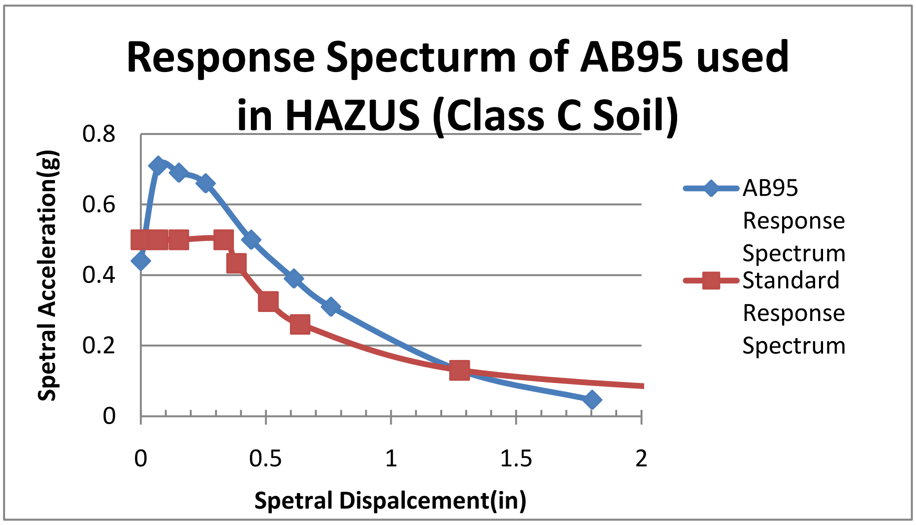

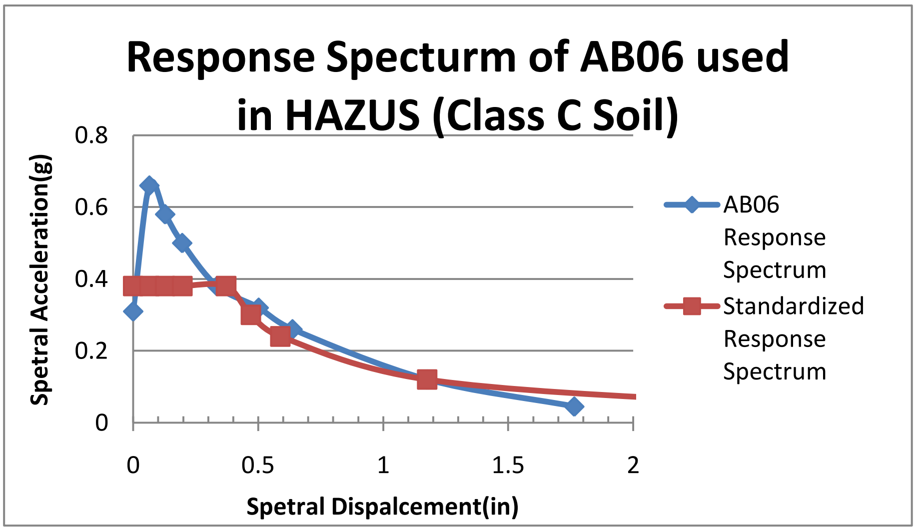

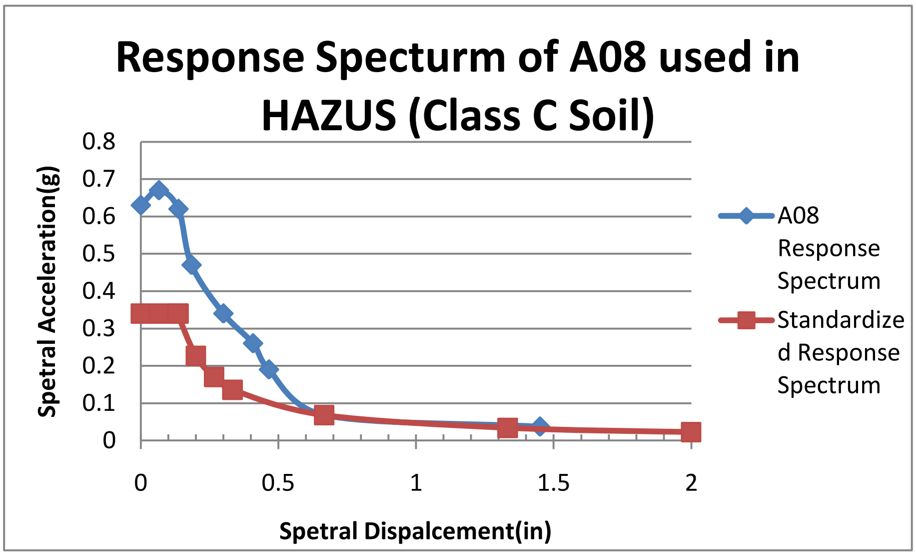

Figure 5-10: Comparison of Standard Response Spectrum used in HAZUS for AB95, AB06 and A08 GMPEs.

In order to analyze the effect of different GMPEs, a weighted average of building damage is calculated. Shown in the event tree below, equal weights are assigned to the North-West and South-West scenarios for the same magnitude and distance. This is because earthquakes in both directions are located in the same seismic source zone (IRM), and hence have equal occurrence probability. Scenarios of different magnitude and distance are assigned weights based on the 2% in 50 years magnitude-distance deaggregation results of each GMPE. A weight is also assigned to each GMPE based on its reliability. AB06 is given the highest weight of 0.5 since it is considered to be the most accurate model among these three (Atkinson, 2008). AB95 and A08 are both assigned a weight of 0.25. The overall weight of each scenario is the product of the weights from location, deaggregation, and GMPEs.

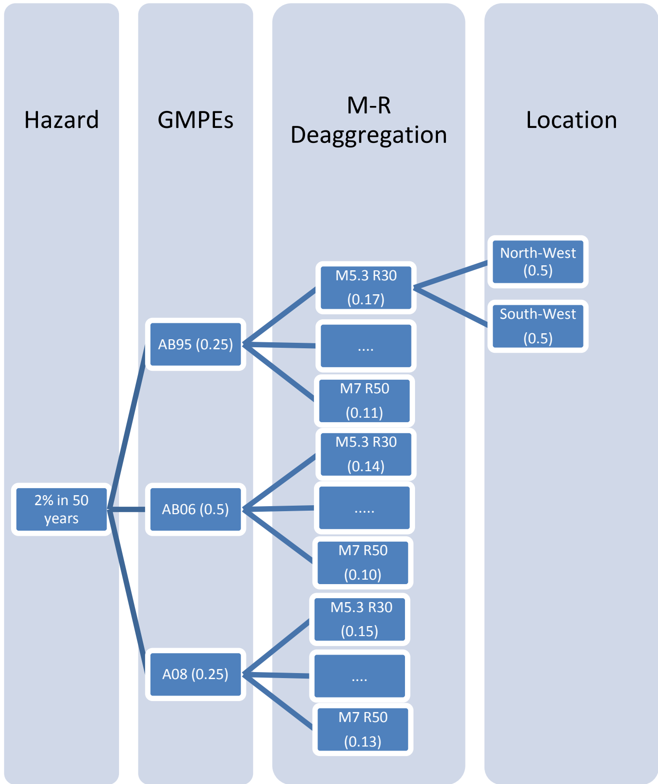

Figure 5-11: Event Tree Showing Scenarios and Their Weights

The distribution of slight damage results are shown in Figure 5-12, similar plots of moderate, extensive, and complete damages are available in Appendix E. It is observed that all three GMPEs have normal distributions where AB95 has the highest expected value, and A08 has the lowest expected value. The weighted average results of direct physical damage caused by a 2% in 50 years hazard are listed in Table 5-7. From the results, it is expected that about 12500 buildings will be slightly damaged, which is 4% of the total building stock in Montreal. 4000 or 1% of the buildings will be moderately damaged. Less than 1% of the buildings will suffer extensive and complete damage. As noticed in Table 5-7, these results are of highly variable, since the standard deviation is very large. Therefore, these results are considered to be approximate estimations, and only provide preliminary assessments of the seismic vulnerability of Montreal. When using these results, one should keep in mind the various uncertainties involved in the process.

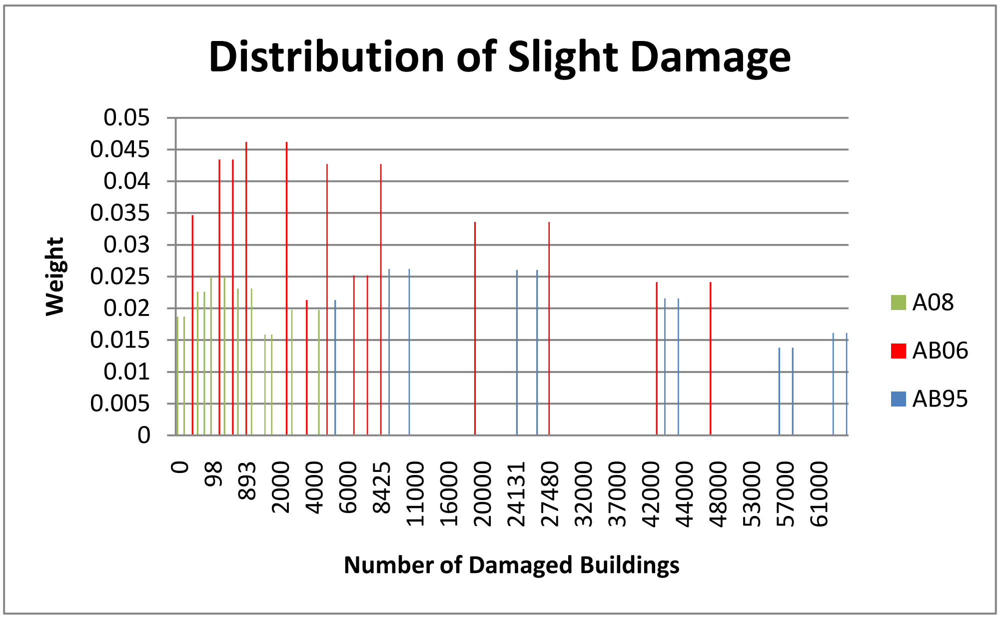

Figure 5-12: Distribution of Slight Damage Results from all Scenarios

Table 5-7: Summary of Weighted Average Damage of all Damage Levels from Direct Physical Damage Results

GMPEs	Slight		Moderate		Extensive		Complete	
	# of Buildings Damaged	% of Total Building	# of Buildings Damaged	% of Total Building	# of Buildings Damaged	% of Total Building	# of Buildings Damaged	% of Total Building
AB95	29854	9.47%	12162	3.86%	3009	0.95%	571	0.18%
AB06	9631	3.06%	1736	0.55%	243	0.08%	37	0.01%
A08	837	0.27%	103	0.03%	144	0.05%	34	0.01%
Weighted Average	**12488**	**3.96%**	**3934**	**1.25%**	**910**	**0.29%**	**170**	**0.05%**
Weighted Std Dev.	**17993**	**5.71%**	**7438**	**2.36%**	**1937**	**0.61%**	**397**	**0.13%**

5.1.2 Building Damage by Occupancy and Structural Type

Using the same weights, the weighted average of building damage by occupancy and structural type is calculated and summarized in Table 5-8, and Table 5-9. Shown in Figure 5-13 and Figure 5-14, most of the damage occurs in residential buildings and wood buildings. This is expected since 95% of the buildings in Montreal are residential buildings, and among these, wood single family houses are the most common ones. For a 2% in 50 years hazard, 9380 or 6% of single family buildings are estimated to suffer damage, followed by 6820 (5%) of multi-family residential buildings. In terms of structural type, 9618(4%) wood buildings are expected to be damaged, followed by 5887(10%) unreinforced masonry buildings. This is also expected, since unreinforced masonry buildings are proven to perform poorly in an earthquake (Lefebvre, 2004).

Table 5-8: Summary of Number of Damaged Buildings by Occupancy Type

GMPEs	Commercial	Education	Government	Industrial	OtherResidential	Religion	SingleFamily
AB95	1774	115	75	512	19371	175	23574
	17%	15%	16%	18%	13%	17%	16%
AB06	482	31	20	137	3956	49	6973
	5%	4%	4%	5%	3%	5%	5%
A08	63	3	2	17	394	6	633
	1%	0%	0%	1%	0%	1%	0%
Weighted Average	700	44	29	196	6820	68	9380
	7%	6%	6%	7%	5%	7%	6%

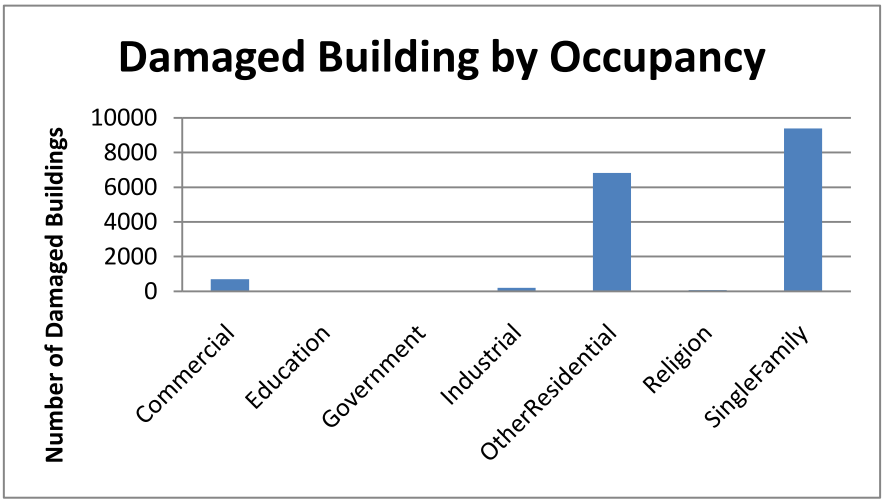

Figure 5-13: Weighted Average Number of Damaged Buildings by Occupancy Type

Table 5-9: Summary of Number of Damaged Buildings by Structural Type

GMPEs	Wood	Steel	Concrete	Precast	RM	URM	MH
AB95	26715	1629	1375	147	1945	13785	1
	12%	14%	16%	22%	14%	24%	20%
AB06	5695	362	326	44	339	4881	0
	3%	3%	4%	6%	2%	9%	9%
A08	366	37	21	5	26	663	0
	0%	0%	0%	1%	0%	1%	0%
Weighted Average	9618	588	506	59	656	5887	0
	4%	5%	6%	9%	5%	10%	10%

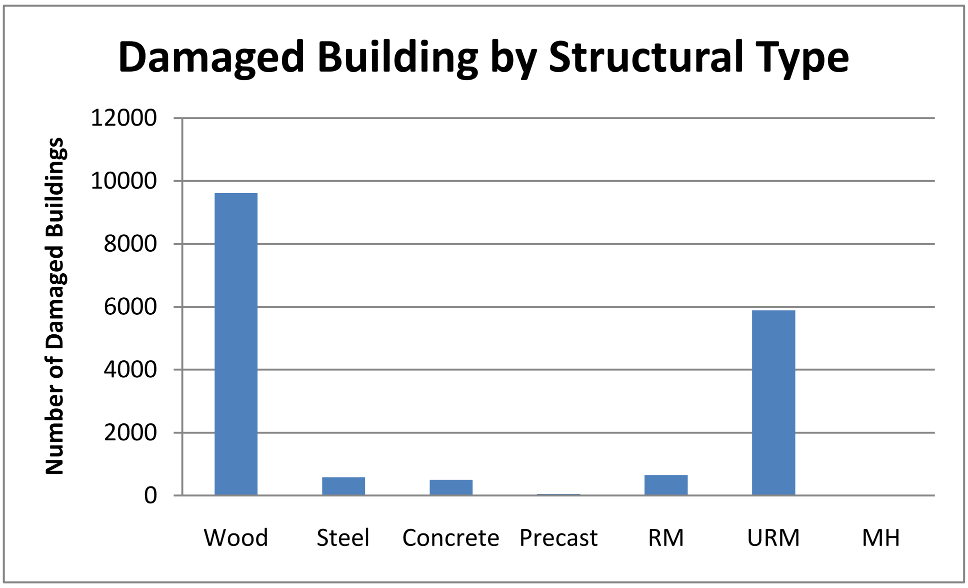

Figure 5-14: Weighted Average Number of Damaged Buildings by Structural Type

5.2 Building Direct Economic Losses

The estimated building direct economic losses (structural, non-structural, content and inventory) are analyzed for all the scenarios. Shown in Table 5-10, the direct economic losses are in the range of 1.42 million to 8.7 billion depending on the magnitude and GMPE chosen. The direct economic losses are related to the level of physical damage suffered in an earthquake. Comparing results for different GMPEs, AB95 results have the largest economic losses with a weighted average of 3.4 billion dollars. AB06 and A08 scenarios give similar levels of losses, with weighted averages of 0.76 billion and 0.7 billion losses respectively. The large difference in economic losses is expected since AB95 scenarios have much higher building damages compared to AB06 and A08 scenarios. Although AB06 scenarios have higher slight and moderate damages than A08 scenarios, the economic losses of AB06 scenarios are only slightly higher than A08 scenarios. This indicates that buildings with slight and moderate damages suffer much smaller economic losses than buildings with extensive and complete damages in HAZUS methodology.

Table 5-10: Direct Building Related Losses in Million Dollars

GMPEs	AB06			A08			AB95		
	Scenarios	**Capital Loss**	**Weight**	**Scenarios**	**Capital Loss**	**Weight**	**Scenarios**	**Capital Loss**	**Weight**
North-West Scenarios	AB06_30NW5.3	$ 1.42	14%	A08_30NW5.3	$ 21.12	15%	AB95_30NW5.3	$ 335.01	15%
	AB06_30NW5.7	$ 23.25	17%	A08_30NW5.7	$ 115.00	18%	AB95_30NW5.7	$ 830.06	18%
	AB06_30NW6	$ 118.05	18%	A08_30NW6	$ 337.66	20%	AB95_30NW6	$ 2,193.92	20%
	AB06_30NW6.3	$ 415.30	17%	A08_30NW6.3	$ 821.44	19%	AB95_30NW6.3	$ 4,167.91	19%
	AB06_30NW6.7	$ 1,493.43	13%	A08_30NW6.7	$ 1,963.12	16%	AB95_30NW6.7	$ 7,165.78	16%
	AB06_30NW7	$ 2,956.28	10%						
	AB06_50NW7	$ 355.04	10%	A08_50NW7	$ 1,036.19	13%	AB95_50NW7	$ 4,567.03	13%
	Weighted Avg	**$ 619.31**		**Weighted Avg**	**$ 684.94**		**Weighted Avg**	**$ 3,120.76**	
South-West Scenarios	AB06_30SW5.3	$ 11.76	14%	A08_30SW5.3	$ 34.40	15%	AB95_30SW5.3	$ 505.45	15%
	AB06_30SW5.7	$ 75.41	17%	A08_30SW5.7	$ 151.68	18%	AB95_30SW5.7	$ 1,146.49	18%
	AB06_30SW6	$ 247.43	18%	A08_30SW6	$ 377.90	20%	AB95_30SW6	$ 2,808.75	20%
	AB06_30SW6.3	$ 725.02	17%	A08_30SW6.3	$ 867.92	19%	AB95_30SW6.3	$ 4,953.85	19%
	AB06_30SW6.7	$ 2,214.71	13%	A08_30SW6.7	$ 2,136.12	16%	AB95_30SW6.7	$ 8,217.18	16%
	AB06_30SW7	$ 3,978.69	10%						
	AB06_50SW7	$ 385.98	10%	A08_50SW7	$ 995.33	13%	AB95_50SW7	$ 4,641.84	13%
	Weighted Avg	**$ 905.55**		**Weighted Avg**	**$ 732.34**		**Weighted Avg**	**$ 3,647.25**	
	Overall Weighted Avg	**$ 762.43**		**Overall Weighted Avg**	**$ 708.64**		**Overall Weighted Avg**	**$ 3,384.00**	

5.3 Social Losses

5.3.1 Displaced Household and Short-Term Shelter Needs

Number of displaced household and the number of people seeking short-term shelters are summarized in Table 5-11 and Table 5-12 respectively. Compare scenarios with different GMPEs, AB95 scenarios have the highest estimations while AB06 scenarios have the lowest. Number of displaced household and number of people seeking short-term shelter are evaluated as functions of the number of extensive and complete damage buildings. Shown in section 5.1, AB95 scenarios have the highest extensive and complete building damage followed by A08 and AB06 scenarios. Therefore, these results are expected. Given the same weights as before, the estimated results from all scenarios using all three GMPEs are calculated. The estimated numbers of displaced household and people seeking short-term shelter are 2490 and 1388 respectively.

Table 5-11: Summary of Number of Displaced Household from All Scenarios

GMPEs	AB06			A08			AB95		
	Scenarios	Number of Displace Household	Weight	Scenarios	Number of Displace Household	Weight	Scenarios	Number of Displace Household	Weight
North-West Scenarios	AB06_30NW5.3	0	14%	A08_30NW5.3	0	15%	AB95_30NW5.3	339	15%
	AB06_30NW5.7	0	17%	A08_30NW5.7	27	18%	AB95_30NW5.7	1151	18%
	AB06_30NW6	5	18%	A08_30NW6	163	20%	AB95_30NW6	4251	20%
	AB06_30NW6.3	81	17%	A08_30NW6.3	613	19%	AB95_30NW6.3	10390	19%
	AB06_30NW6.7	809	13%	A08_30NW6.7	1864	16%	AB95_30NW6.7	23332	16%
	AB06_30NW7	2731	10%						
	AB06_50NW7	41	10%	A08_50NW7	883	13%	AB95_50NW7	17060	13%
	Weighted Avg	**392**		**Weighted Avg**	**557**		**Weighted Avg**	**8880**	
South-West Scenarios	AB06_30SW5.3	0	14%	A08_30SW5.3	0	15%	AB95_30SW5.3	335	15%
	AB06_30SW5.7	0	17%	A08_30SW5.7	25	18%	AB95_30SW5.7	1126	18%
	AB06_30SW6	7	18%	A08_30SW6	135	20%	AB95_30SW6	4107	20%
	AB06_30SW6.3	152	17%	A08_30SW6.3	540	19%	AB95_30SW6.3	9742	19%
	AB06_30SW6.7	1215	13%	A08_30SW6.7	1705	16%	AB95_30SW6.7	21377	16%
	AB06_30SW7	3200	10%						
	AB06_50SW7	34	10%	A08_50SW7	880	13%	AB95_50SW7	15196	13%
	Weighted Avg	**503**		**Weighted Avg**	**512**		**Weighted Avg**	**8181**	
	Overall Weighted Avg for AB06	**447**		**Overall Weighted Avg for A08**	**535**		**Overall Weighted Avg for AB95**	**8530**	

Estimated Displaced Households: 2490

Table 5-12: Summary of Number of People Seeking Short-term Shelter from All Scenarios

GMPEs	AB06			A08			AB95		
	Scenarios	Number of People Seeking Shelter	Weight	Scenarios	Number of People Seeking Shelter	Weight	Scenarios	Number of People Seeking Shelter	Weight
North-West Scenarios	AB06_30NW5.3	0	14%	A08_30NW5.3	0	15%	AB95_30NW5.3	190	15%
	AB06_30NW5.7	0	17%	A08_30NW5.7	13	18%	AB95_30NW5.7	651	18%
	AB06_30NW6	2	18%	A08_30NW6	87	20%	AB95_30NW6	2406	20%
	AB06_30NW6.3	43	17%	A08_30NW6.3	337	19%	AB95_30NW6.3	5851	19%
	AB06_30NW6.7	449	13%	A08_30NW6.7	1019	16%	AB95_30NW6.7	13137	16%
	AB06_30NW7	1547	10%						
	AB06_50NW7	22	10%	A08_50NW7	479	13%	AB95_50NW7	9509	13%
	Weighted Avg	**220**		**Weighted Avg**	**304**		**Weighted Avg**	**4991**	
South-West Scenarios	AB06_30SW5.3	0	14%	A08_30SW5.3	0	15%	AB95_30SW5.3	185	15%
	AB06_30SW5.7	0	17%	A08_30SW5.7	12	18%	AB95_30SW5.7	624	18%
	AB06_30SW6	3	18%	A08_30SW6	72	20%	AB95_30SW6	2282	20%
	AB06_30SW6.3	82	17%	A08_30SW6.3	286	19%	AB95_30SW6.3	5428	19%
	AB06_30SW6.7	633	13%	A08_30SW6.7	903	16%	AB95_30SW6.7	11916	16%
	AB06_30SW7	1740	10%						
	AB06_50SW7	18	10%	A08_50SW7	468	13%	AB95_50SW7	8440	13%
	Weighted Avg	**270**		**Weighted Avg**	**271**		**Weighted Avg**	**4553**	
	Overall Weighted Avg for AB06	**245**		**Overall Weighted Avg for A08**	**288**		**Overall Weighted Avg for AB95**	**4772**	

Estimated Number of People Seeking Short-term Shelter: 1388

5.3.2 Casualty Estimates

During the study, HAZUS failed to give casualty estimation for 85 of the 522 census tracts (Figure 5-15). Due to this technical problem, the casualty estimation of scenario 06M67R30SW was calculated using Excel based on HAZUS methodology. A simplified approach is used for all other scenarios: total casualties in the study region are extrapolated from the casualties of the 437 census tracts calculated by HAZUS. Based on the ratio of total population of the study region and population covered by HAZUS calculation at three time of a day, the multiplication factors used for 2AM, 2PM and 5PM are 1.19, 1.16 and 1.02 respectively. The comparison of these two approaches is presented in Table 5-13, where the casualty results of scenario 06M67R30SW are calculated using both approaches. It is observed that the results from both approaches are similar at all damage level. Therefore, the use of simplified approach is justified.

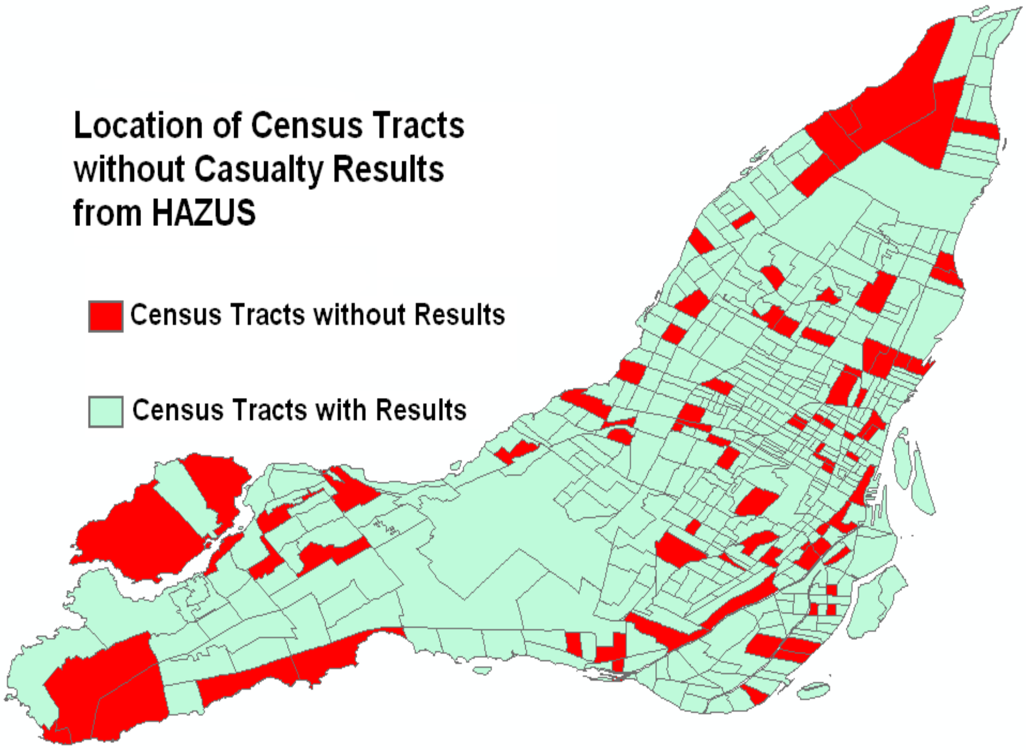

Figure 5-15: Location of Census Tracts Missing Casualty Estimates from HAZUS. The census tracts marked in red are the tracts HAZUS failed to give casualty estimates.

Table 5-13: Comparison of Casualty Estimations using HAZUS and Simplified Methods for Scenario 06M67R30SW

	Number of People Injured			
HAZUS	**Level1**	**Level2**	**Level3**	**Level4**
2am	252	31	2	4
2pm	420	68	7	14
5pm	279	42	4	8
Simplified	**Level1**	**Level2**	**Level3**	**Level4**
2am	262	34	2	5
2pm	425	71	7	15
5pm	249	40	3	8

The weighted average results from all scenarios using different GMPEs are given in Table 5-14. The casualty at 2 AM, 2 PM and 5 PM are estimated for all four injury levels. Based on these results, one could expect the largest casualty if an earthquake occurred during the middle of a day (2PM). Detailed results from individual scenarios can be found in Appendix F.

Table 5-14: Summary of Estimated Casualties at 2AM, 2PM and 5PM from Different GMPEs

	GMPE	Level1	Level2	Level3	Level4
2AM	**AB95**	1004	190	22	43
	AB06	41	4	0	0
	A08	46	9	1	2
	Weighted Avg.	**283**	**52**	**6**	**11**
2PM	**AB95**	1260	253	31	60
	AB06	137	20	2	4
	A08	82	19	2	5
	Weighted Avg.	**404**	**78**	**9**	**18**
5PM	**AB95**	913	181	22	42
	AB06	94	13	1	2
	A08	54	12	1	3
	Weighted Avg.	**289**	**55**	**6**	**12**

Level 1 Injury: minor injury without hospitalization; Level 2 Injury: moderate injury with hospitalization; Level 3 Injury: life-threatening injuries; Level 4 Injury: Death

Comparing the total casualty at three different times of a day, the daytime (2 PM) casualties are much higher than the nighttime (2 AM) and commuting time (5 PM) casualties. This is expected since the daytime population is much higher than the nighttime population in Montreal. It should also be noticed that since the casualty estimates does not include roadway kills. The number estimated is expected to increase for both daytime and commuting time once highway bridges are included into the inventory. Within the total casualty, over 95% of the casualty is not life-threatening level one or level two casualties.

5.4 Detailed Results of Scenario 06M67R30SW

In order to analyze the geographic distribution of all damages, the detailed results of scenarios 06M67R30SW are presented in this section. The scenario is chosen because the damage estimated from this scenario is close to the weighted average results of all scenarios. Therefore, the results from this scenario are representative to damages caused by a 2% in 50 years seismic hazard. By showing the geographic distribution of both physical and economic losses, the seismic vulnerability of different areas of Montreal is examined.

5.4.1 Ground Failure due to Liquefaction and landslide

Damage caused by ground failure is evaluated in HAZUS. The two major contributors of ground failure are liquefaction and landslide. The probabilities of these two hazards are evaluated using default HAZUS methodology for scenario 06M67R30SW and 06M67R30NW. The results are presented in Figure 5-16 to Figure 5-19. These four maps indicate both liquefaction and landslide have low occurrence probabilities under a magnitude M6.7 event. Most of the island is not expected to have liquefaction or landslide. Comparing the results from both North-West scenario and South-West scenario, it is observed that the regions closer to earthquake source generally have higher liquefaction and landslide probability. The location of the earthquake event has great influence in the analysis results.

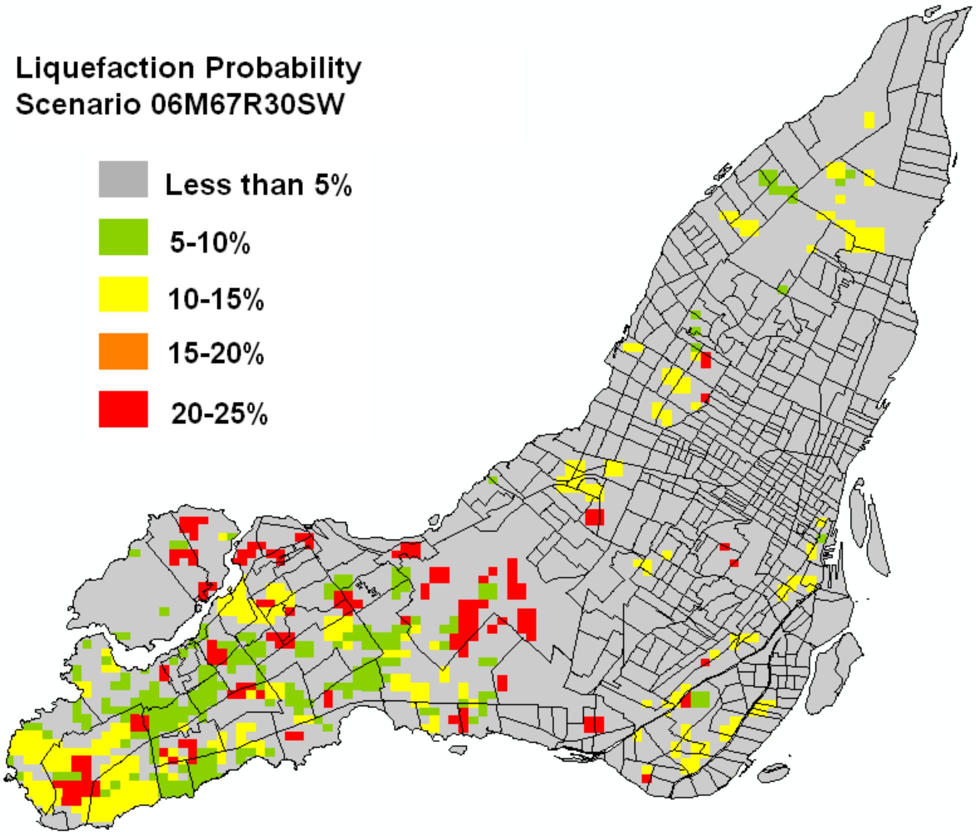

Figure 5-16: Liquefaction Probability Map of Scenario 06M67R30SW

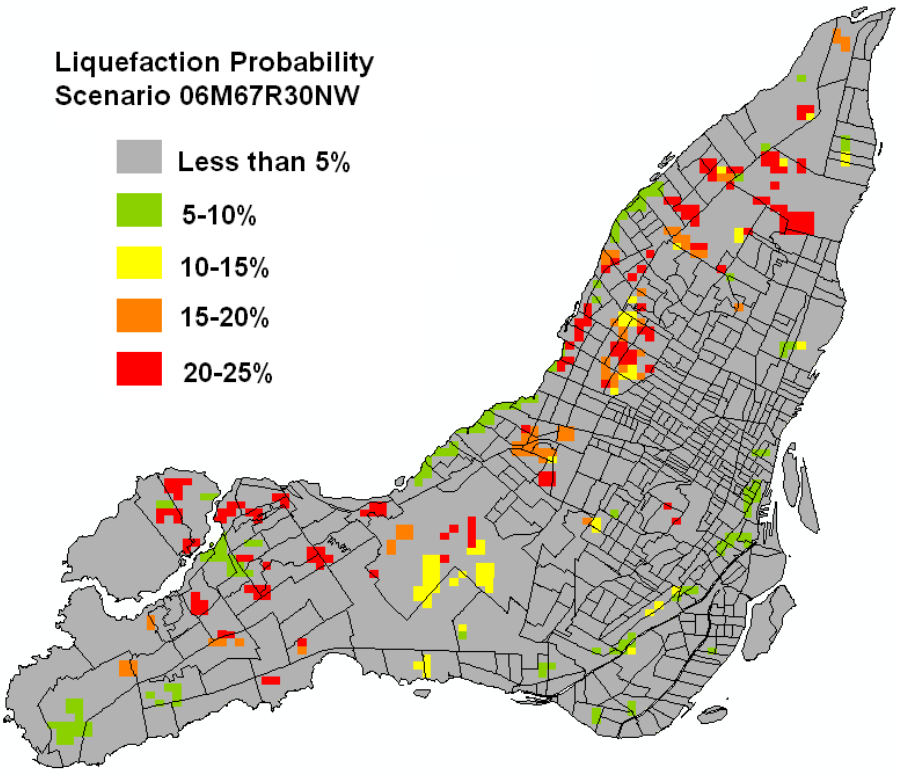

Figure 5-17: Liquefaction Probability Map of Scenario 06M67R30NW

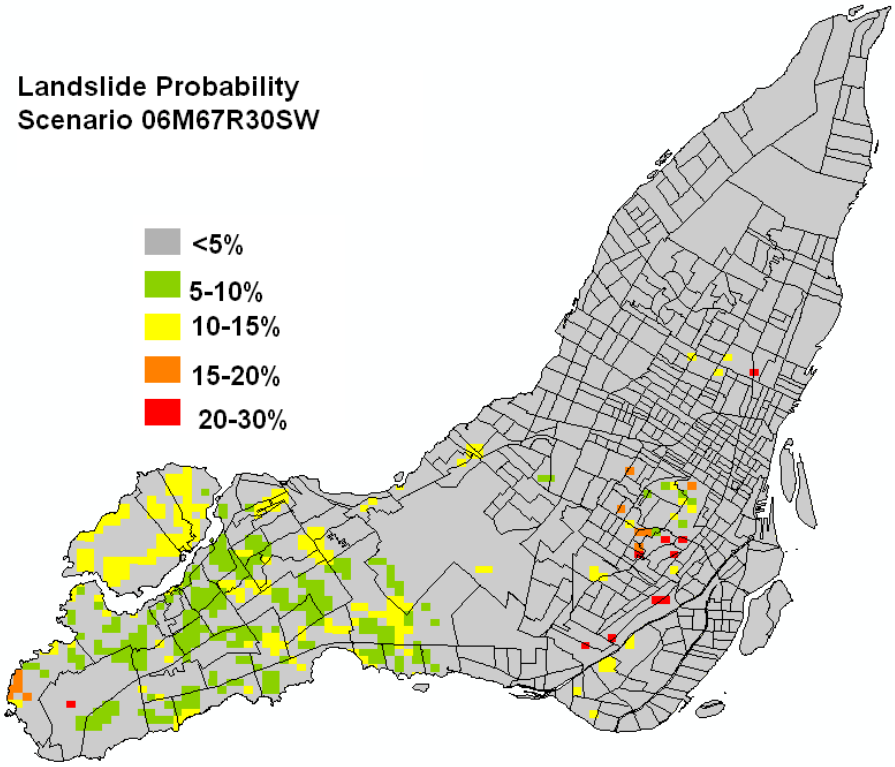

Figure 5-18: Landslide Probability Map of Scenario 06M67R30SW

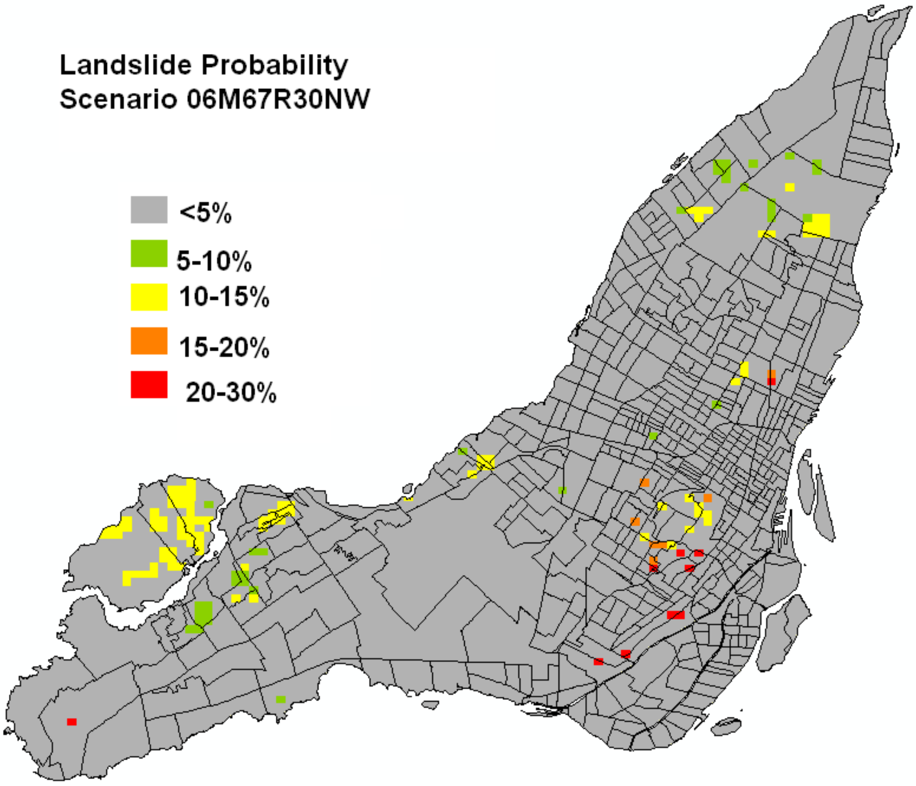

Figure 5-19: Landslide Probability Map of Scenario 06M67R30NW

5.4.2 Direct Physical Damages to GBS

Geographic Distribution of Total Building Damages

The total number of buildings damaged and total area of buildings damaged per census tract are shown in Figure 5-20 and 5-21 for scenario 06M67R30SW. Three trends are found in these two figures: 1) In general, more damage is observed in the western part of the island than eastern part of the island. This is expected since the location of the event is 30km away from the center of Montreal in the south-west direction. Therefore, the census tracts closer to the source are expected to have more damages. This trend is confirmed by the results from the same magnitude-distance event on the North-West direction of Montreal (06M67R30NW). In Figure 5-24 and 5-25, the result shows that the census tracts in Montreal-Nord suffer intensive damages, which is not observed in the south-western part of the island. On the other hand, census tracts with large damages in the South-West scenario only suffer moderate damages. 2) It is also observed that the total damaged area is not proportional to the total number of building damaged in a census tract. In neighborhoods such as Kirkland, Beaconsfield, and Point-Claire, buildings are mostly single family houses with smaller total building area. Therefore, even with high number of damaged building, the total damaged area is still relatively small. 3) The total damage observed is proportional to the size of the census tract. Since the damage result is aggregated to census tract level, the result is biased towards bigger census tract with more population and buildings. In order to exclude this size effect, the total number of buildings damaged and the total area of buildings damaged are normalized with respect to the land area of the census tract. The resulting maps are shown in Figure 5-22 and 5-23.

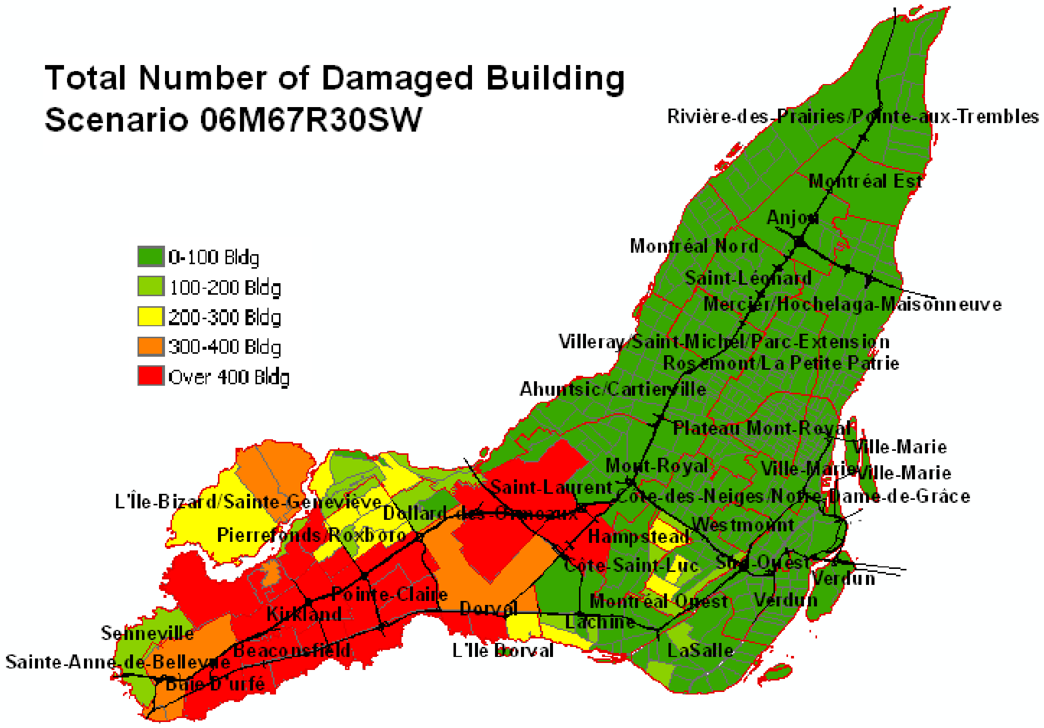

Figure 5-20: Total Number of Buildings Damaged in Each Census Tract.

(The Results are generated for Scenario: 06M67R30SW and aggregated to include all building type and damage levels)

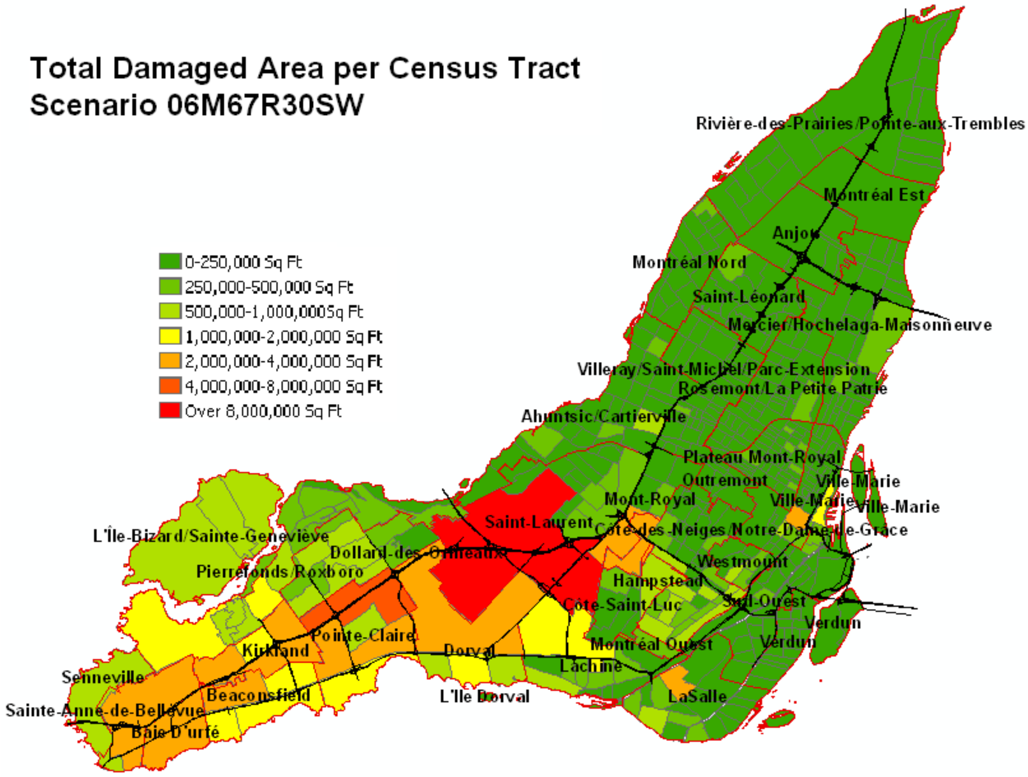

Figure 5-21: Total Area of Building Damage in Each Census Tract

(The Results are generated from Scenario: 06M67R30SW and aggregated to include all building types and damage levels)

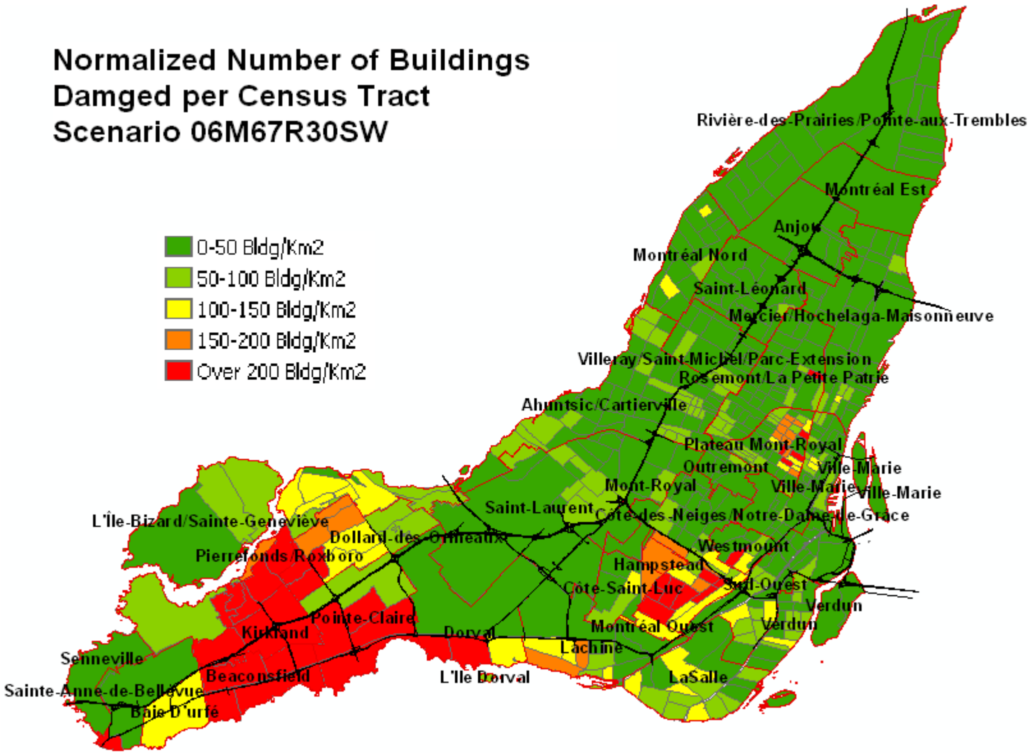

Figure 5-22: Normalized Number of Building Damaged in Each Census Tract (The Results are generated from Scenario: 06M67R30SW and aggregated to include all building types and damage levels. The results are normalized with respect to the total land area of the census tract)

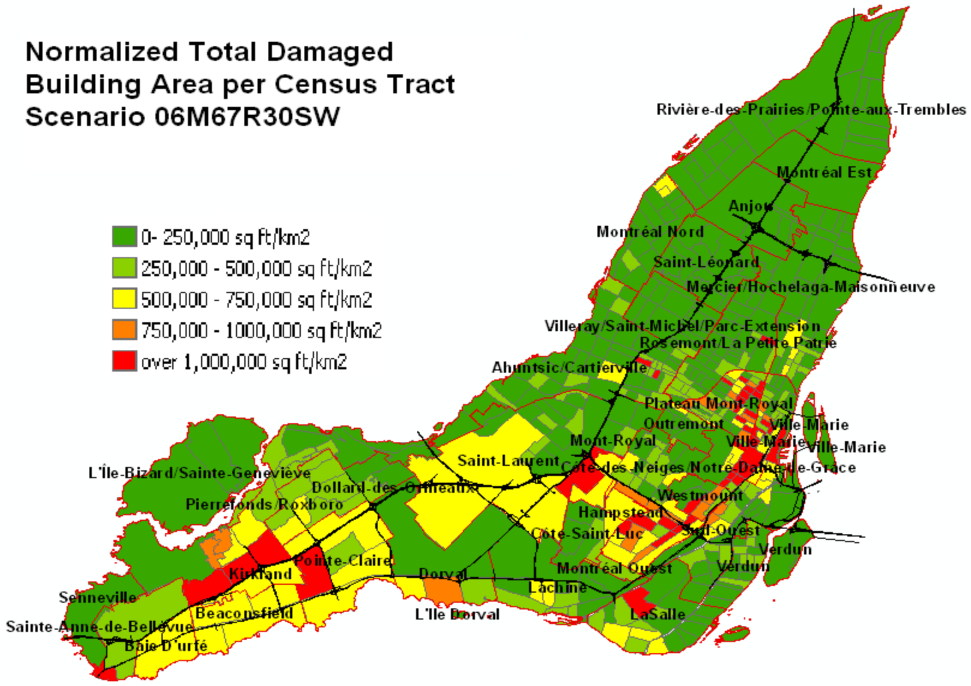

Figure 5-23: Normalized Total Damaged Building Area in Each Census Tract (The Results are generated from Scenario: 06M67R30SW and aggregated to include all building types and damage level. The results are normalized with respect to the total land area of the census tract)

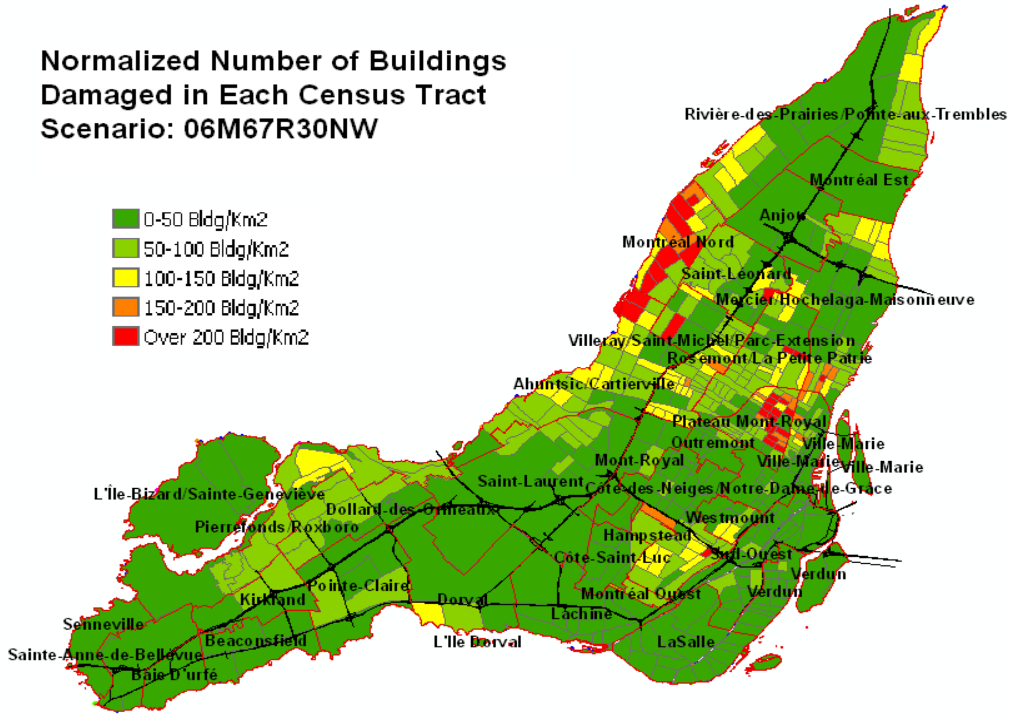

Figure 5-24: Normalized Number of Buildings Damaged in Each Census Tract (The Results are generated from Scenario: 06M67R30NW and aggregated to include all building types and damage levels. The results are normalized with respect to the total land area of the census tract.)

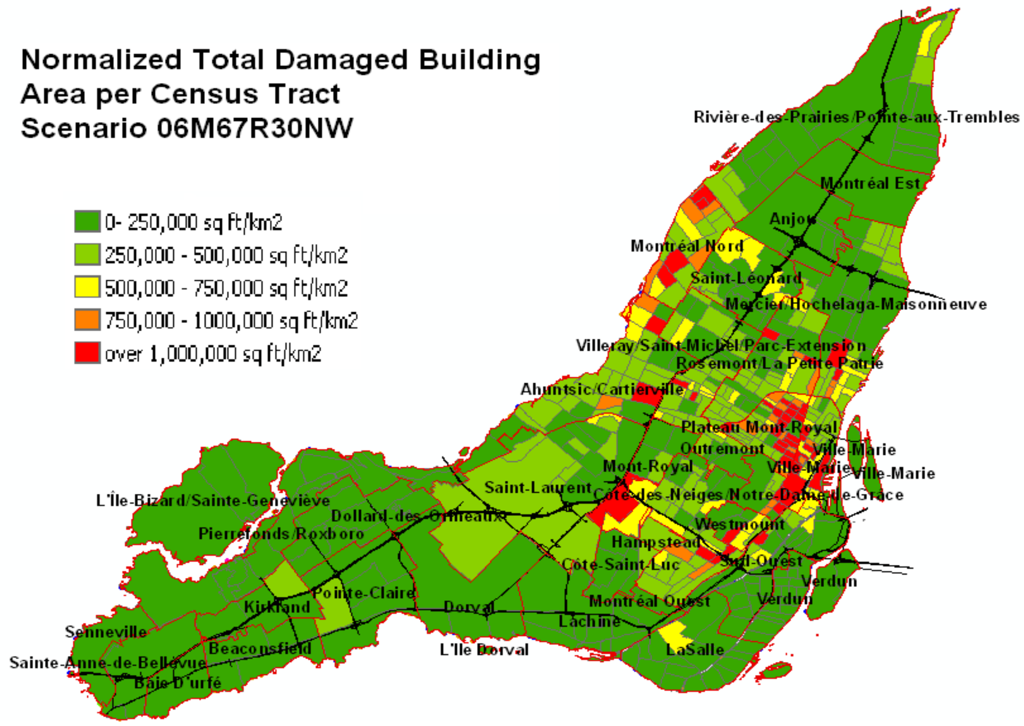

Figure 5-25: Normalized Total Damaged Building Area in Each Census Tract (The Results are generated from Scenario: 06M67R30SW and aggregated to include all building types and damage level. The results are normalized with respect to the total land area of the census tract)

By examining the normalized damaged building area results, it is observed that the boroughs of Ville-Marie, Plateau Mont-Royal, Westmount, and Cote-Des-Neiges/ Nortre-Dame-de-Grace(CDN/NDG) all suffer intensive damages. Shown in Figure 5-26, there are 41 census tracts with intensive damage (damage>1 million square feet per square kilometer). Among all these census tracts, 70% are located in Ville-Marie (12), Plateau Mont-Royal (11), and CDG/NDG(6), making these neighborhoods the most seismic vulnerable areas in Montreal. Comparing to the soil class map in Chapter 3(Figure 3-11), 68% of these census tracts are all located in soil class C or D sites. This demonstrates that soil amplification effect is a contributor to the overall seismic vulnerability of a region. The distribution is shown in Figure 5-27.

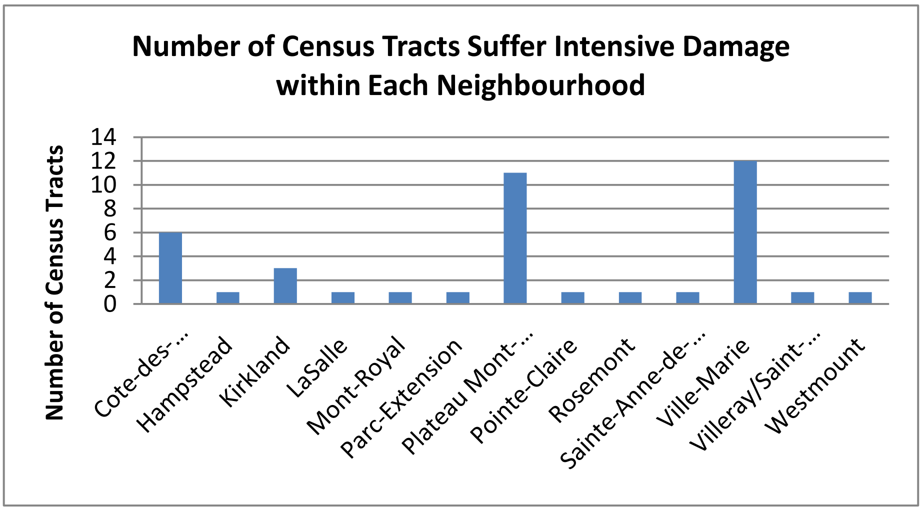

Figure 5-26: Distribution of Census Tracts with Building Damage Greater than 1 million Square Footage per Square Kilometer.

(The Results are generated from Scenario: 06M67R30SW and aggregated to include all building types and damage level.)

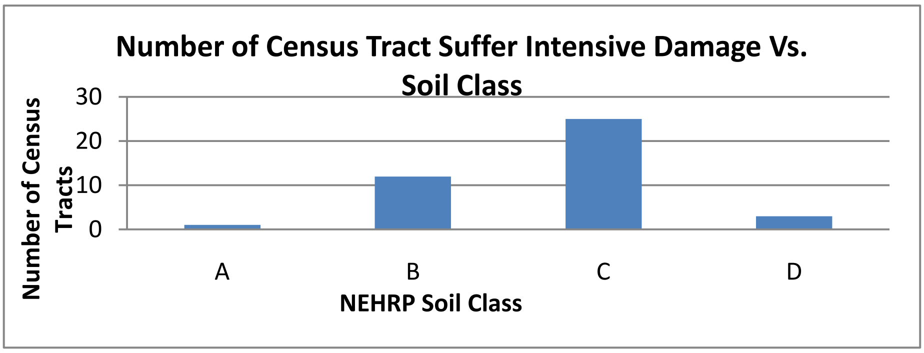

Figure 5-27: Distribution of Census Tracts with Building Damage Greater than 1 million Square Footage per Square Kilometer among Different NEHRP Soil Class. (The Results are generated from Scenario: 06M67R30SW and aggregated to include all building types and damage level.)

Geographic Distribution of Building Damage by Damage Level

The total damaged building area is broken down into four different damage levels. Shown in Figure 5-28, most of the census tracts only suffer slight to moderate damages, which account for 95% of the total damage area. The census tracts with buildings suffering extensive to complete damages are the census tracts in south-west of Montreal, which is closer to the epicenter of the earthquake and with higher estimated liquefaction and landslide probability (Figure 5-16, 5-18). Since ground failure caused by liquefaction and landslide only contributes to extensive and complete damage, the higher level of extensive and complete damage is expected in these areas. The same trend is observed in Figure 5-29 for North-West scenario.

Geographic Distribution of Building Damage by Structural Type

In terms of structural type, 43% of building damage comes from masonry buildings, which accounts for 26% of the total building area. The second highest category for building damage (33%) comes from wood building, which accounts for 51% of the total building area. The rest of the damage comes from steel (18%) and concrete buildings (6%), which consist of 17% and 6% of the total building area. This makes masonry building the most seismic vulnerable structural type among all buildings. It is also observed that the damaged wood buildings are mostly observed in western part of island, where single family wood buildings are the most common structural type. The geographic distribution of building damage by structural type is presented in Figure 5-30 and 5-31 for scenario 06M67R30SW and 06M67R30NW, respectively.

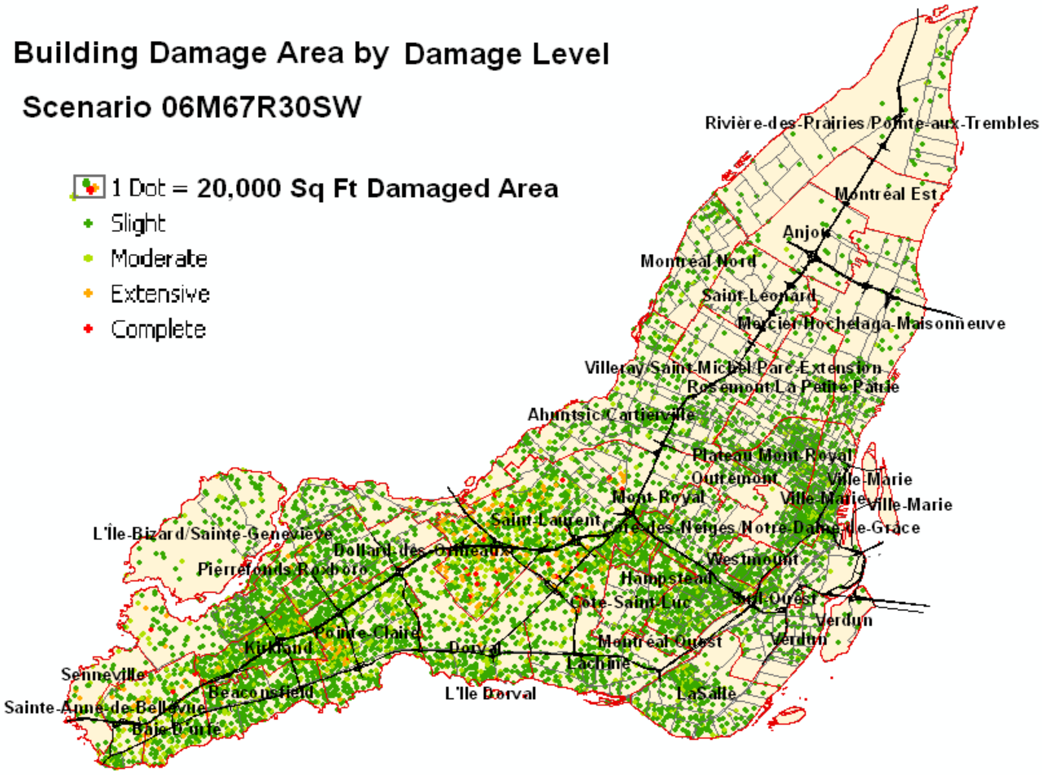

Figure 5-28: Damaged Building Area by Four Different Damage Level (The Results are generated from scenario: 06M67R30SW and aggregated to include all building types.)

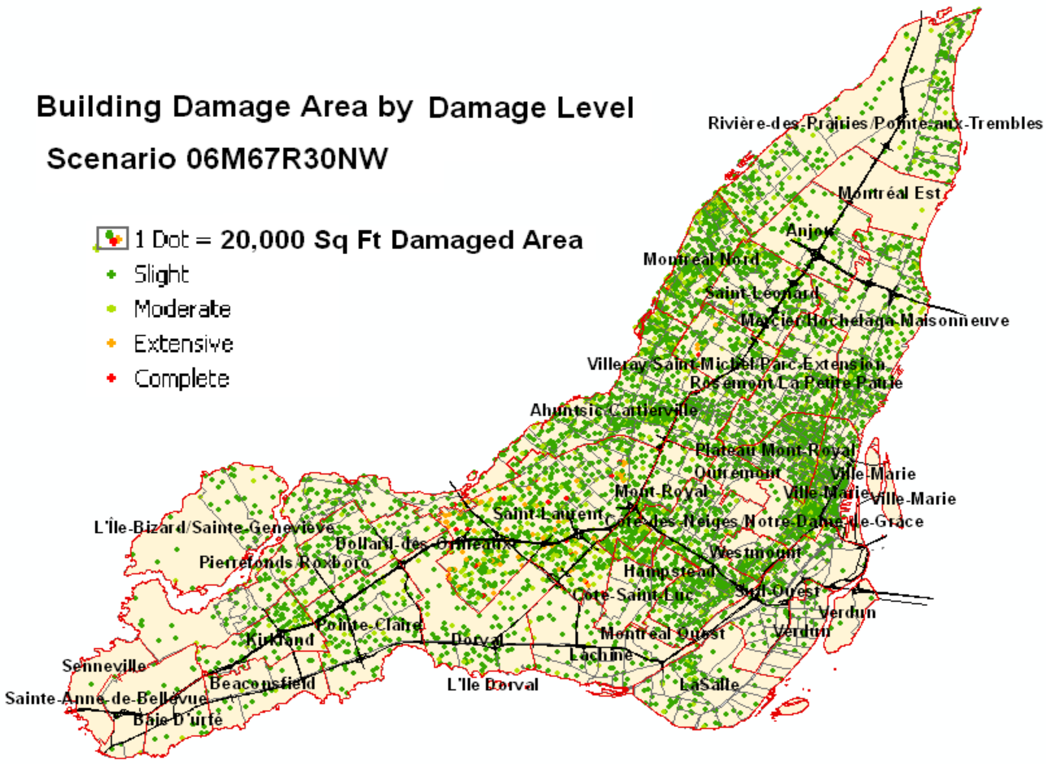

Figure 5-29: Damaged Building Area by Four Different Damage Level (The Results are generated from scenario: 06M67R30NW and aggregated to include all building types.)

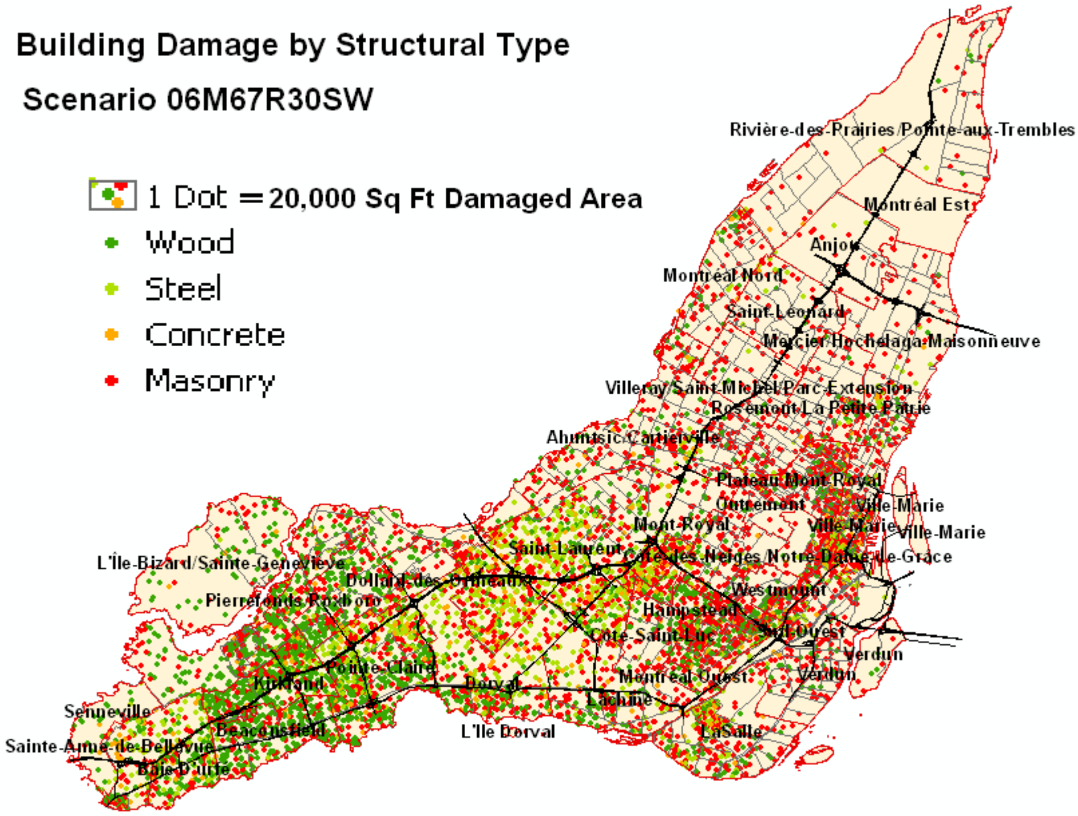

Figure 5-30: Damaged Building Area by Structural Type (The Results are generated from scenario: 06M67R30SW and aggregated to include all building types.)

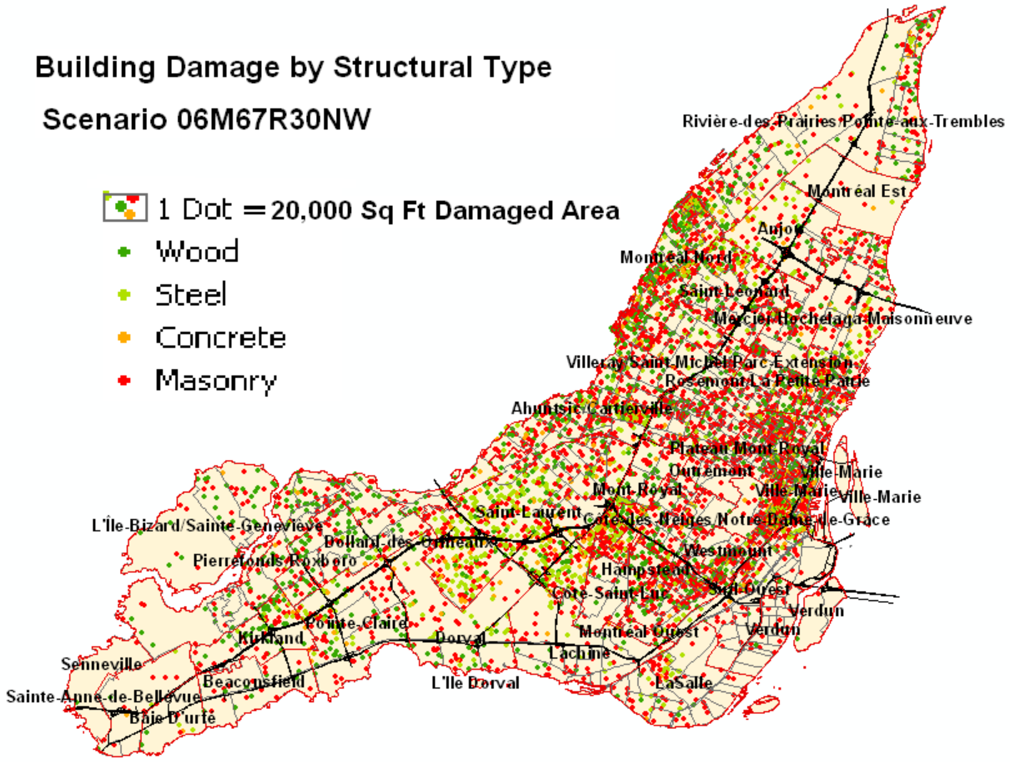

Figure 5-31 Damaged Building Area by Structural Type (The Results are generated from scenario: 06M67R30SW and aggregated to include all building types.)

5.4.3 Direct Economic Losses

The normalized total direct building economic loss is presented in Figure 5-33; this includes economic losses due to structural damage, non-structural damage, building content damage, and business inventory loss. The largest damage per land area occurs in the borough of Ville-Marie, Kirkland, and Point-Claire. This pattern is consistent with the direct physical damage result. The break-down of economic losses shows that building structural and non-structural losses are the largest contributors of all economic losses. In all census tracts with damages, they account for 65% of the total economic losses on average. The rest of the economic losses are shared by content damage and inventory loss, which are 33% and 1% respectively of the total loss on average.

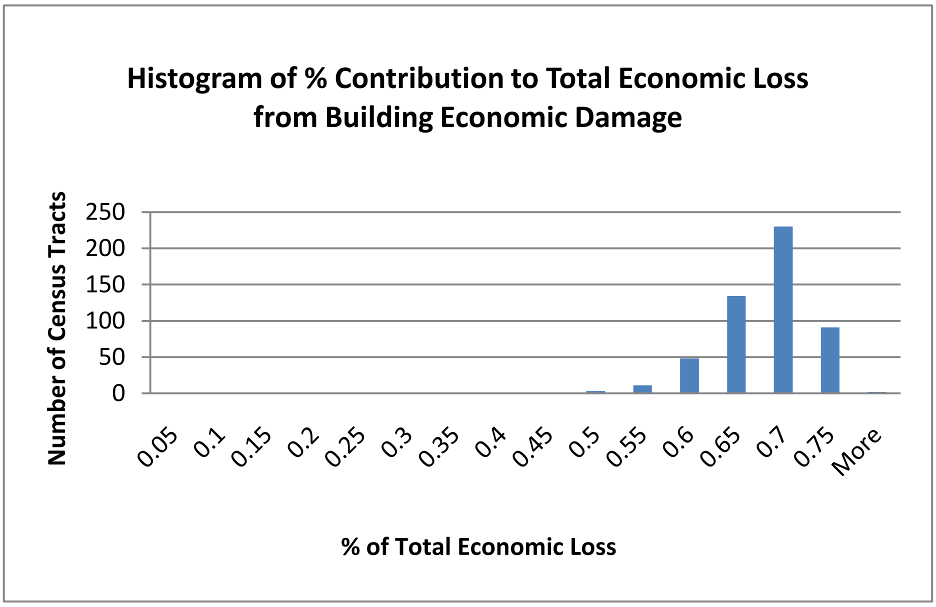

Figure 5-32: Histogram of Percentage Contribution to Total Economic Loss from Building Economic Damage of Scenario 06M67R30SW

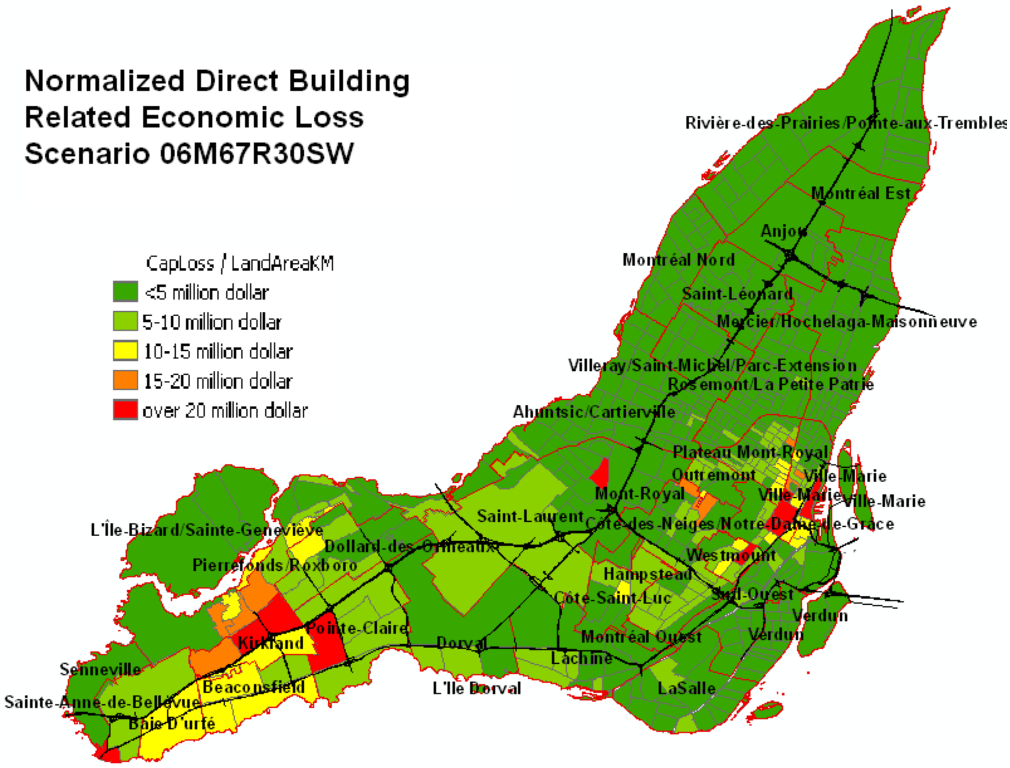

Figure 5-33: Normalized Direct Building Related Economic Loss Map of Scenario 06M67R30SW. (The results are normalized by total land area of the census tract and aggregated to include all building types)

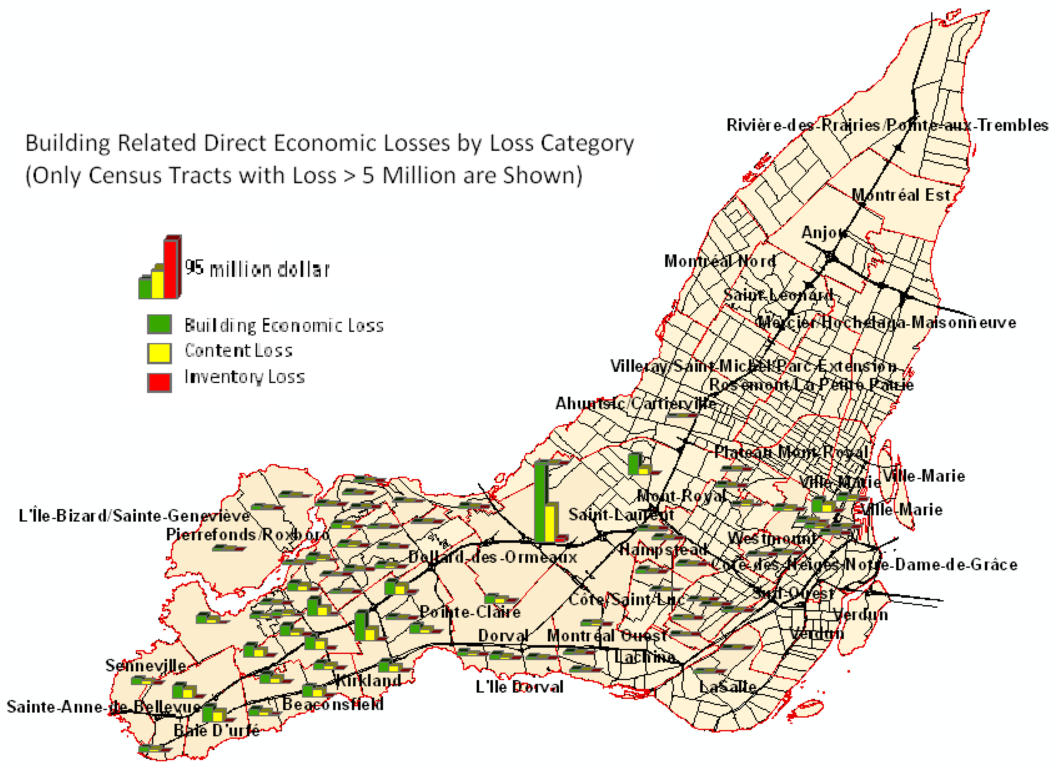

Figure 5-34: Breakdown of the Direct Building Related Economic Loss Map of Scenario 06M67R30SW. (Only Census Tracts with Loss over 5 millions are presented.)

5.4.4 Direct Social Losses

5.4.4.1 Displaced Household and Short-term Shelter Needs

In terms of number of displaced households, 98 out of 522 census tracts are expected to have at least one displaced household. These census tracts are located mostly in the western part of the island, and the census tract expecting the largest number of displaced household is in the neighborhood of Saint-Laurent. The number of people seeking short-term shelter map presented in Figure 5-36 has a similar trend to the number of displaced household(Figure 5-35): 65 out of 522 census tracts are expected to have people seeking short-term shelter.

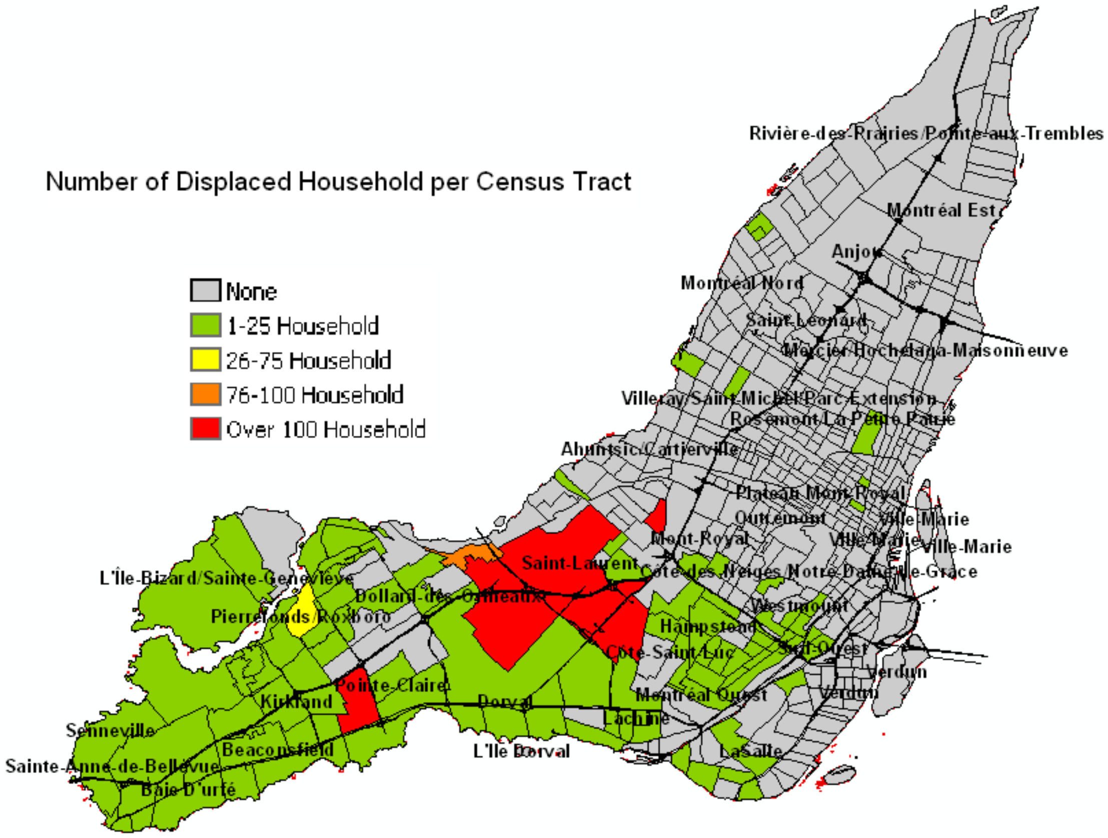

Figure 5-35: Number of Displaced Household per Census Tract for Scenario 06M67R30SW

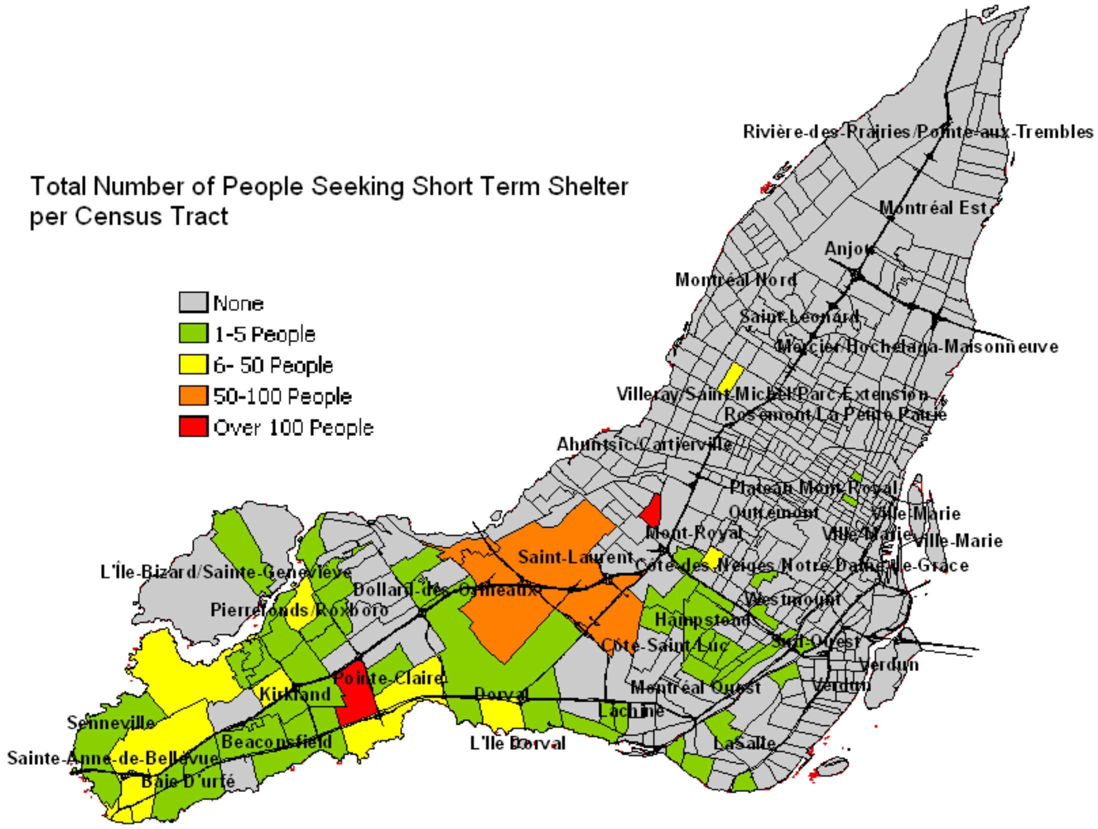

Figure 5-36: Number of People Seeking Short-term Shelter per Census Tract of Scenario 06M67R30SW)

5.4.4.2 Casualty Estimates

During the study, HAZUS failed to give casualty estimates for 85 of the 522 census tracts. Therefore, manual calculation using the HAZUS methodology was performed for scenario 06M67R30SW. The calculation is done in Excel using the methodology described in HAZUS-MH4 technical manual. Only casualties resulting from building damage are estimated. The roadway casualty can be calculated once the highway bridge data is available. The detailed steps involved in the calculation are documented in Appendix F.

The geographic distribution of casualties is shown in Figure 5-37, 5-38, and 5-39 for 2 am, 2pm, and 5pm scenarios respectively. The figures are all normalized by census 2006 population, and therefore shown as the percentage of census population. In all three figures, more casualties are expected in the west of the island than in the east, showing a strong link between the physical building damage and casualty. At 2 PM and 5 PM, higher numbers of casualties are observed in downtown area, which corresponds to the higher population density during the day. For a given census tract, the daytime casualties are higher than the nighttime casualties except for the census tracts in the west-end of the island. The non-normalized casualty estimates are also presented in Figure 5-40 to Figure 5-42 for comparison.

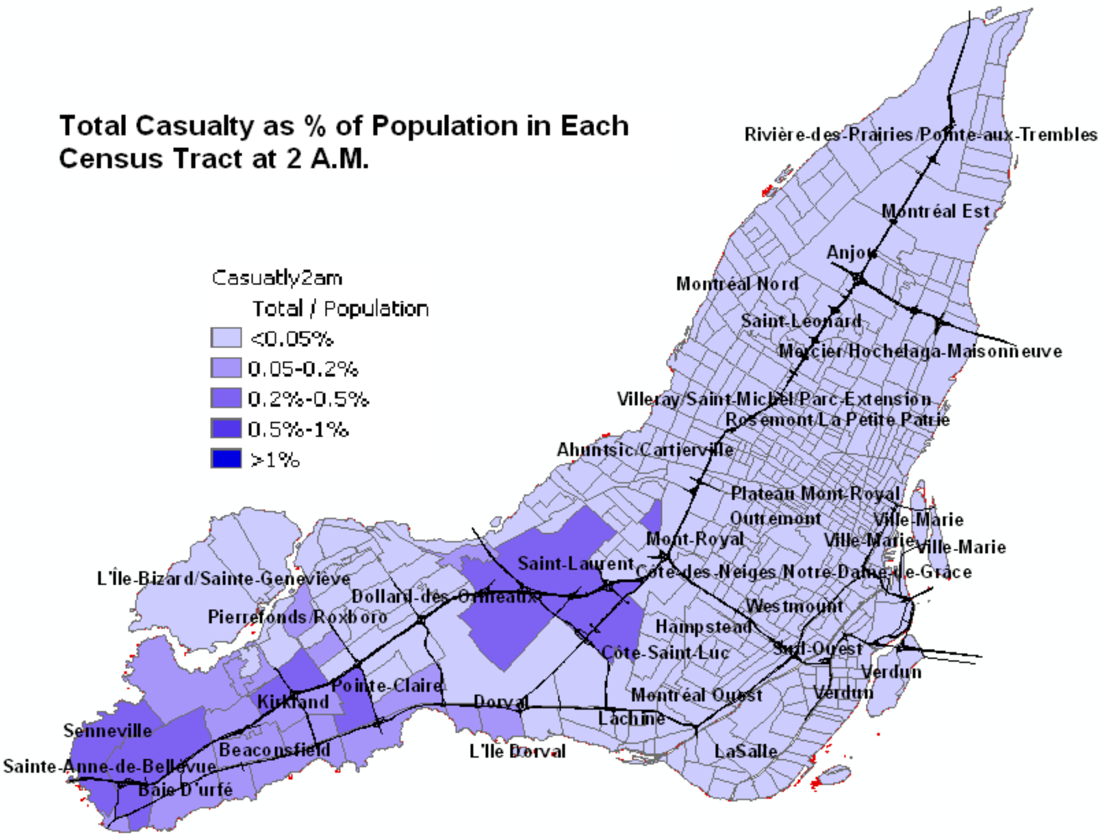

Figure 5-37: Casualty as % Population at 2 AM for Scenario 06M67R30SW

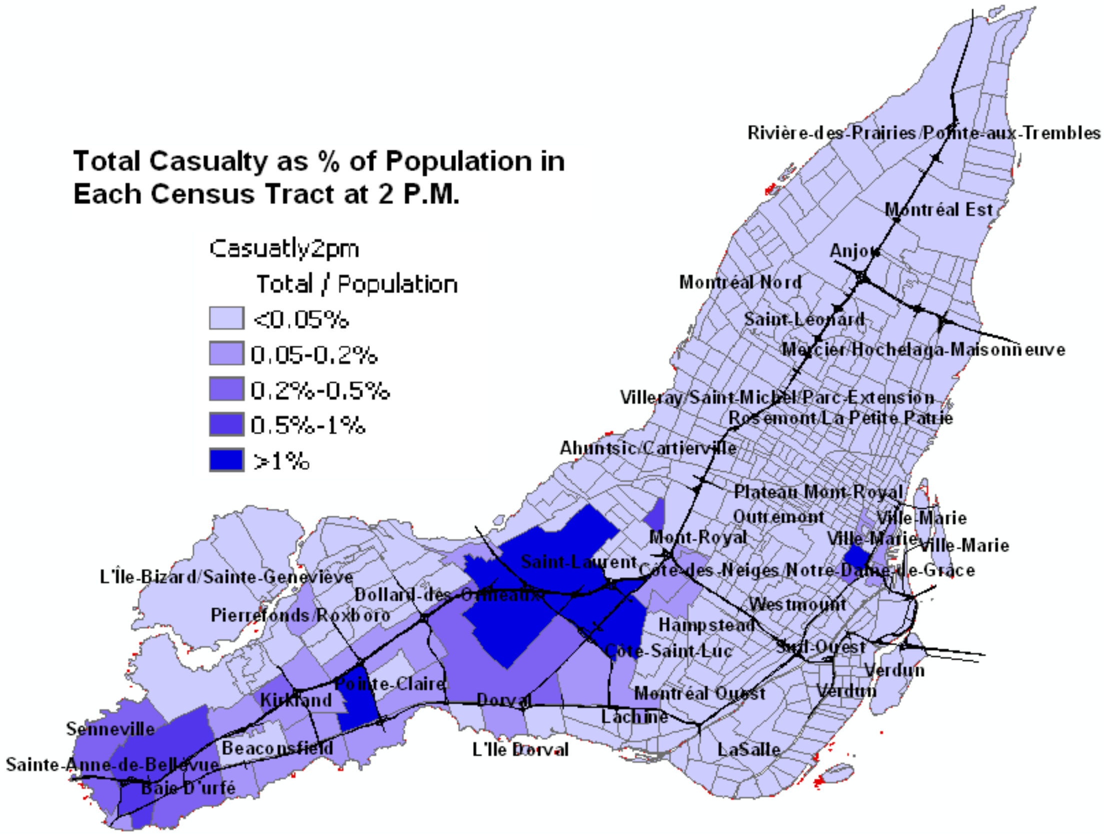

Figure 5-38: Casualty as % Population at 2 PM for Scenario 06M67R30SW

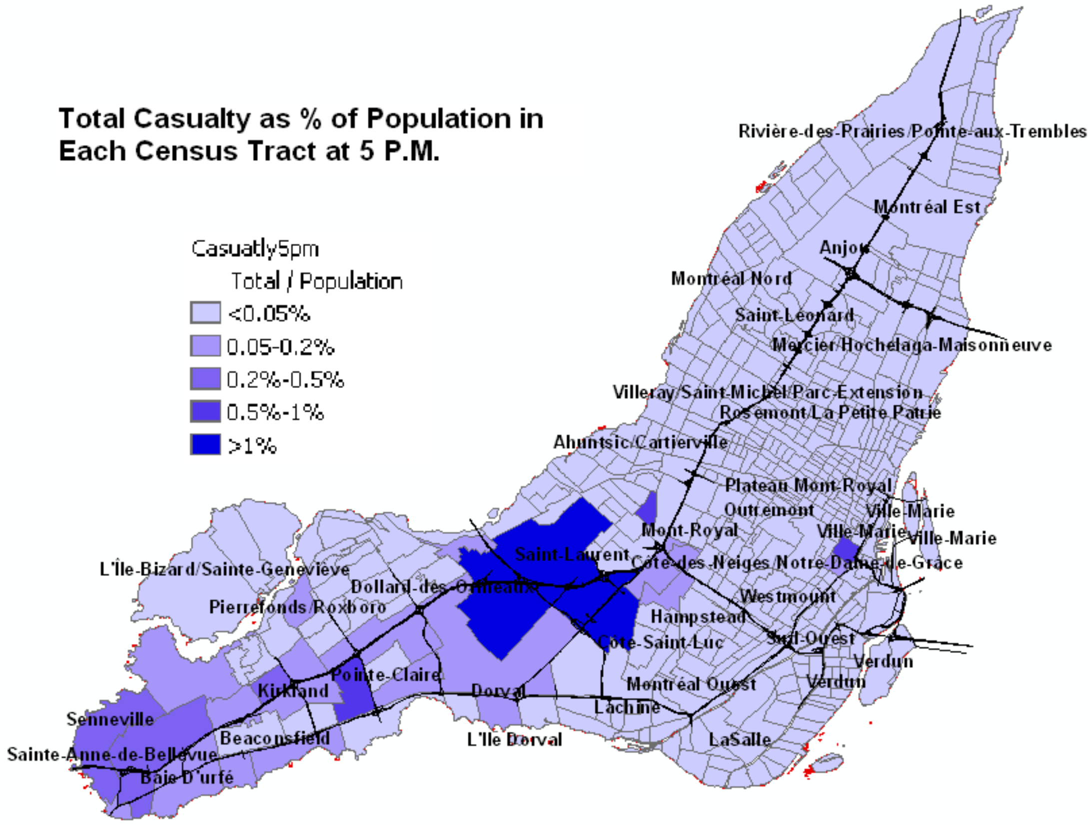

Figure 5-39: Casualty as % Population at 5 PM for Scenario 06M67R30SW

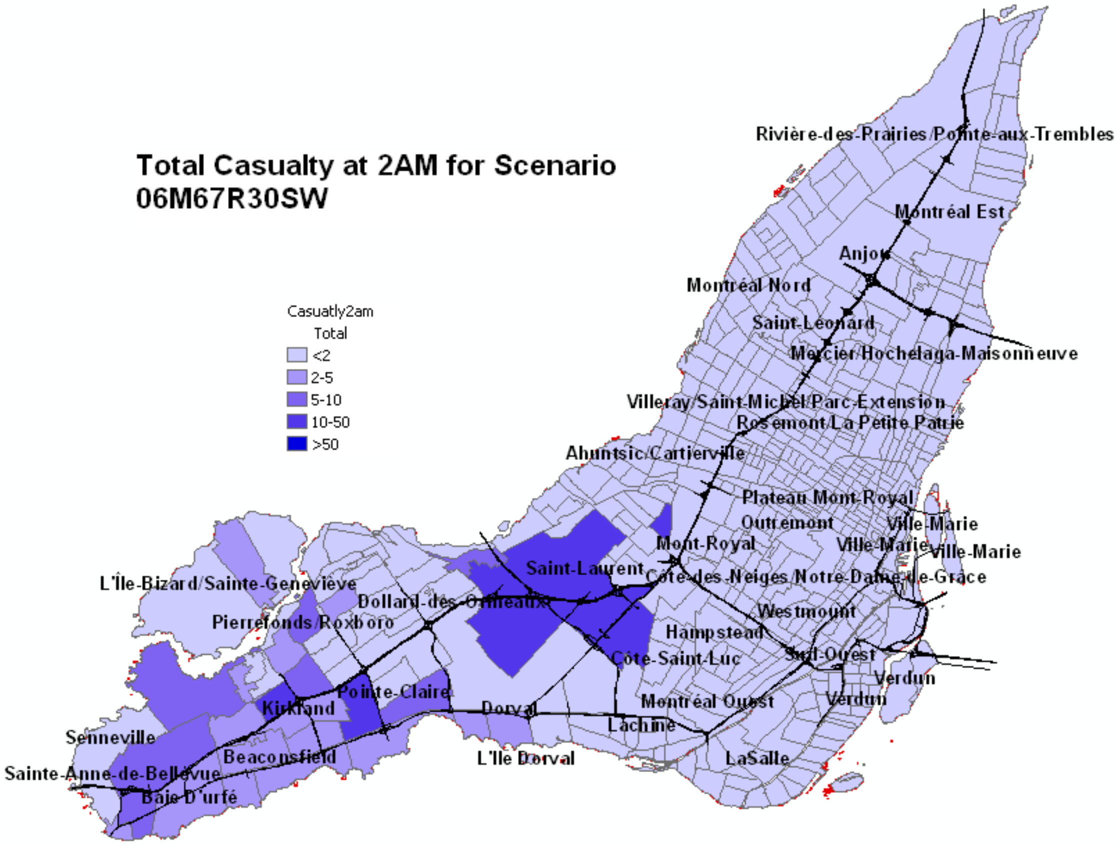

Figure 5-40: Total Number of Casualty at 2 AM for Scenario 06M67R30SW

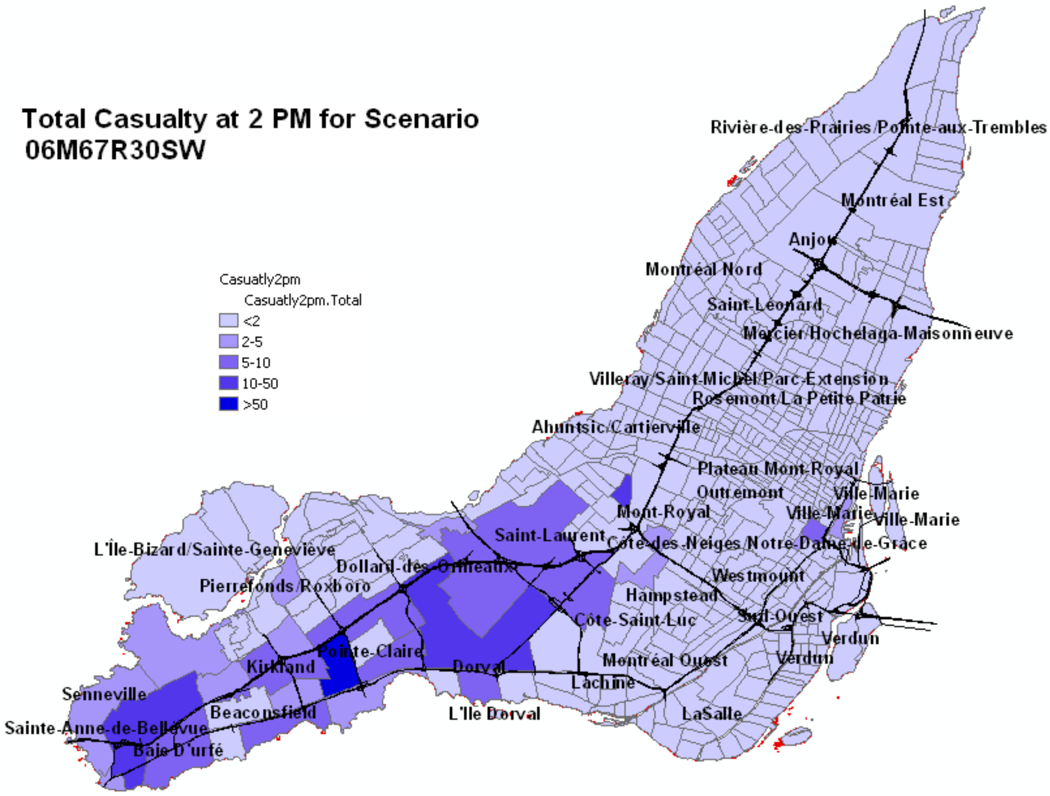

Figure 5-41: Total Number of Casualty at 2 PM for Scenario 06M67R30SW

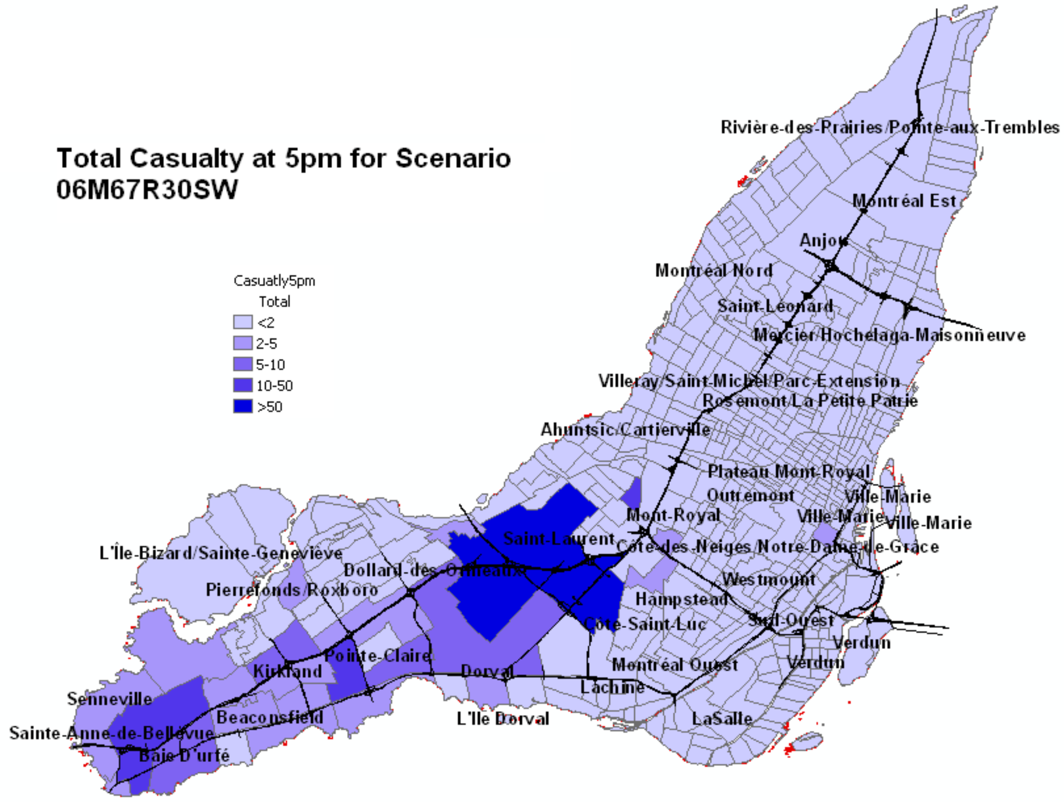

Figure 5-42: Total Number of Casualty at 5 PM for Scenario 06M67R30SW

5.5 Essential Facilities

Since the analysis on essential facilities is performed at individual building level, the result of damage and functionality of essential facilities is highly dependent on the quality of input data. The design level, structural type and location of the building are the required input for such analysis. Since the structural type and design level is missing for essential facilities in Montreal, this study only attempt to conduct a preliminary estimation of the performance of essential facilities in Montreal based on its location and default structural data provided in HAZUS.

The expected weighted average functionality of hospitals, schools, emergency operation centers (EOCs), fire stations, and police stations are summarized in Table 5-15. The functionality by scenario is presented in Appendix G. Roughly 50% of the hospitals and schools will have functionality greater than 50% on the day of the earthquake. No essential facility is expected to experience complete damage on the day of the earthquake.

Table 5-15: Weighted Average Value of functionality of essential facilities by Category

	Total	**At Least Moderate Damage >50% on Day 1**	**Complete Damage >50% on day 1**	**With Functionality > 50% on day 1**
Hospitals	71	1	0	40
Schools	764	16	0	423
EOCs	62	1	0	55
Police Stations	44	0	0	43
Fire Stations	65	0	0	60

Chapter 6. Conclusion sand Recommendations

This study investigates the potential direct physical and social damages in Montreal from a seismic hazard with occurrence of 2% in 50 years. The study region is the island of Montreal, which covers an area of 500 square kilometers with 522 census tracts. There are over 827 thousands of households in the study region with 1.85 million people (Census 2006 Data). There are estimated 315 thousands of buildings in Montreal, 95% of them are residential building. The total replacement value of the general building stock is estimated to be 128,511 millions of dollars. Individual scenarios are chosen based on deaggregation of 2% in 50 years hazard using different ground motion prediction equations. The weighted average result from all scenarios is calculated. The result of this study is a preliminary assessment of the damage caused by 2%/50 yrs seismic hazard, and can be used as a mean to evaluate the scope of potential loss in Montreal and as a pilot study for applying HAZUS software for loss estimation in Montreal region. The conclusion and recommendation of this study is as following.

6.1 Conclusions

1 Expected Damaged of a 2%/50yrs Seismic Event in Montreal

Direct Physical Damages

The direct physical damage to the general building stock is estimated to be 3.96%, 1.25%, 0.29% and 0.05% of the total building stock for slight, moderate, extensive and complete damages respectively. Among all building types, masonry buildings are found to be the most vulnerable building type: 10% of the total unreinforced masonry buildings are expected to experience different levels of damage.

Social Economic Loss

The direct economic loss due to building damages is expected to be 1404 millions of dollars, including content and business inventory losses. There are 2490 displaced households and 1388 people will be seeking short-term shelter. The estimated number of people injured is 352, 509, and 362 if the earthquake happens at 2 AM, 2

PM, and 5 PM respectively.

Geographic Distribution of Damages

The most vulnerable region in Montreal is downtown, where the building and population density is the highest. Both building damage and social-economic damages are expected to be very high.

2 The choice of ground motion prediction equations can strongly influence loss estimation results from HAZUS. By using different GMPEs, the damage results can vary by a factor of a hundred for events with the same magnitude and distance.

3 The earthquake loss estimation is sensitive to the ground motion amplitude, which is determined by magnitude, distance, and site condition.

4 When using HAZUS for earthquake loss estimation on large scale regions like Montreal, the location of earthquake event can influence the results. The regions closer to the earthquake source have significantly higher estimated damages than regions further away.

6.2 Recommendations

1 Overall, the structural type distribution in Montreal is similar to the default building mapping scheme by HAZUS. However, the differences do exist. In order to get more accurate results, a detailed building survey will be beneficial in future studies.

2 This study mainly covers the general building stock, and therefore, the estimated damage is only a portion of the total damage caused by an earthquake. Future studies should include transportation and utility systems once the required datasets are collected.

3 The uncertainties associated with ground motion prediction equations are high for Eastern North American regions. The ground motion amplitude calculated by such equations is of high uncertainties. Therefore, a combination GMPE using the weighted average of different GMPEs can be used to calculate the ground motion amplitude. Such approach has been used by the USGS in the 2002 update of the National Seismic Hazard Maps (Frankel, et al., 2002).

Appendix A: Deaggregation Results from CRISIS 2007

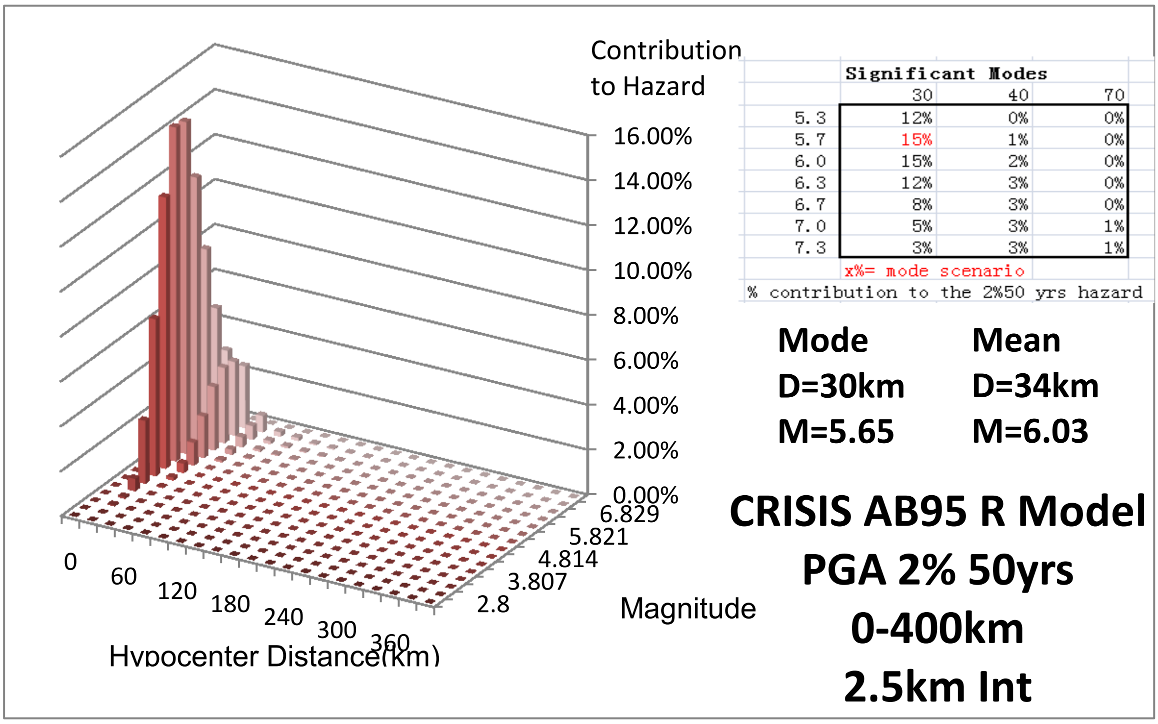

Figure A-1: Deaggreagation results from CRISIS for PGA using ground motion prediction equation AB95

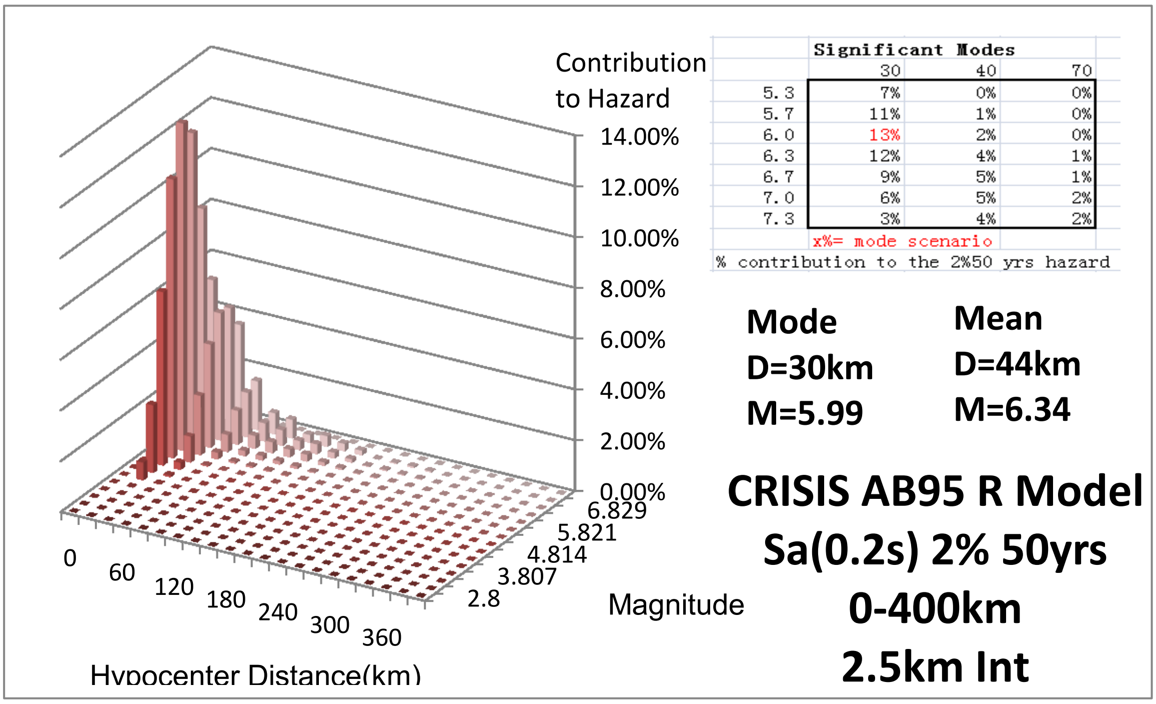

Figure A-2: Deaggreagation results from CRISIS for Sa(0.2s) using ground motion prediction equation AB95

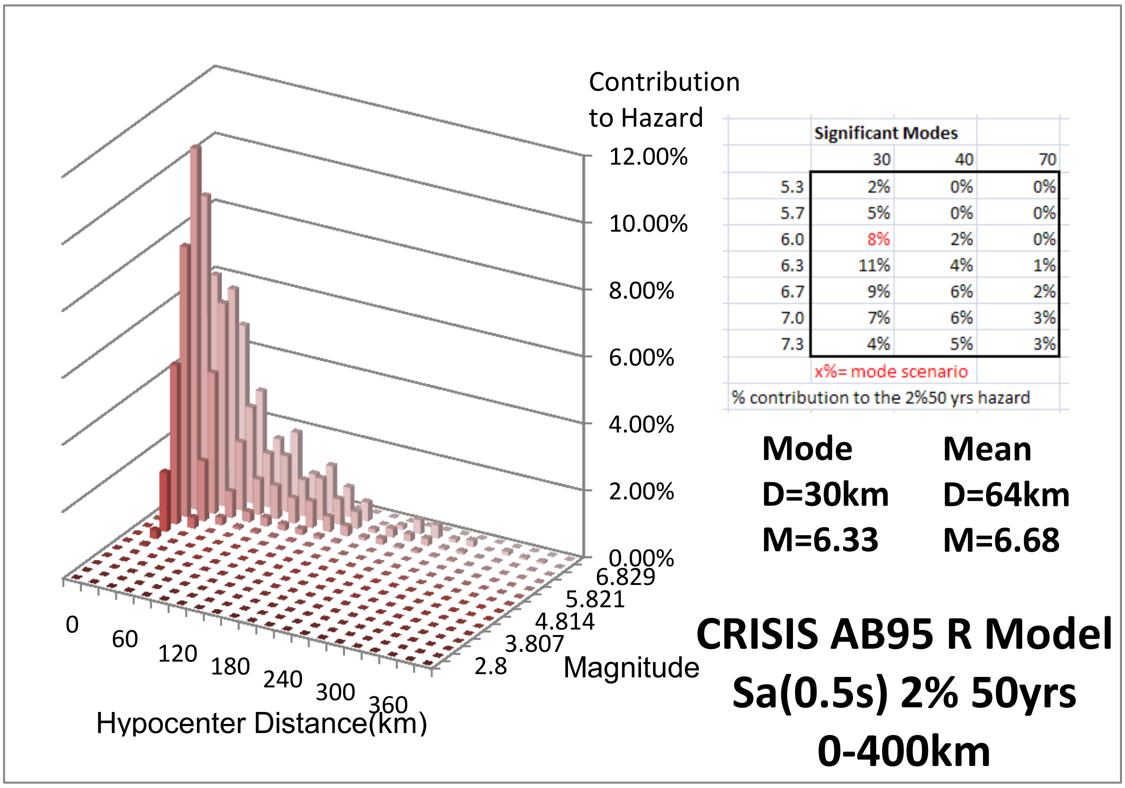

Figure A-3: Deaggreagation results from CRISIS for Sa(0.5s) using ground motion prediction equation AB95

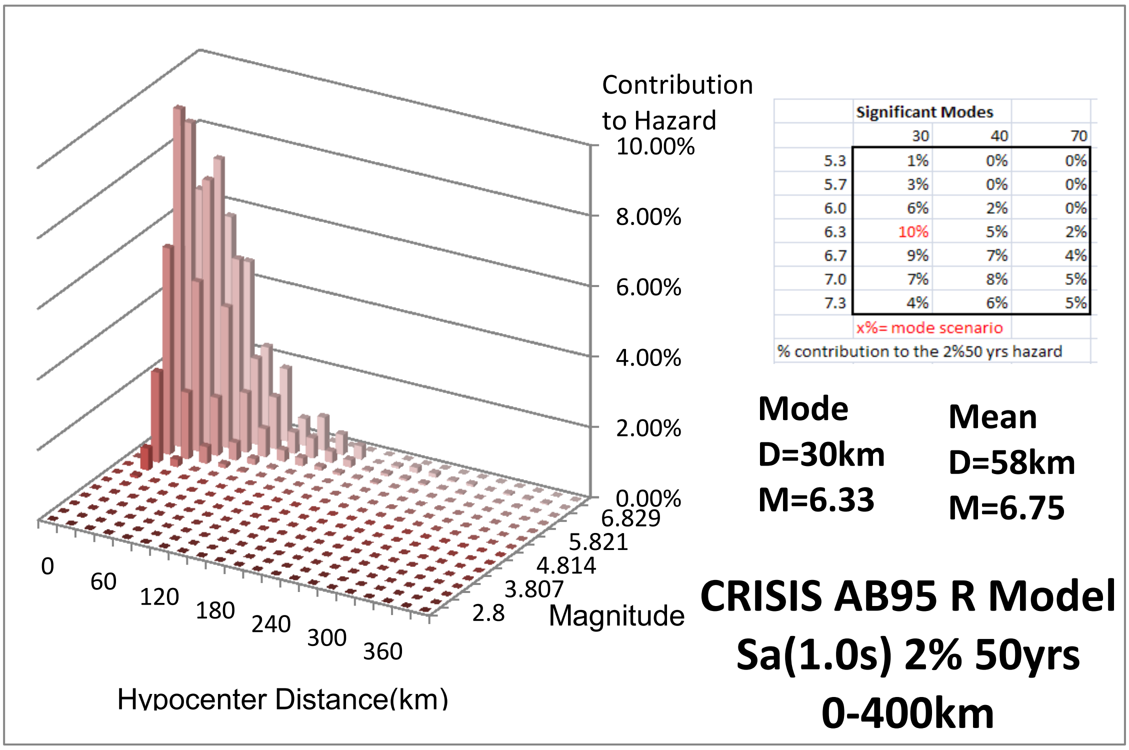

Figure A-4: Deaggregation results from CRISIS for Sa(1.0s) using ground motion prediction equation AB95

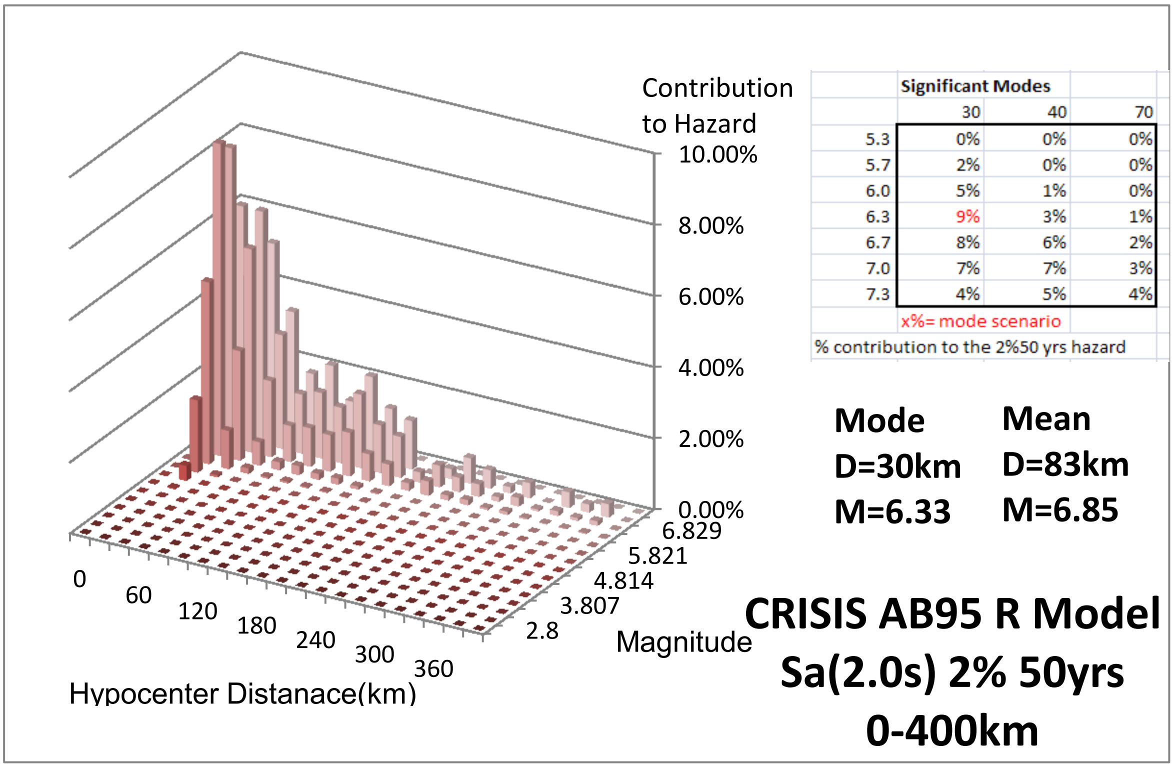

Figure A-5: Deaggregation results from CRISIS for Sa(2.0s) using ground motion prediction equation AB95

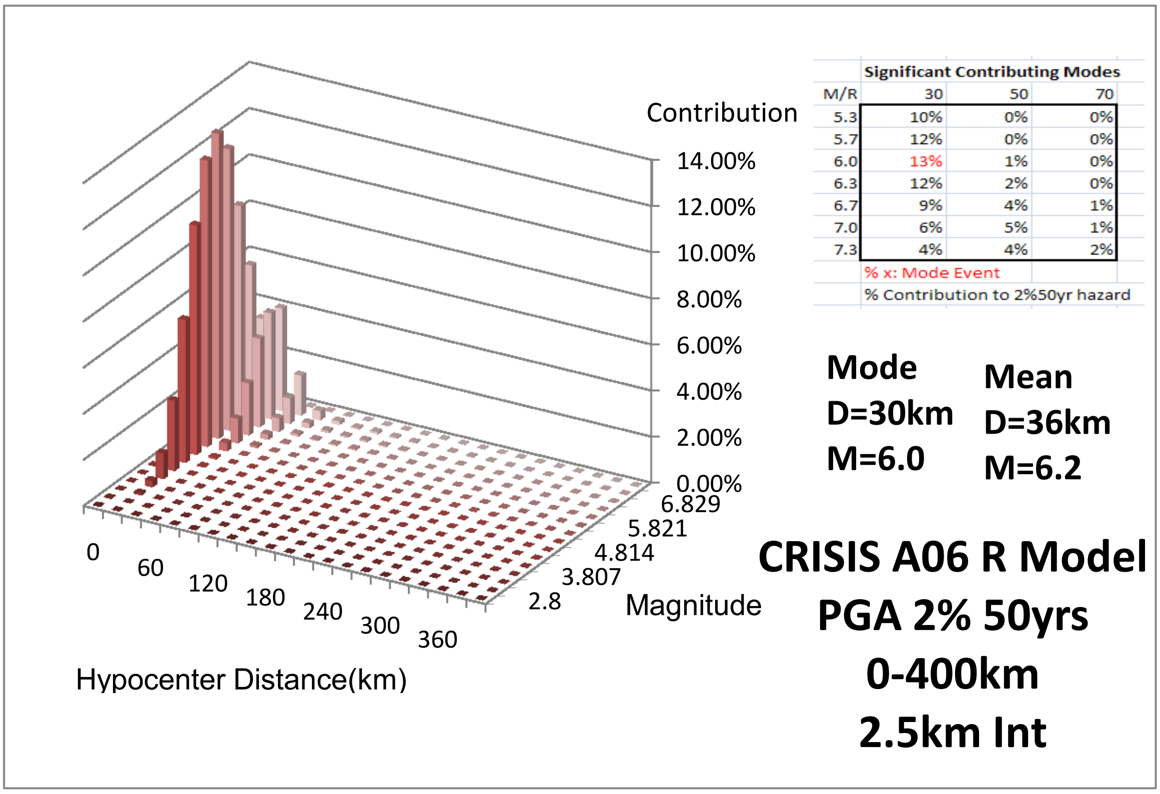

Figure A-6: Deaggregation results from CRISIS for PGA using ground motion prediction equation AB06

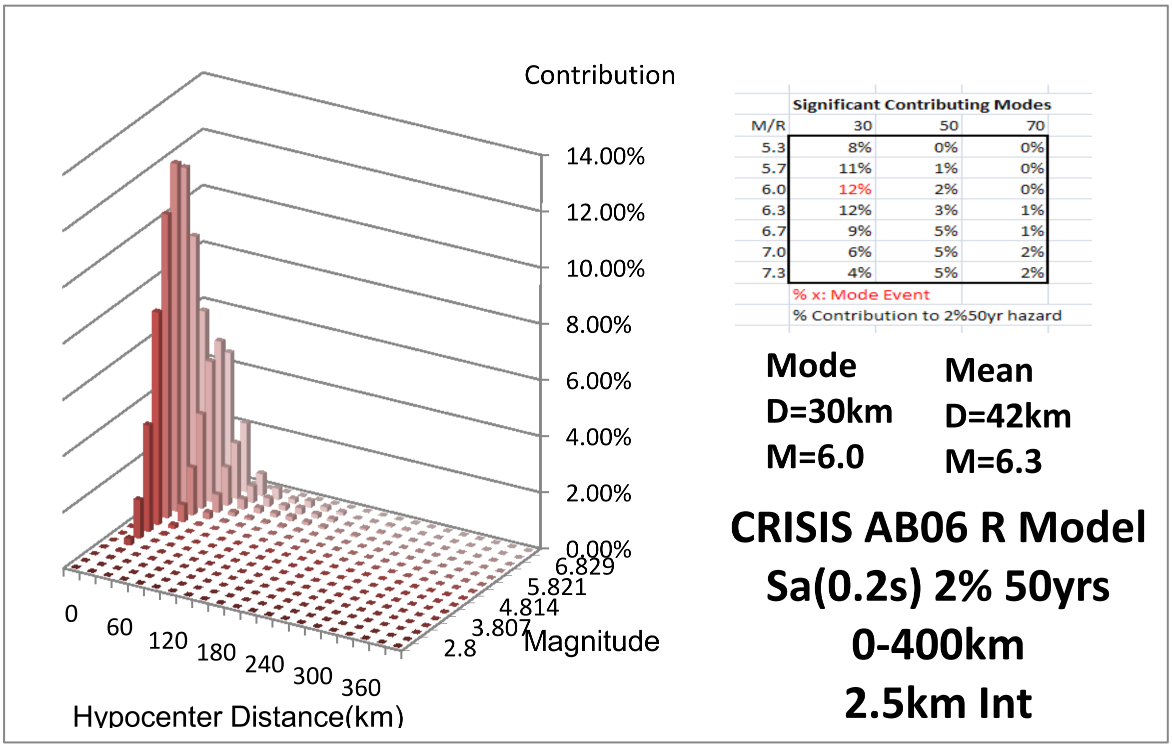

Figure A-7: Deaggregation results from CRISIS for Sa(0.2s) using ground motion prediction equation AB06

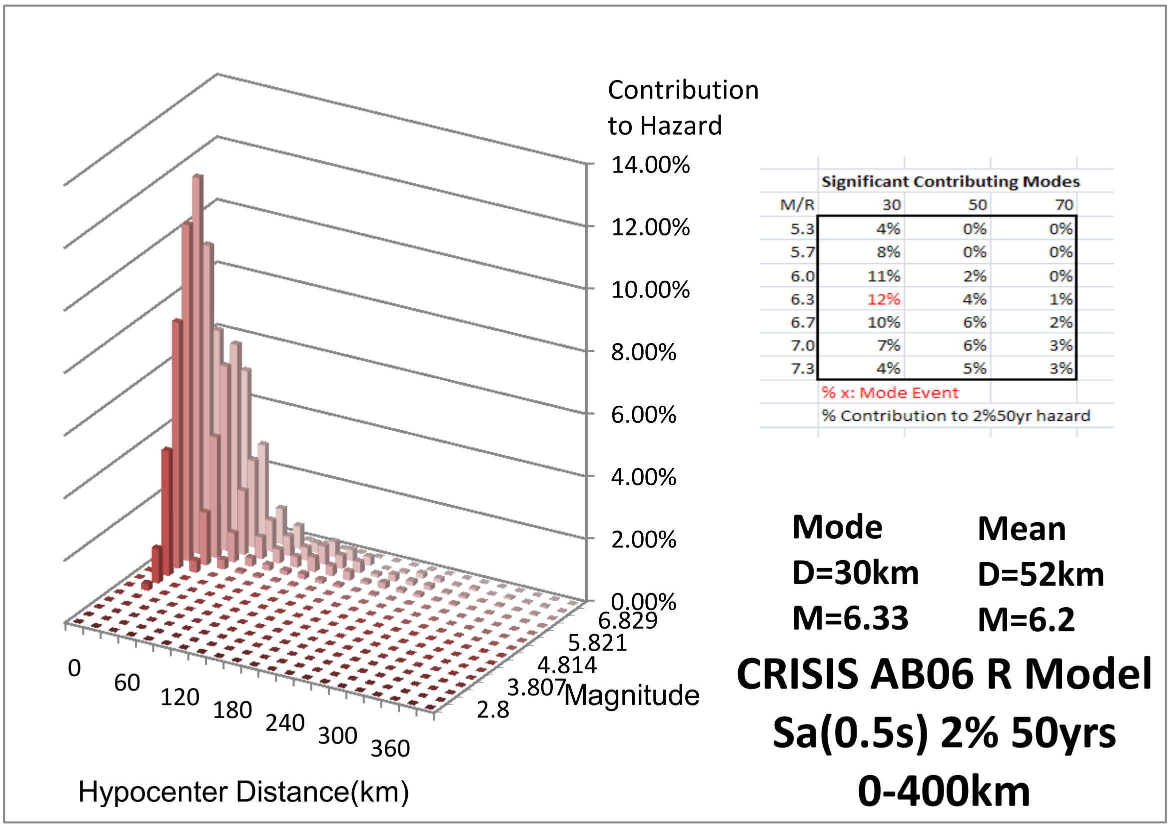

Figure A-8: Deaggregation results from CRISIS for Sa(0.5s) using ground motion prediction equation AB06

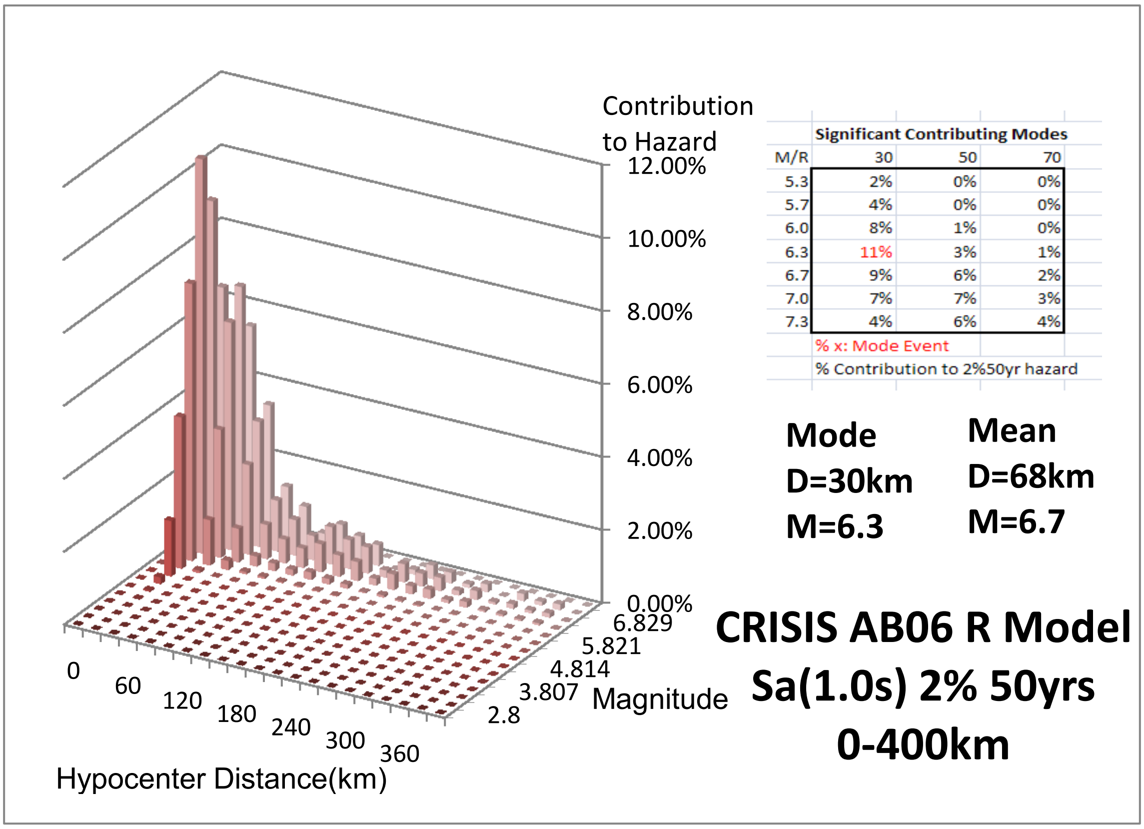

Figure A-9: Deaggregation results from CRISIS for Sa(1.0s) using ground motion prediction equation AB06

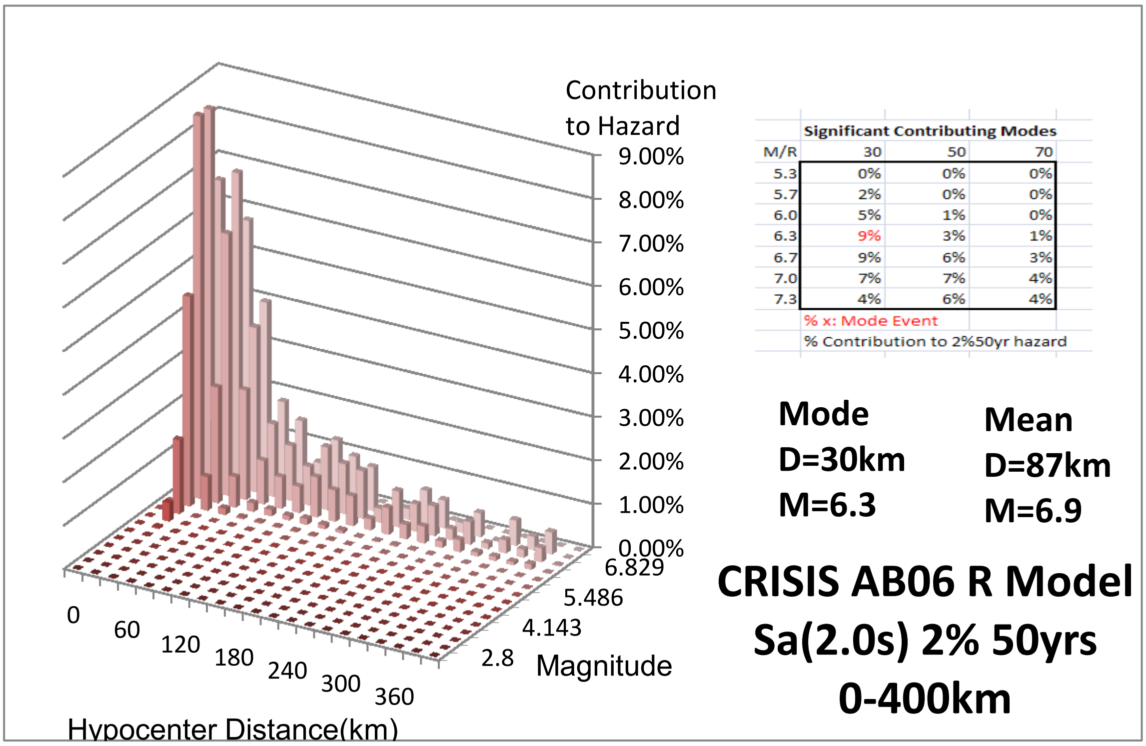

Figure A-10: Deaggregation results from CRISIS for Sa(2.0s) using ground motion prediction equation AB06

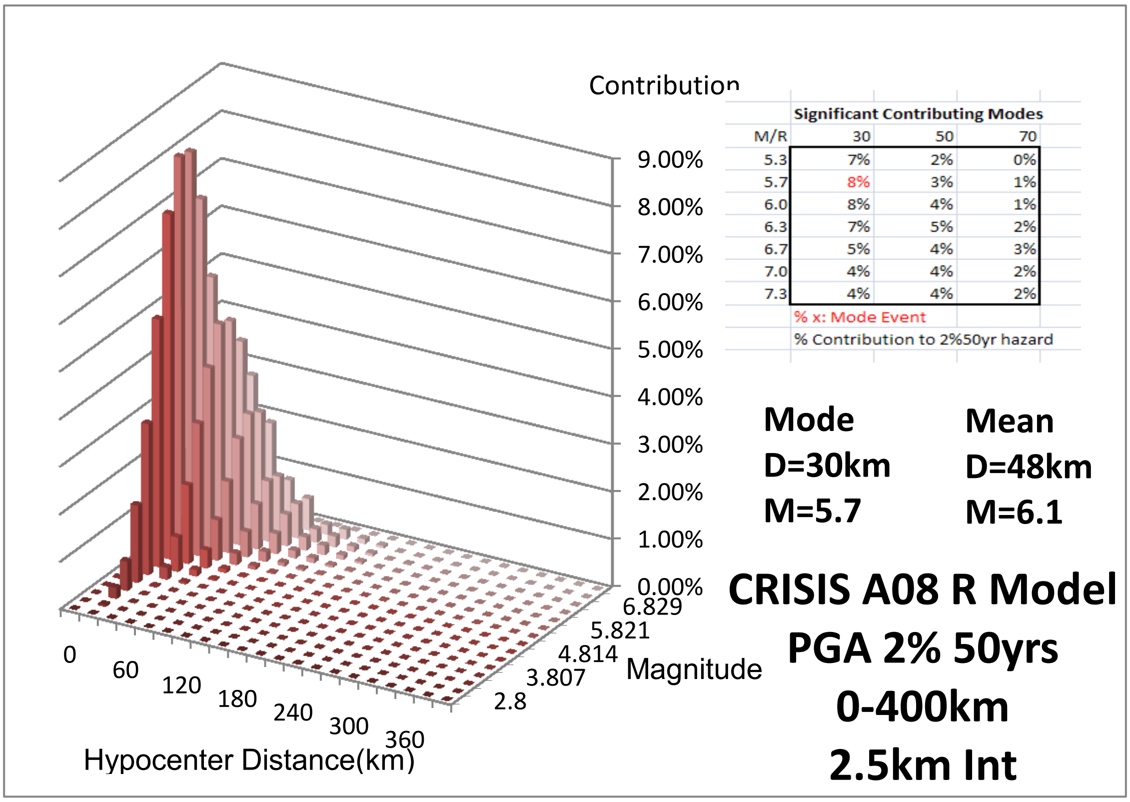

Figure A-11: Deaggregation results from CRISIS for PGA using ground motion prediction equation A08

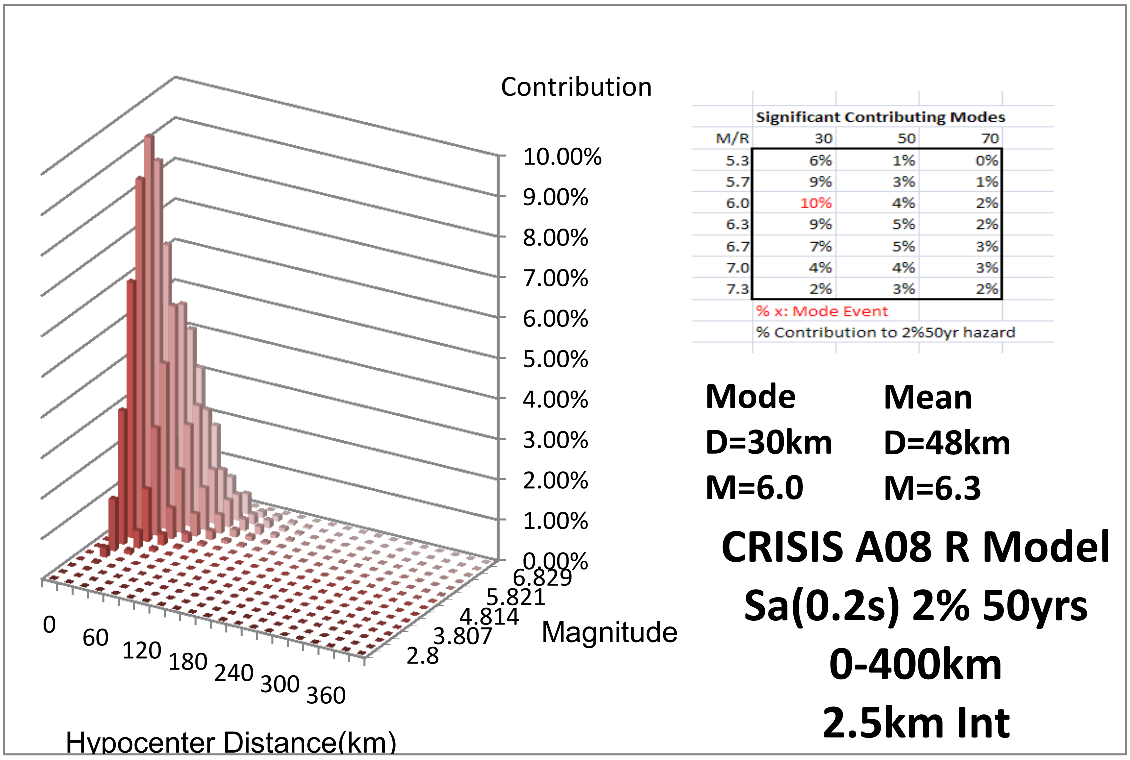

Figure A-12: Deaggregation results from CRISIS for Sa(0.2s) using ground motion prediction equation A08

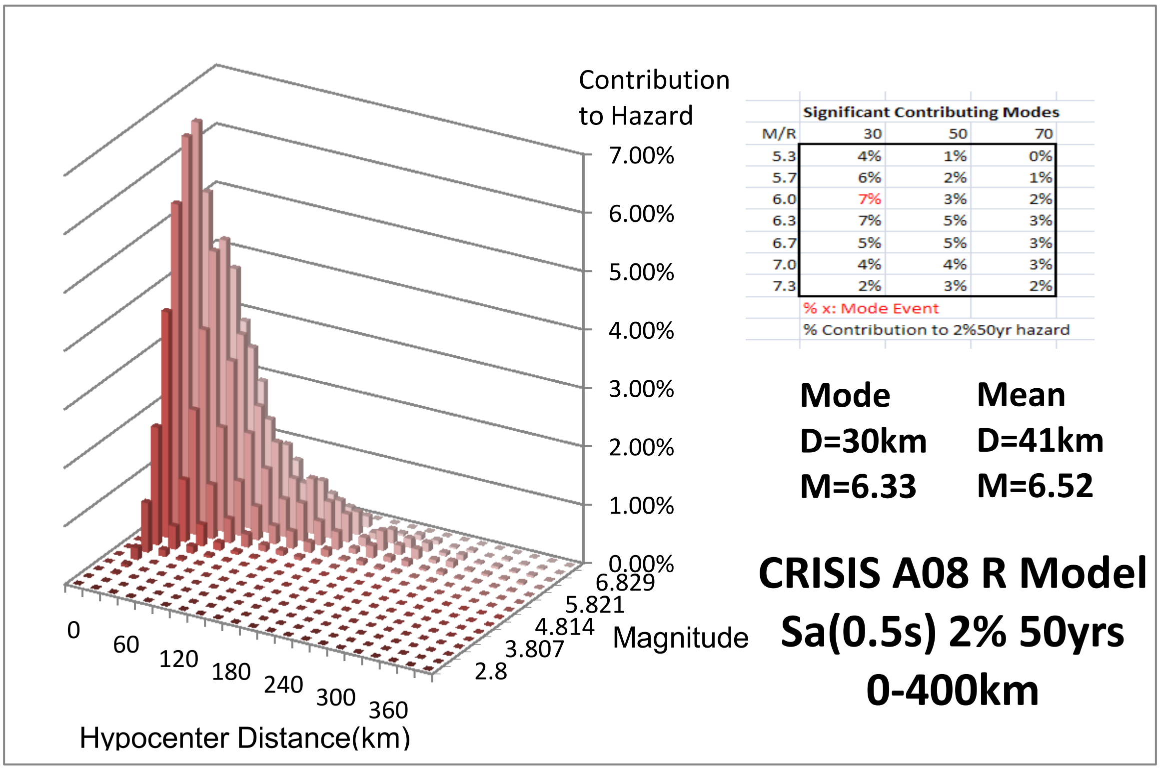

Figure A-13: Deaggregation results from CRISIS for Sa(0.5s) using ground motion prediction equation A08

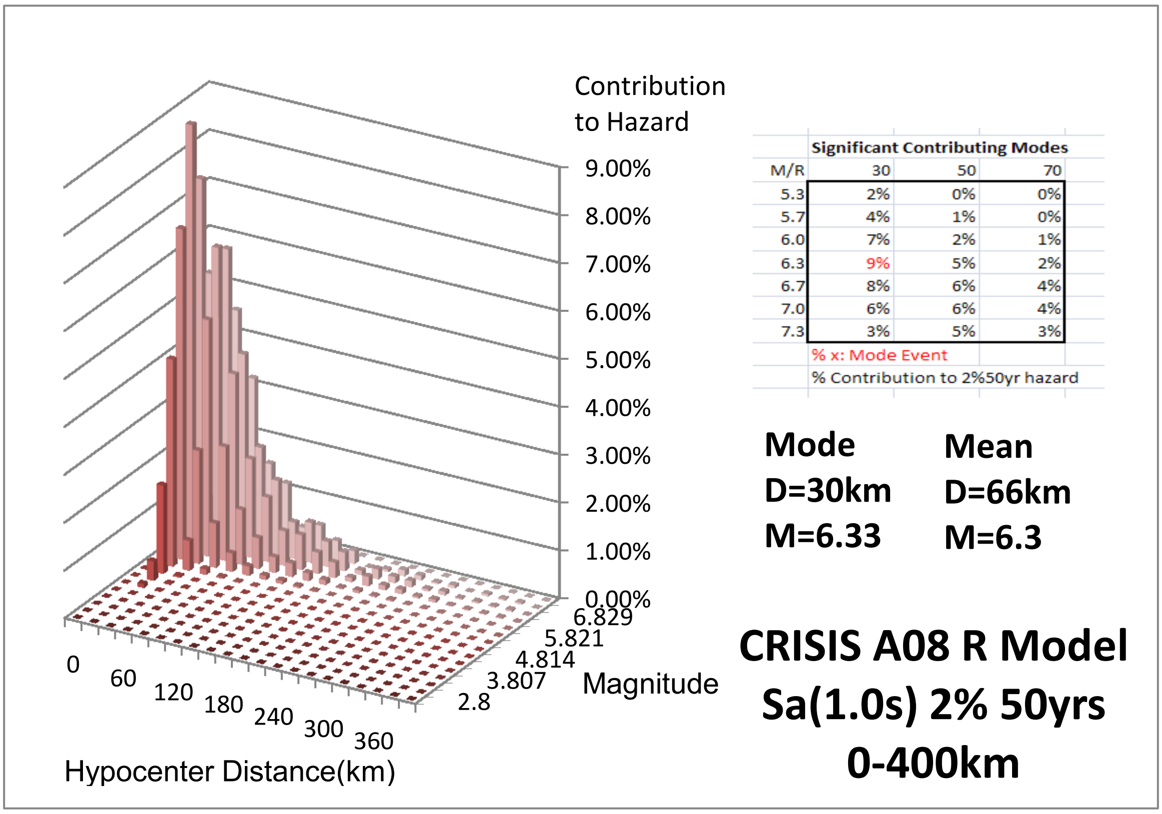

Figure A-14: Deaggregation results from CRISIS for Sa(1.0s) using ground motion prediction equation A08

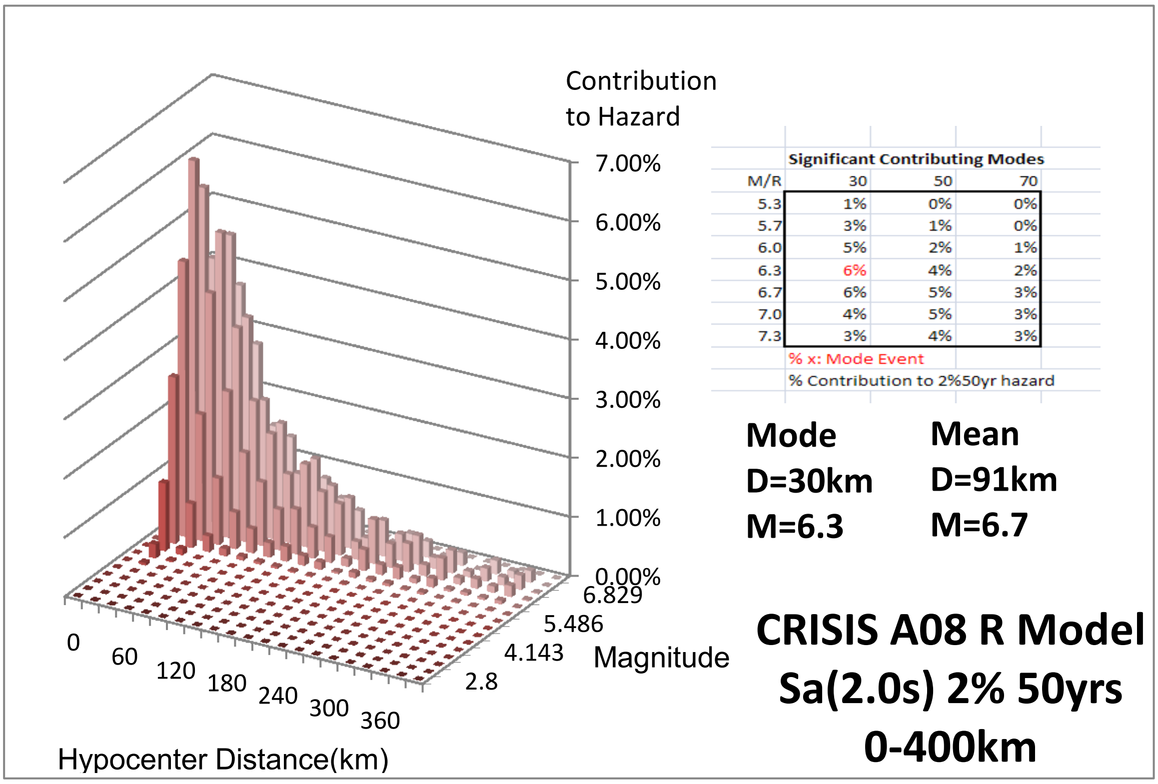

Figure A-15: Deaggregation results from CRISIS for Sa(2.0s) using ground motion prediction equation A08

Appendix B: Ground Motion Parameter Calculation using AB06 and A08

AB06:

$$LogY = c_1 + c_2M + c_3M^2 + (c_4 + c_5M)f_1 + (c_6 + c_7M)f_2 + (c_8 + c_9M)f_0 + c_{10}R_{cd} + S$$

(Atkinson & Boore, 2006)

1) Decide which soil class the site belongs to according to the soil map developed. If the soil class of the site is A, then apply equation using factors in Table B-1. If not, then go to step 2.

2) Calculate Y (PGA, PGV, Sa0.3s, and Sa1.0s) for Site B/C boundary using Table B-2.

3) Calculate S factor based on $PGA_{B/C}$ and Site class for each ground motion parameters depending on the V_{30} value of the site. (V30=1130 for Class B, 560 for Class C, 270 for ClassD)

$$S = \log\left\{exp\left[b_{lin}\ln\left(\frac{V_{30}}{V_{ref}}\right) + b_{ln}\ln\left(\frac{60}{100}\right)\right]\right\} \quad for\ pgaBC \le 60cm/sec^2$$

and

$$S = \log\left\{exp\left[b_{lin}\ln\left(\frac{V_{30}}{V_{ref}}\right) + b_{ln}\ln\left(\frac{pgaBC}{100}\right)\right]\right\} \quad for\ pgaBC > 60cm/sec^2$$

Where

b_{nl} is slope controlling the non-linear factor, defined by the following equations

$$b_{nl} = b_1 \qquad\qquad for\ V_{30} \le V_1$$

$$b_{nl} = \frac{(b_1 - b_2)\ln\left(\frac{V_{30}}{V_2}\right)}{\ln\left(\frac{V_1}{V_2}\right)} + b_2 \qquad\qquad for\ V_1 < V_{30} \le V_2$$

$$b_{nl} = \frac{b_2 \ln\left(\frac{V_{30}}{V_{ref}}\right)}{\ln\left(\frac{V_2}{V_{ref}}\right)} \qquad\qquad for\ V_2 < V_{30} \le V_{ref}$$

$$b_{nl} = 0.0 \qquad\qquad for\ V_{30} > V_{ref}$$

Coefficient Used in the Calculation of Soil Amplification Factor S

Period(s)	**b_{lin}**	**b_1**	**b_2**
Sa(1.0s)	-0.7	-0.44	0
Sa(0.3125s)	-0.445	-0.513	-0.13
Sa(0.25s)	-0.39	-0.518	-0.16
Sa(0.3s)*	-0.434	-0.514	-0.136
PGA	-0.361	-0.641	-0.144
PGV	-0.6	-0.495	-0.06

* blin, b1, and b2 used for Sa(0.3 s) is interpolated from coefficients for Sa(0.3125s) and Sa(0.25s)

4) Add S factor to the corresponding ground motion parameter calculated in step 2, obtaining the ground motion parameter for the site.

Table B-1: Coefficients for Ground Motion Parameters Calculation on Hard Rock Site for the use in AB06 GMPE (Atkinson & Boore, 2006)

Table 6

Coefficients of Equations for Predicting Median ENA Ground Motions on Hard Rock (Horizontal Component, log(10) Values Are Given in cgs Units) for 5% Damped PSA at Stated Frequencies, According to Equation (5)

Frequency (Hz)	Period (sec)	c_1	c_2	c_3	c_4	c_5	c_6	c_7	c_8	c_9	c_{10}
0.20	5.00	−5.41E+00	1.71E+00	−9.01E−2	−2.54E+00	2.27E−01	−1.27E+00	1.16E−01	9.79E−01	−1.77E−01	−1.76E−04
0.25	4.00	−5.79E+00	1.92E+00	−1.07E−01	−2.44E+00	2.11E−01	−1.16E+00	1.02E−01	1.01E+00	−1.82E−01	−2.01E−04
0.32	3.13	−6.04E+00	2.08E+00	−1.22E−01	−2.37E+00	2.00E−01	−1.07E+00	8.95E−02	1.00E+00	−1.80E−01	−2.31E−04
0.40	2.50	−6.17E+00	2.21E+00	−1.35E−01	−2.30E+00	1.90E−01	−9.86E−01	7.86E−02	9.68E−01	−1.77E−01	−2.82E−04
0.50	2.00	−6.18E+00	2.30E+00	−1.44E−01	−2.22E+00	1.77E−01	−9.37E−01	7.07E−02	9.52E−01	−1.77E−01	−3.22E−04
0.63	1.59	−6.04E+00	2.34E+00	−1.50E−01	−2.16E+00	1.66E−01	−8.70E−01	6.05E−02	9.21E−01	−1.73E−01	−3.75E−04
0.80	1.25	−5.72E+00	2.32E+00	−1.51E−01	−2.10E+00	1.57E−01	−8.20E−01	5.19E−02	8.56E−01	−1.66E−01	−4.33E−04
1.0	1.00	−5.27E+00	2.26E+00	−1.48E−01	−2.07E+00	1.50E−01	−8.13E−01	4.67E−02	8.26E−01	−1.62E−01	−4.86E−04
1.3	0.794	−4.60E+00	2.13E+00	−1.41E−01	−2.06E+00	1.47E−01	−7.97E−01	4.35E−02	7.75E−01	−1.56E−01	−5.79E−04
1.6	0.629	−3.92E+00	1.99E+00	−1.31E−01	−2.05E+00	1.42E−01	−7.82E−01	4.30E−02	7.88E−01	−1.59E−01	−6.95E−04
2.0	0.500	−3.22E+00	1.83E+00	−1.20E−01	−2.02E+00	1.34E−01	−8.13E−01	4.44E−02	8.84E−01	−1.75E−01	−7.70E−04
2.5	0.397	−2.44E+00	1.65E+00	−1.08E−01	−2.05E+00	1.36E−01	−8.43E−01	4.48E−02	7.39E−01	−1.56E−01	−8.51E−04
3.2	0.315	−1.72E+00	1.48E+00	−9.74E−02	−2.08E+00	1.38E−01	−8.89E−01	4.87E−02	6.10E−01	−1.39E−01	−9.54E−04
4.0	0.251	−1.12E+00	1.34E+00	−8.72E−02	−2.08E+00	1.35E−01	−9.71E−01	5.63E−02	6.14E−01	−1.43E−01	−1.06E−03
5.0	0.199	−6.15E−01	1.23E+00	−7.89E−02	−2.09E+00	1.31E−01	−1.12E+00	6.79E−02	6.06E−01	−1.46E−01	−1.13E−03
6.3	0.158	−1.46E−01	1.12E+00	−7.14E−02	−2.12E+00	1.30E−01	−1.30E+00	8.31E−02	5.62E−01	−1.44E−01	−1.18E−03
8.0	0.125	2.14E−01	1.05E+00	−6.66E−02	−2.15E+00	1.30E−01	−1.61E+00	1.05E−01	4.27E−01	−1.30E−01	−1.15E−03
10.0	0.100	4.80E−01	1.02E+00	−6.40E−02	−2.20E+00	1.27E−01	−2.01E+00	1.33E−01	3.37E−01	−1.27E−01	−1.05E−03
12.6	0.079	6.91E−01	9.97E−01	−6.28E−02	−2.26E+00	1.25E−01	−2.49E+00	1.64E−01	2.14E−01	−1.21E−01	−8.47E−04
15.9	0.063	9.11E−01	9.80E−01	−6.21E−02	−2.36E+00	1.26E−01	−2.97E+00	1.91E−01	1.07E−01	−1.17E−01	−5.79E−04
20.0	0.050	1.11E+00	9.72E−01	−6.20E−02	−2.47E+00	1.28E−01	−3.39E+00	2.14E−01	−1.39E−01	−9.84E−02	−3.17E−04
25.2	0.040	1.26E+00	9.68E−01	−6.23E−02	−2.58E+00	1.32E−01	−3.64E+00	2.28E−01	−3.51E−01	−8.13E−02	−1.23E−04
31.8	0.031	1.44E+00	9.59E−01	−6.28E−02	−2.71E+00	1.40E−01	−3.73E+00	2.34E−01	−5.43E−01	−6.45E−02	−3.23E−05
40.0	0.025	1.52E+00	9.60E−01	−6.35E−02	−2.81E+00	1.46E−01	−3.65E+00	2.36E−01	−6.54E−01	−5.50E−02	−4.85E−05
PGA	0.010	9.07E−01	9.83E−01	−6.60E−02	−2.70E+00	1.59E−01	−2.80E+00	2.12E−01	−3.01E−01	−6.53E−02	−4.48E−04
PGV	0.011	−1.44E+00	9.91E−01	−5.85E−02	−2.70E+00	2.16E−01	−2.44E+00	2.66E−01	8.48E−02	−6.93E−02	−3.73E−04

Total sigma = 0.30 for all frequencies.

Table B-2: Coefficients for Ground Motion Parameters Calculation on B/C Boundary Site for the use in AB06 GMPE (Atkinson & Boore, 2006)

Coefficients of Equations for Predicting Median ENA Ground Motions for BC Boundary (V_{30} = 760 m/sec) (Horizontal Component, log(10) Values Are Given in cgs Units) for 5% Damped PSA at Stated Frequencies, According to Equation (5)

Frequency (Hz)	Period (sec)	c_1	c_2	c_3	c_4	c_5	c_6	c_7	c_8	c_9	c_{10}
0.20	5.00	−4.85E+00	1.58E+00	−8.07E−02	−2.53E+00	2.22E−01	−1.43E+00	1.36E−01	6.34E−01	−1.41E−01	−1.61E−04
0.25	4.00	−5.26E+00	1.79E+00	−9.79E−02	−2.44E+00	2.07E−01	−1.31E+00	1.21E−01	7.34E−01	−1.56E−01	−1.96E−04
0.32	3.13	−5.59E+00	1.97E+00	−1.14E−01	−2.33E+00	1.91E−01	−1.20E+00	1.10E−01	8.45E−01	−1.72E−01	−2.45E−04
0.40	2.50	−5.80E+00	2.13E+00	−1.28E−01	−2.26E+00	1.79E−01	−1.12E+00	9.54E−02	8.91E−01	−1.80E−01	−2.60E−04
0.50	2.00	−5.85E+00	2.23E+00	−1.39E−01	−2.20E+00	1.69E−01	−1.04E+00	8.00E−02	8.67E−01	−1.79E−01	−2.86E−04
0.63	1.59	−5.75E+00	2.29E+00	−1.45E−01	−2.13E+00	1.58E−01	−9.57E−01	6.76E−02	8.67E−01	−1.79E−01	−3.43E−04
0.80	1.25	−5.49E+00	2.29E+00	−1.48E−01	−2.08E+00	1.50E−01	−9.00E−01	5.79E−02	8.21E−01	−1.72E−01	−4.07E−04
1.0	1.00	−5.06E+00	2.23E+00	−1.45E−01	−2.03E+00	1.41E−01	−8.74E−01	5.41E−02	7.92E−01	−1.70E−01	−4.89E−04
1.3	0.794	−4.45E+00	2.12E+00	−1.39E−01	−2.01E+00	1.36E−01	−8.58E−01	4.98E−02	7.08E−01	−1.59E−01	−5.75E−04
1.6	0.629	−3.75E+00	1.97E+00	−1.29E−01	−2.00E+00	1.31E−01	−8.42E−01	4.82E−02	6.77E−01	−1.56E−01	−6.76E−04
2.0	0.500	−3.01E+00	1.80E+00	−1.18E−01	−1.98E+00	1.27E−01	−8.47E−01	4.70E−02	6.67E−01	−1.55E−01	−7.68E−04
2.5	0.397	−2.28E+00	1.63E+00	−1.05E−01	−1.97E+00	1.23E−01	−8.88E−01	5.03E−02	6.84E−01	−1.58E−01	−8.59E−04
3.2	0.315	−1.56E+00	1.46E+00	−9.31E−02	−1.98E+00	1.21E−01	−9.47E−01	5.58E−02	6.50E−01	−1.56E−01	−9.55E−04
4.0	0.251	−8.76E−01	1.29E+00	−8.19E−02	−2.01E+00	1.23E−01	−1.03E+00	6.34E−02	5.81E−01	−1.49E−01	−1.05E−03
5.0	0.199	−3.06E−01	1.16E+00	−7.21E−02	−2.04E+00	1.22E−01	−1.15E+00	7.38E−02	5.08E−01	−1.43E−01	−1.14E−03
6.3	0.158	1.19E−01	1.06E+00	−6.47E−02	−2.05E+00	1.19E−01	−1.36E+00	9.16E−02	5.16E−01	−1.50E−01	−1.18E−03
8.0	0.125	5.36E−01	9.65E−01	−5.84E−02	−2.11E+00	1.21E−01	−1.67E+00	1.16E−01	3.43E−01	−1.32E−01	−1.13E−03
10.0	0.100	7.82E−01	9.24E−01	−5.56E−02	−2.17E+00	1.19E−01	−2.10E+00	1.48E−01	2.85E−01	−1.32E−01	−9.90E−04
12.6	0.079	9.67E−01	9.03E−01	−5.48E−02	−2.25E+00	1.22E−01	−2.53E+00	1.78E−01	1.00E−01	−1.15E−01	−7.72E−04
15.9	0.063	1.11E+00	8.88E−01	−5.39E−02	−2.33E+00	1.23E−01	−2.88E+00	2.01E−01	−3.19E−02	−1.07E−01	−5.48E−04
20.0	0.050	1.21E+00	8.83E−01	−5.44E−02	−2.44E+00	1.30E−01	−3.04E+00	2.13E−01	−2.10E−01	−9.00E−02	−4.15E−04
25.2	0.040	1.26E+00	8.79E−01	−5.52E−02	−2.54E+00	1.39E−01	−2.99E+00	2.16E−01	−3.91E−01	−6.75E−02	−3.88E−04
31.8	0.031	1.19E+00	8.88E−01	−5.64E−02	−2.58E+00	1.45E−01	−2.84E+00	2.12E−01	−4.37E−01	−5.87E−02	−4.33E−04
40.0	0.025	1.05E+00	9.03E−01	−5.77E−02	−2.57E+00	1.48E−01	−2.65E+00	2.07E−01	−4.08E−01	−5.77E−02	−5.12E−04
PGA	0.010	5.23E−01	9.69E−01	−6.20E−02	−2.44E+00	1.47E−01	−2.34E+00	1.91E−01	−8.70E−02	−8.29E−02	−6.30E−04
PGV	0.011	−1.66E+00	1.05E+00	−6.04E−02	−2.50E+00	1.84E−01	−2.30E+00	2.50E−01	1.27E−01	−8.70E−02	−4.27E−04

Total sigma = 0.30 for all frequencies.

A08:

A08 is the latest attenuation relationship developed by Atkinson (2008) using referenced empirical approach. It is based on the This GMPE is largely based on the relationship developed by Boore and Atkinson (2008). Using the database developed for the PEER-NGA project, BA08 empirically developed an GMPE that describes ground motion parameter(Y) as a function of magnitude scaling (F_M), distance function (F_D), and site amplification (F_s) as shown in the following equation:

$$lnY = F_M(M) + F_D\left(R_{JB}, M\right) + F_s\left(V_{s30}, R_{JB}, M\right) + \varepsilon\sigma_T$$

(Boore & Atkinson, 2008)

Where M is the moment magnitude, R_{JB} is the Joyner-Boore distance.(Boore & Atkinson, 2008)

A08 adopts this relationship and calibrates the equation with ENA database, adding a correction factor F to the equation. This F factor is expressed as a quadratic function of distance R, shown in equation:

$$logF = c_0 + c_1 R_{jb} + c_2 R_{jb}^2$$

(Atkinson, 2008)

The A08 ground motion prediction is simply the product of the ground motion predicted using BA08 equation and the correction factor F.(Atkinson, 2008)

$$Y_{ENA} = FY_{BA07}$$

The calculation steps can be divided into following steps:

1) Calculate distance function F_D from BA08. The coefficients used for ground motion parameters PGA, Sa(0.3s), Sa(1.0s), and PGV are listed here, taken from Table 6 in (Boore & Atkinson, 2008).

$$F_D(R_{JB}, \mathbf{M}) = [c_1 + c_2(\mathbf{M} - \mathbf{M}_{ref})]\ln(R/R_{ref}) + c_3(R - R_{ref}),$$

$$R = \sqrt{R_{JB}^2 + h^2}$$

	PGV	**PGA**	**0.3s**	**1.0s**

c1	-0.8737	-0.6605	-0.5543	-0.8183
c2	0.1006	0.1197	0.01955	0.1027
c3	-0.00334	-0.01151	-0.0075	-0.00334
h	2.54	1.35	2.14	2.54
Mref(Mw)	4.5	4.5	4.5	4.5
Rref(km)*	1	1	1	1

2) Calculate magnitude scaling function F_M. The coefficients used for ground motion parameters PGA, Sa(0.3s), Sa(1.0s), and PGV are listed here, taken from Table 2 and Table 7 in (Boore & Atkinson, 2008). U, SS, NS, RS are dummy variables for different fault type. For Montreal region, the fault type is unknown (U). Therefore, SS, NS, RS are 0 for calculations used in this study.

a) $\mathbf{M} \leq \mathbf{M}_h$

$$F_M(\mathbf{M}) = e_1 U + e_2 SS + e_3 NS + e_4 RS + e_5(\mathbf{M} - \mathbf{M}_h) + e_6(\mathbf{M} - \mathbf{M}_h)^2,$$

b) $\mathbf{M} > \mathbf{M}_h$

$$F_M(\mathbf{M}) = e_1 U + e_2 SS + e_3 NS + e_4 RS + e_7(\mathbf{M} - \mathbf{M}_h),$$

	PGV	**PGA**	**0.3s**	**1.0s**
Mh	8.5	6.75	6.75	6.75
e1	5.00121	-0.53804	0.43825	-0.46896
e2	5.04727	-0.5035	0.44516	-0.43443
e3	4.63188	-0.75472	0.25356	-0.78465
e4	5.0821	-0.5097	0.5199	-0.3933
e5	0.18322	0.28805	0.64472	0.6788
e6	-0.12736	-0.10164	-0.15694	-0.18257
e7	0	0	0.10601	0.05393
U	1	1	1	1
SS	0	0	0	0
NS	0	0	0	0
RS	0	0	0	0

3) Calculate correlation factor F to adapt BA08 to A08.

$$\log F = c_0 + c_1 R_{jb} + c_2 R_{jb}^2,$$

(Atkinson, 2008)

	PGV	PGA	0.3s	1.0s
c1	-1.11E-03	1.20E-03	0.001337	5.56E-04
c2	1.89E-06	2.30E-06	1.08E-06	7.44E-07
c0(avg)	-0.029	0.287	-0.18933	-0.376
c0(std.deviation)	0.223	0.331	0.316	0.288
c0w	0.047	0.163	-0.222	-0.404

4) Calculate site amplification factors F_S according to site class. For soil class B, C, D, E, the S factor is the same as the one presented in AB06 calculation. For soil class A, the factor is based on the ratio of ground motion parameter calculated for soil class B/C boundary(V30=760m/s) and soil class A using AB06 GMPE.

$$F_{sA}=\ln(AB06(rock)/AB06(soilB\&C))$$

(Atkinson, personal communication, 2010)

5) Add up distance function (FD), magnitude scaling function (FM), A08 adaption factor (F) and soil amplification faction. The calculated average ground motion parameters is Y, which is PGA, PGV, Sa(0.3s), and Sa(1.0s) in this study.

$$Ln(Y)=F_D+F_M+\ln(F)+F_s$$

Table B-3: NEHRP Soil Classification

Site Class	Site Class Description	Shear Wave Velocity (m/sec)	
		Minimum	Maximum
A	**HARD ROCK** Eastern United States sites only	1500	
B	**ROCK**	760	1500
C	**VERY DENSE SOIL AND SOFT ROCK** Untrained shear strength $u_s \geq 2000$ psf ($u_s \geq 100$ kPa) or $N \geq 50$ blows/ft	360	760
D	**STIFF SOILS** Stiff soil with undrained shear strength 1000 psf $\leq u_s \leq 2000$ psf (50 kPa $\leq u_s \leq$ 100 kPa) or $15 \leq N \leq 50$ blows/ft	180	360
E	**SOFT SOILS** Profile with more than 10 ft (3 m) of soft clay defined as soil with plasticity index PI > 20, moisture content *w* > 40% and undrained shear strength u_s < 1000 psf (50 kPa) (N < 15 blows/ft)		180
F	**SOILS REQUIRING SITE SPECIFIC EVALUATIONS** **1. Soils vulnerable to potential failure or collapse under seismic loading:** e.g. liquefiable soils, quick and highly sensitive clays, collapsible weakly cemented soils. **2. Peats and/or highly organic clays** (10 ft (3 m) or thicker layer) **3. Very high plasticity clays:** (25 ft (8 m) or thicker layer with plasticity index >75) **4. Very thick soft/medium stiff clays:** (120 ft (36 m) or thicker layer)		

Appendix C: Soil Map Input Data

Table C-1: Mini-Vib Results

ID	X	Y	Vs30	CMP
NDE10050	-73.49441197130	45.66855446830	312.549916	50.000000
NDE10075	-73.49424250180	45.66888976950	302.574698	75.000000
NDE10100	-73.49407303020	45.66922507030	290.306034	100.000000
NDE10125	-73.49397992480	45.66961924100	296.292617	125.000000
NDE10150	-73.49388681800	45.67001341160	295.276919	150.000000
NDE10175	-73.49379370990	45.67040758200	309.406084	175.000000
NDE10200	-73.49370060030	45.67080175230	358.219472	200.000000
NDE10225	-73.49360748940	45.67119592250	313.850204	225.000000
NDE10250	-73.49351437710	45.67159009260	348.312751	250.000000
NDE10275	-73.49342126340	45.67198426260	340.603383	275.000000
NDE10300	-73.49332814840	45.67237843240	335.859479	300.000000
NDE10325	-73.49323503200	45.67277260210	327.930360	325.000000
NDE10350	-73.49314191410	45.67316677170	321.872651	350.000000
NDE10375	-73.49304879500	45.67356094120	311.875168	375.000000
NDE10400	-73.49295567440	45.67395511060	333.835812	400.000000
NDE10425	-73.49286255250	45.67434927980	340.588196	425.000000
NDE10450	-73.49276942920	45.67474344900	321.983716	450.000000
NDE10475	-73.49267630450	45.67513761800	333.708972	475.000000
NDE10500	-73.49258317840	45.67553178690	319.145836	500.000000
NDE10525	-73.49249005100	45.67592595560	303.524258	525.000000
NDE10550	-73.49239692210	45.67632012430	315.566941	550.000000
NDE10575	-73.49230379190	45.67671429280	297.610192	575.000000
NDE10600	-73.49221066040	45.67710846120	308.788800	600.000000
NDE10625	-73.49211752740	45.67750262950	322.294715	625.000000
NDE10650	-73.49202439310	45.67789679770	299.824122	650.000000
NDE10675	-73.49193125740	45.67829096580	290.008385	675.000000
NDE10700	-73.49183812030	45.67868513370	283.252906	700.000000
NDE10725	-73.49174498180	45.67907930150	278.063014	725.000000
NDE10750	-73.49165184200	45.67947346920	300.046015	750.000000
NDE10775	-73.49155870070	45.67986763680	286.584517	775.000000
NDE10800	-73.49146555820	45.68026180430	295.981403	800.000000
NDE10825	-73.49137241420	45.68065597160	296.799633	825.000000
NDE10850	-73.49127926880	45.68105013890	281.221088	850.000000
NDE10875	-73.49118612210	45.68144430600	292.769498	875.000000
NDE10900	-73.49109297400	45.68183847300	284.285116	900.000000
NDE10925	-73.49099982450	45.68223263980	297.286833	925.000000
NDE10950	-73.49090667360	45.68262680660	286.700029	950.000000
NDE10975	-73.49081352140	45.68302097320	281.790099	975.000000
NDE11000	-73.49072036780	45.68341513970	267.490001	1000.000000
NDE11025	-73.49062721280	45.68380930610	280.942169	1025.000000
NDE11050	-73.49053405640	45.68420347240	283.438988	1050.000000
NDE11075	-73.49044089860	45.68459763860	293.049124	1075.000000
NDE11100	-73.49034773950	45.68499180460	283.475123	1100.000000
NDE11125	-73.49025457900	45.68538597050	283.882560	1125.000000
NDE11150	-73.49016141710	45.68578013630	290.433846	1150.000000
NDE11175	-73.49006825390	45.68617430200	279.533058	1175.000000

NDE11200	-73.48997508920	45.68656846760	285.225032	1200.000000
NDE11225	-73.48988192320	45.68696263300	289.402937	1225.000000
NDE11250	-73.48978875580	45.68735679830	280.269177	1250.000000
NDE11275	-73.48969558700	45.68775096350	275.633997	1275.000000
NDE11300	-73.48960241680	45.68814512860	283.394343	1300.000000
NDE11325	-73.48950924530	45.68853929360	284.111541	1325.000000
NDE11350	-73.48941607240	45.68893345840	270.814053	1350.000000
NDE11375	-73.48932289810	45.68932762320	284.216127	1375.000000
NDE11400	-73.48922972240	45.68972178780	291.371046	1400.000000
NDE11425	-73.48913654540	45.69011595230	266.246117	1425.000000
NDE11450	-73.48904336690	45.69051011670	278.795825	1450.000000
NDE11475	-73.48895018710	45.69090428090	275.477396	1475.000000
NDE11500	-73.48885700590	45.69129844500	286.020920	1500.000000
NDE20050	-73.48857235250	45.69232978270	288.914484	50.000000
NDE20075	-73.48843123400	45.69280046260	289.619142	75.000000
NDE20100	-73.48829011300	45.69327114230	278.935324	100.000000
NDE20125	-73.48811931610	45.69365142000	283.131182	125.000000
NDE20150	-73.48794851690	45.69403169740	283.823079	150.000000
NDE20175	-73.48777771530	45.69441197450	268.700362	175.000000
NDE20200	-73.48760691140	45.69479225130	269.651444	200.000000
NDE30050	-73.48662088090	45.69563427670	269.694272	50.000000
NDE30075	-73.48636164720	45.69589122480	228.040203	75.000000
NDE30100	-73.48610241100	45.69614817230	262.226796	100.000000
NDE30125	-73.48584317250	45.69640511920	266.522726	125.000000
NDE30150	-73.48558393150	45.69666206540	285.865769	150.000000
NDE30175	-73.48532468820	45.69691901110	283.411966	175.000000
NDE30200	-73.48506544250	45.69717595610	273.677291	200.000000
NDE30225	-73.48480619440	45.69743290040	254.382916	225.000000
NDE30250	-73.48454694390	45.69768984420	279.770802	250.000000
NDE30275	-73.48428769100	45.69794678730	258.477151	275.000000
NDE30300	-73.48402843570	45.69820372970	269.210968	300.000000
NDE30325	-73.48376917810	45.69846067160	269.529362	325.000000
NDE30350	-73.48350991800	45.69871761280	274.234125	350.000000
NDE30375	-73.48325065560	45.69897455340	271.811353	375.000000
NDE30400	-73.48299139070	45.69923149330	279.645209	400.000000
NDE30425	-73.48285324910	45.69958969430	266.169116	425.000000
NDE30450	-73.48271510570	45.69994789500	301.167943	450.000000
NDW10050	-73.53282445970	45.54858972380	389.270036	50.000000
NDW10075	-73.53263635470	45.54889531400	390.385107	75.000000
NDW10100	-73.53244824760	45.54920090380	411.097776	100.000000
NDW10125	-73.53226013850	45.54950649320	442.026123	125.000000
NDW10150	-73.53207202730	45.54981208230	427.316933	150.000000
NDW10175	-73.53188391400	45.55011767110	437.640610	175.000000
NDW10200	-73.53169579860	45.55042325950	411.119359	200.000000
NDW10225	-73.53150768120	45.55072884750	383.306901	225.000000
NDW10250	-73.53131956170	45.55103443520	387.657118	250.000000
NDW10275	-73.53113144010	45.55134002250	409.957994	275.000000

NDW10300	-73.53094331650	45.55164560950	383.300394	300.000000
NDW10325	-73.53075519080	45.55195119620	383.274033	325.000000
NDW10350	-73.53056706300	45.55225678250	399.389357	350.000000
NDW10375	-73.53037893310	45.55256236840	398.605355	375.000000
NDW10400	-73.53019080120	45.55286795400	409.147742	400.000000
NDW10425	-73.53000266710	45.55317353920	404.837627	425.000000
NDW10450	-73.52981453110	45.55347912410	383.005901	450.000000
NDW10475	-73.52962639290	45.55378470860	447.707502	475.000000
NDW10500	-73.52943825270	45.55409029280	389.417202	500.000000
NDW10525	-73.52925011030	45.55439587670	379.485008	525.000000
NDW10550	-73.52906196600	45.55470146010	397.465280	550.000000
NDW10575	-73.52887381950	45.55500704330	387.262319	575.000000
NDW10600	-73.52868567100	45.55531262600	417.000486	600.000000
NDW10625	-73.52849752040	45.55561820850	413.385439	625.000000
NDW10650	-73.52830936770	45.55592379050	385.955006	650.000000
NDW10675	-73.52812121290	45.55622937230	381.628733	675.000000
NDW10700	-73.52793305610	45.55653495360	421.342317	700.000000
NDW10725	-73.52774489720	45.55684053470	398.791284	725.000000
NDW10750	-73.52755673620	45.55714611530	368.363703	750.000000
NDW10775	-73.52736857310	45.55745169560	390.156842	775.000000
NDW10800	-73.52718040800	45.55775727560	390.967384	800.000000
NDW10825	-73.52699224080	45.55806285520	379.692674	825.000000
NDW10850	-73.52680407150	45.55836843450	392.599918	850.000000
NDW10875	-73.52661590020	45.55867401340	393.462016	875.000000
NDW10900	-73.52642772680	45.55897959200	416.594973	900.000000
NDW10925	-73.52623955130	45.55928517020	413.726058	925.000000
GN10050	-73.61317975280	45.47270973160	407.76171	-50
GN10075	-73.61349397990	45.47293857730	397.3223	-75
GN10100	-73.61380820950	45.47316742220	364.29864	-100
GN10125	-73.61412244160	45.47339626620	441.64298	-125
GN10150	-73.61443667630	45.47362510940	453.38399	-150
GN10175	-73.61475091350	45.47385395180	448.44156	-175
GN10200	-73.61506515320	45.47408279330	440.45941	-200
GN10225	-73.61518092720	45.47425297000	408.88162	-225
GN10250	-73.61529670190	45.47442314650	410.80947	-250
GN10275	-73.61565229370	45.47459623020	420.48831	-275
GN10300	-73.61600788780	45.47476931270	508.28231	-300
GN10325	-73.61664327170	45.47494578350	469.00726	-325
GN10350	-73.61727865970	45.47512225090	408.88159	-350
GN10375	-73.61791405170	45.47529871470	496.65302	-375
GN10400	-73.61854944780	45.47547517500	406.88235	-400
GN10425	-73.61894640060	45.47559249110	396.63745	-425
GN10450	-73.61934335510	45.47570980580	435.41448	-450
GN10475	-73.61974031130	45.47582711910	467.42812	-475
GN10500	-73.62013726910	45.47594443110	485.78562	-500
GN10525	-73.62045154250	45.47617325800	428.11929	-525
GN10550	-73.62076581830	45.47640208420	511.79796	-550

GN10575	-73.62108009680	45.47663090950	465.55556	-575
GS10050	-73.61127234040	45.47223649280	361.63834	50
GS10075	-73.61095812630	45.47200764100	388.95473	75
GS10100	-73.61064391480	45.47177878850	423.89915	100
GS10125	-73.61000858570	45.47160228480	430.47845	125
GS10150	-73.60937326070	45.47142577770	323.06612	150
GS10175	-73.60873793970	45.47124926710	374.6859	175
GS10200	-73.60810262280	45.47107275290	383.22045	200
GS10225	-73.60778842810	45.47084389270	342.80465	225
GS10250	-73.60747423600	45.47061503160	314.95812	250
GS10275	-73.60716004640	45.47038616970	322.55149	275
GS10300	-73.60684585940	45.47015730690	352.9445	300
GS10325	-73.60668876680	45.47004287520	369.15674	325
GS10350	-73.60653167490	45.46992844320	302.64561	350
GS10375	-73.60621749290	45.46969957880	286.71529	375
JB10050	-73.55533617110	45.55840380040	225.96385	-50
JB10075	-73.55533040520	45.55862875480	221.33066	-75
JB10100	-73.55596508850	45.55886180850	217.72754	-100
JB10125	-73.55651626370	45.55922881980	221.76232	-125
JB10150	-73.55675124950	45.55943431400	228.98166	-150
JB10175	-73.55698422120	45.55971854190	246.73639	-175
JB10200	-73.55721719510	45.56000276930	238.94539	-200
JB10225	-73.55769322460	45.56017755230	247.03544	-225
JB10250	-73.55816925710	45.56035233330	267.17069	-250
JB10275	-73.55864529250	45.56052711230	294.72787	-275
JB10300	-73.55912133100	45.56070188940	294.32755	-300
JB10325	-73.55975749070	45.56087868370	333.58453	-325
JB10350	-73.56039365460	45.56105547460	314.92354	-350
JB10375	-73.56102982240	45.56123226200	367.45545	-375
JB10400	-73.56166599440	45.56140904590	367.19754	-400
JB10425	-73.56214061510	45.56164004930	402.32863	-425
JB10450	-73.56262097710	45.56164609570	529.58141	-450
JB10500	-73.56357596810	45.56188313770	375.43242	-500

Figure C-1: Downhole Data

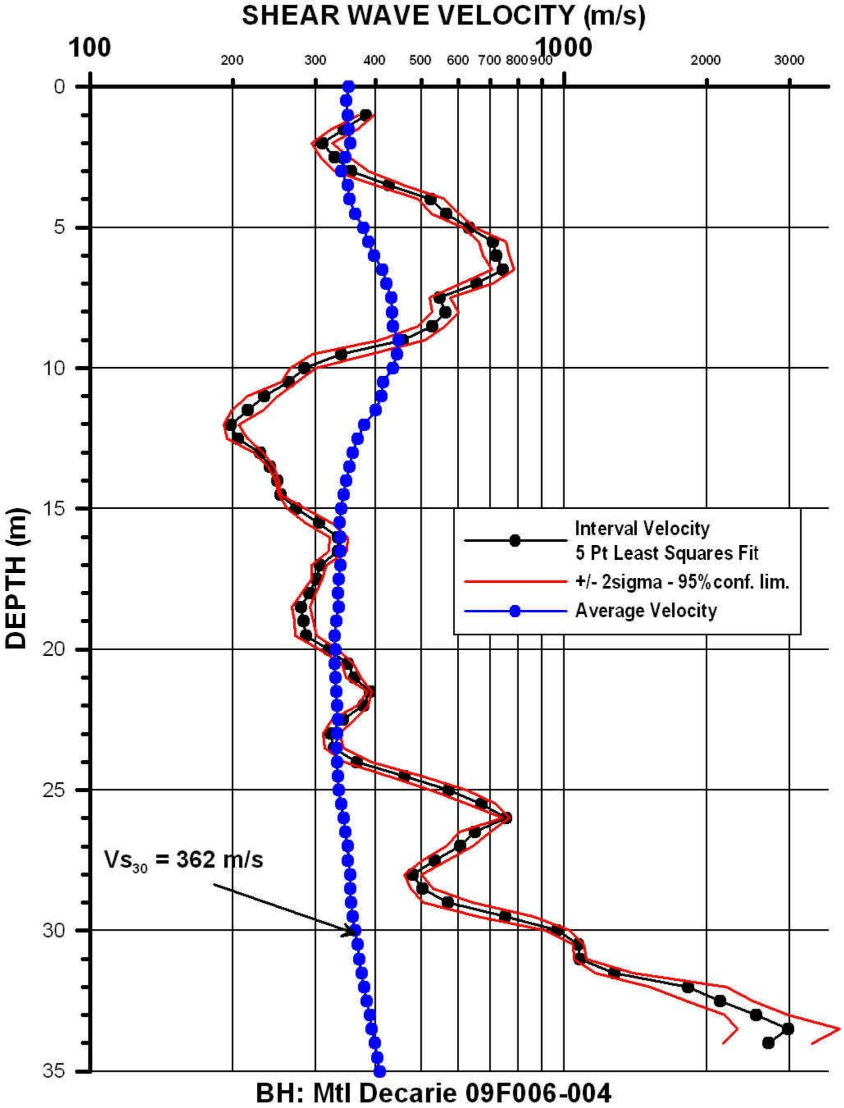

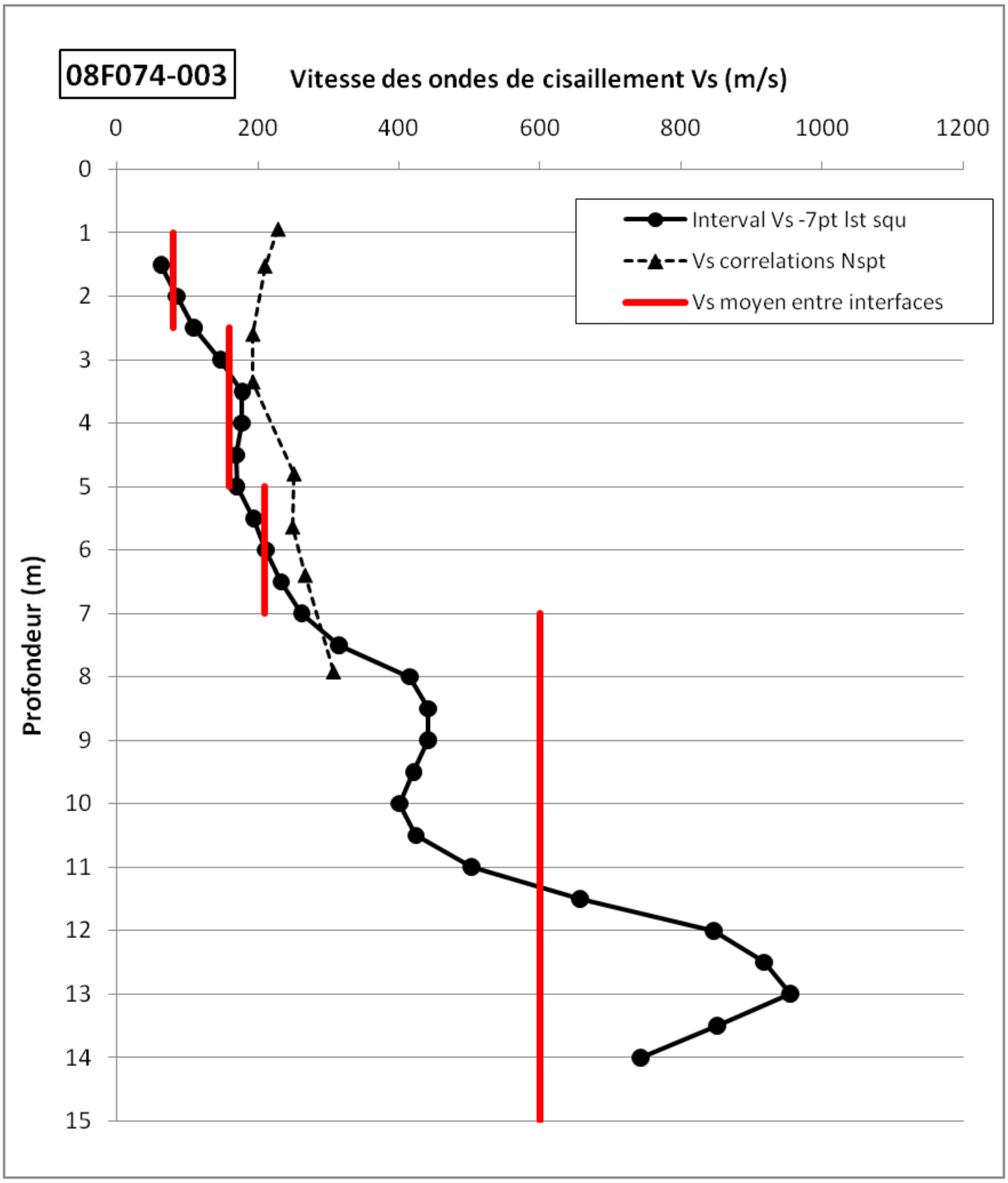

	$V_{S,30}$ estimée (m/s)	$V_{S,30}$ mesurée (m/s)
08F074-003	750 - 870	420 - 570
08F074-004	980 - 1200	520 - 690
	Type B	Type C

(City of Montreal, 2009)

Appendix D: Building Types Observed in Montreal for Low-rise Residential Buildings

17: Single storey masonry building

Foundation	Stone
Wall	stone/rubble stone
Floor	
Roof	Sloped
Material	Brick/wood
Structure:	Masonry bearing wall
Year:	-1840
Location:	
HAZUS code:	UMB

2: Urban Townhouse

Foundation	Masonry foundation wall
Wall	Load bearing firewalls on sides (wood studs+infill bricks)
Floor	Timber beam goes into bearing walls
Roof	Mansard with crushed stone+membrance
Material	Brick/wood
Structure:	Masonry bearing wall+ wood frame
Year:	Around 1900 towards 1920's
Location:	Square mile, Rue laval
HAZUS code:	UMB

Role 2005 ID: 11292000

Role 2005 ID: 53093500

Role 2005 ID: 54116600

Role 2005 ID: 28137900

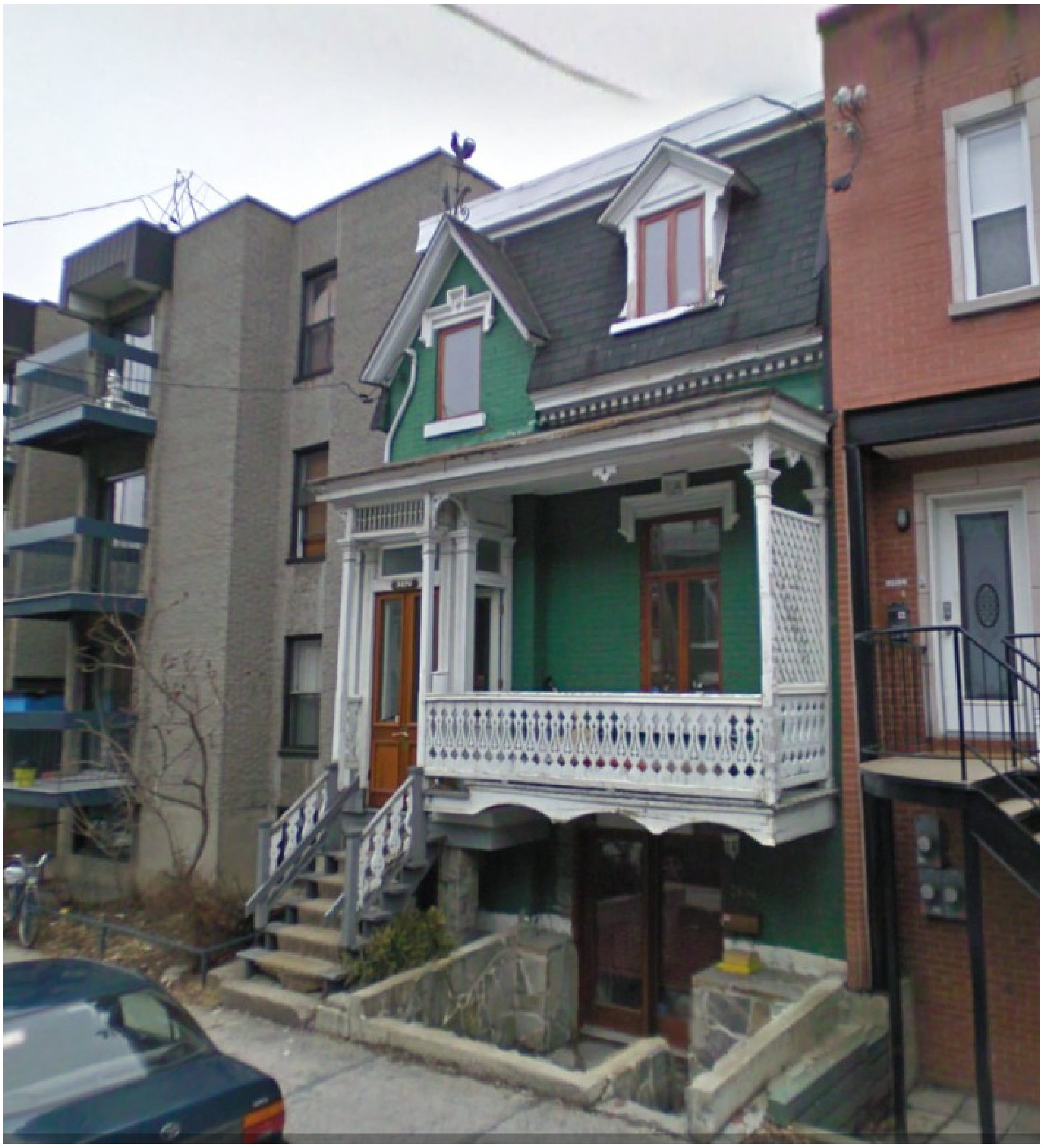

Maisons en rangée, rue de Bullion

quartier Saint-Loius (près de Roy). Construites vers 1875-80

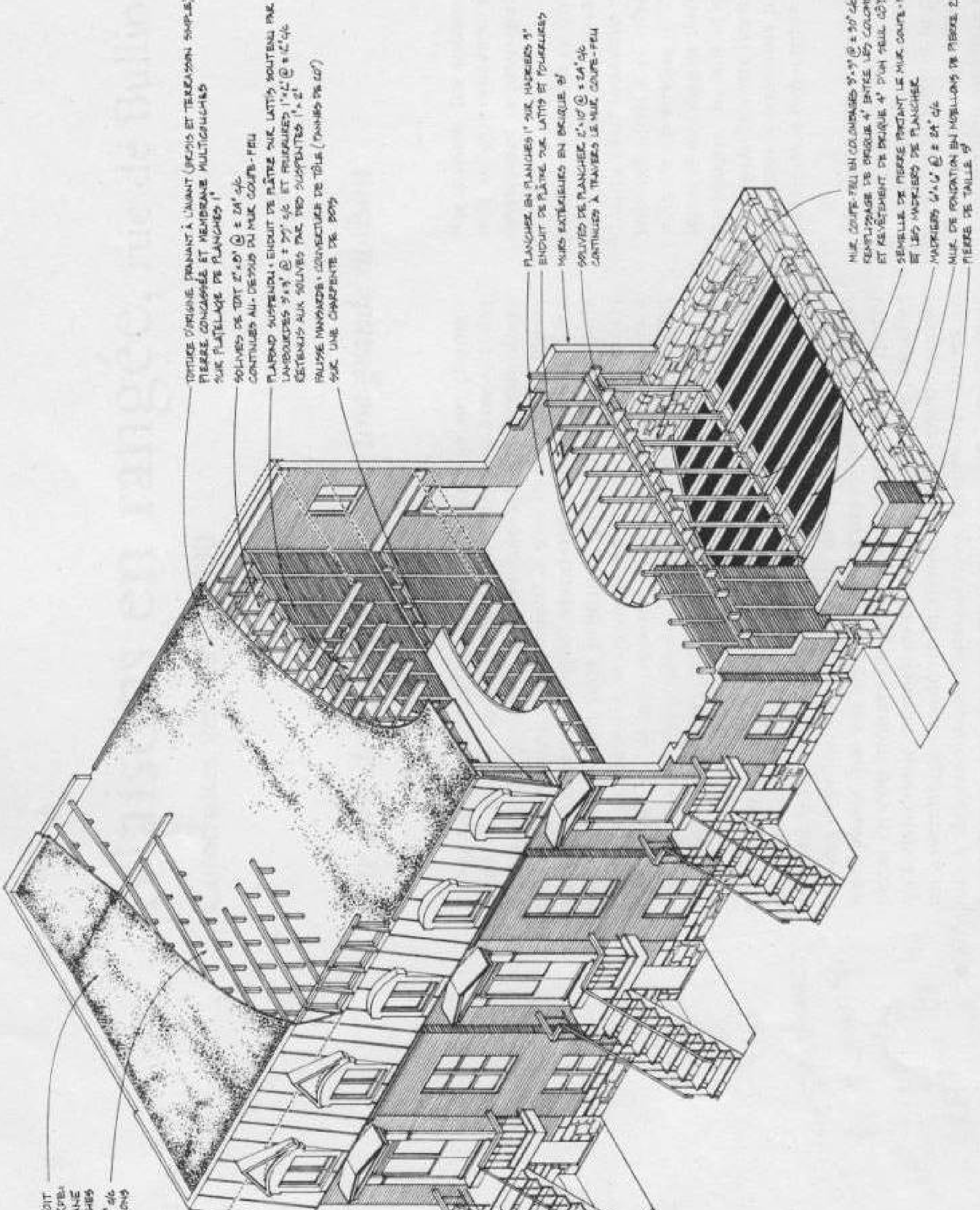

(Auger & Roquet, 1998)

3 : 2-storey apartment

Foundation	?
Wall	Load bearing firewalls on sides
	Wood frame with thin brick exterior wall
Roof	Flat roof
Others	Built right on the sidewalk, no front stairs.
Material	Brick/wood
Structure:	Masonry bearing wall+ wood frame
Year:	Around 1900
Location:	East of square mile, Rue Ontario, Lasalle
HAZUS code:	UMB

Role: 24087800

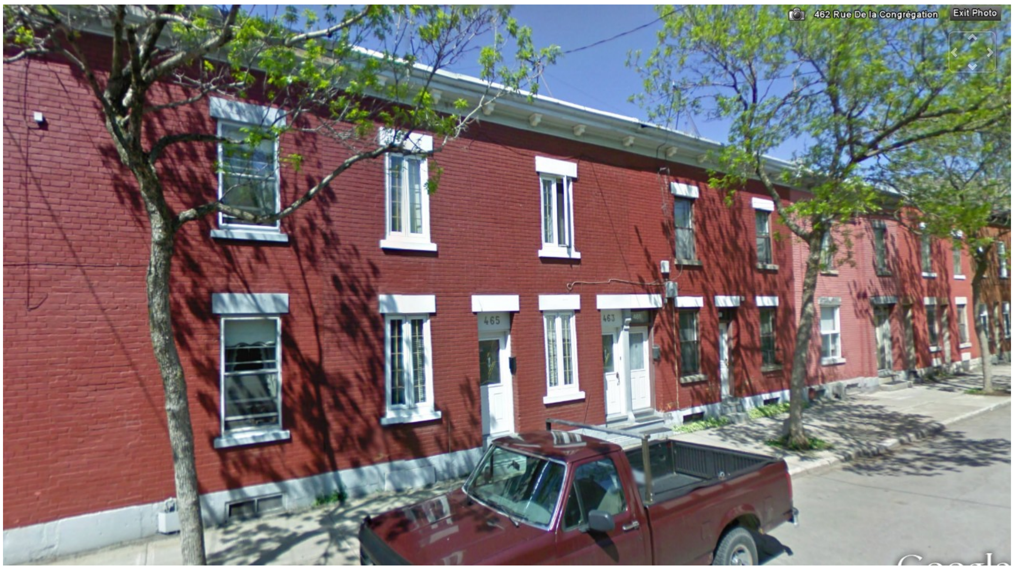

53049

Role 2005 ID: 50111900

18: Buildings with opening on ground floor (originally with second building in the back)

wall	brick
Foundation	Stone
Floor	
Roof	Flat
Material	Masonry and Wood
Structure:	Masonry bearing wall and wood frame
Year:	1875-1912
Location:	
HAZUS code:	UMB

Role 2005 ID: 42031900

Triplex jumelés et maison de fond de lot

1271-85, rue Champlain. Construit vers 1880

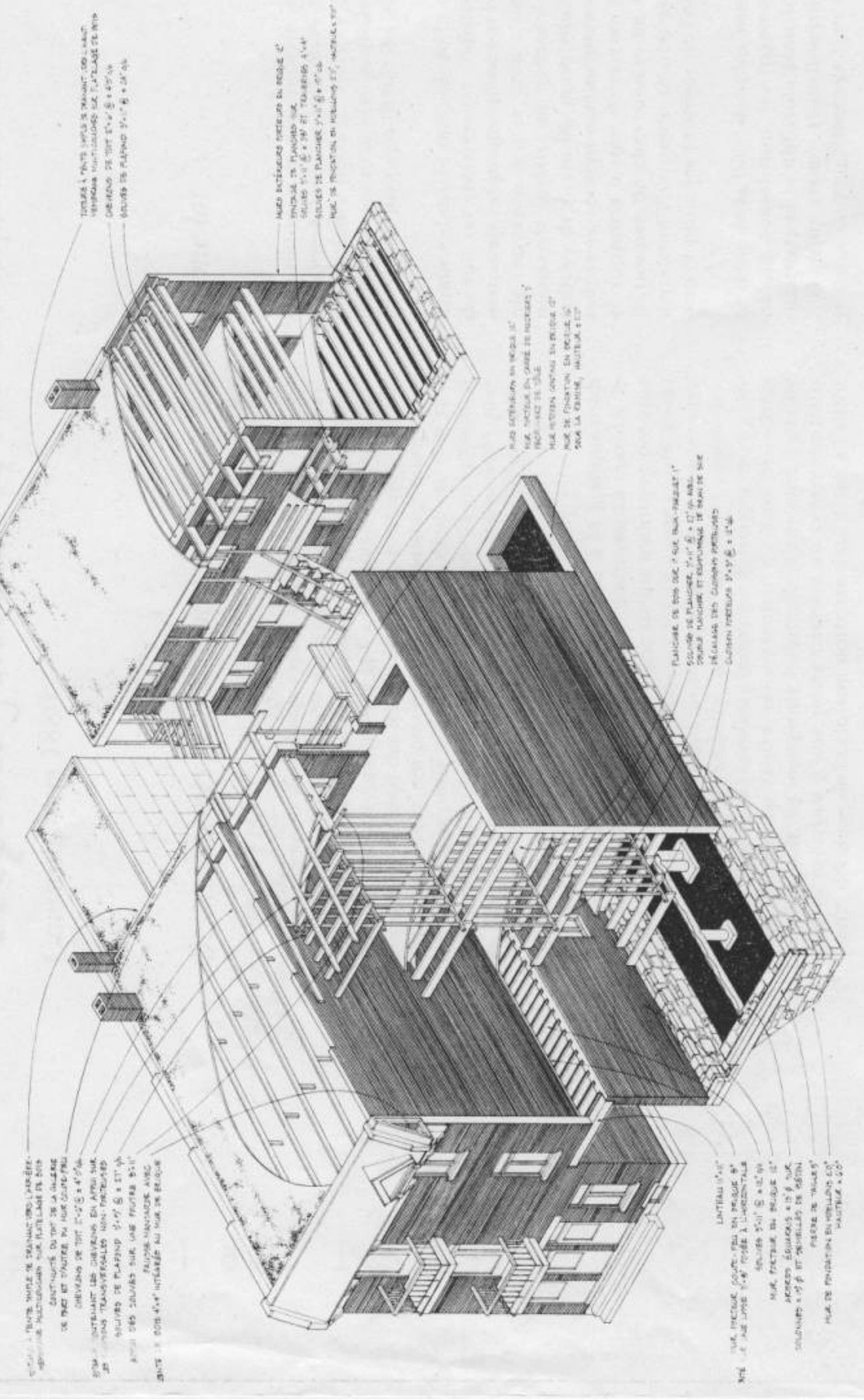

(Auger & Roquet, 1998)

16 : Residential two storey

wall	brick/wood , LOWER HALF BRICK, UPPER WOOD SHEATHING
Foundation	
Floor	
Roof	flat
Material	wood
Structure:	wood frame
Year:	1950'S-1970'S
Location:	
HAZUS code:	W1(LWF)

Role 2005 ID: 80289514

19 : Two storey building with semi-basement parking garage

wall	
Foundation	
Floor	
Roof	Flat
Material	Wood/concrete
Structure:	
Year:	1950'S-1980'S
Location:	
HAZUS code:	W1(LWF)

Role 2005 ID: 1310340

Role 2005 ID: 78046700

20: Semi-detached/detached two storey houses

wall	
Foundation	
Floor	
Roof	flat
Material	Wood/brick/concrete
Structure:	
Year:	1920'S-1950'S
Location:	
HAZUS code:	W1(LWF)

Role 2005 ID: 44043200

Role 2005 ID: 496500

4: Semi-detached triplex

wall	Exterior brick wall serving as load bearing walls Interior load bearing partition wall
Foundation	Concrete primeter wall +3 3"x11" timber beam & column
Floor	3"x11" timber member , direction could vary at the same floor level
Roof	flat
Material	Wood/brick
Structure:	Side bearing wall/wood frame
Year:	1900’S-1920’S
Location:	
HAZUS code:	UMB

Role 2005 ID: 21084900

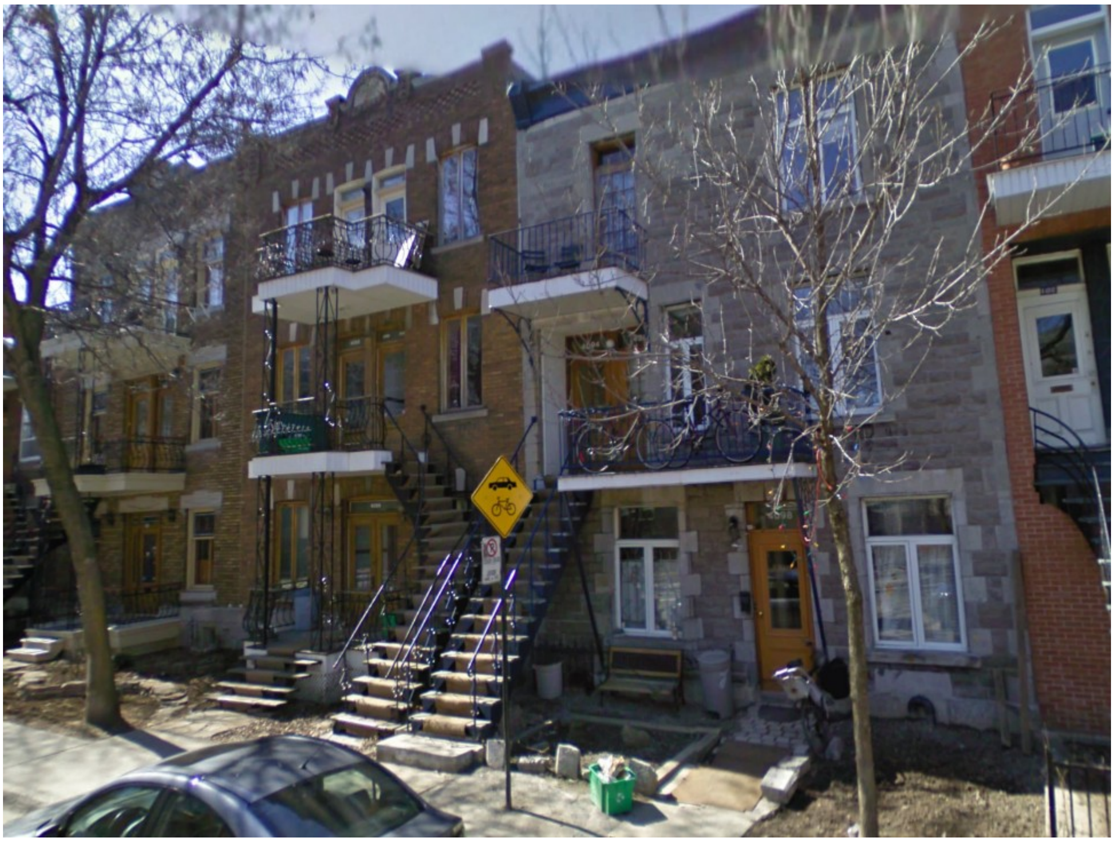

Cinq-plex, 4704-12, rue Garnier, Montréal

Typique des quartiers résidentiels (plateau Mont-Royal, Verdun, Hochelaga-Maisonneuve). Construit vers 1910

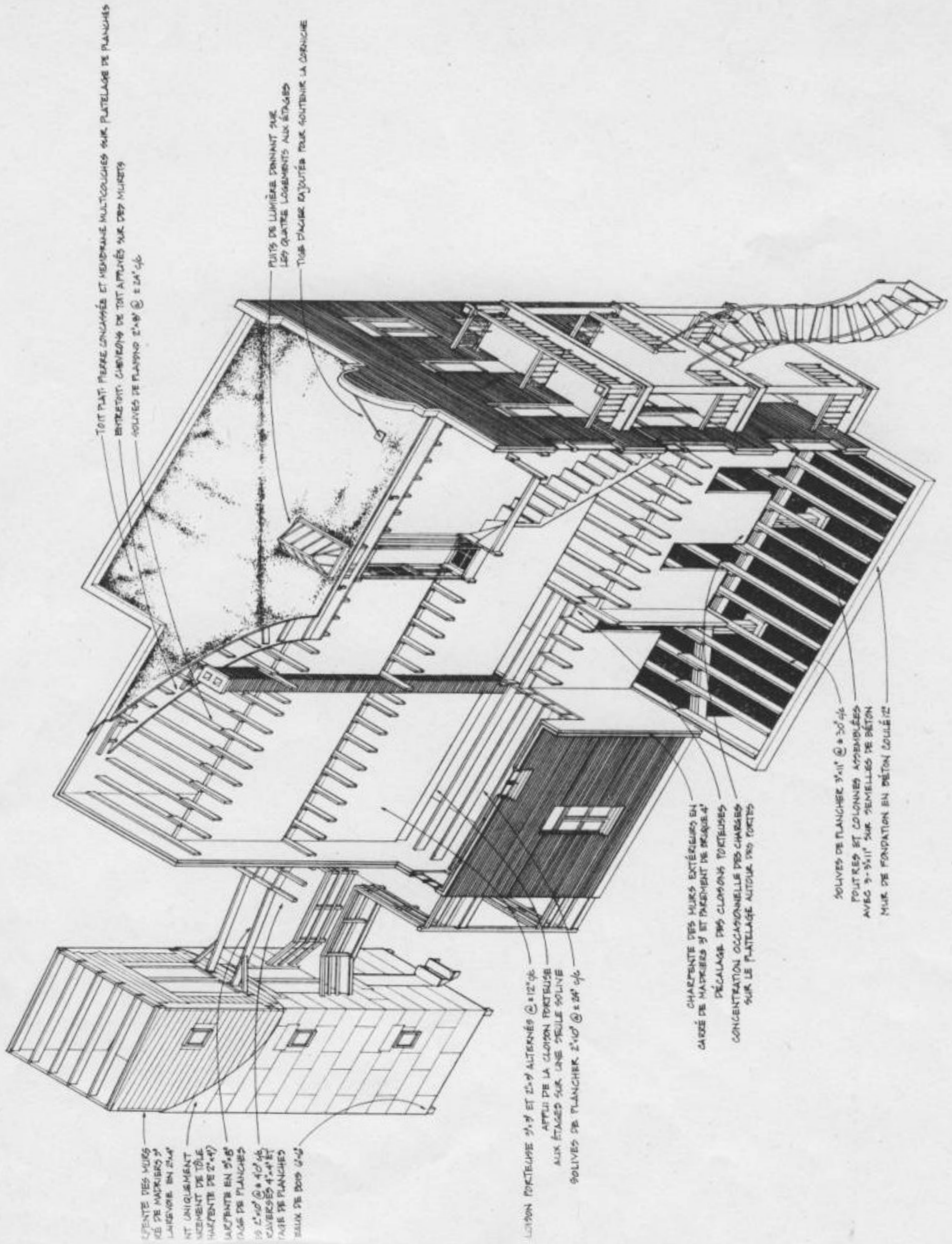

(Auger & Roquet, 1998)

5: Detached triplex

wall	Exterior brick wall serving as load bearing walls Interior load bearing partition wall
Foundation	Concrete primeter wall +3 3"x11" timber beam & column
Floor	3"x11" timber member going into side walls
Roof	flat
Material	Wood/brick
Structure:	Side bearing wall/wood frame
Year:	1900’S-1920’S
Location:	
HAZUS code:	UMB

Role 2005 ID: 54175100

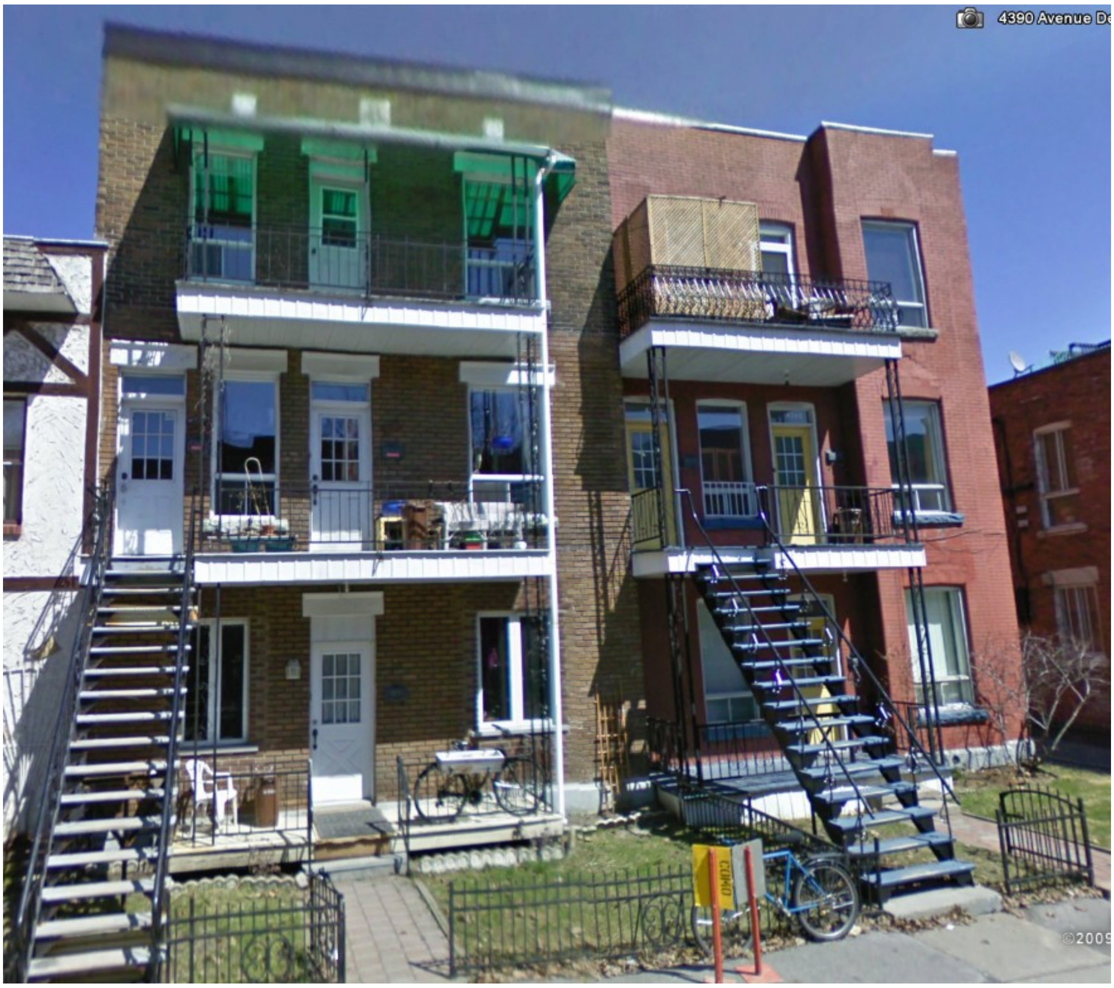

Triplex et cinq-plex jumelés

7094-7108, Christophe-Colomb. Typiques des quartiers résidentiels (Plateau Mont-Royal, Villeray, Maisonneuve, Verdun) avec escaliers extérieurs et logements en «L». Construit vers 1915-1920

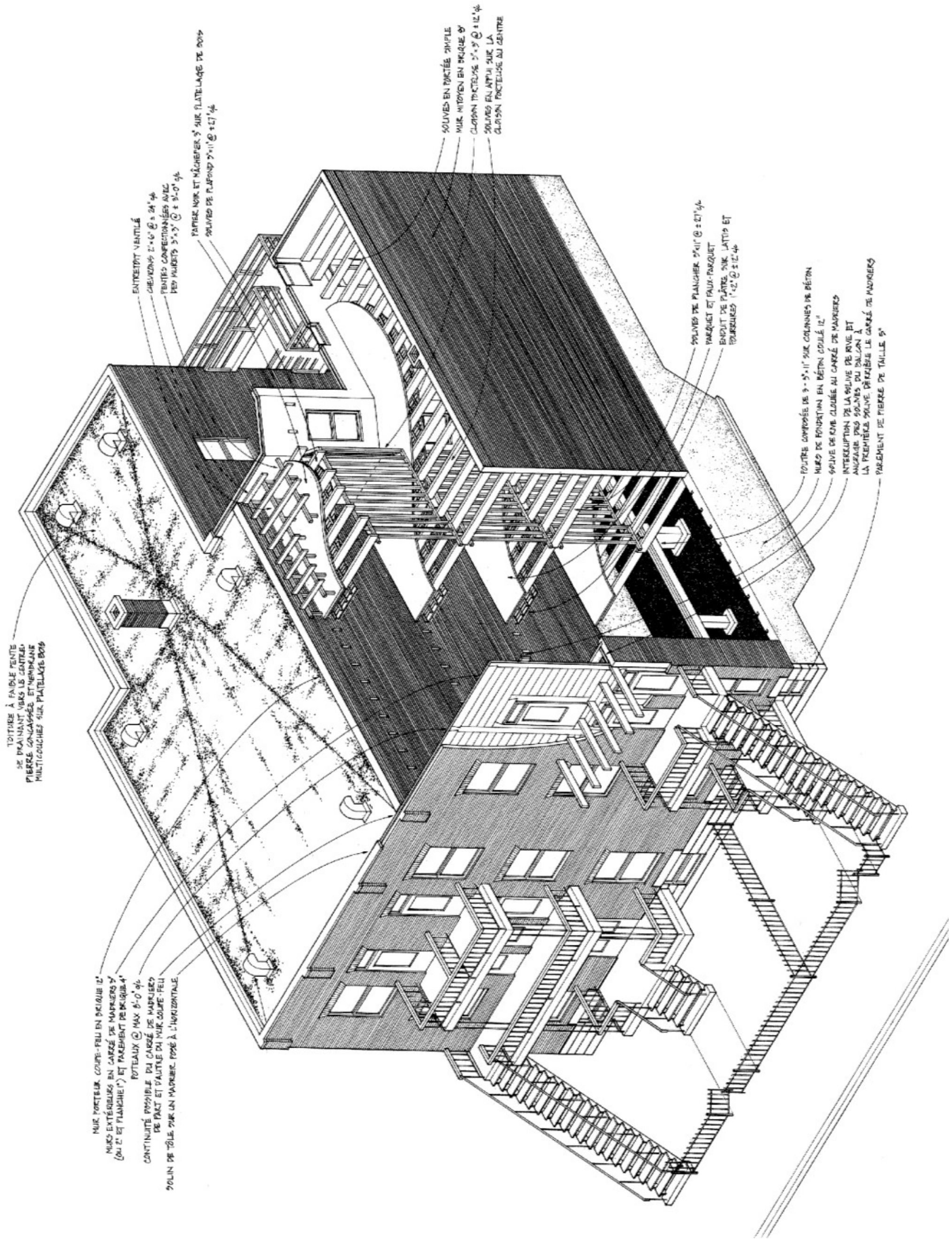

(Auger & Roquet, 1998)

6: Multiplex apartment (3 and half storey)

Foundation	Load bearing concrete block wall + steel framing
	Semi-basement lodging
Wall	Wood square plank as exterior/ wall studs with plywood sheathing
	Interior load bearing wood stud wall
Floor	2"x10" timber/lumber at 12"c/c+plywood decking
Roof	Flat roof with ventilation
Material	Wood/brick
Structure:	wood frame
Year:	1950's
Location:	
HAZUS code:	LWF(W1)

Role 2005 ID: 7311721

Role 2005 ID: 31243960

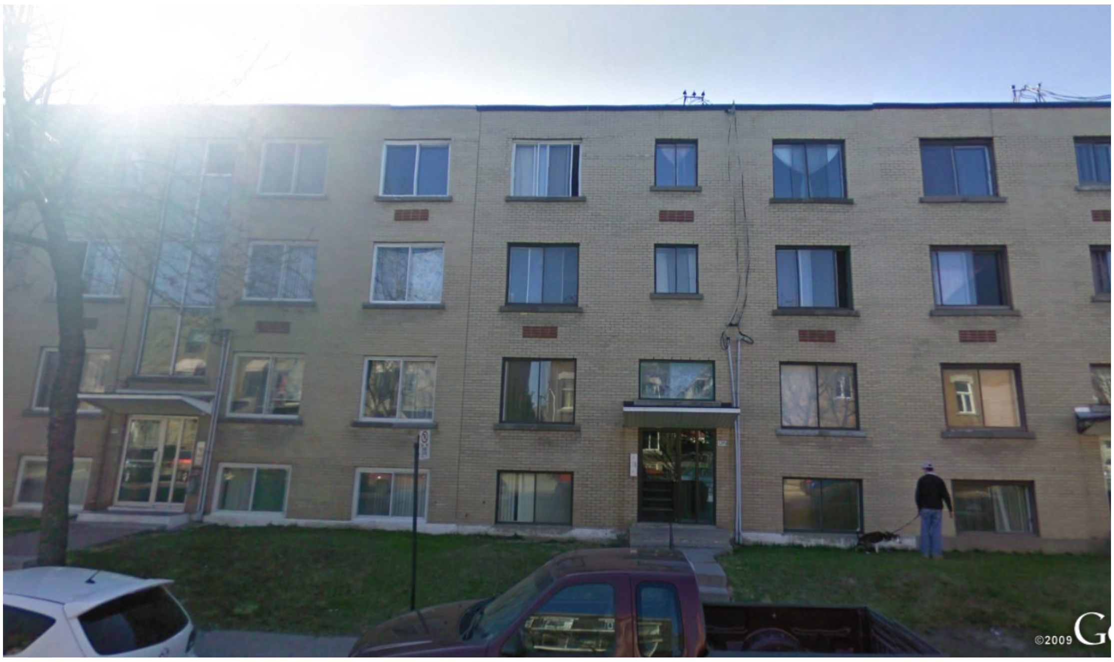

Bâtiment à logements multiples

détaché avec distribution par corridors et système de chauffage central (Côte des neiges, Notre-Dame-de-Grâce, Ville Saint-Michel, Plateau Mont-Royal). 3600, rue Fullum, vers 1960

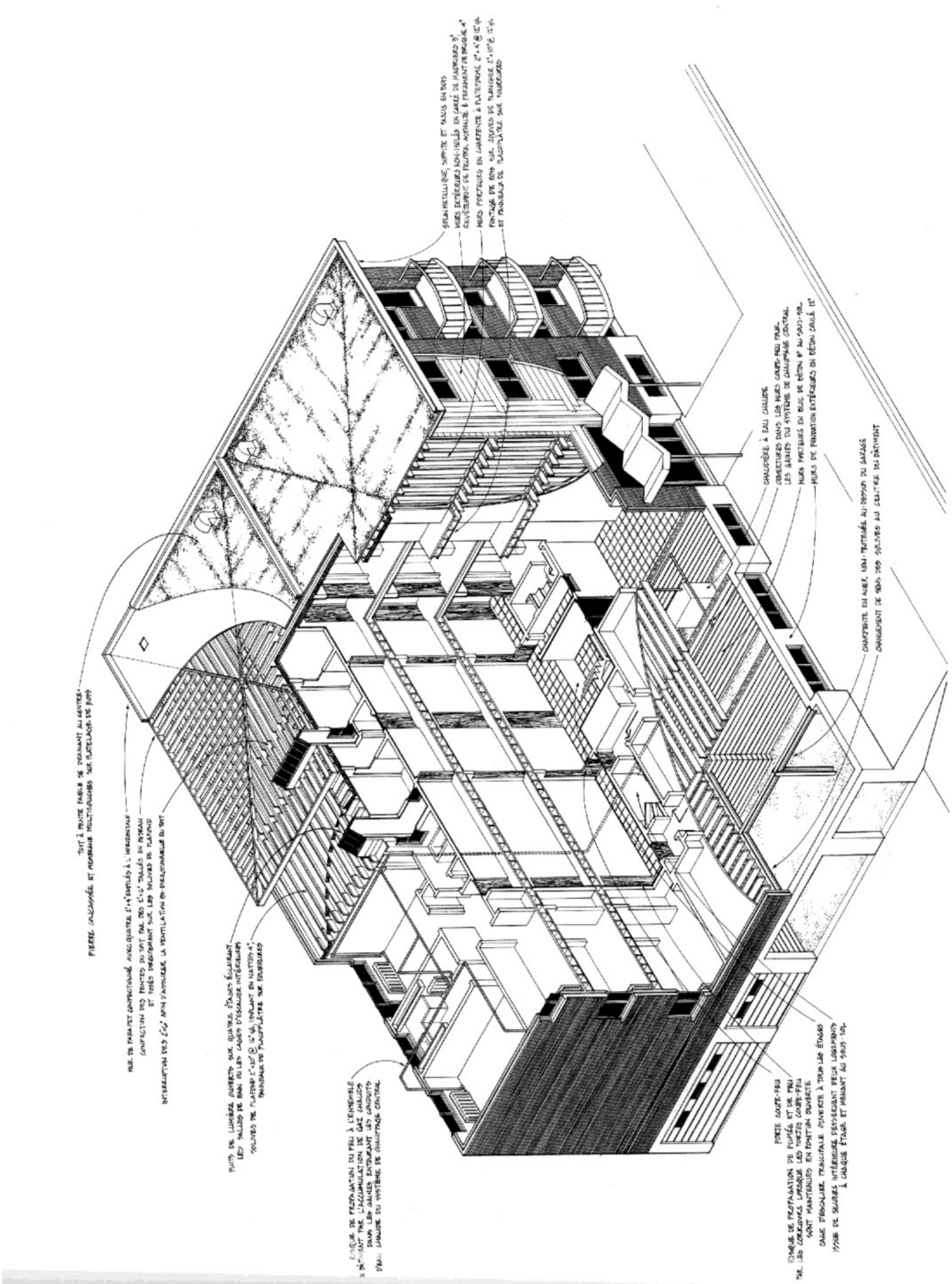

(Auger & Roquet, 1998)

7: Commercial/residential(triplex converted)

Foundation	Masonry Primeter wall
Wall	Cast-ion column at first floor
	wood wall stud at second floor
	Brick fire walls on sides(load bearing)
Roof	Multilayer membrane on plywood deck+crushed stone
Floor	steel beam at ground floor, wood at second
Material	Brick/Wood
Structure:	Bearing wall/wood frame
Year:	
Location:	
HAZUS code:	UMB

Role 2005 ID: 287500

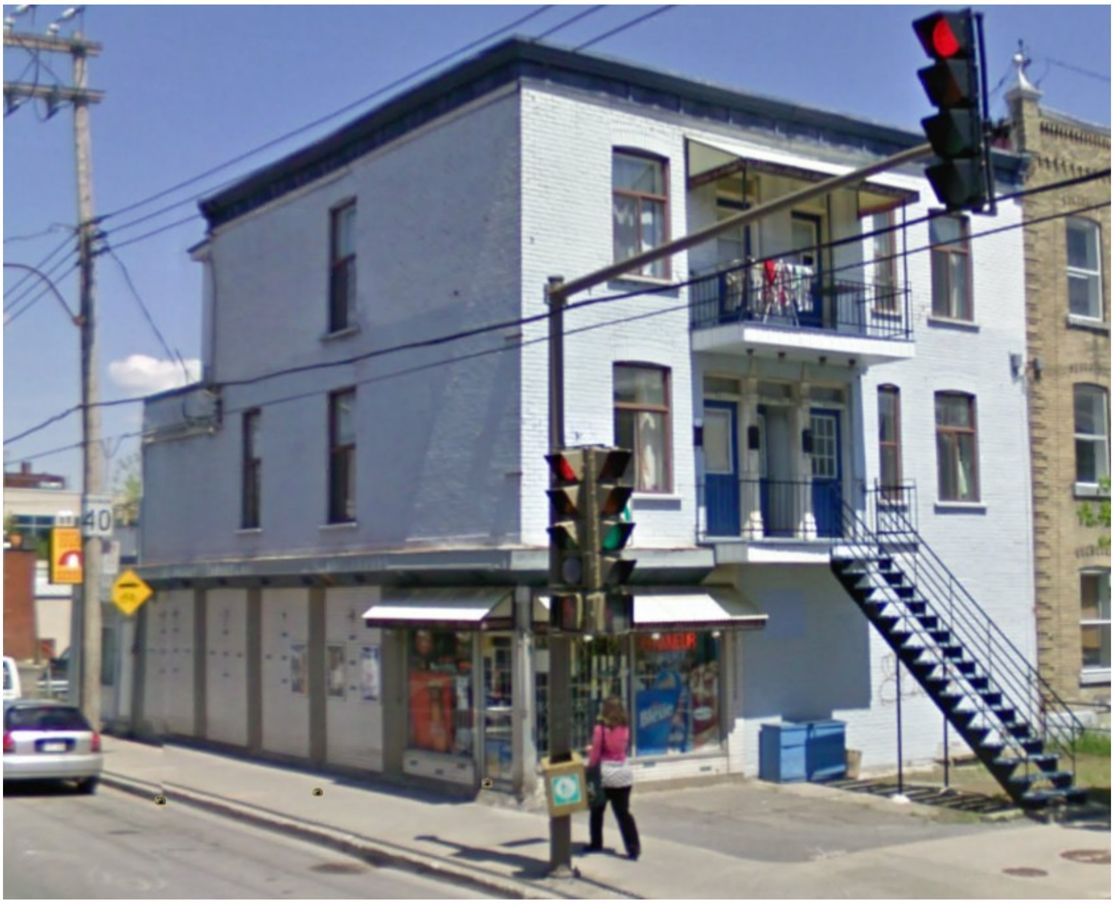

Commerce-résidences, rue Laurier, Montréal. Construit vers 1910

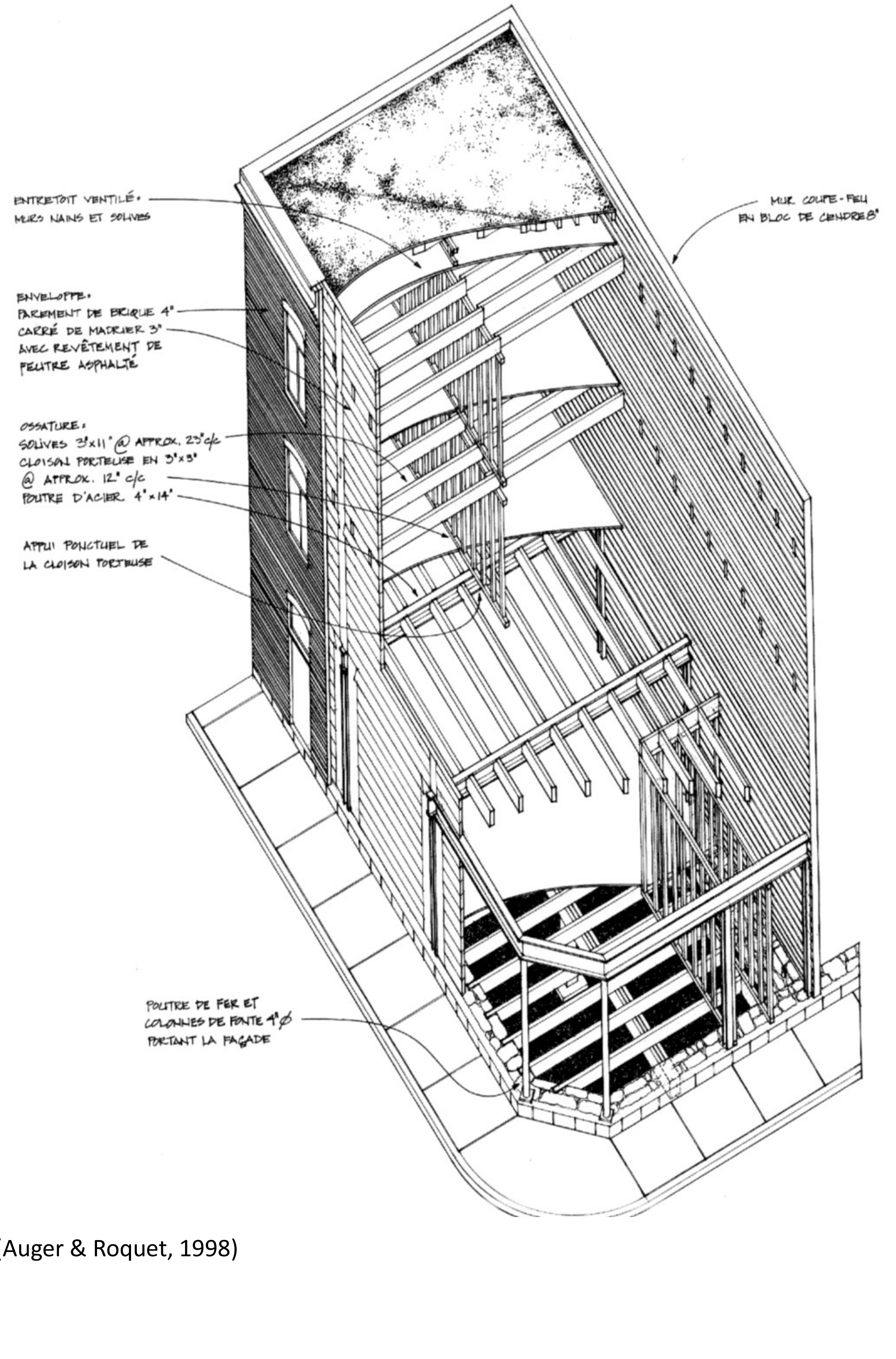

(Auger & Roquet, 1998)

8: Multiplex Apartment(Less than 4 storey)

Foundation	Concrete: perimeter wall (12") interior wall (8")
Wall	Concrete block (8") as bearing walls on sides
	Brick front and rear walls
	Wood frame/prefabricated wood product as interior wall
Roof	Flat roof with ventilation
	Multilayer membrane on plywood deck+crushed stone
Floor	joist at 12"c/c +plywood decking
Others	Balcony-Plywood decking on steel framing
Material	Wood/brick
Structure:	wood frame
Year:	1950's to now
Location:	
HAZUS code:	LWF(W1)

Role 2005 ID: 543595

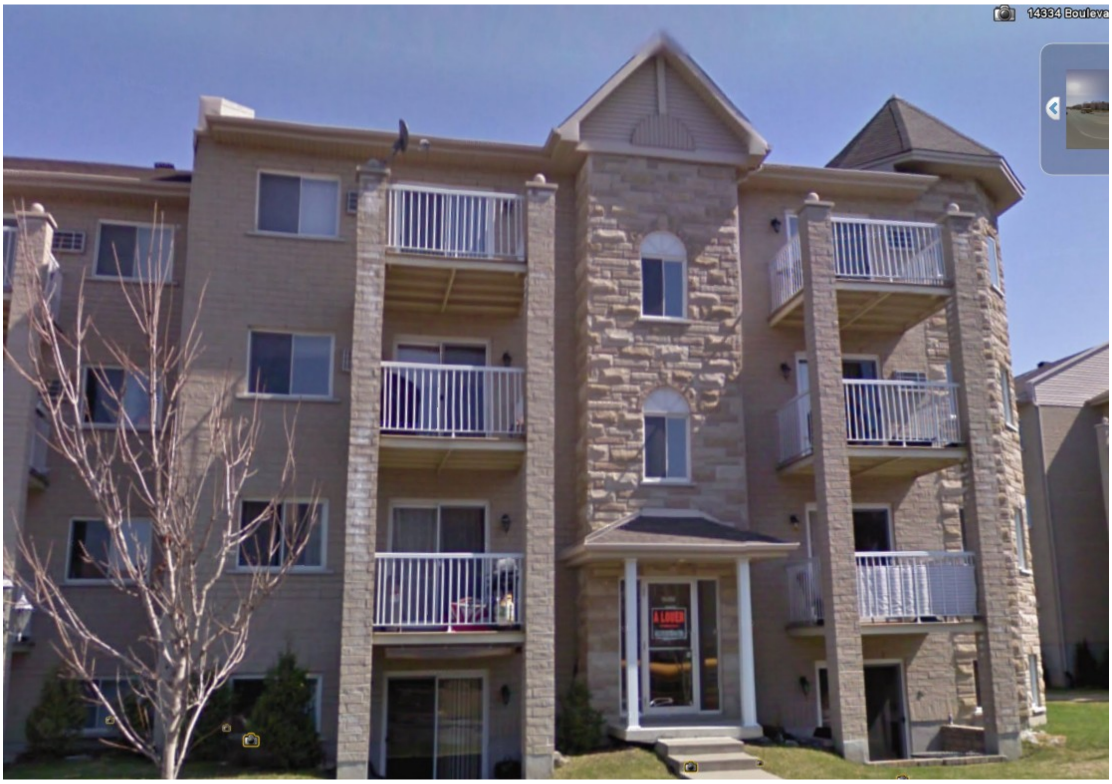

Six-plex de Montréal et des banlieues

Cage d'escalier intérieure et issue de secours extérieure. Après 1960

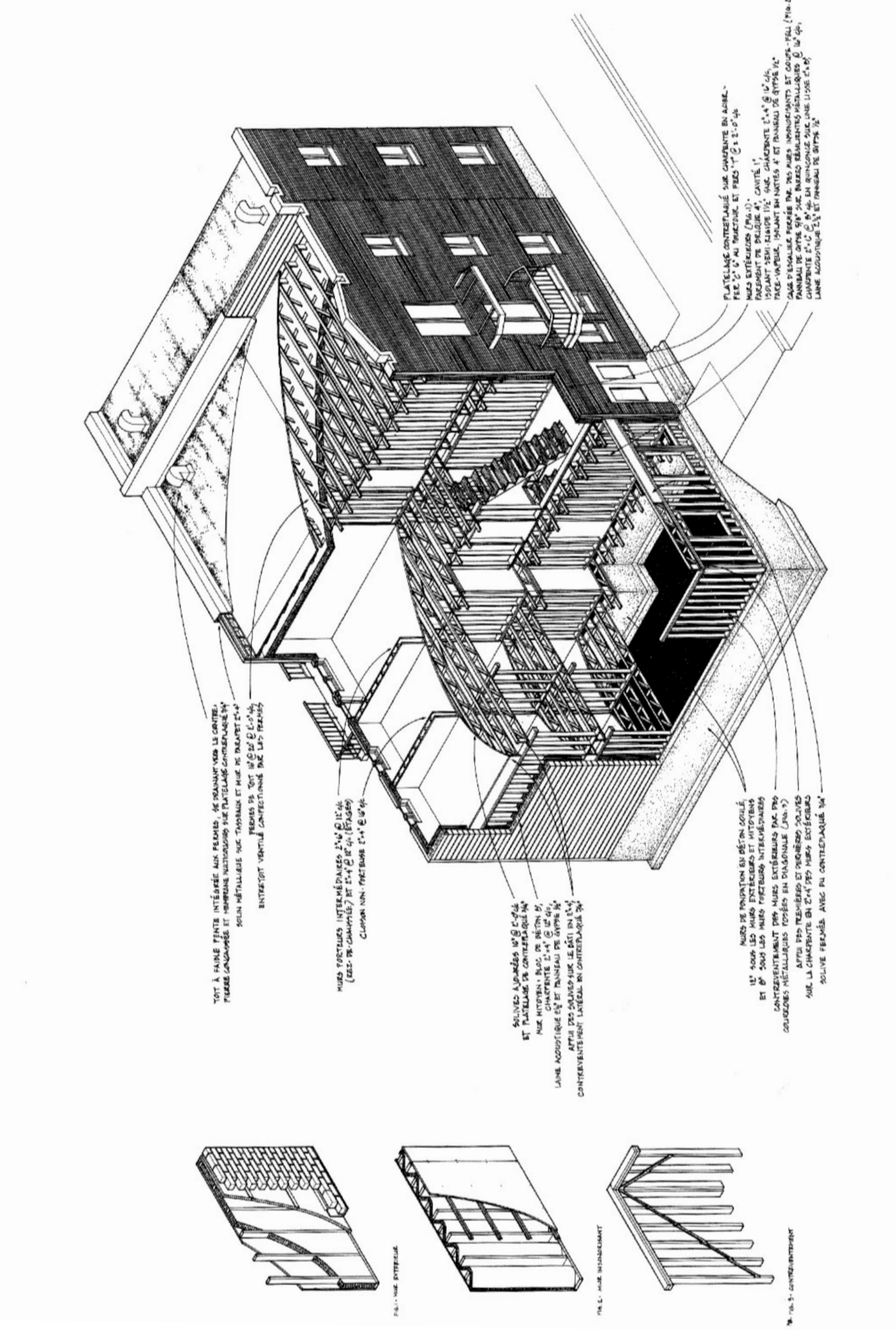

(Auger & Roquet, 1998)

21: Three storey apartment building

Foundation	Concrete
Wall	
Roof	Flat
Floor	
Material	Wood
Structure:	wood frame/Platform construction
Year:	1940’s-1990’s
Location:	East, Central Montreal
HAZUS code:	LWF(W1)

Role 2005 ID: 66082840

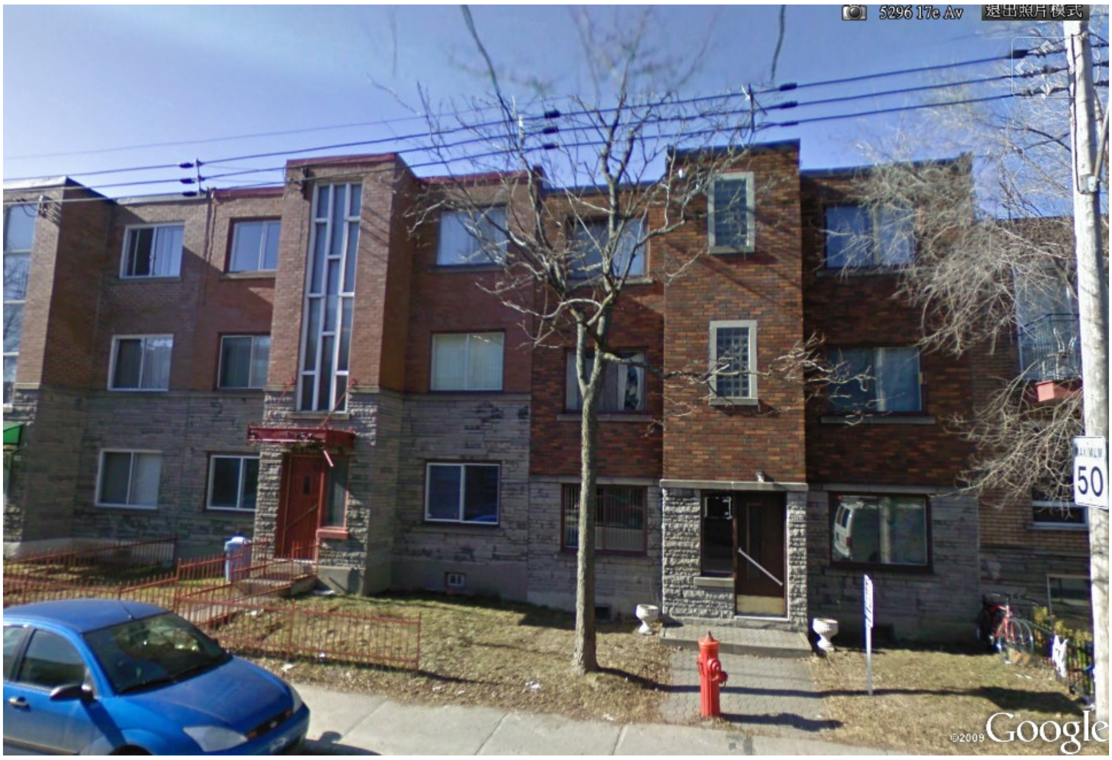

Appendix E: Direct Building Damage by Individual Scenario

Figure E-1 Distribution of Number of Damaged Buildings

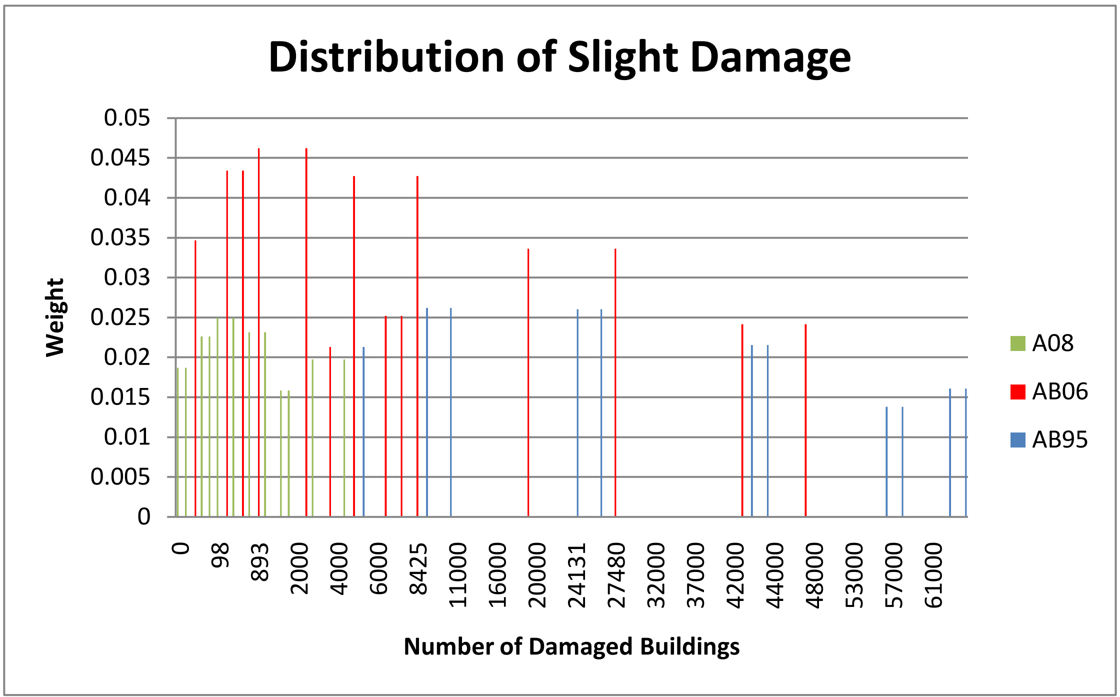

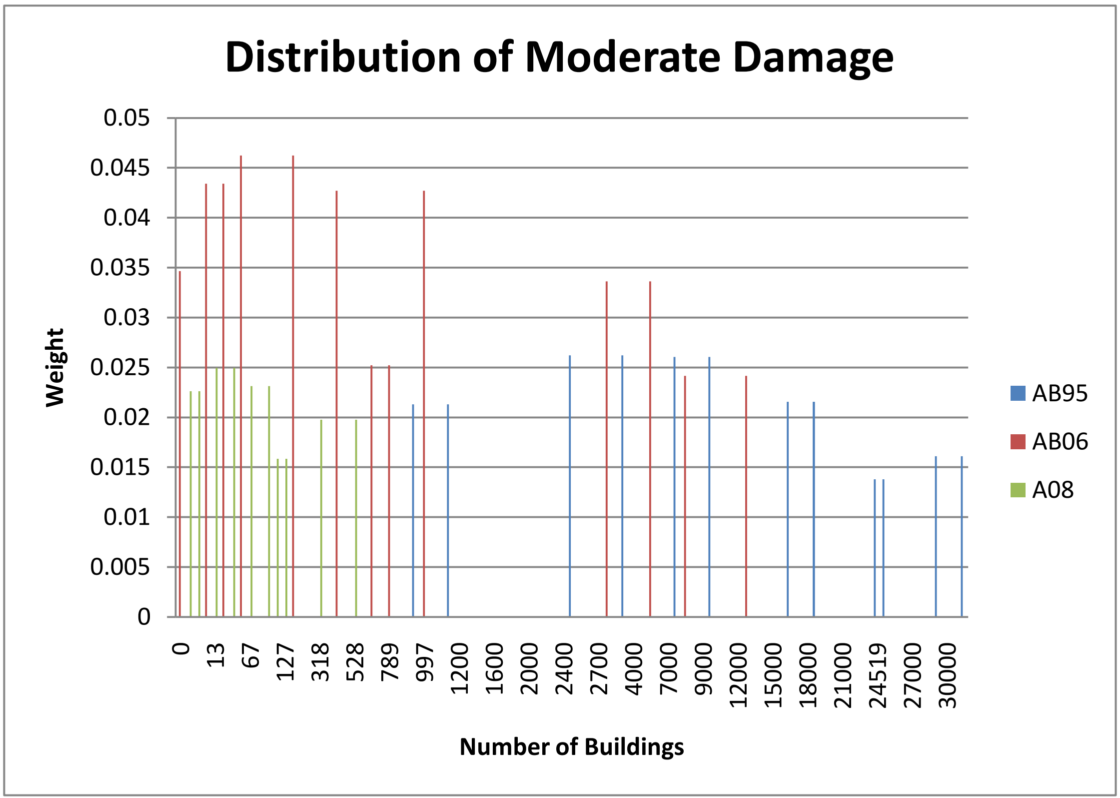

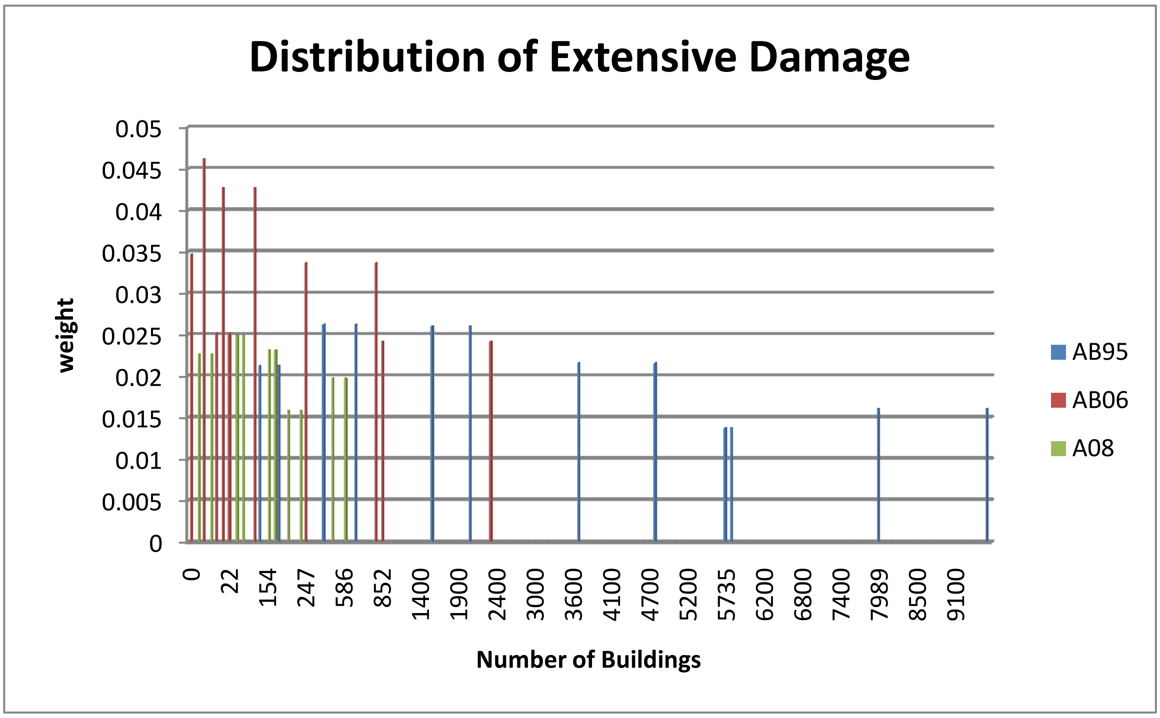
Distribution of Extensive Damage
0.05
0.045
0.04
0.035
0.03
0.025
0.02
0.015
0.01
0.005
0
weight
0
22
154
247
586
852
1400
1900
2400
3000
3600
4100
4700
5200
5735
6200
6800
7400
7989
8500
9100
Number of Buildings
AB95
AB06
A08

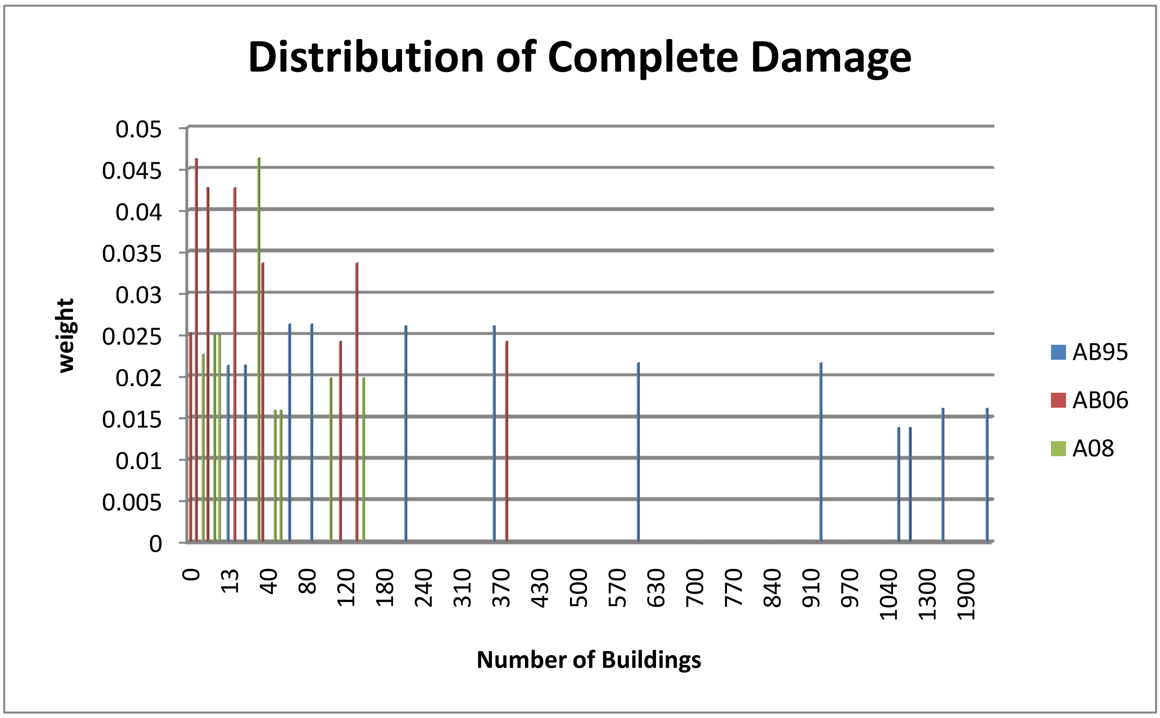
Distribution of Complete Damage
0.05
0.045
0.04
0.035
0.03
0.025
0.02
0.015
0.01
0.005
0
weight
0
13
40
80
120
180
240
310
370
430
500
570
630
700
770
840
910
970
1040
1300
1900
Number of Buildings
AB95
AB06
A08

Table E-1: Building Damage by Occupancy Type of All Scenarios

Scenarios	Commercial	Education	Government	Industrial	OtherResidential	Religion	SingleFamily	Contribution Factor	Weight
AB95_30NW5.3	225 2.2%	14 1.8%	9 1.9%	75 2.6%	2308 1.6%	24 2.3%	1980 1.3%	12.06	17.0%
AB95_30NW5.7	529 5.1%	33 4.3%	21 4.5%	174 6.1%	5775 3.9%	53 5.1%	5322 3.5%	14.84	21.0%
AB95_30NW6	1344 13.1%	86 11.3%	53 11.4%	429 15.1%	15913 10.8%	137 13.0%	15653 10.3%	14.75	20.8%
AB95_30NW6.3	2439 23.7%	157 20.6%	100 21.5%	755 26.5%	29341 19.9%	238 22.7%	29776 19.6%	12.21	17.2%
AB95_30NW6.7	3969 38.6%	260 34.1%	167 35.9%	1196 42.0%	47906 32.4%	376 35.8%	49074 32.3%	9.12	12.9%
AB95_50NW7	3603 35.0%	239 31.4%	154 33.1%	1080 37.9%	41678 28.2%	337 32.1%	41727 27.5%	7.81	11.0%
Weighted Avg	**1759** **17%**	**114** **15%**	**73** **16%**	**542** **19%**	**20750** **14%**	**170** **16%**	**20776** **14%**		
AB95_30SW5.3	256 2.5%	17 2.2%	10 2.1%	69 2.4%	1888 1.3%	28 2.7%	3728 2.5%	12.06	17.0%
AB95_30SW5.7	583 5.7%	37 4.8%	23 4.9%	158 5.6%	4773 3.2%	62 5.9%	8930 5.9%	14.84	21.0%
AB95_30SW6	1437 14.0%	90 11.8%	61 13.1%	385 13.5%	13382 9.1%	149 14.2%	22608 14.9%	14.75	20.8%
AB95_30SW6.3	2498 24.3%	161 21.1%	107 23.0%	665 23.4%	25109 17.0%	253 24.1%	38729 25.5%	12.21	17.2%
AB95_30SW6.7	3920 38.1%	258 33.9%	172 36.9%	1041 36.6%	41622 28.2%	386 36.8%	58717 38.6%	9.12	12.9%
AB95_50SW7	3520 34.2%	233 30.6%	154 33.0%	970 34.1%	37959 25.7%	338 32.2%	44496 29.3%	7.81	11.0%
Weighted Avg	**1789** **17%**	**116** **15%**	**77** **16%**	**481** **17%**	**17992** **12%**	**179** **17%**	**26372** **17%**		
Total Weighted Avg	**1774** **17%**	**115** **15%**	**75** **16%**	**512** **18%**	**19371** **13%**	**175** **17%**	**23574** **16%**		

Scenarios	Commercial	Education	Government	Industrial	OtherResidential	Religion	SingleFamily	Contribution Factor	Weight
AB06_30NW5.3	0 0.0%	0 0.0%	0 0.0%	0 0.0%	1 0.0%	0 0.0%	1 0.0%	9.9	13.9%
AB06_30NW5.7	4 0.0%	0 0.0%	0 0.0%	2 0.1%	56 0.0%	1 0.1%	46 0.0%	12.4	17.4%
AB06_30NW6	43 0.4%	3 0.4%	1 0.2%	15 0.5%	471 0.3%	5 0.5%	414 0.3%	13.2	18.5%
AB06_30NW6.3	214 2.1%	14 1.8%	8 1.7%	77 2.7%	2355 1.6%	24 2.3%	2146 1.4%	12.2	17.1%
AB06_30NW6.7	1014 9.9%	64 8.4%	41 8.8%	336 11.8%	10626 7.2%	102 9.7%	10488 6.9%	9.6	13.4%
AB06_30NW7	2337 22.7%	148 19.4%	95 20.4%	749 26.3%	23637 16.0%	216 20.6%	24012 15.8%	6.9	9.7%
AB06_50NW7	354 3.4%	23 3.0%	15 3.2%	121 4.3%	3467 2.3%	37 3.5%	3189 2.1%	7.2	10.1%
Weighted Avg	**443** **4%**	**28** **4%**	**18** **4%**	**146** **5%**	**4562** **3%**	**44** **4%**	**4504** **3%**		
AB06_30SW5.3	0 0.0%	0 0.0%	0 0.0%	0 0.0%	1 0.0%	0 0.0%	12 0.0%	9.9	13.9%
AB06_30SW5.7	12 0.1%	1 0.1%	0 0.0%	3 0.1%	43 0.0%	2 0.2%	291 0.2%	12.4	17.4%
AB06_30SW6	74 0.7%	6 0.8%	3 0.6%	20 0.7%	354 0.2%	11 1.0%	1872 1.2%	13.2	18.5%
AB06_30SW6.3	332 3.2%	22 2.9%	14 3.0%	82 2.9%	1721 1.2%	39 3.7%	7340 4.8%	12.2	17.1%
AB06_30SW6.7	1270 12.3%	81 10.6%	55 11.8%	314 11.0%	7794 5.3%	133 12.7%	23975 15.8%	9.6	13.4%
AB06_30SW7	2474 24.0%	158 20.7%	110 23.6%	595 20.9%	17231 11.7%	244 23.2%	42041 27.7%	6.9	9.7%
AB06_50SW7	382 3.7%	24 3.1%	16 3.4%	99 3.5%	2667 1.8%	41 3.9%	4998 3.3%	7.2	10.1%
Weighted Avg	**521** **5%**	**34** **4%**	**23** **5%**	**128** **4%**	**3349** **2%**	**55** **5%**	**9443** **6%**		
Total Weighted Avg	**482** **5%**	**31** **4%**	**20** **4%**	**137** **5%**	**3956** **3%**	**49** **5%**	**6973** **5%**		

Scenarios	Commercial	Education	Government	Industrial	OtherResidential	Religion	SingleFamily	Contribution Factor	Weight
A08_30NW5.3	0 0.0%	0 0.0%	0 0.0%	0 0.0%	0 0.0%	0 0.0%	0 0.0%	7.2	15.0%
A08_30NW5.7	2 0.0%	0 0.0%	0 0.0%	0 0.0%	8 0.0%	0 0.0%	9 0.0%	8.7	18.1%
A08_30NW6	12 0.1%	0 0.0%	0 0.0%	3 0.1%	71 0.0%	1 0.1%	70 0.0%	9.6	20.0%
A08_30NW6.3	56 0.5%	2 0.3%	1 0.2%	16 0.6%	340 0.2%	4 0.4%	323 0.2%	8.9	18.5%
A08_30NW6.7	194 1.9%	11 1.4%	7 1.5%	59 2.1%	1715 1.2%	18 1.7%	1447 1.0%	7.6	15.8%
A08_50NW7	93 0.9%	4 0.5%	3 0.6%	28 1.0%	724 0.5%	8 0.8%	630 0.4%	6.1	12.7%
Weighted Avg	**56 1%**	**3 0%**	**2 0%**	**16 1%**	**441 0%**	**5 0%**	**384 0%**		
A08_30SW5.3	0 0.0%	0 0.0%	0 0.0%	0 0.0%	0 0.0%	0 0.0%	2 0.0%	7.2	15.0%
A08_30SW5.7	4 0.0%	0 0.0%	0 0.0%	0 0.0%	7 0.0%	0 0.0%	42 0.0%	8.7	18.1%
A08_30SW6	17 0.2%	1 0.1%	0 0.0%	4 0.1%	53 0.0%	1 0.1%	216 0.1%	9.6	20.0%
A08_30SW6.3	68 0.7%	4 0.5%	2 0.4%	17 0.6%	258 0.2%	6 0.6%	856 0.6%	8.9	18.5%
A08_30SW6.7	260 2.5%	15 2.0%	9 1.9%	68 2.4%	1335 0.9%	25 2.4%	3660 2.4%	7.6	15.8%
A08_50SW7	96 0.9%	4 0.5%	3 0.6%	25 0.9%	596 0.4%	9 0.9%	749 0.5%	6.1	12.7%
Weighted Avg	**70 1%**	**4 1%**	**2 0%**	**18 1%**	**346 0%**	**6 1%**	**883 1%**		
Total Weighted Avg	**63 1%**	**3 0%**	**2 0%**	**17 1%**	**394 0%**	**6 1%**	**633 0%**		

Table E-2: Building Damage by Structural Type

Scenarios	Wood	Steel	Concrete	Precast	RM	URM	MH	Contribution Factor	Weight
AB95_30NW5.3	1453 0.7%	148 1.2%	137 1.6%	24 3.5%	253 1.8%	2619 4.6%	0 0.0%	12.06	17.0%
AB95_30NW5.7	4924 2.2%	391 3.3%	354 4.0%	54 7.9%	610 4.2%	5574 9.8%	0 0.0%	14.84	21.0%
AB95_30NW6	17524 7.9%	1147 9.6%	1018 11.6%	125 18.4%	1580 11.0%	12220 21.6%	0 0.0%	14.75	20.8%
AB95_30NW6.3	36333 16.3%	2295 19.3%	1957 22.3%	207 30.4%	2843 19.7%	19170 33.8%	1 33.3%	12.21	17.2%
AB95_30NW6.7	63223 28.4%	4057 34.1%	3313 37.8%	312 45.9%	4677 32.5%	27366 48.3%	2 50.0%	9.12	12.9%
AB95_50NW7	52252 23.5%	3656 30.7%	3034 34.6%	291 42.7%	4292 29.8%	25292 44.7%	2 50.0%	7.81	11.0%
Weighted Avg	**25108 11%**	**1668 14%**	**1409 16%**	**149 22%**	**2067 14%**	**13783 24%**	**1 18%**		
AB95_30SW5.3	2555 1.1%	156 1.3%	145 1.7%	26 3.8%	213 1.5%	2901 5.1%	0 0.0%	12.06	17.0%
AB95_30SW5.7	7340 3.3%	400 3.4%	363 4.1%	54 7.9%	520 3.6%	5891 10.4%	0 0.0%	14.84	21.0%
AB95_30SW6	22079 9.9%	1139 9.6%	995 11.3%	122 17.9%	1368 9.5%	12407 21.9%	0 0.0%	14.75	20.8%
AB95_30SW6.3	41671 18.7%	2189 18.4%	1854 21.1%	200 29.4%	2481 17.2%	19124 33.8%	2 50.0%	12.21	17.2%
AB95_30SW6.7	67961 30.5%	3762 31.6%	3083 35.2%	297 43.6%	4109 28.5%	26902 47.5%	2 66.7%	9.12	12.9%
AB95_50SW7	52609 23.6%	3437 28.9%	2860 32.6%	278 40.8%	3945 27.4%	24542 43.3%	2 50.0%	7.81	11.0%
Weighted Avg	**28322 13%**	**1589 13%**	**1341 15%**	**145 21%**	**1823 13%**	**13786 24%**	**1 23%**		
Total Weighted Avg	**26715 12%**	**1629 14%**	**1375 16%**	**147 22%**	**1945 14%**	**13785 24%**	**1 20%**		

Scenarios	Wood	Steel	Concrete	Precast	RM	URM	MH	Contribution Factor	Weight
AB06_30NW5.3	0 0.0%	0 0.0%	0 0.0%	0 0.0%	0 0.0%	2 0.0%	0 0.0%	9.9	13.9%
AB06_30NW5.7	6 0.0%	2 0.0%	1 0.0%	0 0.0%	2 0.0%	97 0.2%	0 0.0%	12.4	17.4%
AB06_30NW6	130 0.1%	19 0.2%	15 0.2%	5 0.7%	23 0.2%	762 1.3%	0 0.0%	13.2	18.5%
AB06_30NW6.3	1190 0.5%	119 1.0%	105 1.2%	23 3.4%	147 1.0%	3254 5.7%	0 0.0%	12.2	17.1%
AB06_30NW6.7	8855 4.0%	765 6.4%	713 8.1%	101 14.9%	865 6.0%	11371 20.1%	1 33.3%	9.6	13.4%
AB06_30NW7	24167 10.8%	2084 17.5%	1870 21.3%	215 31.6%	2232 15.5%	20626 36.4%	1 33.3%	6.9	9.7%
AB06_50NW7	1707 0.8%	237 2.0%	221 2.5%	38 5.6%	247 1.7%	4758 8.4%	0 0.0%	7.2	10.1%
Weighted Avg	**3927 2%**	**352 3%**	**320 4%**	**43 6%**	**387 3%**	**4716 8%**	**0 8%**		
AB06_30SW5.3	1 0.0%	0 0.0%	0 0.0%	0 0.0%	0 0.0%	14 0.0%	0 0.0%	9.9	13.9%
AB06_30SW5.7	73 0.0%	4 0.0%	4 0.0%	1 0.1%	2 0.0%	267 0.5%	0 0.0%	12.4	17.4%
AB06_30SW6	873 0.4%	34 0.3%	36 0.4%	7 1.0%	21 0.1%	1367 2.4%	0 0.0%	13.2	18.5%
AB06_30SW6.3	4687 2.1%	185 1.6%	180 2.1%	31 4.6%	123 0.9%	4345 7.7%	0 0.0%	12.2	17.1%
AB06_30SW6.7	19164 8.6%	889 7.5%	790 9.0%	109 16.0%	664 4.6%	12006 21.2%	1 33.3%	9.6	13.4%
AB06_30SW7	37581 16.9%	1979 16.6%	1716 19.6%	198 29.1%	1640 11.4%	19736 34.8%	2 66.7%	6.9	9.7%
AB06_50SW7	2781 1.2%	230 1.9%	212 2.4%	38 5.6%	189 1.3%	4776 8.4%	0 0.0%	7.2	10.1%
Weighted Avg	**7464 3%**	**373 3%**	**332 4%**	**44 7%**	**292 2%**	**5047 9%**	**0 11%**		
Total Weighted Avg	**5695 3%**	**362 3%**	**326 4%**	**44 6%**	**339 2%**	**4881 9%**	**0 9%**		

Scenarios	Wood	Steel	Concrete	Precast	RM	URM	MH	Contribution Factor	Weight
A08_30NW5.3	0 0.0%	0 0.0%	0 0.0%	0 0.0%	0 0.0%	0 0.0%	0 0.0%	7.2	15.0%
A08_30NW5.7	4 0.0%	0 0.0%	0 0.0%	0 0.0%	0 0.0%	15 0.0%	0 0.0%	8.7	18.1%
A08_30NW6	41 0.0%	8 0.1%	2 0.0%	0 0.0%	4 0.0%	103 0.2%	0 0.0%	9.6	20.0%
A08_30NW6.3	197 0.1%	34 0.3%	14 0.2%	4 0.6%	22 0.2%	473 0.8%	0 0.0%	8.9	18.5%
A08_30NW6.7	947 0.4%	118 1.0%	74 0.8%	18 2.6%	112 0.8%	2181 3.9%	0 0.0%	7.6	15.8%
A08_50NW7	351 0.2%	54 0.5%	29 0.3%	7 1.0%	44 0.3%	1004 1.8%	0 0.0%	6.1	12.7%
Weighted Avg	**240 0%**	**33 0%**	**18 0%**	**4 1%**	**28 0%**	**583 1%**	**0 0%**		
A08_30SW5.3	0 0.0%	0 0.0%	0 0.0%	0 0.0%	0 0.0%	2 0.0%	0 0.0%	7.2	15.0%
A08_30SW5.7	12 0.0%	1 0.0%	0 0.0%	0 0.0%	0 0.0%	39 0.1%	0 0.0%	8.7	18.1%
A08_30SW6	74 0.0%	9 0.1%	4 0.0%	1 0.1%	3 0.0%	200 0.4%	0 0.0%	9.6	20.0%
A08_30SW6.3	399 0.2%	39 0.3%	20 0.2%	5 0.7%	17 0.1%	732 1.3%	0 0.0%	8.9	18.5%
A08_30SW6.7	2240 1.0%	154 1.3%	102 1.2%	21 3.1%	96 0.7%	2760 4.9%	0 0.0%	7.6	15.8%
A08_50SW7	371 0.2%	54 0.5%	26 0.3%	7 1.0%	36 0.2%	987 1.7%	0 0.0%	6.1	12.7%
Weighted Avg	**492 0%**	**40 0%**	**24 0%**	**5 1%**	**23 0%**	**744 1%**	**0 0%**		
Total Weighted Avg	**366 0%**	**37 0%**	**21 0%**	**5 1%**	**26 0%**	**663 1%**	**0 0%**		

Appendix F: Casualty Estimation

F.1 Casualty Estimation Results

Table F-1: Casualty Estimation of Scenarios using GMEP AB95

2am

Scenarios	Level1	Level2	Level3	Level4	Weight
AB95_30NW5.3	58	7	1	1	17.00%
AB95_30NW5.7	170	23	1	5	21.00%
AB95_30NW6	574	93	10	18	20.80%
AB95_30NW6.3	1320	239	25	53	17.20%
AB95_30NW6.7	2835	572	71	137	12.90%
AB95_50NW7	2134	414	52	98	11.00%
Weighted Avg	**993**	**186**	**22**	**42**	
AB95_30SW5.3	65	8	0	1	17.00%
AB95_30SW5.7	187	29	2	5	21.00%
AB95_30SW6	627	107	11	20	20.80%
AB95_30SW6.3	1398	260	30	59	17.20%
AB95_30SW6.7	2904	598	73	144	12.90%
AB95_50SW7	1981	381	47	89	11.00%
Weighted Avg	**1015**	**194**	**22**	**44**	
Total Weighted Avg	**1004**	**190**	**22**	**43**	

2pm

Scenarios	Level1	Level2	Level3	Level4	Weight
AB95_30NW5.3	69	9	0	1	17.00%
AB95_30NW5.7	202	33	2	7	21.00%
AB95_30NW6	651	110	12	22	20.80%
AB95_30NW6.3	1546	293	35	66	17.20%
AB95_30NW6.7	3412	714	92	174	12.90%
AB95_50NW7	2602	516	63	122	11.00%
Weighted Avg	**1183**	**231**	**28**	**54**	
AB95_30SW5.3	86	12	1	1	17.00%
AB95_30SW5.7	259	44	5	8	21.00%
AB95_30SW6	823	153	19	34	20.80%
AB95_30SW6.3	1816	367	45	88	17.20%
AB95_30SW6.7	3883	863	115	221	12.90%
AB95_50SW7	2572	515	64	123	11.00%
Weighted Avg	**1338**	**275**	**35**	**66**	
Total Weighted Avg	**1260**	**253**	**31**	**60**	

5pm

Scenarios	Level1	Level2	Level3	Level4	Weight
AB95_30NW5.3	69	9	0	1	17.00%
AB95_30NW5.7	149	22	2	3	21.00%
AB95_30NW6	487	81	10	16	20.80%
AB95_30NW6.3	1143	214	24	49	17.20%
AB95_30NW6.7	2498	520	66	126	12.90%
AB95_50NW7	1896	377	48	90	11.00%
Weighted Avg	**872**	**169**	**21**	**39**	
AB95_30SW5.3	62	9	0	1	17.00%
AB95_30SW5.7	183	30	2	7	21.00%
AB95_30SW6	588	107	12	23	20.80%
AB95_30SW6.3	1302	259	31	60	17.20%
AB95_30SW6.7	2755	602	78	150	12.90%
AB95_50SW7	1835	365	45	87	11.00%
Weighted Avg	**953**	**193**	**23**	**46**	
Total Weighted Avg	**913**	**181**	**22**	**42**	

Table F-2: Casualty Estimation of Scenarios using GMPE AB06

2am

Scenarios	Level1	Level2	Level3	Level4	Weight
AB06_30NW5.3	0	0	0	0	13.90%
AB06_30NW5.7	0	0	0	0	17.40%
AB06_30NW6	5	0	0	0	18.50%
AB06_30NW6.3	28	1	0	0	17.10%
AB06_30NW6.7	176	18	1	2	13.40%
AB06_30NW7	476	56	5	7	9.70%
AB06_50NW7	36	1	0	0	10.10%
Weighted Avg	**33**	**3**	**0**	**0**	
AB06_30SW5.3	0	0	0	0	13.90%
AB06_30SW5.7	1	0	0	0	17.40%
AB06_30SW6	7	0	0	0	18.50%
AB06_30SW6.3	48	4	0	0	17.10%
AB06_30SW6.7	262	34	2	5	13.40%
AB06_30SW7	638	89	6	13	9.70%
AB06_50SW7	36	2	0	0	10.10%
Weighted Avg	**49**	**5**	**0**	**1**	
Total Weighted Avg	**41**	**4**	**0**	**0**	

2pm

Scenarios	Level1	Level2	Level3	Level4	Weight
AB06_30NW5.3	0	0	0	0	13.90%
AB06_30NW5.7	0	0	0	0	17.40%
AB06_30NW6	6	0	0	0	18.50%
AB06_30NW6.3	36	3	0	0	17.10%
AB06_30NW6.7	246	34	3	6	13.40%
AB06_30NW7	616	84	9	14	9.70%
AB06_50NW7	45	1	0	0	10.10%
Weighted Avg	**104**	**13**	**1**	**2**	
AB06_30SW5.3	0	0	0	0	13.90%
AB06_30SW5.7	1	0	0	0	17.40%
AB06_30SW6	9	0	0	0	18.50%
AB06_30SW6.3	71	9	1	1	17.10%
AB06_30SW6.7	425	71	7	15	13.40%
AB06_30SW7	961	158	17	33	9.70%
AB06_50SW7	49	2	0	0	10.10%
Weighted Avg	**169**	**27**	**3**	**5**	
Total Weighted Avg	**137**	**20**	**2**	**4**	

5pm

Scenarios	Level1	Level2	Level3	Level4	Weight
AB06_30NW5.3	0	0	0	0	13.90%
AB06_30NW5.7	0	0	0	0	17.40%
AB06_30NW6	2	0	0	0	18.50%
AB06_30NW6.3	26	2	0	0	17.10%
AB06_30NW6.7	171	22	1	3	13.40%
AB06_30NW7	437	57	3	9	9.70%
AB06_50NW7	34	2	0	0	10.10%
Weighted Avg	**73**	**9**	**0**	**1**	
AB06_30SW5.3	0	0	0	0	13.90%
AB06_30SW5.7	0	0	0	0	17.40%
AB06_30SW6	7	0	0	0	18.50%
AB06_30SW6.3	49	7	0	1	17.10%
AB06_30SW6.7	284	45	3	9	13.40%
AB06_30SW7	659	105	9	21	9.70%
AB06_50SW7	34	1	0	0	10.10%
Weighted Avg	**115**	**18**	**1**	**3**	
Total Weighted Avg	**94**	**13**	**1**	**2**	

Table F-3: Casualty Estimation of Scenarios using GMPE A08

2am

Scenarios	Level1	Level2	Level3	Level4	Weight
A08_30NW5.3	0	0	0	0	15.00%
A08_30NW5.7	1	0	0	0	18.10%
A08_30NW6	13	2	0	0	20.00%
A08_30NW6.3	52	11	1	2	18.50%
A08_30NW6.7	157	32	2	7	15.80%
A08_50NW7	76	14	1	2	12.70%
Weighted Avg	**47**	**9**	**1**	**2**	
A08_30SW5.3	0	0	0	0	15.00%
A08_30SW5.7	2	0	0	0	18.10%
A08_30SW6	11	2	0	0	20.00%
A08_30SW6.3	46	10	1	1	18.50%
A08_30SW6.7	161	32	4	6	15.80%
A08_50SW7	74	14	1	2	12.70%
Weighted Avg	**46**	**9**	**1**	**1**	
Total Weighted Avg	**46**	**9**	**1**	**2**	

2pm

Scenarios	Level1	Level2	Level3	Level4	Weight
A08_30NW5.3	0	0	0	0	15.00%
A08_30NW5.7	3	0	0	0	18.10%
A08_30NW6	26	7	0	1	20.00%
A08_30NW6.3	100	23	3	6	18.50%
A08_30NW6.7	226	52	6	14	15.80%
A08_50NW7	128	30	3	8	12.70%
Weighted Avg	**76**	**18**	**2**	**5**	
A08_30SW5.3	0	0	0	0	15.00%
A08_30SW5.7	7	1	0	0	18.10%
A08_30SW6	26	6	0	1	20.00%
A08_30SW6.3	94	23	3	6	18.50%
A08_30SW6.7	299	69	8	19	15.80%
A08_50SW7	133	31	3	8	12.70%
Weighted Avg	**88**	**20**	**2**	**5**	
Total Weighted Avg	**82**	**19**	**2**	**5**	

5pm

Scenarios	Level1	Level2	Level3	Level4	Weight
A08_30NW5.3	0	0	0	0	15.00%
A08_30NW5.7	3	0	0	0	18.10%
A08_30NW6	17	5	0	0	20.00%
A08_30NW6.3	64	14	1	3	18.50%
A08_30NW6.7	156	35	3	9	15.80%
A08_50NW7	84	20	1	5	12.70%
Weighted Avg	**51**	**12**	**1**	**3**	
A08_30SW5.3	0	0	0	0	15.00%
A08_30SW5.7	3	0	0	0	18.10%
A08_30SW6	17	3	0	0	20.00%
A08_30SW6.3	60	14	1	2	18.50%
A08_30SW6.7	195	43	6	10	15.80%
A08_50SW7	87	20	1	6	12.70%
Weighted Avg	**57**	**13**	**1**	**3**	
Total Weighted Avg	**54**	**12**	**1**	**3**	

F.2 Casualty Estimation Using HAZUS Methodology

1) Calculate indoor and outdoor population distribution within each census tract using the default relationship provided by HAZUS. (FEMA, 2003) The calculations are done for all occupancy classes (Residential, Commercial, Educational, Industrial, Hotels) at three time scenarios of a day (2a.m., 2 p.m., and 5 p.m.). In addition to the population in all occupancy classes, the commuting population is also calculated. The commuting population is used to calculate road kills resulted from the failure of highway bridges, which is not included in the scope of this study.

Table F-4: Distribution of People in Census Tract (FEMA, 2003)

Distribution of People in Census Tract			
Occupancy	**2:00 a.m.**	**2:00 p.m.**	**5:00 p.m.**
Indoors			
Residential	(0.999)0.99(NRES)	(0.70)0.75(DRES)	(0.70)0.5(NRES)
Commercial	(0.999)0.02(COMW)	(0.99)0.98(COMW) + (0.80)0.20(DRES) + 0.80(HOTEL) + 0.80(VISIT)	0.98[0.50(COMW) + 0.10(NRES)+ 0.70(HOTEL)]
Educational		(0.90)0.80(GRADE) + 0.80(COLLEGE)	(0.80)0.50(COLLEGE)
Industrial	(0.999)0.10(INDW)	(0.90)0.80(INDW)	(0.90)0.50(INDW)
Hotels	0.999(HOTEL)	0.19(HOTEL)	0.299(HOTEL)
Outdoors			
Residential	(0.001)0.99(NRES)	(0.30)0.75(DRES)	(0.30)0.5(NRES)
Commercial	(0.001)0.02(COMW)	(0.01)0.98(COMW) + (0.20)0.20(DRES) + (0.20)VISIT + 0.50(1-PRFIL)0.05(POP)	0.02[0.50(COMW) + 0.10(NRES) + 0.70(HOTEL)] + 0.50(1-PRFIL) [0.05(POP) + 1.0(COMM)]
Educational		(0.10)0.80(GRADE) + 0.20(COLLEGE)	(0.20)0.50(COLLEGE)
Industrial	(0.001)0.10(INDW)	(0.10)0.80(INDW)	(0.10)0.50(INDW)
Hotels	0.001(HOTEL)	0.01(HOTEL)	0.001(HOTEL)
Commuting			
Commuting in cars	0.005(POP)	(PRFIL)0.05(POP)	(PRFIL)[0.05(POP) + 1.0(COMM)]
Commuting using other modes		0.50(1-PRFIL)0.05(POP)	0.50(1-PRFIL) [0.05(POP) + 1.0(COMM)]

where:

POP	is the census tract population taken from census data
DRES	is the daytime residential population inferred from census data
NRES	is the nighttime residential population inferred from census data
COMM	is the number of people commuting inferred from census data
COMW	is the number of people employed in the commercial sector
INDW	is the number of people employed in the industrial sector
GRADE	is the number of students in grade schools (K-12)

COLLEGE	is the number of students on college and university campuses in the census tract
HOTEL	is the number of people staying in hotels in the census tract
PRFIL	is a factor representing the proportion of commuters using automobiles, inferred from profile of the community (0.60 for dense urban, 0.80 for less dense urban or suburban, and 0.85 for rural). The default is 0.80.
VISIT	is the number of regional residents who do not live in the study area, visiting the census tract for shopping and entertainment. Default is set to zero.

2) Download structural damage state from HAZUS. This is done by downloading the structural damage by building area table in HAZUS result. The tables are converted into percentage damage and aggregated into four damage states. The format of a sample slight damage probability table is shown in the following figure. Moderate, extensive and complete damage probability tables are also created.

Tract	HAZUSTract	W1	W2	S1L	....	*Building*	*Types*	....	URML	URMM	MH
4620001.0	36061000100	0.004801	0.012179	0.005595					0.07052	0	0
4620002.0	36061000200	0.004798	0.010989	0.005435					0.070088	0	0
4620003.0	36061000300	0.004801	0.011884	0.005766					0.070209	0	0
4620004.0	36061000400	0.002298	0.002122	0.000588					0.038876	0	0
4620005.0	36061000500	0.016001	0.037654	0.02112					0.130632	0	0
4620006.0	36061000600	0.004799	0.01238	0.005703					0.07016	0	0
4620007.0	36061000700	0.000703	0.002667	0.000553					0.024459	0	0
4620008.0	36061000800	0.004805	0.012411	0.005792					0.070116	0	0
4620009.0	36061000900	0.013299	0.012755	0.005739					0.10483	0	0
4620010.0	36061001000	0.013306	0.012712	0.005731					0.105145	0	0
4620011.0	36061001100	0.000702	0.002821	0.000696					0.024632	0	0
4620012.0	36061001201	0.000709	0.002656	0.001022					0.024444	0	0
4620012.0	36061001202	0.000696	0.002351	0.000739					0.024714	0	0
4620013.0	36061001300	0.002303	0.002464	0.0007					0.039523	0	0
4620014.0	36061001401	0.004798	0.012256	0.005738					0.072568	0	0
4620014.0	36061001402	0.013242	0.012887	0.005715					0.107244	0	0
4620015.0	36061001500	0.013297	0.012496	0.005709					0.103538	0	0
4620016.0	36061001600	0.0133	0.012987	0.006349					0.102813	0	0
4620017.0	36061001700	0.013295	0.012966	0.005708					0.10306	0	0
4620018.0	36061001800	0.013295	0.012598	0.005557					0.103117	0	0
4620019.0	36061001900	0.0133	0.01271	0.005687					0.10305	0	0
4620021.0	36061002100	0.013304	0.012848	0.005734					0.103665	0	0
4620022.0	36061002200	0.013303	0.013233	0.005229					0.102787	0	0
....											

Figure F-1: Slight Damage within Each Building Types as % of Total Building Area

3) Calculate casualty for each building type and casualty level within each occupancy class using the following formula.

$$Casualty_i = Population_i \sum_{j=1}^{n} \%DamageLevel_j * CasualtyRate_{ji}$$

Where

Population $_i$= Number of people in individual building type i within each occupancy class calculated based on occupancy-structural type distribution table(Table F-5) and distribution of people in census tract (Table F-4).

% Damage Level $_j$= % building damaged in each damage level j (slight, moderate, extensive, complete with collapse, and complete without collapse) and

Casualty Rate $_{ij}$= Casualty rate from HAZUS for building type i and damage level j

Damage Level is the five structural damage levels: slight, moderate, extensive, and complete with collapse and complete without collapse. The collapse rate of each building type is given in Table x. The casualty rates of different injury levels are given for all five structural damage levels from HAZUS technical manual (FEMA,2003) The population within each building type and occupancy class is calculated based on the default occupancy-structural type distribution table.

4) Sum up casualties resulted from all building types (W1 to MH). This should be done for all occupancy classes and time scenarios. The aggregated results are the

estimated casualties at four injury levels within each occupancy class at three time of a day.

Table F-5: Occupancy-structural type distribution by HAZUS default NY Inventory

	W1	W2	S1L	S2L	S3	S4L	S5L	C1L	C2L	C3L	PC1	PC2L	RM1L	RM2L	URML	MH
RES1	0.85								0.01						0.14	
RES2																1
RES3	0.62			0.03				0.02	0.02				0.05	0.04	0.22	
RES4	0.48		0.05	0.04			0.04	0.08	0.04		0.03	0.03	0.03	0.03	0.15	
RES5	0.07		0.07	0.06			0.06	0.17	0.06	0.03	0.08	0.06	0.05	0.05	0.24	
RES6	0.22		0.11	0.08			0.08	0.08	0.03	0.02	0.04	0.03	0.05	0.04	0.22	
COM1		0.14	0.2	0.15	0.05		0.16	0.03	0.02		0.02		0.04	0.02	0.17	
COM2		0.1	0.21	0.15	0.07		0.16	0.03	0.02		0.02		0.03	0.04	0.17	
COM3		0.25	0.07	0.05	0.11		0.05	0.03	0.02		0.02		0.06	0.04	0.3	
COM4		0.26	0.11	0.08	0.04		0.09	0.04	0.02		0.03		0.05	0.04	0.24	
COM5		0.13	0.13	0.09	0.13		0.1	0.05	0.03		0.02	0.02	0.05	0.03	0.22	
COM6		0.02	0.22	0.15			0.18	0.1	0.04	0.02	0.05	0.04	0.03	0.02	0.13	
COM7		0.24	0.1	0.07	0.15		0.08	0.03	0.02		0.03		0.04	0.04	0.2	
COM8		0.19	0.19	0.13	0.06		0.15	0.03	0.02		0.02		0.03	0.03	0.15	
COM9		0.05	0.2	0.13	0.12	0.02	0.16	0.07	0.02		0.03	0.03	0.03	0.02	0.12	
COM10			0.1	0.07			0.08	0.3	0.11	0.06	0.14	0.12			0.02	
IND1		0.05	0.22	0.15	0.04	0.02	0.17	0.07	0.03		0.03	0.03	0.03	0.03	0.13	
IND2		0.1	0.15	0.09	0.15		0.11	0.05	0.03		0.02	0.02	0.04	0.05	0.19	
IND3		0.07	0.25	0.18	0.03		0.19	0.04	0.02		0.02	0.02	0.03	0.02	0.13	
IND4		0.07	0.26	0.19	0.03		0.2	0.03	0.02		0.02		0.02	0.03	0.13	
IND5		0.05	0.25	0.17	0.03	0.02	0.2	0.07	0.03		0.03	0.03		0.02	0.1	
IND6		0.1	0.21	0.14	0.07	0.02	0.16	0.05	0.02		0.02	0.02	0.02	0.03	0.14	
AGR1		0.48	0.08	0.06	0.12		0.07	0.02					0.03	0.02	0.12	
REL1	0.36		0.04	0.04			0.03	0.02	0.02		0.02		0.07	0.06	0.34	
GOV1		0.07	0.24	0.16	0.03		0.19	0.05	0.03		0.02	0.01	0.03	0.03	0.13	
GOV2		0.08	0.16	0.11	0.04		0.13	0.08	0.03	0.02	0.04	0.03	0.04	0.05	0.19	
EDU1		0.13	0.17	0.13			0.13	0.05	0.03		0.02	0.02	0.05	0.05	0.22	
EDU2		0.04	0.18	0.13			0.14	0.08	0.03	0.02	0.04	0.03	0.05	0.04	0.22	

Appendix G: Functionality of Essential Facilities by Scenario

Essential Facility Functionality-Hospital

Scenarios	At Least Moderate Damage >50% on Day 1	Complete Damage >50% on day 1	With Functionality > 50% on day 1	Weight
AB95_30NW5.3	0	0	71	17%
AB95_30NW5.7	0	0	50	21%
AB95_30NW6	0	0	3	21%
AB95_30NW6.3	2	0	0	17%
AB95_30NW6.7	18	0	0	13%
AB95_50NW7	4	0	0	11%
Weighted Avg	**3**	**0**	**23**	
AB95_30SW5.3	0	0	69	17%
AB95_30SW5.7	0	0	52	21%
AB95_30SW6	1	0	11	21%
AB95_30SW6.3	2	0	0	17%
AB95_30SW6.7	13	1	0	13%
AB95_50SW7	3	0	0	11%
Weighted Avg	**3**	**0**	**25**	
Total Weighted Avg	**3**	**0**	**24**	

Scenarios	At Least Moderate Damage >50% on Day 1	Complete Damage >50% on day 1	With Functionality > 50% on day 1	Weight
AB06_30NW5.3	0	0	71	14%
AB06_30NW5.7	0	0	71	17%
AB06_30NW6	0	0	61	18%
AB06_30NW6.3	0	0	21	17%
AB06_30NW6.7	0	0	0	13%
AB06_30NW7	0	0	0	10%
AB06_50NW7	0	0	1	10%
Weighted Avg	**0**	**0**	**37**	
AB06_30SW5.3	0	0	71	14%
AB06_30SW5.7	0	0	68	17%
AB06_30SW6	0	0	63	18%
AB06_30SW6.3	0	0	16	17%
AB06_30SW6.7	3	0	0	13%
AB06_30SW7	4	0	0	10%
AB06_50SW7	0	0	8	10%
Weighted Avg	**1**	**0**	**37**	
Total Weighted Avg	**0**	**0**	**37**	

Scenarios	At Least Moderate Damage >50% on Day 1	Complete Damage >50% on day 1	With Functionality > 50% on day 1	Weight
A08_30NW5.3	0	0	71	15%
A08_30NW5.7	0	0	71	18%
A08_30NW6	0	0	71	20%
A08_30NW6.3	0	0	70	19%
A08_30NW6.7	0	0	38	16%
A08_50NW7	0	0	55	13%
Weighted Avg	**0**	**0**	**64**	
A08_30SW5.3	0	0	71	15%
A08_30SW5.7	0	0	71	18%
A08_30SW6	0	0	70	20%
A08_30SW6.3	0	0	65	19%
A08_30SW6.7	0	0	48	16%
A08_50SW7	0	0	53	13%
Weighted Avg	**0**	**0**	**64**	
Total Weighted Avg	**0**	**0**	**64**	

Essential Facility Functionaly-School

Scenarios	At Least Moderate Damage >50% on Day 1	Complete Damage >50% on day 1	With Functionality > 50% on day 1	Weight
AB95_30NW5.3	0	0	731	17%
AB95_30NW5.7	0	0	531	21%
AB95_30NW6	0	0	12	21%
AB95_30NW6.3	35	0	0	17%
AB95_30NW6.7	218	0	0	13%
AB95_50NW7	58	0	0	11%
Weighted Avg	**41**	**0**	**238**	
AB95_30SW5.3	0	0	706	17%
AB95_30SW5.7	1	0	538	21%
AB95_30SW6	22	0	119	21%
AB95_30SW6.3	59	1	3	17%
AB95_30SW6.7	189	13	0	13%
AB95_50SW7	62	0	0	11%
Weighted Avg	**46**	**2**	**258**	
Total Weighted Avg	**43**	**1**	**248**	

Scenarios	At Least Moderate Damage >50% on Day 1	Complete Damage >50% on day 1	With Functionality > 50% on day 1	Weight
AB06_30NW5.3	0	0	764	14%
AB06_30NW5.7	0	0	763	17%
AB06_30NW6	0	0	666	18%
AB06_30NW6.3	0	0	148	17%
AB06_30NW6.7	0	0	3	13%
AB06_30NW7	32	0	3	10%
AB06_50NW7	0	0	28	10%
Weighted Avg	**3**	**0**	**390**	
AB06_30SW5.3	0	0	764	14%
AB06_30SW5.7	0	0	713	17%
AB06_30SW6	0	0	600	18%
AB06_30SW6.3	5	0	220	17%
AB06_30SW6.7	52	0	3	13%
AB06_30SW7	84	2	3	10%
AB06_50SW7	0	0	124	10%
Weighted Avg	**16**	**0**	**391**	
Total Weighted Avg	**10**	**0**	**391**	

Scenarios	At Least Moderate Damage >50% on Day 1	Complete Damage >50% on day 1	With Functionality > 50% on day 1	Weight
A08_30NW5.3	0	0	764	15%
A08_30NW5.7	0	0	764	18%
A08_30NW6	0	0	764	20%
A08_30NW6.3	0	0	727	19%
A08_30NW6.7	0	0	338	16%
A08_50NW7	0	0	569	13%
Weighted Avg	**0**	**0**	**665**	
A08_30SW5.3	0	0	764	15%
A08_30SW5.7	0	0	757	18%
A08_30SW6	0	0	724	20%
A08_30SW6.3	0	0	674	19%
A08_30SW6.7	1	0	456	16%
A08_50SW7	0	0	534	13%
Weighted Avg	**0**	**0**	**660**	
Total Weighted Avg	**0**	**0**	**663**	

Essential Facility Functionaly-Emergency Operation Center

Scenarios	At Least Moderate Damage >50% on Day 1	Complete Damage >50% on day 1	With Functionality > 50% on day 1	Weight
AB95_30NW5.3	0	0	61	17%
AB95_30NW5.7	0	0	60	21%
AB95_30NW6	0	0	50	21%
AB95_30NW6.3	1	0	50	17%
AB95_30NW6.7	2	0	46	13%
AB95_50NW7	1	0	45	11%
Weighted Avg	**1**	**0**	**53**	
AB95_30SW5.3	0	0	60	17%
AB95_30SW5.7	0	0	57	21%
AB95_30SW6	0	0	48	21%
AB95_30SW6.3	7	0	44	17%
AB95_30SW6.7	10	0	36	13%
AB95_50SW7	2	0	43	11%
Weighted Avg	**3**	**0**	**49**	
Total Weighted Avg	**2**	**0**	**51**	

Scenarios	At Least Moderate Damage >50% on Day 1	Complete Damage >50% on day 1	With Functionality > 50% on day 1	Weight
AB06_30NW5.3	0	0	62	14%
AB06_30NW5.7	0	0	62	17%
AB06_30NW6	0	0	58	18%
AB06_30NW6.3	0	0	54	17%
AB06_30NW6.7	0	0	50	13%
AB06_30NW7	1	0	50	10%
AB06_50NW7	0	0	50	10%
Weighted Avg	**0**	**0**	**56**	
AB06_30SW5.3	0	0	62	14%
AB06_30SW5.7	0	0	61	17%
AB06_30SW6	0	0	58	18%
AB06_30SW6.3	0	0	50	17%
AB06_30SW6.7	3	0	42	13%
AB06_30SW7	11	0	38	10%
AB06_50SW7	0	0	50	10%
Weighted Avg	**1**	**0**	**53**	
Total Weighted Avg	**1**	**0**	**54**	

Scenarios	At Least Moderate Damage >50% on Day 1	Complete Damage >50% on day 1	With Functionality > 50% on day 1	Weight
A08_30NW5.3	0	0	62	15%
A08_30NW5.7	0	0	62	18%
A08_30NW6	0	0	62	20%
A08_30NW6.3	0	0	62	19%
A08_30NW6.7	0	0	54	16%
A08_50NW7	0	0	62	13%
Weighted Avg	**0**	**0**	**61**	
A08_30SW5.3	0	0	62	15%
A08_30SW5.7	0	0	62	18%
A08_30SW6	0	0	61	20%
A08_30SW6.3	0	0	59	19%
A08_30SW6.7	0	0	56	16%
A08_50SW7	0	0	58	13%
Weighted Avg	**0**	**0**	**60**	
Total Weighted Avg	**0**	**0**	**60**	

Essential Facility Functionaly-Police Station

Scenarios	At Least Moderate Damage >50% on Day 1	Complete Damage >50% on day 1	With Functionality > 50% on day 1	Weight
AB95_30NW5.3	0	0	44	17%
AB95_30NW5.7	0	0	43	21%
AB95_30NW6	0	0	43	21%
AB95_30NW6.3	0	0	43	17%
AB95_30NW6.7	1	0	43	13%
AB95_50NW7	0	0	43	11%
Weighted Avg	**0**	**0**	**43**	
AB95_30SW5.3	0	0	43	17%
AB95_30SW5.7	0	0	43	21%
AB95_30SW6	1	0	43	21%
AB95_30SW6.3	1	0	43	17%
AB95_30SW6.7	1	0	41	13%
AB95_50SW7	1	0	43	11%
Weighted Avg	**1**	**0**	**43**	
Total Weighted Avg	**0**	**0**	**43**	

Scenarios	At Least Moderate Damage >50% on Day 1	Complete Damage >50% on day 1	With Functionality > 50% on day 1	Weight
AB06_30NW5.3	0	0	44	14%
AB06_30NW5.7	0	0	44	17%
AB06_30NW6	0	0	43	18%
AB06_30NW6.3	0	0	43	17%
AB06_30NW6.7	0	0	43	13%
AB06_30NW7	0	0	43	10%
AB06_50NW7	0	0	43	10%
Weighted Avg	**0**	**0**	**43**	
AB06_30SW5.3	0	0	44	14%
AB06_30SW5.7	0	0	43	17%
AB06_30SW6	0	0	43	18%
AB06_30SW6.3	1	0	43	17%
AB06_30SW6.7	1	0	43	13%
AB06_30SW7	1	1	42	10%
AB06_50SW7	0	0	43	10%
Weighted Avg	**0**	**0**	**43**	
Total Weighted Avg	**0**	**0**	**43**	

Scenarios	At Least Moderate Damage >50% on Day 1	Complete Damage >50% on day 1	With Functionality > 50% on day 1	Weight
A08_30NW5.3	0	0	44	15%
A08_30NW5.7	0	0	44	18%
A08_30NW6	0	0	44	20%
A08_30NW6.3	0	0	43	19%
A08_30NW6.7	0	0	43	16%
A08_50NW7	0	0	43	13%
Weighted Avg	**0**	**0**	**44**	
A08_30SW5.3	0	0	44	15%
A08_30SW5.7	0	0	44	18%
A08_30SW6	0	0	43	20%
A08_30SW6.3	0	0	43	19%
A08_30SW6.7	0	0	43	16%
A08_50SW7	0	0	43	13%
Weighted Avg	**0**	**0**	**43**	
Total Weighted Avg	**0**	**0**	**43**	

Essential Facility Functionaly-Fire Station

Scenarios	At Least Moderate Damage >50% on Day 1	Complete Damage >50% on day 1	With Functionality > 50% on day 1	Weight
AB95_30NW5.3	0	0	64	17%
AB95_30NW5.7	0	0	64	21%
AB95_30NW6	0	0	56	21%
AB95_30NW6.3	1	0	56	17%
AB95_30NW6.7	1	0	51	13%
AB95_50NW7	1	0	54	11%
Weighted Avg	**0**	**0**	**58**	
AB95_30SW5.3	0	0	65	17%
AB95_30SW5.7	0	0	65	21%
AB95_30SW6	0	0	56	21%
AB95_30SW6.3	0	0	54	17%
AB95_30SW6.7	2	0	44	13%
AB95_50SW7	1	0	51	11%
Weighted Avg	**0**	**0**	**57**	
Total Weighted Avg	**0**	**0**	**58**	

Scenarios	At Least Moderate Damage >50% on Day 1	Complete Damage >50% on day 1	With Functionality > 50% on day 1	Weight
AB06_30NW5.3	0	0	65	14%
AB06_30NW5.7	0	0	65	17%
AB06_30NW6	0	0	61	18%
AB06_30NW6.3	0	0	59	17%
AB06_30NW6.7	0	0	56	13%
AB06_30NW7	3	0	56	10%
AB06_50NW7	0	0	56	10%
Weighted Avg	**0**	**0**	**60**	
AB06_30SW5.3	0	0	65	14%
AB06_30SW5.7	0	0	65	17%
AB06_30SW6	0	0	65	18%
AB06_30SW6.3	0	0	57	17%
AB06_30SW6.7	0	0	53	13%
AB06_30SW7	3	0	49	10%
AB06_50SW7	0	0	56	10%
Weighted Avg	**0**	**0**	**60**	
Total Weighted Avg	**0**	**0**	**60**	

Scenarios	At Least Moderate Damage >50% on Day 1	Complete Damage >50% on day 1	With Functionality > 50% on day 1	Weight
A08_30NW5.3	0	0	65	15%
A08_30NW5.7	0	0	65	18%
A08_30NW6	0	0	65	20%
A08_30NW6.3	0	0	64	19%
A08_30NW6.7	0	0	59	16%
A08_50NW7	0	0	63	13%
Weighted Avg	**0**	**0**	**64**	
A08_30SW5.3	0	0	65	15%
A08_30SW5.7	0	0	65	18%
A08_30SW6	0	0	65	20%
A08_30SW6.3	0	0	65	19%
A08_30SW6.7	0	0	62	16%
A08_50SW7	0	0	64	13%
Weighted Avg	**0**	**0**	**64**	
Total Weighted Avg	**0**	**0**	**64**	

Reference:

Abrahamson, N. A. (2007). Unpublished Report. http://www.ce.memphis.edu/7137/schedule.htm

Adams, J. (1989). Seismicity and Seismotectonics of Southeastern Canada. *Earthquake Hazards and the Design of Constructed Facilities in the Eastern United States, Annals of the New York Academy of Sciences, 558*, 40-53.

Adams, J., & Halchuk, S. (2003). *Fourth generation seismic hazard maps of Canada: Values for over 650 Canadian localities intended for the 2005 National Building Code of Canada*.

Adams, J., & Halchuk, S. (2004). *Fourth-Generation Seismic Hazard Maps for the 2005 National Building Code of Canada*. Paper presented at the 13th World Conference on Earthquake Engineering.

Adams, J., Rogers, G., Halchuk, S., McCormack, D., & Cassidy, J. (2002). *The case for an advanced national earthquake monitoring system for Canada's cities at risk.* Paper presented at the 7th U.S. National Conference on Earthquake Engineering, Boston, United States.

Atkinson, G. M. (2008). Ground-Motion Prediction Equations for Eastern North America from a Referenced Empirical Approach: Implications for Epistemic Uncertainty. *Bulletin of the Seismological Society of America, 98*(3), 1304-1318.

Atkinson, G. M., & Boore, D. M. (1995). Ground-motion relations for eastern North America. *Bulletin of the Seismological Society of America, 85*(1), 17-30.

Atkinson, G. M., & Boore, D. M. (2006). Earthquake Ground-Motion Prediction Equations for Eastern North America. *Bulletin of the Seismological Society of America, 97*(3), 1032-.

Auger, J., & Roquet, N. (1998). *Mémoire de bâtisseurs du Québec : répertoire illustré de systèmes de construction du 18e siècle à nos jours*. Montréal: Méridien.

Bazzurro, P., & Allin Cornell, C. (1999). Disaggregation of seismic hazard. *Bulletin of the Seismological Society of America, 89*(2), 501-520.

Belvaux, M. (2009a). CRISIS Attenuation Table using AB95 Ground Motion Prediction

Equation.

Belvaux, M. (2009b). CRISIS Input File: R-Model used in NBCC2005.

Boore, D. M., & Atkinson, G. M. (2008). Ground-Motion Prediction Equations for the Average Horizontal Component of PGA, PGV, and 5%-Damped PSA at Spectral Periods between 0.01 s and 10.0 s. *Earthquake Spectra, 24*(1), 99-138.

Boyer, L. (1985). *Geology of Montreal, Province of Quebec, Canada*. Lawrence, KS: Association of Engineering Geologists.

Campbell, K. W. (2003). Prediction of Strong Ground Motion Using the Hybrid Empirical Method and Its Use in the Development of Ground-Motion (Attenuation) Relations in Eastern North America. *Bulletin of the Seismological Society of America, 93*(3), 1012-1033.

Chouinard, L., Rosset, P., De la Puente, A., Madriz, R., Mitchell, D., & Adams, J. (2004). *Seismic Hazard Analysis for Montreal*. Paper presented at the 13th World Conference on Earthquake Engineering.

CIMTU (2003). Enquête Origine-destination 2003.

City of Montreal (2010). Role foncier securite 2009. Montreal.

Coburn, A. W., & Spence, R. J. S. (1992). *Factors Determining Human Casualty Levels in Earthquakes: Mortality Prediction in Building Collapse.* Paper presented at the 10 WCEE, Madrid, Spain.

Crawford, C. B. (1968). Quick clays of eastern Canada. *Engineering Geology, 2*, 239-265.

Durkin, M. E., & Thiel, C. C. (1991). *Integrating Earthquake Casualty and Loss Estimation.* Paper presented at the Workshop on Modeling Earthquake Casualties for Planning and Response, Sacramento.

Earthquakes Canada, G. Earthquake Search (On-line Bulletin). Retrieved 2010.08.13, from Nat. Res. Can.: http://seismo.nrcan.gc.ca/stnsdata/nedb/bull_e.php

Elkady, A. M. (2010). CRISIS Attenuation Input Tables using AB06 and A08 Ground Motion Prediction Equations.

Elnashai, A. S., Di Sarno, L., & Wiley, I. (2008). Fundamentals of earthquake engineering, from http://dx.doi.org/10.1002/9780470024867

Elnashai, A. S., & Sarno, L. D. (2008). *Fundamentals of Earthquake Engineering*: Wiley.

FEMA (1992). *NEHRP Handbook for Seismic Evaluation of Existing Buildings*.

FEMA (1997). 1997 NEHRP Recommended Provisions for Seismic Regulations for New Buildings. Washington, D. C.

FEMA (2003). *Multi-hazard Loss Estimation Methodology Earthquake Model HAZUS®MH MR4 Technical Manual*. Washington, D.C.: National Institute of Building Sciences.

Forsyth, D. A. (1981). Characteristics of the western Quebec seismic zone. *Can. J. Earth Sci. , 18*, 103-119.

Frankel, A. D., Peterson, M. D., Mueller, C. S., Haller, K. M., Wheleler, R. L., Leyendecker, E. V., et al. (2002). *Documentation for the 2002 Update of the National Seismic Hazard Maps*: USGS.

Gates, A. E., & Ritchie, D. (2007). *Encyclopedia of Earthquakes and Volcanoes, Third Edition*. New York, NY: Facts On File.

Halchuk, S., Adams, J., & Anglin, F. (2007). *Revised Deaggregation of Seismic Hazard for Selected Canadian Cities*. Paper presented at the Ninth Canadian Conference on Earthquake Engineering.

Harmsen, S., Perkins, D., & Frankel, A. (1999). Deaggregation of probabilistic ground motions in the central and eastern United States. *Bulletin of the Seismological Society of America, 89*(1), 1-13.

Harrald, J. R., Abchee, M., Alharthi, H., & Boukari, D. (1991). *The Development of a Methodology for American Red Cross Staffing of a Disaster Under the Federal Response Plan*: George Washington Univ.

Joseph, B. J. P. (2005). *Liquefaction Hazard Mapping for the Island of Montreal.* McGill University, Montreal.

Journeay, M., & Hastings, N. Risk-Based Planning & Disaster Mitigation for District of North Vancouver, from http://georisk.info/WSHome.aspx?ws=NorthVan&locale=en-CA

Leblanc, G. (1981). A closer look at the September 16, 1732, Montreal earthquake. *Canadian Journal of Earth Sciences, 18*(3), 539-550.

Lefebvre, K. (2004). *Caracterisation structurale et evaluation de la vulnerabilite sismique des batiments historiques en maconnerie du Vieux-Montreal*

Unpublished M.Ing. dissertation, Ecole de Technologie Superieure (Canada), Canada., Montreal, Quebec, Canada.

Liao, S. S., Veneziano, D., & Whitman, R. V. (1988). Regression Models for Evaluating Liquefaction Probability. *Journal of Geotechnical Engineering, 114*(4).

Mahaney, J. A., Paret, T. F., Kehoe, B. E., & Freeman., S. A. (1993). *The Capacity Spectrum Method for Evaluating Structural Response during the Loma Prieta Earthquake.* Paper presented at the 1993 United States National Earthquake Conference, Memphis, Tennessee. .

Makdisi, F. I., & Seed, H. B. (1978). Simplified Procedure for Estimating Dam and Embankment Earthquake-Induced Deformations. *Journal of the Geotechnical Engineering Division,American Society of Civil Engineers, 104*(GT7, July), 849-867.

Marcusson, W. F. (1978). Definition of Terms Related to Liquefaction. *Journal Geotechnical Engineering Division, ASCE, 104*(GT9), 1197-1200.

Marsan, J.-C. (1981). *Montreal in Evolution:historical analysis of the development of Montreal's architecture and urban environment* McGill-Queen's University Press.

Molina-Palacios, S., & Lindholm, C. D. (2004). *HAZUSICG V1.0: User and Technical Manual*.Unpublished manuscript, Kjeller, Norway.

Oliveira, C. S., Roca, A., & Goula, X. (2006). *Assessing and managing earthquake risk : geo-scientific and engineering knowledge for earthquake risk mitigation : developments, tools, techniques*. Dordrecht: Springer.

Ordaz, M., Aguilar, A., & Arboleda, J. (2007). CRISIS (Version 1.2). UNAM, Mexico: Instituto de Ingeniería.

Park, C. B. (2010). *MASW Analysis*: Park Seismic LLC Perkins, J. B. (1992). *Estimates of Uninhabitable Dwelling Units in Future Earthquakes Affecting the San Francisco Bay Region.* Paper presented at the ABAG, Oakland, California.

Ploeger, S. K. (2008). *Applying the HAZUS-MH software tool to assess seismic hazard and vulnerability in downtown Ottawa, Canada.* Carleton University, Ottawa, Canada.

Power, M. S., Dawson, A. W., Streiff, D. W., Perman, R. G., & Haley, S. C. (1982). *Evaluation of Liquefaction Susceptibility in the San Diego, California Urban Area.* Paper presented at the 3rd International Conference on Microzonation.

Prest, V. K., & Hode-Keyser, J. (1982). *Caracteristiques Geologiques et Geotechniques des DepotsMeubles de l'Ile de Montreal et des Environs, Quebec*. Ottawa, Canada: Commission Geologique du Canada.

Quebec:RessourcesNaturellesetFaune (Cartographer). (1999). *Base de données topographiques du Québec. 31H05101-31H12202*

Rosset, P., & Chouinard, L. (2008). Characterization of site effects in Montreal, Canada. *Natural Hazards, 48*(2), 295-308.

Rosset, P., De la Puente, A., Madirz, R., Chouinard, L., Mitchell, D., & Adams, J. (2003). Identification of site effects in the Montreal Urban Community, Canada: Pilot study and methodological developments. Unpublished Report. Department of Civil Engineering and Applied Mechanics, McGill University

Sadigh, K., Egan, J. A., & Youngs, R. R. (1986.). Specification of Ground Motion for Seismic Design of Long Period Structures. *Earthquake Notesrelationships are tabulated in Joyner and Boore (1988) and Youngs and others (1987). 57*(1), 13.

Seed, H. B., & Idriss, I. M. (1982). *Ground Motions and Soil Liquefaction During Earthquakes*. Oakland, California: Earthquake Engineering Research Institute.

Singhroy, V., Mattar, K. E., & Gray, A. L. (1998). Landslide characterisation in Canada using interferometric SAR and combined SAR and TM images. [doi: DOI: 10.1016/S0273-1177(97)00882-X]. *Advances in Space Research, 21*(3), 465-476.

Smalley, I. (1976). Factors relating to the landslide process in Canadian quickclays. *Earth Surface Processes, 1*(2), 163-172.

Smith, S. B., & Coull, A. (1991). *Tall building structures : analysis and design*. New York: Wiley.

Somerville, P., Collins, N., Abrahamson, R., & Saikia, C. (2001). *Ground-motion Attenuation Relationships for the Central and Eastern United States*: final report to the U.S. Geological Survey.

StatisticCanada 2006 Census of Canada (Montreal) Using E-STAT (distributor). Retrieved September, 16, 2009: http://estat.statcan.gc.ca/cgi-win/cnsmcgi.exe?Lang=E&EST-Fi=EStat\English\SC_RR-eng.htm

StatisticCanada Census 2006: Geographic Files - Digital Boundary Files & Digital Cartographic Retrieved Nov. 06, 2010 http://www.edrs.mcgill.ca/StatCan/geogfiles/census2006/canadafiles/index.html

StatisticsCanada (2006). 2006 Cumulative Profile, Montréal (878 Census tracts) (table). *2006 Census of Population*, 2009, from http://estat.statcan.gc.ca/cgi-win/cnsmcgi.exe?Lang=E&EST-Fi=EStat\English\SC_RR-eng.htm

Toro, G. R., Abrahamson, N. A., & Schneider, J. F. (1997). Engineering Model of Strong Ground Motions from Earthquakes in the Central and Eastern United States. *Seismological Research Letters, 68*, 41-57.

U.S.GeologicalSurvey (2006). Prince William Sound, Alaska,1964 March 28 03:36 UTC Magnitude 9.2, Largest Earthquake in Alaska *Historic Earthquakes* Retrieved Jan. 11th, 2011, from http://earthquake.usgs.gov/earthquakes/states/events/1964_03_28.php

Wieczorek, G. F., Wilson, R. C., & Harp, E. L. (Cartographer). (1985). *Map of Slope Stability During Earthquakes in San Mateo County, California*.

Wilson, R. C., & Keefer, D. K. (1985). Predicting Areal Limits of Earthquake Induced Landsliding, Evaluating Earthquake Hazards in the Los Angeles Region. *U.S. Geological Survey Professional Paper*(1360), 317-493.

Youd, T. L., & Perkins, D. M. (1978). Mapping of Liquefaction Induced Ground Failure Potential. *Journal of the Geotechnical Engineering Division, 104*(4), 433-446.